Untangling the complexity of yeast hybrids and flavour production

A thesis submitted to the University of Manchester for the degree of
Doctor of Philosophy
in the Faculty of Biology, Medicine and Health

2022

Federico Visinoni

School of Biological Sciences

Table of contents

Total word count: 37.122

List of figures

List of tables

List of abbreviations

ATP	Adenosine triphosphate
ABV	Alcohol by volume
ANOVA	Analysis of variance
bp	Base pair
Chr	Chromosome
cDNA	Complementary DNA
CNV	Copy Number Variation
DNA	Deoxyribonucleic acid
DE	Differential expressed
Dr	Dilution Rate
DME	Dry malt extract
ESI	Electrospray ionization
FACS	Fluorescence-activated cell sorting
GC	Gas Chromatography
GO	Gene ontology
GMO	Genetic Modified Organism
HPLC	High throughput liquid chromatography
ITS	Internal transcribed region of the rRNA
Kb	kilo base
LC	Liquid chromatography
LOD	Logarithm of the odds
MS	Mass Spectroscopy
MAT	Mating type
mtDNA	Mitochondrial DNA
F*n*	*n*-th filial generation
OD	Optical Density
OG	Original gravity
PEG	Polyethylene glycol
PCR	Polymerase Chain Reaction
QTL	Quantitative Trait Locus
QTN	Quantitative Trait Nucleotide
RHA	Reciprocal hemizygosis analysis

RT-qPCR	Retro transcriptase quantitative polymerase chain reaction
RNA	Ribonucleic acid
Sc	*Saccharomyces cerevisiae*
Se	*Saccharomyces eubayanus*
Sj	*Saccharomyces jurei*
Sk	*Saccharomyces kudriavzevii*
Su	*Saccharomyces uvarum*
SNP	Single nucleotide polymorphism
SPME	Solid Phase Micro Extraction
μmax	Specific Growth Rate
TOF	Time of flight
VDK	Vicinal Diketones
wt	Wild type
YP	Yeast extract peptone medium
YNB	Yeast Nitrogen Base media

Abstract

The University of Manchester

Federico Visinoni

Doctor of Philosophy

Untangling the complexity of yeast hybrids and flavour production

The brewing yeast strains underwent centuries of domestication, being improved for growth and aroma profile through spontaneous mutations and selection. While genetic modifications have achieved promising results, allowing improvements in both fitness and aroma profiles, their application must deal with the stigma and the regulations associated with GMO products. Researchers must also face the complexity of the fermentation process, in term of variable feedstock, lack of reproducibility, and of the industrial strains used, which are hindering the application of predictive quantitative approaches. Indeed, brewing yeasts commonly evolved as sterile hybrids and often present copy number variations, duplications, and aneuploidy.

In this thesis, we applied a combination of genomics and metabolomics tools to untangle the genomic complexity of industrial hybrids and of the brewing process itself, revealing new strategies for both strain and process development.

First, I studied how growth rate affects the aroma profile of *S. cerevisiae* type strain (NCYC 505) in chemostat experiments at different dilution rates. The study allowed to identify a correlation between growth and the production of the major volatile compounds, shedding new light on how yeast physiology may drive their production. Moreover, the data generated allowed to design a feeding profile to effectively manipulate aroma compound production through nutrient availability.

Second, I applied state-of-the-art techniques to harness the biodiversity of *Saccharomyces species* and study how hybridisation and natural variation affect traits of industrial interest. I presented a novel platform to study inter-species hybrids by crossing geographically distant strains from different species through rare mating, effectively restoring fertility in hybrid strains and allowing quantitative genetics studies. The pipeline developed allowed to identify species-specific and hybrid-specific features responsible for traits of biotechnological interest for the production of fermented beverages, and for antifungal resistance. Furthermore, it allowed to dissect the complexity of the hybrid genome and to assess the genome-wide effect of mito-nuclear interactions on the QTL landscape. Lastly, I explored the brewing potential of *Saccharomyces jurei* in lab-scale and pilot-scale fermentations, assessing both the

fermentation capabilities and the aroma profile of this recently discovered species. Moreover, through spore-to-spore-mating, novel *S. jurei x S. cerevisiae* hybrids of great interest for the beverage industry were generated, presenting good fermentation performances and unique aroma profiles. Overall, the combination of approaches and studies presented in this thesis allowed us to help untangle the complexity of the brewing yeast, refine the industrial process, and to highlight the incredible potential of natural strains and novel hybrids in brewing.

Rationale for submitting the thesis in a journal format

The thesis is presented in a journal format consisting of published results (Chapter 3 and 5) and chapters formatted for submission to a peer-reviewed journal (Chapter 2 and 4). Therefore, the references are presented at the end of each chapter and the reference style is unified throughout the thesis for consistency. As a consequence of the thesis format, there are some overlaps in introduction, methodology and references. However, it is thought that the result is a clear and concise thesis summarising the valuable work of this doctoral project.

Declaration

I declare that no portions of the work referred to in the thesis has been submitted in support of an application for another degree or qualification of this or any other university or other institutes of learning

Copyright statement

i The author of this thesis (including any appendices and/or schedules to this thesis) owns certain copyright or related rights in it (the "Copyright") and s/he has given The University of Manchester certain rights to use such Copyright, including for administrative purposes.

ii Copies of this thesis, either in full or in extracts and whether in hard or electronic copy, may be made **only** in accordance with the Copyright, Designs and Patents Act 1988 (as amended) and regulations issued under it or, where appropriate, in accordance with licensing agreements which the University has from time to time. This page must form part of any such copies made.

iii The ownership of certain Copyright, patents, designs, trademarks and other intellectual property (the "Intellectual Property") and any reproductions of copyright works in the thesis, for example graphs and tables ("Reproductions"), which may be described in this thesis, may not be owned by the author and may be owned by third parties. Such Intellectual Property and Reproductions cannot and must not be made available for use without the prior written permission of the owner(s) of the relevant Intellectual Property and/or Reproductions.

iv Further information on the conditions under which disclosure, publication and commercialisation of this thesis, the Copyright and any Intellectual Property and/or Reproductions described in it may take place is available in the University IP Policy (see http://documents.manchester.ac.uk/DocuInfo.aspx?DocID=24420), in any relevant Thesis restriction declarations deposited in the University Library, The University Library's regulations (see http://www.library.manchester.ac.uk/about/regulations/) and in The University's policy on Presentation of Theses.

Acknowledgements

I would like to thank my Supervisor, Prof. Daniela Delneri, and my Co-Supervisor, Dr. James Winterburn, for all their support and guidance throughout my PhD, for showing me my strengths and for offering me this amazing opportunity.

This thesis would not have been possible without our amazing collaborators: Katherine Hollywood and Rehana Sung from the Manchester Institute of Biotechnology for bearing with me during all my troubles with HPLC and GC-MS, offering both technical and emotional support; Urska Vrhovsek team in Fondazione Edmund Mach, and Penghan Zhang in particular, for welcoming in Trento during my secondments and for showing me the wonder of GC-GC-MS; Prof. Ed Louis team in Leicester for the amazing contributions to QTL analysis and hybrids construction. I had the chance to meet and thank in person only Ed and Yue Hue but I must also thank Alex Roberts for all the help and guidance his thesis gave me. I must also acknowledge the incredible support from the Bioinformatic Core Facilities and the Genomic Technologies facility in Manchester, and especially to Rachel Scholey for the QTL analysis.

I cannot thank enough my friends and colleagues in the Delneri research group and, in particular, Samina Naseeb, Konstantina Giannakou, and Soukaina Timouma which contributed to the work presented here with experiments and analysis. I always felt part of a family here and I will always be grateful to every one of you: Natalia Balarezo, Zorana Carter, Jose Aguiar, Javier Pinto, Alkisti Manousaki, Marcin Fraczek, Steven Parker, Alistair Hanak, and Tanda Qi.

To all my friends back home, thank you for sticking with me even though I was physically escaping from you. Thank you, Matteo, Silvia, Federica, Alessio, and Claudio Aglio, I would be lost without you. Thank you, Carlo, for distracting me every day from work and gifting me wonderful figures in return. Thank you to the most amazing emotional supports cats in the world: Granola and GattaKiwi.

Most of all, thank you to my family for always supporting me, worrying about me and trying to cheer me up. To my brother and my sister, to my parents, to my civvie, I owe this thesis to you.

Finally, I want to thank the European Union's Horizon 2020 research for sponsoring my work through the grant (H2020-MSCA-ITN-2017 – 764364) and allowing me to enjoy the amazing group of the Innovative Training Network Aromagenesis.

Chapter 1 – General introduction

1.1 Yeast physiology

The eight species of the *Saccharomyces* genus have a worldwide distribution and occupy different environmental habitats. The genus is comprised of thermo-tolerant species (*S. cerevisiae*) able to grow up to 45°C, generalists (*S. paradoxus* and *S. mikatae*), and cold-tolerant species (*S. kudriavzevii*, *S. arboricola*, *S. eubayanus*, *S. uvarum* and *S. jurei*) (Naseeb, et al. 2017). The variation observed in thermal and stress adaptation within the genus has been exploited for centuries for industrial applications. In fact, while this thesis will delve deeper on *Saccharomyces* role in the production of fermented beverage, the industrial applications of these species are manifold. *S. cerevisiae*, in particular, is almost ubiquitous in industry, with an important role in food, biopharmaceuticals and biofuel production (Borneman and Pretorius, 2015). Moreover, it's one of the most characterized model system and the first eukaryote to be completely sequenced (Goffeau et al., 1996). Yeasts in the *Saccharomyces* genus are described as facultative anaerobes: able to use oxygen for cellular respiration and to grow in anaerobicity thanks to the fermentation pathway. In both conditions, sugars are converted into pyruvate in the glycolytic pathway. When oxygen is present, pyruvate is directed towards the tricarboxylic acid (TCA) cycle and the respiratory chain, producing energy through oxidative phosphorylation. In anaerobic conditions, pyruvate is converted into ethanol and CO_2 in a two-step process, thus energy is produced only through substrate-level phosphorylation in the glycolytic pathway. Interestingly, yeasts belonging to the *Saccharomyces* species use alcoholic fermentation even in the presence of oxygen even if it is less energy efficient than cellular respiration (Pfeiffer and Morley, 2014). This trait, typical of Crabtree-positive species, occurs due to a repression of the respiratory pathway in glucose abundance (De Deken 1966) and characterizes the early stage of most industrial batch processes.

The most common species used to in the production of fermented beverages are *Saccharomyces cerevisiae* and *S. pastorianus,* a hybrid between *S. cerevisiae* and *S. eubayanus* (Bokulich and Bamforth, 2013). These brewing yeasts strains show particular and unique physiology as a result of their domestication. Brewing strains often exhibit limited respiratory capacity and, irrespective of oxygen concentrations, maintain a fermentative metabolism all throughout the process (Boulton and Quain, 2008). Moreover, their physiology is greatly affected by the numerous stresses which arise during the fermentation process. Yeast is subjected to low pH, elevated ethanol and CO_2

concentrations, reduced water activity and high hydrostatic pressure, especially in large vessels (Boulton and Quain, 2008; Querol et al., 2003). The preference of brewing yeast to accumulate carbohydrates as glycogen and trealose (Cheong et al., 2007) is an example of how yeast evolved to alter its metabolism to withstand such stresses.

Another important trait of the brewing yeast is the capability to utilise a wide variety of nutrients and efficiently ferment wort sugars as maltose and maltotriose. Yeasts usually show a preference for easily assimilated sugars, both in their uptake and utilizations. Sucrose is the first sugar fermented, followed by fructose and glucose whose assimilations happens simultaneously. After glucose is depleted, yeasts start the fermentation of the predominant sugars in wort: maltose and maltotriose (D'Amore et al., 1989). While maltose is commonly fermented by *Saccharomyces* species, albeit with various degree of efficiency, the assimilation of maltotriose is a trait almost exclusively described in brewing strains (Gallone et al., 2018; Krogerus et al., 2015). Moreover, lager strains are able to ferment melibiose, a unique trait in brewing (Quain, 1986).

1.2 Yeast life cycle

The life cycle of yeast populations is complex as cells can stably exist in both haploid and diploid state. Moreover, yeast cells modify their growth in response to stresses and switch between dividing asexually by mitosis and sexual reproduction by meiosis and sporulation. In favourable conditions, yeast is able to grow both in haploid and diploid state following an asexual cell cycle, via a process known as budding. During this mitotic cycle a small bud is formed on the mother cell wall containing an exact copy of the parental chromosomes and organelles. The new daughter cell continues to grow, reaching almost the same size of the mother cell, until it separates (Beran, 1968) (Figure 1-1).

Under stressful conditions, yeasts cells exit the mitotic cycle from the G1 phase as unbudded cells. At this stage, diploids undergo meiosis to generate four haploid spores surrounded by an ascus, which acts as a wall and grants the spores resistance to a variety of environmental stresses (Smits et al., 2001). The ascus is maintained until an improvement of environmental conditions occurs. Then, the ascus is disrupted, and the released spores can develop into haploid cells or mate to form diploids (Herskowitz, 1988).

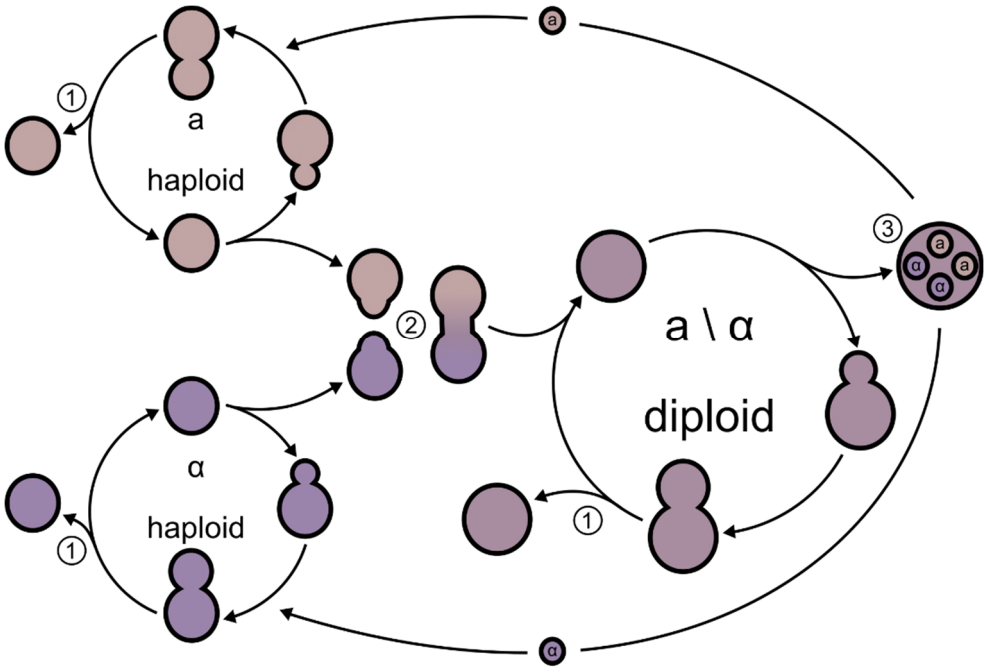

Figure 1-1 | Life cycle of yeast cells. 1 In favourable conditions both haploid and diploid cells reproduce by mitosis via budding. **2** Haploid cells of different mating type (a and α) can also mate to generate a new diploid via conjugation. **3** Under nutrient constraints diploid cells undergo sporulation, generating four haploid ascospores which will be released from the ascus after an improvement of environmental conditions. (Adapted from Masur, 2007)

Sexual reproduction occurs between cells of opposite mating type, in a process called conjugation or mating. Mating-competent cells, or maters, can exist as two different mating type, a and α, differentiated by the production of a corresponding mating pheromone, a- or α-factor. These differences are due to two non-homologous alleles, *MATa* or *MATα*, at the mating type (MAT) locus located on chromosome III (Haber, 2012) which encodes for regulators of the mating pheromones. When in the proximity of a cell of the opposing mating type, maters respond arresting the mitotic cycle and undergoing cell fusion.

In homothallic strains, the expressed MAT locus is flanked by two unexpressed loci: HML and HMR, containing a silent copy of MAT α and MAT a, respectively (Hanson and Wolfe, 2017). Thanks to a homologous recombination event initiated by the HO endonuclease, homothallic strains can undergo a mating-type switch and self-fertilise (Strathern et al., 1982). The HO gene encodes for a site-specific endonuclease able to create a double strand break in the MAT locus. This double strand break will be repaired, in most cases, using the opposite silent copy located in the HML or HMR (Wu and Haber, 1996). Strains with a loss-of-function mutation in the HO gene are defined as heterothallic and are unable to self-

fertilise. Thus, heterothallic strains can be easily maintained as haploids with stable mating types, provided they are not brought into contact of a cell of the opposite mating type.
After mating, haploid cells of different mating type fuse to form a cell possessing a heterozygous MATa/MATα genotype. The combination of the information encoded by these loci triggers the repression of haploid-specific genes, silencing both HO and the mating pheromone production, while activates diploid-specific genes (Breeden and Nasmyth, 1985). Therefore, the resulting diploid is unable to produce mating pheromones and mate between each other. However, in rare cases, spontaneous mutations can arise in diploid or polyploid cells resulting in loss of heterozygosity at the MAT locus and a restoration of fertility (Gunge and Nakatomi, 1972).

1.3 Yeast hybridization

Hybridization constitutes an important mechanism for evolution as it enhances genetic flexibility and phenotypic plasticity (Querol et al., 2003). It is defined as the fusion of two genetically divergent gametes (Sipiczki, 2008) of the same species (intraspecific hybridization) or from different ones (interspecific hybridization).

In yeast, interspecific hybridization commonly occurs in the *Saccharomyces* genus generating sterile hybrids able to undergo mitosis but which can barely produce viable spores (Sipiczki, 2008). To overcome the inability to undergo meiosis efficiently, yeast usually form allotetraploid or homoploid hybrids prone to genomic rearrangements and genetic drift (Belloch et al., 2009). In the brewing industry, the use of interspecific hybrids is commonplace. Since the 15th century *S. pastorianus* has been employed for the production of beer thanks to its unique characteristics. This hybrid possesses both the high fermentative capacity of *S. cerevisiae*, and the cryotolerant nature of *S. eubayanus*, which give it a fitness advantage during the regime of brewing carried out at temperatures around 7 and 13°C (Monerawela and Bond, 2018). Interspecific hybrids are not only selected for their capability to combine advantageous traits of the parent strains. They can also show improved phenotype traits due to the phenomena of heterosis or hybrid vigour. In fact, parental phenotypes don't usually interact in an additive manner (Shull, 1948). Instead, it is often the case that hybrid traits are different than the average of the parental strains (Hochholdinger and Hoecker, 2007). The peculiar conditions in which beer fermentation is carried out can represent a perfect fertile ground for the hybrids to grow and evolve (Replansky et al., 2008). The broad phenotypic variance of newly generated hybrids will undergo natural selection in the relatively harsh

process conditions of beer fermentation. Furthermore, hybrids will be able to draw from the genetic material of both the parental strains in the process of adaptive evolution to this stressful environment (Querol et al., 2003). While *S. pastorianus* is the most common hybrid in beer fermentation, hybrids between *Saccharomyces* species have been isolated in domesticated and wild environments alike (Barbosa et al., 2016). In particular, *S. cerevisiae* x *S. kudriavzevii* and *S. cerevisiae* x *S. uvarum* hybrids, as well as *S. cerevisiae*, *S. uvarum* and *S. eubayanus* triple hybrid (*S. bayanus*), found use in winemaking and in the fermentation of cider and Belgian beers (Gallone et al., 2019; Gonzalez et al., 2006; Le Jeune et al., 2007).

1.3.1 Artificial hybrids

Recently, much work has gone into the generation of *de novo* yeast hybrids, exploiting their potential for the production of biofuels (Peris et al., 2017; Snoek et al., 2015), brewing (Krogerus et al., 2015; Mertens et al., 2015), and winemaking (Bellon et al., 2013; Origone et al., 2018).

Saccharomyces species can be hybridized by a variety of methods: spore-to-spore mating, mass mating, rare mating and protoplast fusion among others that will not be discussed in this thesis.

Spore-to-spore mating and mass mating exploit sexual hybridization events between haploid cells of different species and mating type. The former is performed by manually placing spores from two parent strains near each other in an agar plate using a micromanipulator. Mass mating is somewhat less refined and is accomplished by randomly mixing spores together in liquid media. For this reason, it usually requires selection markers to identify *de novo* hybrids. These approaches boast high hybridization frequencies and genetic stability but requires parental strains able to form viable spores (Pérez-Través et al., 2012; Steensels et al., 2014b).

When parents show little to no spore viability, rare mating and protoplast fusion can still be employed. Rare mating is applied on diploids strains which lose heterozygosity of the MAT locus spontaneously or after genetic mutations. These diploids can rarely, hence the name, undergo mating to produce a tetraploid containing the genome of both the parental strains. However, hybrids constructed this way are less stable and requires selection markers (Alexander et al., 2016; Fukuda et al., 2016). To overcome the low frequency of the hybridization through rare mating, genetic modification is often needed to construct homozygotic diploids able to mate (Greig et al., 2002; Krogerus et al., 2017a).

Lastly, protoplast fusion is an approach which allows the production of intergeneric hybrids employing more disruptive techniques (Lucca et al., 2002). In fact, the parent strains have their cell walls digested before a fusion event occurs between the two cells (van Solingen and van der Plaat, 1977). This method can be used in a large variety of applications, thanks to his aspecificity. However, it encounters the same problems as rare mating: low hybridization frequency, genome instability and it requires the need of selection markers (Krogerus et al., 2017a).

The flourishing current research on *de novo* yeast hybrids opened a new path for the improvement of industrial strains achieving faster growth rate, higher stress tolerance and an increase in the production of aroma compounds (Baker et al., 2019; Bellon et al., 2011; Krogerus et al., 2015, 2018; Mertens et al., 2015; Snoek et al., 2015; Steensels et al., 2014a).

Moreover, yeast hybridisation has become a vital resource in studying evolutionary pathways and speciation mechanisms. Recently, *Saccharomyces* hybrids have been employed to study the evolutionary and fitness effect of loss of heterozygosis, aneuploidies, and epistasis (Bendixsen et al., 2022; Gorter de Vries et al., 2019; Lancaster et al., 2019; Zhang et al., 2020). In particular, *Saccharomyces* hybrids have become a vital resource to study mito-nuclear epistasis and have been recently exploited in the generation of strain possessing unique mito-nuclear genotypes (Nguyen et al., 2020; Szabo et al., 2020). The growing body of research on the role of the mitochondria in yeast hybrids has revealed a genome-wide effect exercised by mitochondrial DNA and suggested mitochondria exchanges might be an overlooked tool for industrial strain development.

1.4 Domestication

Domestication is defined as the modification of the gene pool of a population due to the combined effect of natural selection and selective breeding (Kincaid, 1993). Typical signs of domestication, for pets and feedstocks alike, are changes in the reproductive cycle and adaptations to new sources of food (Baur, 1992; Driscoll et al., 2009). Domesticated species are also characterized by an higher frequency of chromosome abnormalities such as rearrangements, duplications, aneuploidy and loss of genetic information (Bergström et al., 2014; Borneman et al., 2016, 2011; Sheltzer et al., 2011).

Domestication of the brewing yeast probably started between the 16th and the 17th century, when the brewing process moved from small scale home brewing to professional large scale-brewing (Hornsey, 2003). That the start of the process could predate the discovery of microbes was possible due to the practice of back-slopping, described as reusing fermented

product as inoculum for a new fermentation. This is also one of the reasons why yeast strains used for beer production show a higher degree of domestication than the one used to ferment wine (Gallone et al., 2016). The practice of back-slopping has now evolved in what we call re-pitching, defined as re-using pure cultures from a previous fermentation. In this way the population escapes completely the process of natural selection in harsh natural environments which happens during harvest season (Boulton and Quain, 2008).

The effects of domestication in yeast are manifold. Industrial strains were first selected for their ability to thrive in the artificial habitat of the fermentor. During the fermentation, yeast cells are exposed to hyperosmotic stress, due to the high sugar concentration of wort, ionic stress, high ethanol concentration and nutrient starvation (Querol et al., 2003). The strong selection pressure derived from these stressors drove evolution of industrial strains toward accumulating features like aneuploidy and chromosomal rearrangements (Colson et al., 2004) alongside numerous mutations and copy number variations (CNV) in genes involved in metabolism and ion transport (Bergström et al., 2014; Gallone et al., 2016). The most evident example is the amplification of genes involved in maltose and maltotriose metabolism in beer and sake subpopulations which made brewing strains able to efficiently ferment these sugars (Ernandes et al., 1993). Moreover, yeast strains were selected for traits linked to aroma production and efficient flocculation (Bergström et al., 2014; Van Mulders et al., 2010).

As a result of a relaxed selection industrial yeast lost specific traits that were not useful to survive in a man-made niche. In fact, as the organism is subjected to a new environment, the natural selection pressure on specific traits weakens or disappears. This, for example, brought large systematic differences regarding the reproduction cycle of industrial yeast. As shown by Gallone et al., (2016) strains domesticated for beer fermentation lose the ability to undergo sexual reproduction and show reduced spore viability. This is due to the practice of re-pitching, which grant uninterrupted growth in rich medium to the population and relax the pressure on survival strategies adopted by yeast in the absence of nutrients. Moreover, domesticated yeasts used to produce alcoholic beverages show a reduced or absent capability to produces compounds classified as off-flavour, such as 4-vinyl guaiacol (4VG). This phenotype is characteristic of highly domesticated strain and may results in a decreased fitness in natural environments (Gallone et al., 2016). In fact, 4VG production, mediated by the *PAD1* and *FDC1* enzymes, is a result of the decarboxylation of toxic plant-derived phenylacrylic acids found in plant cell walls (Stratford et al., 2007).

Interesting insights on how the domestication process unfolded can also be derived from the recent characterization of kveik yeast from Norwegian farmhouse breweries. This group evolved independently from the industrial strain in a less controlled and regulated environment. Nevertheless, kveik yeasts show similar domestication traits, with high sugars uptake, POF- phenotype, ethanol tolerance and high flocculation efficiency (Preiss et al., 2018). Thus, industrial traits which are considered signatures of the domestication process may have different origins and causes, outside of the niche environment of industrial breweries.

1.5 Yeast mitochondria

In the *Saccharomyces* genus, the mitochondrial genome encodes only for eight proteins, while the majority of the mitochondrial proteome is nuclear-encoded, with *ca.* a thousand proteins which interplay with each other and with mitochondrially encoded proteins (Morgenstern et al., 2017). This interrelationship manifests as stable protein-protein interactions between nuclear- and mitochondrial- encoded proteins, as for the subunits of the ATP synthase complex, as well as in the mito-nuclear interactions found to affect mitochondrial replication (Ellison and Burton, 2010), transcription (Chou et al., 2010), and translation (Lee et al., 2008). This functional interplay has driven an intense coevolution of the mitochondrial and nuclear genomes and became a fertile ground for the development of incompatibilities between ecologically distant strains and species (Visinoni and Delneri, 2022).

Thus, understanding the dynamics of mito-nuclear interactions arising in *Saccharomyces* hybrids is necessary for further development of industrial strains, such as *S. pastorianus*, and for the development on new hybrid strains. To date, mito-nuclear interactions in both intra- and inter-species hybrids were investigated for their role as post-zygotic barriers (Szabo et al., 2020), and were found to affect respiration (Albertin et al., 2013; Spirek et al., 2014), fermentation (Paliwal et al., 2014) thermotolerance (EmilyClare P. Baker et al., 2019; Hewitt et al., 2020; Li et al., 2019; Szabo et al., 2020), nuclear transcription (Hewitt et al., 2020), and nuclear stability in hybrids (Antunovics et al., 2005; Peris et al., 2020).

Moreover, the role of the mitochondria in shaping industry relevant traits in *Saccharomyces* yeasts has been the subject of an increasing number of studies. In particular, mitochondrial DNA resulted one of the main players in defining thermotolerance in *S. cerevisiae* x *S. uvarum* hybrids. Genome-wide non-complementation studies by Li et al. (2019) revealed that nuclear

genes exerted only a limited effect on the hybrid phenotype, while mitochondrial genes strongly influenced hybrid fitness in both high and low temperatures (Li et al., 2019). Additionally, mitochondrial inheritance in *S. cerevisiae* x *S. uvarum* hybrids was found to exert a strong environmental and temperature-dependant transcriptome effect resulting in remarked allele preference of one species over the other in respiratory conditions. The biotechnological importance of the mitochondria, however, is not just limited to shaping yeast thermotolerance and fermentation capabilities. Recent studies in *Saccharomyces* hybrids have unearthed a correlation between the parental origin of the mitochondrial DNA and resistance to biomass drying, as well as to a different aroma profile (Pérez et al., 2022; Picazo et al., 2015). In wine fermentations, in fact, *Saccharomyces* hybrids were found to inherit an aroma profile closer to the parent whose mitochondrial DNA they inherited (Pérez et al., 2022).

1.6 Applications of continuous culturing

Continuous culturing has been widely used to study and perform adaptive evolution of microorganisms (Brickwedde et al., 2017; Dunn et al., 2013; Ferea et al., 1999; Gresham et al., 2008; Wenger et al., 2011; Weusthuis et al., 1994) as it enables precise control of the selective pressure. The two main systems used to attain continuous culturing are the chemostat and the turbidostat. Both systems can be described as bioreactors in which cells grow continuously in a fixed volume, thanks to continuous addition of medium and removal of an equivalent volume culture. Eventually, these systems are able to reach a condition of equilibrium, or steady state, in which the growth rate of the cells and the dilution rate are equal and constant (Monod, 1949; Novick and Szilard, 1950).

In the chemostat, the dilution rate is maintained fixed in a single-nutrient-limited environment. When the steady state is reached, the concentration of the limiting nutrient will dictate the cell density and the main selection pressure. In this way, cells grow in a chemically defined environment and the growth rate can be modulated by both the concentration of the limiting nutrient and the dilution rate. Instead, in the turbidostat the cell density is constantly monitored and kept steady in conditions of nutrient abundance. The limiting factor for growth in this system is not a particular nutrient but an intrinsic property of the cell (e.g. nutrient uptake, rate of organelle biogenesis, resistance to a stressor) (Gresham and Dunham, 2014).

The conditions in which the adaptive evolution unfold in continuous culturing are different than the more common serial transfer in batch cultures. First, in these systems, the selective pressure is maintained constant and defined all throughout the experiment, without any fluctuations (Gresham and Dunham, 2014). Moreover, the nature of these systems makes them better candidates for long-term selection experiments. Once the steady state is reached, they can be easily maintained until there is a constant supply of fresh media and no contaminations occurs. Thus, continuous culturing represents an important tool to study the physiology of a yeast strain in a defined environment in the first 20 generations (Jansen et al., 2002), but also as a way to enhance specific traits through adaptive evolution, which occur in the following generations (Brickwedde et al., 2017; Jansen et al., 2004).

Thanks to the refined control exerted on the selection pressure and the environment with these devices, adaptive evolutions in continuous cultures are ideally suited to be complemented with whole genome and transcriptome analysis (Bull, 2010; Delneri et al., 2008). Moreover, chemostats evolution experiments possess the same trends as domestication, with a high frequency of aneuploidies, chromosomal translocations and copy number variations (Gresham and Hong, 2015). Therefore, they are not only ideal systems to improve and study the genetics and the physiology of industrial strains but also to investigate how the evolution process of the brewing strain unfolded.

1.7 Brewing process

Brewing can be described as a three-stage process in which wort, an aqueous medium containing sugars from cereal sources, is fermented into beer (Figure 1-2).

The process starts with the production of the wort from dried, sprouted barley. This is accomplished by combining malted barley with water and heating (mashing) to allow the enzymes in the malt to break down the starch into sugars (Montanari et al., 2005). The mash is then separated from the residual grains into clear liquid wort in the lautering step and then boiled so to extract desirable compounds from the hops and stabilize the wort (O'Neill 1960). In the final steps of wort production, the wort undergoes a process known as whirlpooling, being pumped at rapid velocity in a vessel to ease the removal of the hops and then it's finally cooled (Tretter, 1989).

The second stage is represented by the fermentation of the wort by yeast cells. In this step, components of the wort are assimilated and converted in ethanol, carbon dioxide and the

numerous secondary metabolites which constitute beer. Finally, in the last stage, the beer is maturated as to be rendered suitable to consumption (Godtfredsen and Ottesen, 1982).

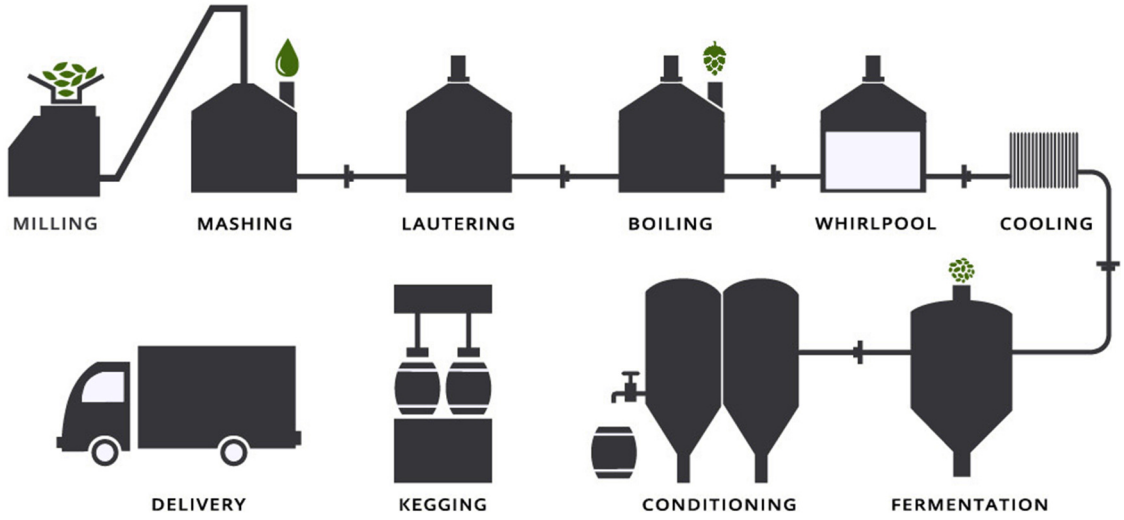

Figure 1-2 | The brewing process

Even though the scientific literature on *Saccharomyces* yeasts and on *S. cerevisiae* in particular is extensive and detailed, the biological processes that make up the fermentation stage of the brewing process are hard to characterize in depth. The reasons are manifold; first, wort is a natural product composed of numerous components whose concentrations can vary from batch to batch. Wort processing is also deeply influenced by the material and methods used in industry and this stage is not easily translated in a laboratory setting. Moreover, brewing is generally conducted as a batch process where both the fermentation parameters and the concentrations of metabolites are in constant state of flux (Boulton and Quain, 2008). The process is also carried out without agitation and in conditions of transient aerobiosis as the fermentation starts with a pulse of oxygen necessary for the biosynthesis of unsaturated fatty acids and sterols (David and Kirsop, 1972).

For these reasons, the fermentation step is characterized by an accentuated unsteady state, in which yeast physiology cannot be followed and described easily (Boulton and Quain, 2008).

1.8 Aroma-active compounds in fermented beverages

A broad and diverse range of compounds are responsible for the complex aroma and taste of fermented beverages. The main yeast-derived sensory-active compounds are often by-

products of the main metabolism, produced as secondary metabolites at trace quantities (Verstrepen et al., 2003). However, thanks to a synergistic interaction between each other, they manage to play an important role in the flavour composition, even below their threshold value (Meilgaard, 1975).

Aroma-active compounds can be broadly classified in: esters, higher alcohols, vicinal diketones, phenolic and sulfur compounds.

Each of these classes will be individually tackled in the following sections, focusing on the metabolic pathway involved in their production and the possible strain modifications which could improve their production. However, it's important to keep in mind that the strain used is just one of the many parameters that influence the concentration of aroma compounds in the final product. A strong effect is also exerted by parameters like temperature, aeration, pitching rate, raw materials used to produce the wort and by the beer maturation process (Boulton and Quain, 2008; Kucharczyk and Tuszyński, 2015.).

1.8.1 Higher alcohols

The main higher (fusel) alcohols in alcoholic beverages are propanol, butanol, isobutanol, phenylethanol and isoamyl alcohol (Dzialo et al., 2017). These compounds contribute with a desirable effect on the product flavour, imparting the characteristic alcoholic taste, a floral, rose like-fragrance (phenylethanol), and a banana, fruity flavour (isoamyl alcohol) (Etschmann et al., 2002; Harada et al., 1985). However, negative effects on the overall aroma can be detected if those compounds are present in excess (>300 mg/L) (Olaniran et al., n.d.). Their importance for the aroma composition is, in fact, also due to their absolute concentrations: the highest of the secondary metabolites (Verstrepen et al., 2003).

Table 1-1 | Main higher alcohols properties in lager beer. Reworked from Procopio et al. 2011 (Procopio et al., 2011)

HIGHER ALCOHOLS	STANDARD VALUES (PPM)	THRESHOLD LEVEL (PPM)	MAIN AMINO ACID PRECURSOR	AROMA IMPRESSION
PROPANOL	2 - 10	21	Threonine	Solvent-like, alcoholic
ISOBUTANOL	5 – 10	10 - 100	Threonine	Alcoholic
ISOAMYL ALCOHOL	30 - 50	60 – 65	Leucine	Banana, fruity flavour
PHENYL ETHANOL	6 – 44	100	Phenylalanine	Floral, rose-like

Higher alcohols are mainly produced as a result of amino acid catabolism in the Ehrlich pathway (Hazelwood et al., 2008; Saerens et al., 2008). After the uptake mediated by numerous transporters, amino acids are deaminated by an aminotransferase (BCAATases). The α-

ketoacid resulting from the transamination is first decarboxylated into an aldehyde and then reduced to produce the corresponding higher alcohol (Ehrlich and Bertheim, 1907). Additionally, higher alcohols can results from a tightly controlled anabolic pathways for the synthesis of branched chain amino acids (Saerens et al., 2008; Yuan et al., 2017) as shown in Figure 1-3.

Higher alcohols are a result of a very robust and complex pathways, due to their close link to amino acid metabolism. Several engineered strains displaying increased higher alcohol production were generated overexpressing enzyme involved in the Ehrlich pathway or increasing the flux towards amino acid productions (Park et al., 2014; Shen et al., 2016). However, there is a need for refined metabolic engineering as simple mutations often don't exert the desired effect, as the overexpression of *ARO8* (Yin et al., 2015) producing the same phenotype as its deletion (Romagnoli et al., 2015). Due to the limitations of GMO use in food & beverages and the complexity of the pathways involved, a more promising approach to increase higher alcohols could be modulating the process parameters. In fact, as higher alcohols are produced by the metabolism of amino acids, their synthesis is correlated with cell growth (Dzialo et al., 2017; Vidal et al., 2015). Thus, an increase in the nitrogen and amino acids content of the media represents a direct and effective way to increase higher alcohol titres (Lei et al., 2013; Vidal et al., 2013).

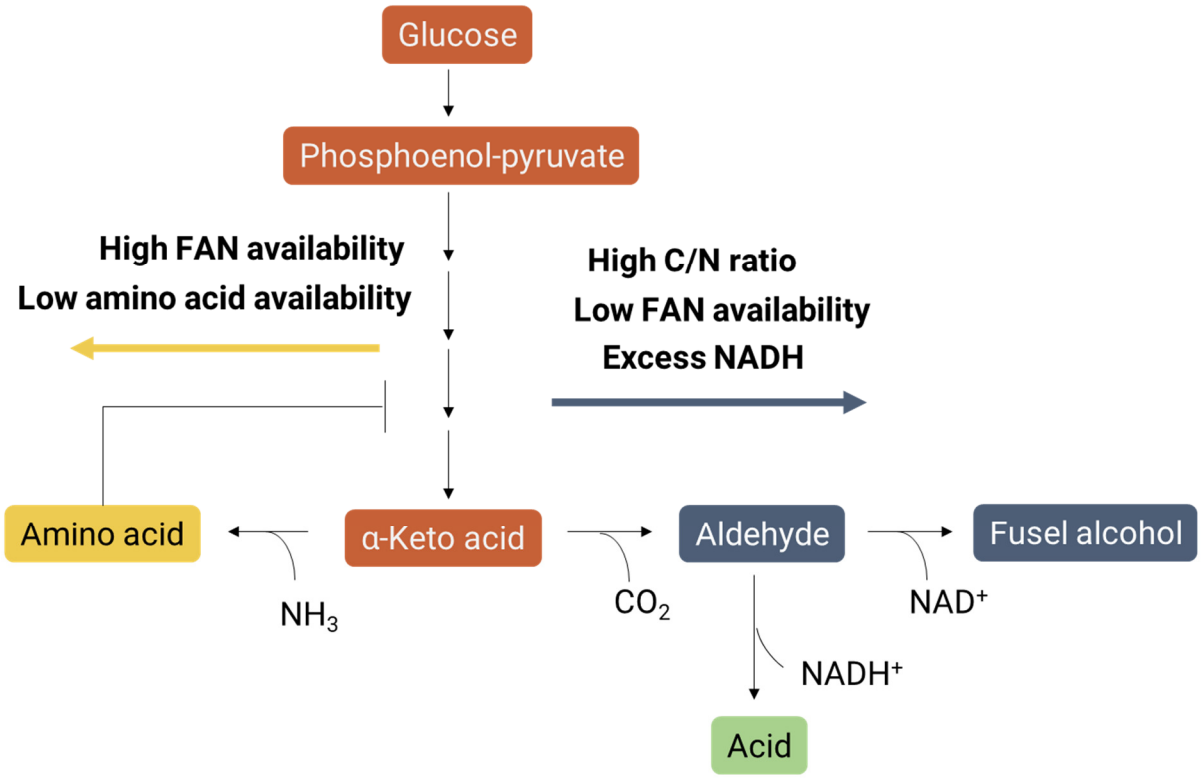

Figure 1-1 | Anabolic pathway of higher alcohol production. An α-Keto acid, derived by the glycolytic pathway or by the combination of glycolysis and the pentose-phosphate pathway can be transaminated to produce the corresponding amino acid or carboxylated to an aldehyde. The metabolic fate of the α-Keto acid is regulated by free amino nitrogen (FAN) availability, the concentration of amino acid, which regulates the pathway through a negative feedback loop, and by the carbon to nitrogen (C/N) ratio.

1.8.2 Esters

The volatile nature of esters, together with their synergistic effect, makes them one of the main contributor of the flavour and aroma of beer, even though only produced at trace levels (few parts per billion) (Lambrechts and Pretorius, 2000). With fusel alcohols, they grant a pleasant, fruity aroma to the beer in moderate quantities, but excess concentrations are considered undesirable. Esters can be classified in acetate esters and fatty acid esters: the former are produced by a condensation reaction between an alcohol and acetyl-CoA, the latter between ethanol and acyl-CoA. In the first group, the most important compounds are isoamyl acetate (pineapple, banana aroma), isobutyl acetate (fruity), ethyl acetate (solvent) and phenylethyl acetate (floral fragrance). Fatty acid esters are ethyl hexanoate (aniseed, apple) and ethyl octanoate (sour apple) (Nordström, 1966).

The condensation reaction for ester synthesis is catalysed by alcohol-O-acetyl (acyl) transferases (AATase). In *S. cerevisiae* Atf1 and Atf2 are the main enzyme responsible for the synthesis of acetate esters, while Eeb1 and Eht1 catalyse the production of ethyl esters (Cherry et al., 2012). An additional enzyme, Eat1, was recently described as able to produce ethyl acetate, via an esterase reaction (Kruis et al., 2017).

Table 1-2 | Main esters properties in lager beer. Reworked from Procopio et al., 2011.

ESTERS	STANDARD VALUES (PPM)	THRESHOLD LEVEL (PPM)	ALCOHOL PRECURSOR	ACYL-COA PRECURSOR	AROMA IMPRESSION
ETHYL ACETATE	15 - 25	21 - 30	Ethanol	Acetyl-CoA	Solvent-like
ISOAMYL ACETATE	0.5 – 1.5	1 – 1.6	Isoamyl alcohol	Acetyl-CoA	Pineapple, banana
PHENYL ETHYL ACETATE	1 - 5	3	Phenyl ethanol	Acetyl-CoA	Floral, rose-like
ETHYL HEXANOATE	0.005 – 0.3	0.14	Ethanol	Hexanoyl-CoA	Aniseed, apple
ETHYL OCTANOATE	004 – 0.053	0.17	Ethanol	Octanoyl-CoA	Sour apple

Due to the strong synergistic effect of esters and their low threshold level, a lot of effort has gone into improving their production. However, as an improved production of esters does not seem to grant any fitness advantage in yeast, it has been difficult to select for better performing strains. For this reason, the most successful approach to date consisted of engineering strains by rational design to improve the activity and expression of enzymes involved in esters production (Aritomi et al., 2004; Lilly et al., 2006, 2000).

To successfully apply adaptive evolution approaches we will need to better understand the role of ester synthesis in yeast. In fact, while it is known their role as insect semiochemicals, it is still under debate if they possess a role in yeast physiology. It has been proposed that they could have a role in the maintenance of redox balance (Malcorps and Dufour, 1992) or they could be the result of conjugation reactions of toxic medium-chain fatty acids to ease their removal (Nordström, 1964). More recently it has been hypothesized that they could be produced due to the stresses resulting in the late stages of fermentation to help maintain plasma membrane fluidity (Mason and Dufour, 2000).

The few conditions which have shown potential to improve esters production are growth with leucine and phenylalanine analogues (Fukuda et al., 2001, 1990; Oba et al., 2005) or the addition of harmful steroid like pregnenolone which favours the activity of Atf1/2 and consequently esters production (Kitagaki and Kitamoto, 2013). Recently, experimental evolutions experiments have been conducted also using compounds able to inhibit lipid synthesis for a similar effect, selecting strain which were able to relieve this repression (Takahashi et al., 2017).

1.8.3 Vicinal diketones

Another class of flavour-active compounds linked with the metabolism of amino acids is the one of vicinal diketones (VDKs). During the fermentation, a build-up of acetolactate and aceto-hydroxy-butyrate can vary due to inefficiencies in the valine and isoleucine biosynthetic pathway. These compounds are then released into the media, where they are chemically decarboxylated in VDKs, diacetyl (2,3-butanedione) and 2,3-pentanedione.

The concentration of vicinal diketones has a significant role in the production of fermented beverages. While at low quantity they grant a nutty, toasty-like aroma (Bartowsky and Henschke, 2004; Molimard and Spinnler, 1996), above their threshold level they add an undesirable buttery and rancid note to the flavour (Bartowsky and Henschke, 2004; Krogerus and Gibson, 2013a).

Diacetyl has attracted more focus from industries and the research community due to its low sensory threshold. The classic approach to decrease the concentration of this compound is to subject the beer to a maturation phase of 2-3 weeks. During this phase, diacetyl can be re-assimilated by yeast and enzymatically reduced to acetoin and 2,3-butanediol, lowering its effect on the overall aroma. However, a long maturation process can be economically taxing, lowering productivity and requiring a large amount of storage space. To overcome this problem, new promising approaches have focused on improving the metabolic flux towards the production of amino acids to consume the excess of acetolactate during the fermentation (Krogerus and Gibson, 2013b; Kusunoki and Ogata, 2012).

1.8.4 Phenolic compounds

Between the various phenolic compounds present in beer, the main flavour-active constituents are simple volatile phenols (Lentz, 2018). These compounds are generally considered as negative contributors to the aroma and are classified as off-flavours.

Phenolic compounds are produced by the decarboxylation of hydroxycinnamic acids (HCAs), which act as inhibitors of microbial growth (Klinke et al., 2004). In *S. cerevisiae*, HCAs (ferulic acid, *p*-coumaric acid and caffeic acid) are first converted in 4-vinylguaiacol (4-VG), 4-cinylphenol (4-VP) and 4-vinylcatechol (4-VC) by the synergistic activity of *PAD1* (phenyl-acrylic acid decarboxylase) and FDC1 (ferulic acid decarboxylase) (Bornscheuer, 2018; Lin et al., 2015, p. 1; Payne et al., 2015). A further reaction, catalysed by vinyl-phenol reductase, can reduce these compounds in 4-ethylguaiacol (4-EG), 4-ethylphenol (4-EP) and 4-ethylcatechol (4-VC) (Vanbeneden et al., 2008; Vanderhaegen et al., 2006).

Highly domesticated industrial yeast shows a reduced or absent ability to detoxify HCAs and are classified as POF-negative, as unable to produce phenolics off-flavours (Gallone et al., 2016). The need of a POF- phenotype in brewing yeast represents a strong limiting factor for the generations of de-novo hybrids, as wild type strains often possess functionals *PAD1* and *FDC1* genes. Thus, it is necessary to laboriously screen and select hybrid progeny for their POF- phenotype or backcross the newly generated hybrid with a POF- strain (Krogerus et al., 2017b).

1.8.5 Sulfur compounds

Volatile sulfur compounds which influence the aroma are derived from sulfate anions present in the feedstock, especially in malt. Their production is a result of the combination of the processing of raw materials and the metabolism of brewing yeast (Boulton and Quain, 2008).

Unlike other classes of flavour-active compounds, sulfur compounds do not influence the aroma in a consistent manner. Molecules like H_2S and mercaptans are generally considered off-flavours, with a rotten-egg, cabbage odour, while several thiols, like furfurylthiol, grant positive notes (Dzialo et al., 2017). The majority of the aroma-enhancing thiols in fermented beverages are derived from grape must and have a significant role only in the wine industry (Fretz et al., 2005).

In beer, sulfur compounds are generally desirable only at very low concentration (*e.g.,* DMS) and are usually described as off-flavours. Significant work has been done to reduce the level of H_2S, modulating the process parameters. It has been shown that nitrogen additions reduce the production of H_2S, as driving the flux towards amino acids production increase the cell need for sulfur assimilation (Jiranek et al., 1995; Mendes-Ferreira et al., 2004). In the same way, genetic approaches have focused on targeting genes connected with sulfur utilization (Cordente et al., 2009; Linderholm et al., 2010) and increasing its flux towards his assimilation into amino acids (Linderholm et al., 2008; Tezuka et al., 1992).

1.9 Aims & objectives

This project aims to identify the major genetic features responsible for desirable traits of commercial hybrid yeasts and generate new strains with enhanced properties relevant to the food industry, including a deeper understanding of the biological processes underlying the production of aromas compounds in fermented beverages. The results obtained in this thesis untangle the genetic complexity of the hybrid strains and present new strain and process development approaches to enhance the aroma profile. The key objectives of the project are:

(1) Investigate a possible relationship between growth rate and aroma production of *S. cerevisiae* type strain NCYC505 through continuous culturing in chemostat at different dilution rates. This study, presented in chapter 2, allowed to characterize yeast physiology during various stage of the fermentation process and shed new lights on the physiological role of aroma compounds. Moreover, the resulting data was exploited to direct new strategies to manipulate the final aroma profile of brewing fermentations through a careful modulation of yeast growth.

(2) Introduce yeast hybrids into the realm of quantitative genetics, allowing to study the genomic complexity of yeast hybrids through genome-wide studies and to exploit natural diversity to identify novel genes and pathways on industrial interest.

a. In chapter 3, I set out to screen a library of multigenerational yeast hybrids in industrial stressors to dissect the genetic basis underlying industrially relevant traits like cold- and acid-tolerance. The combination of high-throughput screening and quantitative genetics techniques allowed to select phenotypical outliers for each condition and to dissect the genetic traits underlying the phenotypic variations. Study of the QTL data from different hybrids crossing contributed greatly to untangle the complexity of yeast hybrids and to the identification of new pathways for strain development.

b. In chapter 4, a library of F12 *S. cerevisiae* x *S. kudriavzevii* hybrids was screened at sub-lethal concentrations of six different antifungal to study the role of hybridisation and natural variation in the development of antifungal resistance. Analysis of the QTL regions allowed the identification of several possible marker of resistance to fluconazole, flucytosine and micafungin which will accelerate the development of new drugs and combinational therapies.

(3) Explore the brewing potential of the recently discovered *S. jurei* and generate a new breed of *S. jurei*/*S. cerevisiae* hybrids through non-GMO techniques for potential application in the fermented beverage industry. In chapter 5, the capability of *S. jurei* strains to assimilate brewing sugars and to sustain the stressors intrinsic to the brewing process was evaluated. Moreover, spore-to-spore mating was employed to accelerate the application of new brewing strains harbouring *S. jurei* backbone in brewing. The hybrids strains were studied in lab-scale and pilot-scale fermentation and their aroma profile was extensively characterised to reveal new notes and aroma characters of great interest to the craft beer market.

Chapter 2 - Volatile aroma compound production is affected by growth rate in *S. cerevisiae*

Federico Visinoni[1], Penghan Zhang[2], Katherine Hollywood[1], Silvia Carlin[2], Urska Vrhovsek[2], James Winterburn[3], Daniela Delneri[1]

[1]*Manchester Institute of Biotechnology, University of Manchester, 131 Princess Street Manchester M1 7DN, UK*

[2]*Foundation Edmund Mach, Via Edmund Mach 1, 38010 San Michele all'Adige TN, Italy*

[3]*Department of Chemical Engineering, The University of Manchester M13 9PL, UK*

2.1 Foreword

The work in this chapter has been published in Applied and Environmental Microbiology (2022): e01509-22 and is available at doi: https://doi.org/10.1128/aem.01509-22. References used within the manuscript are presented at the end of the chapter.

Author contributions: FV, DD and JW designed the research. FV carried out the fermentation experiments and conducted the HPLC analysis of yeast exometabolome under the supervision of DD and JW. KH performed the UPLC-MS analysis for the quantification of intercellular amino acids. FV, PZ and SC performed the GC-MS analysis under the supervision of UV. FV, JW and DD wrote the manuscript with the input of PZ and KH.

2.2 Abstract

The initial growth rate of a yeast strain is a key parameter in the production of fermented beverages. Fast growth is linked with higher fermentative capacity and results in less slow and stuck fermentations, unable to reach the expected final gravity. As concentrations of metabolites are in constant state of flux, quantitative data on how growth rate affects the production of aromatic compounds becomes an important factor for brewers. Chemostats allow to set and keep a specific dilution rate throughout the fermentation and are ideal system to study the effect of growth on aroma production.

In this study, we run chemostats alongside batch and fed-batch cultures, compared volatile profiles detected at different growth rates, and identified those affected by the different feeding profiles. Specifically, we quantified six abundant aroma compounds produced in

anaerobic glucose-limited continuous cultivations of *S. cerevisiae* at different dilution rates. We found that volatile production was affected by the growth rate in four out of six compounds assayed, with higher alcohols and esters following opposite trends. Batch and fed-batch fermentations were devised to study the extent by which the final concentration of volatile compounds is influenced by glucose availability. When compared to the batch system, fed-batch fermentations, where the yeast growth was artificially limited by a slow constant release of nutrients in the media, resulted in a significant increase in concentration of higher alcohols, mirroring the results obtained in continuous fermentations. This study paves the way to further process development optimization for the production of fermented beverages.

2.3 Introduction

The invention of brewing, as fermentation of cereal sources to produce alcoholic beverages, pre-dates history and represents a hallmark of civilization (Hornsey, 2003). Brewing yeast strains underwent centuries of domestication, being improved for growth and aroma profile through spontaneous mutations and selection. However, while the scientific literature on the brewer's yeast, *S. cerevisiae*, is extensive and detailed, little is known of the effect that cellular growth has on the most abundant aroma compounds and on the biosynthetic mechanisms which regulate their production. Amongst the broad and diverse range of compounds responsible for the complex aroma and taste of fermented beverages, the main yeast-derived contributors to the flavour of aroma and beer are higher alcohols and esters (Lambrechts and Pretorius, 2000). These compounds give a pleasant, often fruity aroma to the beer when present in moderate quantities and are closely connected to the yeast's main metabolism, being produced as secondary metabolites in trace quantities (Verstrepen et al., 2003b).

Higher alcohols are produced as a result of amino acid metabolism in the Ehrlich pathway through the catabolism of amino acids or through an anabolic route from pyruvate (Hazelwood et al., 2008). Esters are produced by a condensation reaction between an alcohol and acetyl-CoA (acetate esters), or between ethanol and acyl-CoA (fatty acid esters) (Nordström, 1966). Due to the high concentrations of higher alcohols reached in the fermentation process and the low odour threshold level of esters, a lot of effort has gone into improving their production through synthetic biology approaches (Aritomi et al., 2004; Lilly et al., 2006, 2000). However, to successfully apply adaptive evolution approaches and fine-

tune their production, the impact of cell physiology on the synthesis of higher alcohols and esters must be understood.

Researchers must also face the complexity of the fermentation process, as brewing is generally conducted as a batch process where both the fermentation parameters and the concentrations of metabolites are in constant state of flux (Boulton and Quain, 2008). The process is also carried out without agitation and in conditions of transient aerobiosis as the fermentation starts with a pulse of oxygen which favours the production of unsaturated fatty acids and sterols (David and Kirsop, 1972). For these reasons, the fermentation step is characterized by an accentuated unsteady state, in which yeast physiology cannot be followed nor easily described (Boulton and Quain, 2008; Vázquez-Lima et al., 2014). Nonetheless, to develop new rational approaches for the optimization of fermentation processes it is necessary to understand how the ever-changing cell physiological state may affect and regulate production of aroma compounds.

Thus, it is of foremost importance to follow the fermentation process in a controlled environment where the agents contributing to shaping the aroma profile can be singled out and studied. A key tool in achieving this is the chemostat, a bioreactor in which cells grow continuously in a fixed volume, thanks to continuous addition of medium and removal of an equivalent volume culture. In fact, eventually, these systems are able to reach a condition of equilibrium, or steady state, in which the growth rate of the cells and the dilution rate are equal and constant and metabolite concentrations are stable over time (Monod, 1949; Novick and Szilard, 1950).

Several studies have been carried out to describe the metabolic fluxes of *S. cerevisiae* strains in anaerobic, glucose limited continuous cultures at different dilution rates (Nissen et al., 1997; Verduyn et al., 1990). However, the scope of these studies was limited to the characterization of yeast core metabolism and not of the secondary pathways responsible for the production of volatile compounds. More recently, classic continuous fermentations have been conducted to study the effect of oxygenation, temperature and nitrogen sources on the aroma profile (Aceituno et al., 2012; Boer et al., 2007; Pizarro et al., 2008). However, no quantitative data on how specific growth rate affects aroma profile in glucose limited fermentations is currently available in the literature.

In this study, the link between yeast growth rate and aroma compound production is elucidated, by characterizing the production of the most abundant higher alcohols and esters

in continuous culture at different dilution rates in a *S. cerevisiae* type strain (NCYC 505). The results obtained from the chemostat cultures were subsequently used to devise feeding strategies to modulate the production of both higher alcohols and esters (Figure 2-1).

Our study show that the production of volatile compounds can be enhanced and manipulated to yield different and improved aroma profiles via the implementation of feeding profiles. Moreover, these results will help defining synthetic and experimental evolution approaches to generate strains able to produce higher titres of desired volatile compounds in both wine and beer fermentations.

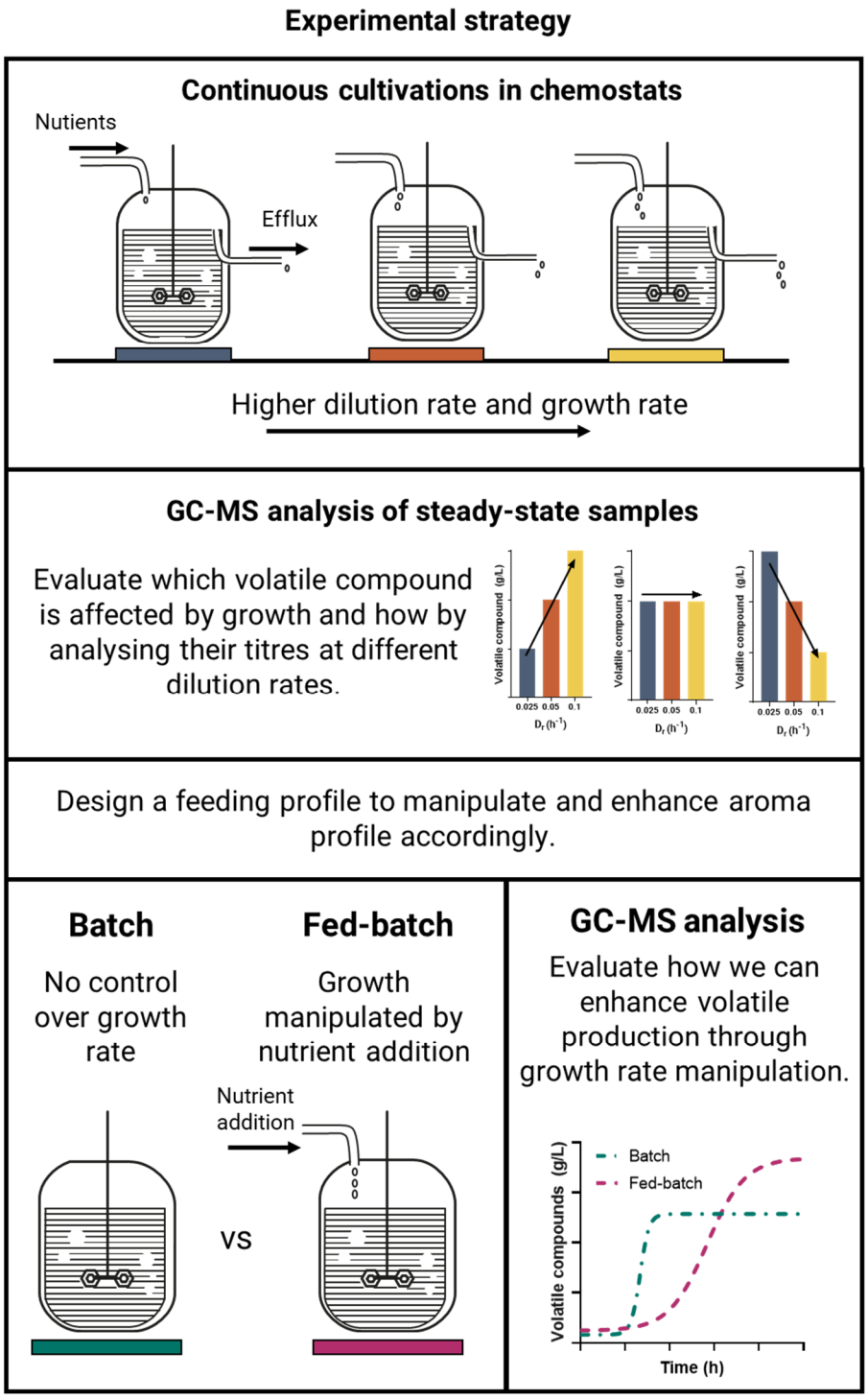

Figure 2-1 | Experimental strategy. Continuous cultivations in chemostats will be employed to single out the effect yeast growth rate could have on the production of volatile compounds. The resulting GC-MS data from steady state samples at different dilution rates will be used to design a feeding profile to enhance the production of selected aroma compounds by artificially manipulating growth rate through nutrients additions.

2.4 Results and discussion

2.4.1 Metabolic characterization of NCYC 505 in continuous carbon-limited cultures

To single out the effect exerted by the growth rate on the production of aroma compounds continuous cultivations in glucose limited chemostats were performed, as described in Methods. The cultures were initially grown in batch mode, until 50 hours when the continuous culture was activated with a constant feed of YNB + 2% glucose at different dilution rates (D_r): 0.025, 0.05, and 0.1 h^{-1}

We found that the biomass decreased linearly with increased dilution rate, an effect likely due the uncoupling between anabolism and catabolism under substrate sufficient conditions (Liu, 1998; Verduyn et al., 1990). Efflux samples at the steady state for the cultures grown at 0.025 and 0.05 h^{-1} D_r showed little to no glucose in the medium, whilst at 0.1 h^{-1} D_r, 7.1 g/L of residual glucose was detected. Nonetheless, no washout or decrease in biomass was registered during the 200 hours of fermentation.

HPLC analysis of the main exometabolites is consistent with the aforementioned work of Nissen and Verduyn (Nissen et al., 1997). Ethanol concentrations decreased with increasing growth rate, while its productivity and specific concentration (calculated as g/(L·OD_{600})) increased at higher dilution rates as a result of the increased availability of carbon source (Table 2-1, Figure 2-2). Similarly, a positive correlation between growth rate and glycerol production was observed, which can be easily attributed to its vital role in balancing the NADH used in anabolic reactions in anaerobic conditions (Nissen et al., 1997; Verduyn et al., 1990). Moreover, at the highest dilution rate tested, a significant increase in the concentration of acetic acid was registered, produced at higher rates than previously described (Nissen et al., 1997) (Figure. 1). As residual glucose was detected in the medium at 0.1 h^{-1} D_r, it is likely that acetic acid production is an effect of overflow metabolism similarly to what has been reported in other species (de Groot et al., 2020; Majewski and Domach, 1990; Stöckmann et al., 2003).

Table 2-1 | Biomass, specific and volumetric concentrations of exometabolites and yield on substrate of NYCY 505 at different dilution rates. Yield is represented by the ratio between Qp, specific productivity (metabolite concentration (g/L) · flow rate (L/h) / volume (L)), and Qs, specific substrate uptake rate (substrate feed concentration (g/L) · flow rate (L/h) / volume (L)

		Ethanol				**Glycerol**				**Acetic Acid**			
D_r	OD_{600}	g/L	g/(L·OD)	g/(L·h)	Qp/Qs	g/L	g/(L·OD)	g/(L·h)	Qp/Qs	g/L	g/(L·OD)	g/(L·h)	Qp/Qs
0.025	7.2	8.37	1.16	0.21	0.42	0.46	0.06	0.01	0.02	0.07	0.01	0.00	0.00
0.05	5.4	7.15	1.32	0.36	0.36	0.81	0.15	0.04	0.04	0.08	0.01	0.00	0.00
0.1	2.4	5.24	2.18	0.52	0.43	0.83	0.35	0.08	0.07	1.42	0.59	0.14	0.12

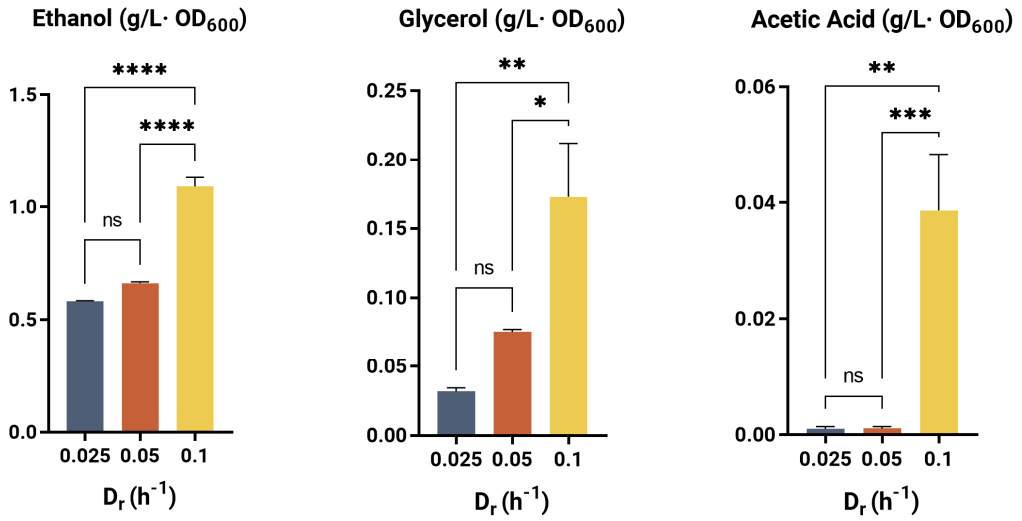

Figure 2-2 | Effect of growth rate on metabolite production of NYCY 505 in synthetic medium. Specific concentrations of ethanol, glycerol, and acetic acid were measured by HPLC from steady-state samples of chemostats at different dilution rates and normalized by cell density as described Materials & Methods. Error bars represent the standard deviation of the mean of 3 consecutive steady-state samples of independent technical replicates. Statistical tests between sets were analysed using ANOVA with * $p < 0.05$ ** $p < 0.01$ *** $p < 0.001$ **** $p < 0.0001$; ns =no significant change.

2.4.2 Production of volatile compounds by NCYC 505 is affected by growth rate

The efflux samples of steady state chemostats operated at different dilution rates were assayed through SPME GC-MS for the most abundant volatile compounds present in alcoholic beverages. To be able to establish a clear, reproducible, and unambiguous correlation between growth rate and aroma compound production, a standard synthetic medium (YNB) was utilized. Six compounds, belonging to three different classes; aldehydes, esters, and higher alcohols, and relevant to the beverage industry, were successfully semi-quantified. The analysis was complicated by the low levels of aroma compounds produced in synthetic media and by their constant removal due to nature of the continuous system. However, these conditions are necessary to establish a clear and unambiguous correlation between growth rate and aroma compound production.

Acetaldehyde is the most abundant aldehyde in beer (Adams et al., 2000) contributing a pleasant, fruity aroma at concentrations lower than its odour threshold (10ug/g)

(Meilgaard, 1993). In continuous fermentations, the specific acetaldehyde concentration followed the trend observed for acetic acid, its oxidation product (Figure 2-3). In fact, a spike in acetaldehyde production at 0.1 h^{-1} D_r was observed, which can be ascribed to an effect of overflow metabolism and an oversaturated flux towards ethanol fermentation.

Ester production was similarly affected by the growth rate. There is a positive linear correlation between growth rate and ethyl octanoate production, the most abundant ethyl ester in conventional brewing fermentations (Procopio et al., 2011). Moreover, an increase in the specific concentration of ethyl hexanoate was recorded from 0.25 to 0.1 h^{-1} D_r (Figure 2-3). The findings confirm the link between ester production and yeast growth suggested by Saerens at al. (Saerens et al., 2008), who reported an increasing production of ethyl esters during the log phase, which decreased gradually after the consumption of 70% of the sugar content. Moreover, as ethyl ester formation is dependent on the concentration of its precursors, ethanol and acyl-CoA, the result is consistent with the higher specific concentration of ethanol detected at increasing dilution rate.

Higher alcohols production, conversely, mainly decreased with dilution rate with both isobutanol and isoamyl alcohol exhibiting a clear downward trend, while phenylethyl alcohol specific concentrations remained stable across the different dilution rates (Figure 2-3).

These results confirm the association between production of higher alcohols and cell growth, which has already been formulated in literature (Dzialo et al., 2017; Vidal et al., 2015), as higher alcohol production results from amino acid metabolism via the Ehrlich pathway. Here, however, it is shown that higher alcohol production is also dependant on the physiological state of the cell, and that it is enhanced when the growth rate is severely limited by the carbon source. The observed trend of higher alcohol production is opposite to that of glycerol at higher dilution rates. Thus, while higher alcohols are thought to have a possible role in the maintenance of the redox balance (Quain, 1985), in the *S. cerevisiae* strain NCYC 505, glycerol production seems to be the preferred and predominant pathway to regenerate NAD^+.

Previous work mainly focused on the modulation of higher alcohol levels through an increase in the nitrogen and amino acid content in the medium (Lei et al., 2013; Vidal

et al., 2013). However, these results suggest a modulation of the carbon source by the use of a defined feed profile could improve their titres, similar to the processes for the production of amino acids (D'Este et al., 2018; El-Dalatony et al., 2019).

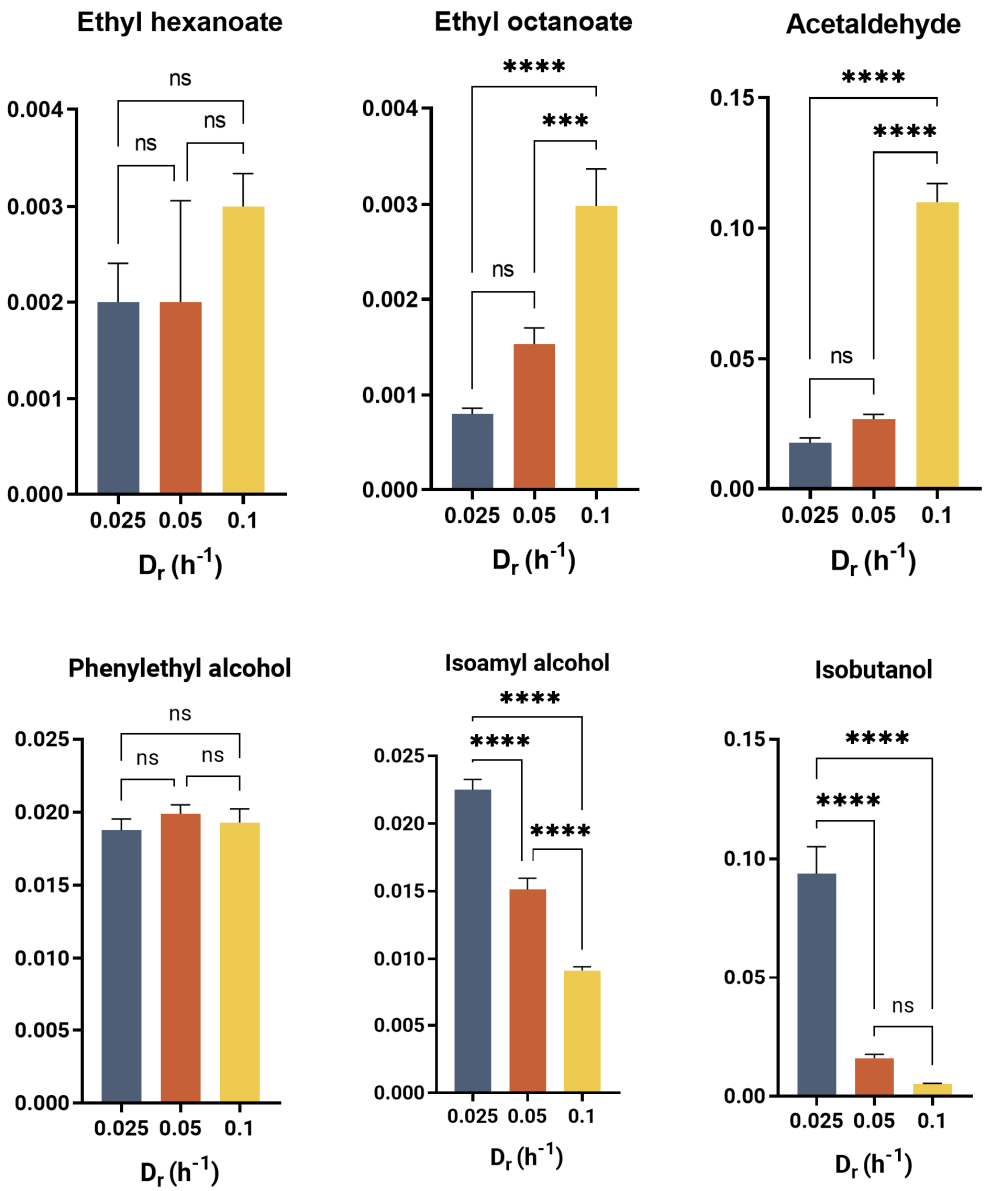

Figure 2-3 | Volatile compounds production is greatly affected by growth rate in chemostats cultivation of NYCY 505 in synthetic media. Semi quantification measurement of volatile compounds were obtained through GC-MS-SPME. Error bars represent the standard deviation of the mean of 3 consecutive steady-state samples of independent technical replicates. Statistical tests between sets were analysed using ANOVA with * $p < 0.05$ ** $p < 0.01$ *** $p < 0.001$ **** $p < 0.0001$; ns =no significant change.

The anabolic pathway leading to higher alcohol production is regulated by the availability of their respective amino acid precursor. Thus, the intracellular levels of phenylalanine, leucine and valine were quantified, being the precursors of phenylethyl alcohol, isoamyl alcohol and isobutanol, respectively. Leucine and valine showed a significant decrease in their specific concentration at 0.05 and 0.1 h^{-1} D_r (Figure 2-4), consistent with the downward trend in the production of their respective higher alcohols observed at high dilution rate. Phenylalanine showed no significant difference in intracellular levels between the chemostats operated at 0.025 and 0.05 0.1 h^{-1} D_r. However, the decrease recorded at 0.1 h^{-1} D_r, while comparable with the one observed in leucine and valine levels, did not impact the specific concentrations of phenylethyl alcohol produced. Thus, the decreasing availability of intracellular amino acids may not be the only factor in play in the regulation of this pathway at different dilution rates.

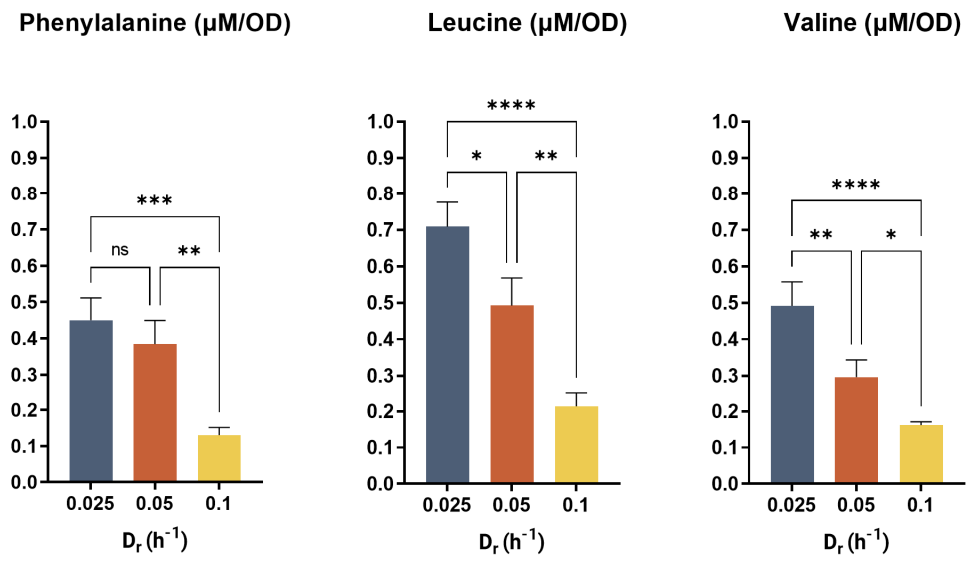

Figure 2-4 | Intracellular amino acid specific concentrations. Quantification of intracellular amino acids was obtained through LC-MS/MS. Error bars represent the standard deviation of the mean of 3 consecutive steady-state samples of independent technical replicates. Statistical tests between sets were analysed using ANOVA with * $p < 0.05$ ** $p < 0.01$ *** $p < 0.001$ **** $p < 0.0001$; ns =no significant change.

2.4.3 Controlled feeding profiles can be used to modulate the production of aroma compounds in conventional fermentations

To evaluate the effect of growth rate in the production of aroma compounds in conventional fermentations, the concentrations of selected compounds were assayed at different timepoints in batch and fed-batch experiments (Figure 2-1). NCYC 505 was grown in batch in two-fold YNB (13.4 g/L) + 4% glucose at 20°C and in fed batch where the starting nutrient concentrations were halved compared to the batch and the remaining nutrients were fed at a constant flow over the course of 20h after 48h. Thus, the growth in the fed-batch experiment was artificially limited after 48h, to replicate a lower growth rate. Profiles of growth, glucose consumption and ethanol productions are shown in Figure 2-5. Interestingly, no significant difference in ethanol and glycerol concentrations were found at the end of fermentations, with their concentration increasing linearly with glucose consumed. End-point fermentation samples were obtained after 76h of fermentation, after glucose was depleted in both batch and fed-batch fermentations, and after 146h. The end-point fermentation samples were assayed through SPME-GC-MS for esters and higher alcohol concentrations to evaluate their production profile and final titres (Figure 2-6)

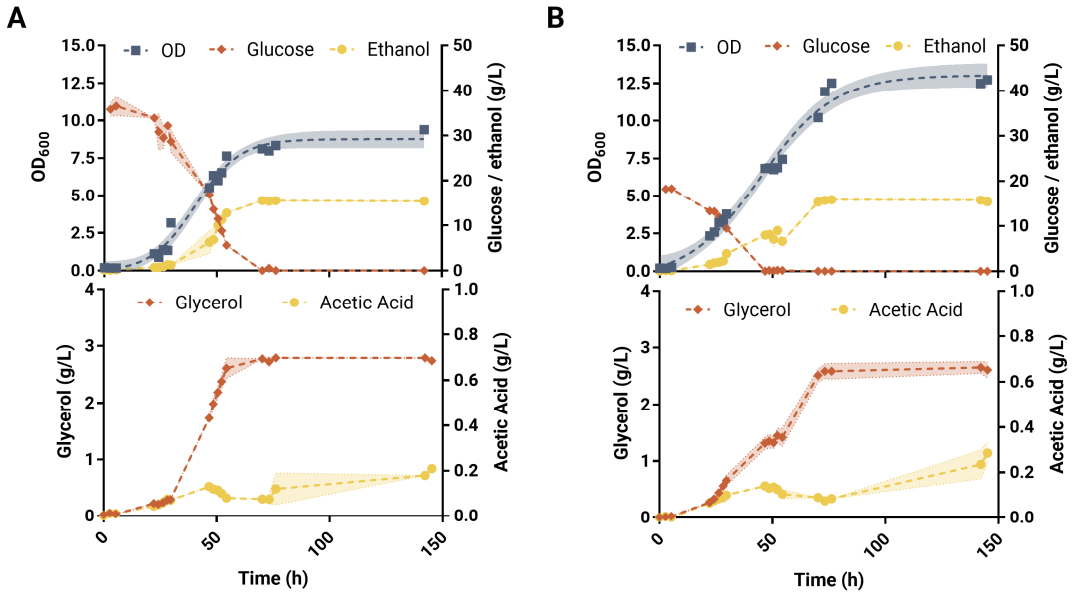

Figure 2-5 | Profile of growth, glucose consumption and ethanol, glycerol, and acetic acid production in batch (A) and fed batch (B) fermentation of NCYC505 at 20°C. Standard deviation of two biological replicates is shown in lighter shades in the lines connecting each sample.

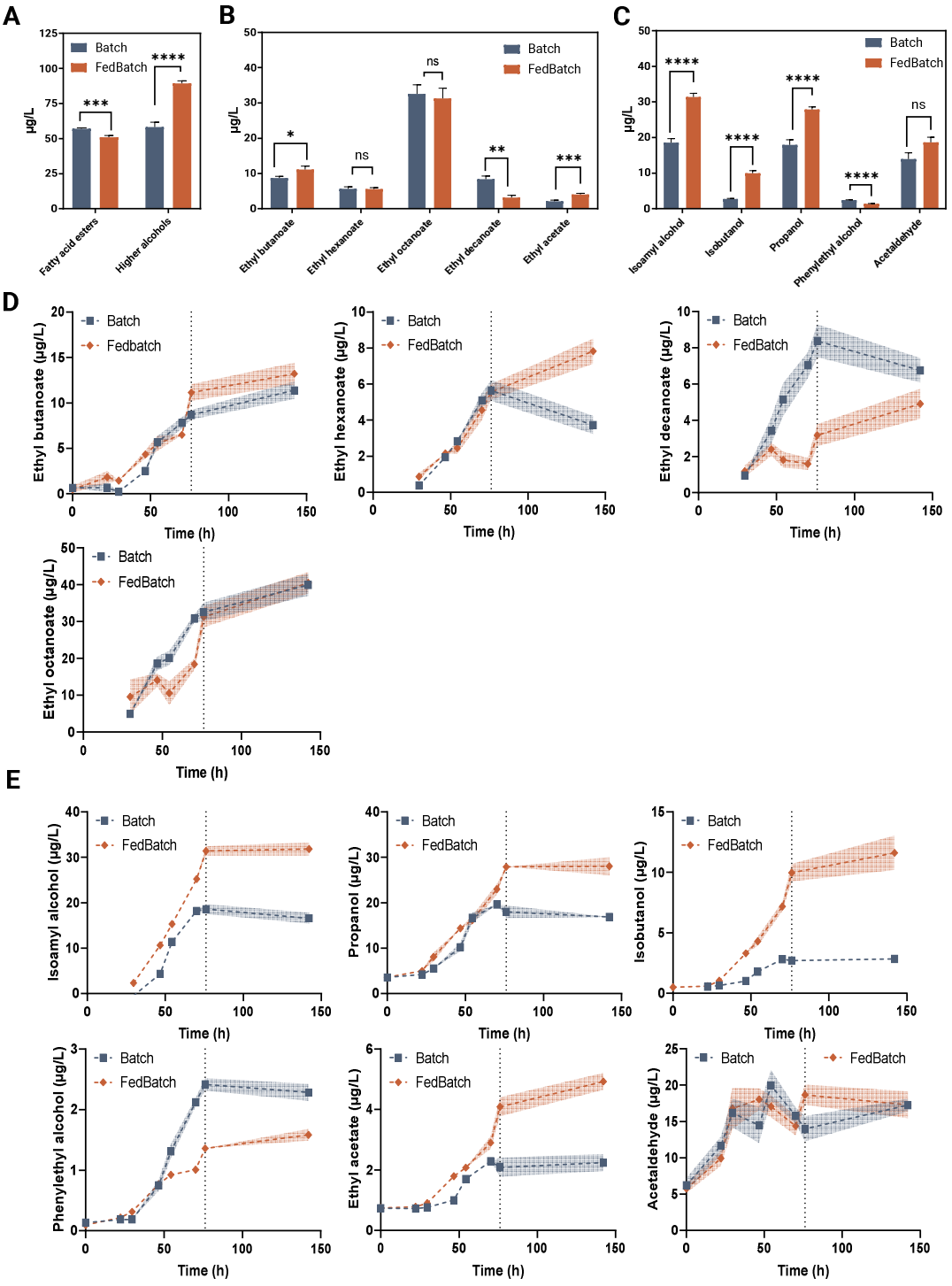

Figure 2-6 | A controlled feeding profile can modulate the production of volatile compounds. (A) Cumulative concentrations of the detected fatty acid esters (ethyl butanoate, hexanoate, octanoate, caprinate) and higher alcohols (isoamyl alcohol, isobutanol, propanol, phenylethyl alcohol). (B) Quantitative measurement of esters, and (C) higher alcohols and acetaldehyde were obtained through GC-MS-SPME after 76h of fermentation in batch and fed batch. Error bars represent the

standard error of biological replicates. Statistical tests between sets were analysed using t-test with * $p < 0.05$ ** $p < 0.01$ *** $p < 0.001$ **** $p < 0.0001$; ns =no significant change (D, E). Production kinetics of fatty acid esters, higher alcohols, ethyl acetate and acetaldehyde in batch and fed-batch fermentations. Standard deviation of two biological replicates is shown in lighter shades in the lines connecting each sample. A vertical dashed line represents the timepoint when glucose was depleted in both batch and fed-batch fermentations, after 76 hours.

Thanks to the higher concentrations reached in the end-point samples compared to the chemostat fermentations, it was possible to increase the number of volatile compounds assayed with five esters (ethyl butanoate, ethyl hexanoate, ethyl octanoate, ethyl decanoate and ethyl acetate), four higher alcohols (isoamyl alcohol, isobutanol, propanol and phenylethyl alcohol), and acetaldehyde being quantified (Figure 2-6A, B, C). Moreover, the concentrations of these compounds were determined throughout the course of the fermentation to highlight the active phases of production (Figure 2-6D, E). The production of seven out of ten volatile compounds were found to be modulated by the feeding profile. The batch experiment reached a higher concentration of fatty acid esters and significantly lower titres of higher alcohols, confirming the general trends observed in chemostat (Figure 2-6A).

However, no significant difference was observed in the production of ethyl hexanoate and ethyl octanoate concentrations between the two experiments after 76h, which in chemostat experiments resulted enhanced by growth rate. Conversely, ethyl butanoate titres slightly increased in fed-batch by 2.45 µg/L, while ethyl decanoate production was almost tripled in batch. These results suggest that high growth and sugar concentrations mainly stimulate the production of esters derived from longer-chain fatty acids, as in the case of ethyl decanoate.

The prolonged period of growth in the fed-batch fermentation resulted in higher levels of ethyl acetate, an acetate ester produced by a condensation reaction between acetyl-CoA and ethanol (Dzialo et al., 2017) (Figure 2-6B). Production profile of ethyl acetate followed the one observed for ethanol in both experiments. Thus, the ethanol fermentation over the course of the entire 76h in the fed-batch might have resulted in higher concentrations of ethyl acetate, compared to the batch. Acetaldehyde titres increased the most in the first 30 hours of fermentation, both in batch and fed-batch (Figure 2-6E). The concentration remained mostly stable during the course of the

fermentation. As a result, the final concentration of acetaldehyde did not differ between batch and fed-batch fermentations (Figure 2-6C).

Consistent with the results observed in chemostat fermentations, a 60% increase in the levels of total higher alcohols was recorded in fed-batch fermentation, where the lower availability of glucose resulted in fewer hours of sustained specific growth rate compared to the batch (Figure 2-6C). In particular, the feeding protocol in fed-batch resulted in a 2.5-fold increase in the levels of propanol, and over 50% higher titres of isoamyl alcohol and isobutanol (Figure 2-6C). Phenylethyl alcohol levels resulted higher in batch as its production was greatly reduced in the second phase of the fed-batch fermentation (Figure 2-6E). In the initial stages of the fermentation, the yield on glucose of phenylethyl alcohol was similar in both experiments (0.49 μg/g in batch and 0.47 μg/g in fed-batch). However, the yield in the fed-batch decreased dramatically to 0.22 μg/g when new nutrients were drip-fed into the media while the batch reached a final yield 0.60 μg/g. Thus, we propose that phenylethyl alcohol production in NCYC 505 might be enhanced when nutrients levels in the media are in excess, and decrease when nutrients become limiting, as observed in fed-batch fermentations.

Lower levels of higher alcohol were reported to be a cause of unbalanced flavour profile higher in high-gravity brewing, characterised by high starting sugar concentrations (He et al., 2014; Verstrepen et al., 2003a). Moreover, our results suggest that the final titres of higher alcohols could be effectively modulated through the use of fed batch fermentations, moving the focus from strain development to process optimisation. In fact, classical experimental evolution methodologies, which tends to select for high-growth strains, may result in an unbalanced flavour profile with higher concentrations of esters and a decreased amount of higher alcohols. In chemostats we observed that the concentrations of isobutanol and isoamyl alcohol were closely linked with one of their intracellular amino acid precursors. Thus, evolution experiments in media with high carbon to nitrogen ratio, without amino acids, might enhance the anabolic route of the Ehrlich pathway and lead to an increase in the production of higher alcohols.

2.5 Conclusions

The incredible recent growth of the craft beer market has fuelled the need to develop new beverages catering to the consumer need for a wider choice of flavours and beer styles. While synthetic biology approaches helped identify and modulate the pathways responsible for aroma compound production, the limitations in the use of genetically modified organisms in food and beverages has restricted these applications. Recent developments in the field of yeast hybridisation have helped develop new strains able to produce new and complex aroma profiles (Giannakou et al., 2021; Krogerus et al., 2017; Pérez et al., 2022).

However, little is known about the interplay between physiology and volatile compound production in yeast, and this is hindering evolution experiments. Thus, it is of foremost important to dissect the pathways connected with aroma profile and understand how they can be manipulated to enhance the aroma profile of fermented beverages. In this study, a potential link between the production of aroma compounds and growth rate was investigated in the *Saccharomyces cerevisiae* type strain NCYC 505. Continuous fermentation experiments in anaerobic conditions at different dilution rates allowed unambiguous correlation of yeast growth rate with the production of four out of the six volatile compounds assayed. In particular, ethyl octanoate and acetaldehyde levels increased with growth rate while the synthesis of two higher alcohols, propanol and isoamyl alcohol, was found to be inversely correlated with growth. The enhanced production of higher alcohols was also found to be directly correlated with the intracellular levels of their respective amino acid precursor, which were more abundant at lower dilution rates. Moreover, higher alcohols were found to play little to no role in redox balance at high dilution rate, with glycerol synthesis being the preferred pathway to regenerate NADH used in anabolic reactions. The continuous fermentation experiment confirmed esters and higher alcohols as tightly linked with cell metabolism and suggest that their metabolism is influenced by the physiological state of the cell. Thus, modulation of the nutrient availability might be an important tool for exerting control on the final aroma profile of a fermented product.

Guided by these results, fermentation experiments in batch and fed-batch were devised to investigate the extent the aroma profile could be manipulated by limiting nutrients availability. The concentrations of seven out of ten volatile compounds

detected were found to be significantly different in the end-point sample of the fermentations. In particular, higher alcohols levels increased by 60% in fed-batch fermentations where yeast growth was limited by nutrients availability, with propanol increasing 2.5-fold over batch levels, while ethyl decanoate concentrations tripled in batch fermentation. Thus, the newly described link between growth rate and aroma compound production was successfully exploited to increase the titres of higher alcohol in NCYC 505 and carefully modulate its aroma profile through rational design of the fermentation process. The implementation of feeding profiles to artificially regulate growth will be an important tool to cater to consumer needs and generate new fermented beverages harbouring new and varied aroma profiles.

2.6 Materials and Methods

2.6.1 Strain and media

All experiments were performed with the industrial yeast *S. cerevisiae* type strain NCYC 505 purchased from the National Collection of Yeast Cultures (NCYC). The yeast was maintained on YPD agar (agar 15 g/L, yeast extract 10 g/L, peptone 20 g/L, glucose 20 g/L). Precultures were grown overnight in shake flask cultures on 50 ml YPD (yeast extract 10 g/L, peptone 20 g/L, glucose 20 g/L) at 30°C. Biomass was recorded via optical density measurement at 600 nm with a spectrophotometer (BioSpectrometer, Eppendorf).

2.6.2 Bioreactor fermentations

1L stirred tank bioreactors (Multifors, Infors-HT) were used to perform all fermentation experiments. A washed overnight culture was used to inoculate the fermentors at an initial OD_{600} of 0.1. Cells were grown in 500 mL of YNB without amino acids and with ammonium sulfate with glucose as the carbon source. Temperature was controlled at 20°C and agitation set at 300 rpm. pH was adjusted by the addition of 2M sodium hydroxide (NaOH) to maintain a constant value of 5. An influx of oxygen was maintained for 5 min to saturate the vessel with air, prior the start of the fermentation. After inoculation, oxygenation was set to 0%. Aliquots were collected at different time intervals for optical measurements reading. The samples were then centrifuged (13,000 g for 5 minutes) and stored at 20°C for further analysis.

Batch fermentations were performed in two-fold YNB (13.4 g/L) + 4% glucose at 20°C. Fed-batch fermentations were performed as described above in 500 ml of YNB (6.7 g/L) + 2% glucose. After 48 h, 25 ml of 40% glucose (w/v) and YNB 20x (134 g/L) were fed at a constant flow of 1.25 ml/·h for 20 h until the fermentation was reverted to a batch.

2.6.3 Continuous fermentations

For chemostats, the fermentation was started as described above in 500 ml of 6.7 g/L of YNB + 2% glucose. The process was conducted in batch for the first 36h, and then maintained in continuous for 10 days. A constant feed of fresh batch media was pumped in the fermenter at different dilution rates (Dr = 0.025, 0.05, 0.1 h^{-1}) with a peristaltic pump (Infors-HT). The efflux was removed through a sampling tube connected to a peristaltic pump in order to keep the volume constant. The steady state was defined as the situation in which at least a volume change had passed after the last change in OD_{600} measured and where the measured ethanol and glycerol concentrations were constant.

2.6.4 HPLC analysis

The concentration of metabolites (glucose, glycerol, acetic acid, and ethanol) was measured by HPLC using a 1260 Infinity II LC System with a Refractive Index Detector (Agilent). A 300x7.8 mm Hi-Plex HPLC Column (Agilent) was equilibrated with 5 mM H_2SO_4 in HPLC grade water at 55° at a 0.8 mL/min flow rate. Compounds were identified by retention times and quantified using calibration curves generated from authentic standards. For chemostat efflux samples the concentration is expressed as specific concentration, calculated dividing the concentration in g/L by the OD_{600} value for each timepoint.

2.6.5 Aroma compound analysis

Volatile compounds were detected and analyzed by using a Thermo Scientific TSQ Quantum GC Triple Quadropole GC-MS. 0.5 ml of sample were prepared in a 20 ml vial added with 25 µl of the internal standard 2-octanol (2.5 mg/L) and 0.5 g of NaCl. The samples were incubated for 10 min at 40°C. The volatile compounds were collected on a Divinylbenzene–Carboxen- Polydimethylsiloxane 2 cm fiber (DVB-CAR-PDMS Supelco) for an extraction time of 30 min. A VF-wax column (Agilent) 30 m/I.D 0.25 mm/Film 0.25 µm was used for the separation.

The oven was kept at 40 °C for 4 min then increased by 6 °C/min to 250 °C and kept at the final temperature for 5 min. The injector and interface temperatures were kept at 250 °C as well. Helium was used as the carrier gas with a flow rate of 1.2 ml/min. The time for thermal desorption of analytes was 4 min. The MS detector was operated in full scan mode at 70 eV with a scan range from 40 to 300 m/z for 44 min.

Data analysis was performed using the software ThermoXcalibur (Version 2.2 SP1.48, Thermo scientific). Chromatogram peak annotation was based on the retention time of the reference standard and comparison with a mass spectral database (NIST version 2.0). The absolute concentration of the compound in the sample was calculated with calibration curves generated from pure reference standards. Measurement bias was corrected with the internal standard.

2.6.6 Amino acid analysis

Intracellular amino acids were extracted as described in Gent and Slaugther (1998) (Gent and Slaughter, 1998). LC-MS/MS analysis was conducted using an ultra-performance liquid chromatography system (Waters Acquity UPLC H-class) coupled to a Xevo TQ-S triple-quadrupole mass spectrometer (Waters Corporation, MA, USA) equipped with an electrospray ionization source (ESI). The desolvation gas flow rate was set to 300L/h at a temperature of 600 °C. The cone gas flow rate was fixed at 150 L/h and the source temperature at 150 °C. The source offset was set to 50 V. The capillary voltage was optimized at 1.5 kV for negative mode (ESI-). The following compounds were monitored in ESI- mode as follows; Valine (SIR of mass 116.07, 0.2-1.2 min); Leucine/Isoleucine (SIR of mass 130.09, 0.75-1.4 min); Phenylalanine (MRM 164.07->146.60, 2.0-3.0 min). MassLynx v 4.1 (Waters) software was used to process the quantitative data obtained from calibration standards and from diluted samples. The mobile phases, columns, column temperature and gradient programs were set based on the specific chemical properties of the target analytes. A Waters Acquity BEH C18 column (50 mm x 2.1 mm, 1.7 µm) was used at 45 °C, flow rate 0.3 mL/min. An optimum separation gradient was obtained with a binary mobile phase A (H_2O + 0.1% Formic Acid) and B (Acetonitrile +0.1% Formic Acid). The gradient elution program was: 0- 1.2 min at 100% A; 1.2 -2.5 min to 90% A, hold at 90% A for 2.5 min; reduce to 5% A over 0.5 min, hold for 0.5 min before returning to 100% A for 1 min. The total run time was 7 min. The inject volume was 5 µL.

2.7 Acknowledgments

This work was supported by the European Commission (H2020-MSCA-ITN-2017) grant number 764364 awarded to DD and UV. The authors would also like to acknowledge the support received from the Manchester Institute of Biotechnology analytical facility for the HPLC analysis and the helpful discussions with Claire Lin Lin on amino acids quantification.

2.8 Bibliography

Aceituno, F.F., Orellana, M., Torres, J., Mendoza, S., Slater, A.W., Melo, F., Agosin, E., 2012. Oxygen Response of the Wine Yeast Saccharomyces cerevisiae EC1118 Grown under Carbon-Sufficient, Nitrogen-Limited Enological Conditions. Appl Environ Microbiol 78, 8340–8352. https://doi.org/10.1128/AEM.02305-12

Adams, M.R., Moss, M. O., Moss, Maurice O., 2000. Food Microbiology. Royal Society of Chemistry.

Aritomi, K., Hirosawa, I., Hoshida, H., Shiigi, M., Nishizawa, Y., Kashiwagi, S., Akada, R., 2004. Self-cloning yeast strains containing novel FAS2 mutations produce a higher amount of ethyl caproate in Japanese sake. Biosci. Biotechnol. Biochem. 68, 206–214.

Boer, V.M., Tai, S.L., Vuralhan, Z., Arifin, Y., Walsh, M.C., Piper, M.D.W., de Winde, J.H., Pronk, J.T., Daran, J.-M., 2007. Transcriptional responses of Saccharomyces cerevisiae to preferred and nonpreferred nitrogen sources in glucose-limited chemostat cultures. FEMS Yeast Res. 7, 604–620. https://doi.org/10.1111/j.1567-1364.2007.00220.x

Boulton, C., Quain, D., 2008. Brewing Yeast and Fermentation. John Wiley & Sons.

David, M.H., Kirsop, B.H., 1972. The Varied Response of Brewing Yeasts to Oxygen and Sterol Treatment. Proceedings. Annual meeting - American Society of Brewing Chemists 30, 14–16. https://doi.org/10.1080/00960845.1972.12005950

de Groot, D.H., Lischke, J., Muolo, R., Planqué, R., Bruggeman, F.J., Teusink, B., 2020. The common message of constraint-based optimization approaches: overflow metabolism is caused by two growth-limiting constraints. Cell. Mol. Life Sci. 77, 441–453. https://doi.org/10.1007/s00018-019-03380-2

D'Este, M., Alvarado-Morales, M., Angelidaki, I., 2018. Amino acids production focusing on fermentation technologies – A review. Biotechnology Advances 36, 14–25. https://doi.org/10.1016/j.biotechadv.2017.09.001

Dzialo, M.C., Park, R., Steensels, J., Lievens, B., Verstrepen, K.J., 2017. Physiology, ecology and industrial applications of aroma formation in yeast. FEMS Microbiol Rev 41, S95–S128. https://doi.org/10.1093/femsre/fux031

El-Dalatony, M.M., Saha, S., Govindwar, S.P., Abou-Shanab, R.A.I., Jeon, B.-H., 2019. Biological Conversion of Amino Acids to Higher Alcohols. Trends in Biotechnology 37, 855–869. https://doi.org/10.1016/j.tibtech.2019.01.011

Gent, Slaughter, 1998. Intracellular distribution of amino acids in an slp1 vacuole-deficient mutant of the yeast Saccharomyces cerevisiae. J Appl Microbiol 84, 752–758. https://doi.org/10.1046/j.1365-2672.1998.00406.x

Giannakou, K., Visinoni, F., Zhang, P., Nathoo, N., Jones, P., Cotterrell, M., Vrhovsek, U., Delneri, D., 2021. Biotechnological exploitation of Saccharomyces jurei and its hybrids in craft beer fermentation uncovers new aroma combinations. Food Microbiology 100, 103838. https://doi.org/10.1016/j.fm.2021.103838

Hazelwood, L.A., Daran, J.-M., Maris, A.J.A. van, Pronk, J.T., Dickinson, J.R., 2008. The Ehrlich Pathway for Fusel Alcohol Production: a Century of Research on Saccharomyces cerevisiae Metabolism. Appl. Environ. Microbiol. 74, 2259–2266. https://doi.org/10.1128/AEM.02625-07

He, Y., Dong, J., Yin, H., Zhao, Y., Chen, R., Wan, X., Chen, P., Hou, X., Liu, J., Chen, L., 2014. Wort composition and its impact on the flavour-active higher alcohol and ester formation of beer – a review. Journal of the Institute of Brewing 120, 157–163. https://doi.org/10.1002/jib.145

Hornsey, I.S., 2003. A History of Beer and Brewing. Royal Society of Chemistry.

Krogerus, K., Magalhães, F., Vidgren, V., Gibson, B., 2017. Novel brewing yeast hybrids: creation and application. Appl Microbiol Biotechnol 101, 65–78. https://doi.org/10.1007/s00253-016-8007-5

Lambrechts, M.G., Pretorius, I.S., 2000. Yeast and its Importance to Wine Aroma - A Review. S. Afr. J. Enol. Vitic. 21, 33.

Lei, H., Li, H., Mo, F., Zheng, L., Zhao, H., Zhao, M., 2013. Effects of Lys and His supplementations on the regulation of nitrogen metabolism in lager yeast. Appl. Microbiol. Biotechnol. 97, 8913–8921. https://doi.org/10.1007/s00253-013-5137-x

Lilly, M., Bauer, F.F., Styger, G., Lambrechts, M.G., Pretorius, I.S., 2006. The effect of increased branched-chain amino acid transaminase activity in yeast on the production of higher alcohols and on the flavour profiles of wine and distillates. FEMS Yeast Res. 6, 726–743. https://doi.org/10.1111/j.1567-1364.2006.00057.x

Lilly, M., Lambrechts, M.G., Pretorius, I.S., 2000. Effect of increased yeast alcohol acetyltransferase activity on flavor profiles of wine and distillates. Appl. Environ. Microbiol. 66, 744–753.

Liu, Y., 1998. Energy uncoupling in microbial growth under substrate-sufficient conditions. Appl Microbiol Biotechnol 49, 500–505. https://doi.org/10.1007/s002530051204

Majewski, R.A., Domach, M.M., 1990. Simple constrained-optimization view of acetate overflow in E. coli. Biotechnology and Bioengineering 35, 732–738. https://doi.org/10.1002/bit.260350711

Meilgaard, M.C., 1993. Individual differences in sensory threshold for aroma chemicals added to beer. Food Quality and Preference 4, 153–167. https://doi.org/10.1016/0950-3293(93)90158-3

Monod, J., 1949. The Growth of Bacterial Cultures. Annual Review of Microbiology 3, 371–394. https://doi.org/10.1146/annurev.mi.03.100149.002103

Nissen, T.L., Schulze, U., Nielsen, J., Villadsen, J., 1997. Flux Distributions in Anaerobic, Glucose-Limited Continuous Cultures of Saccharomyces Cerevisiae. Microbiology 143, 203–218. https://doi.org/10.1099/00221287-143-1-203

Nordström, K., 1966. Formation of Esters from Acids by Brewer's Yeast: Formation from Unsaturated Acids. Nature 210, 99–100. https://doi.org/10.1038/210099a0

Novick, A., Szilard, L., 1950. Description of the Chemostat. Science 112, 715–716. https://doi.org/10.1126/science.112.2920.715

Pérez, D., Denat, M., Pérez-Través, L., Heras, J.M., Guillamón, J.M., Ferreira, V., Querol, A., 2022. Generation of intra- and interspecific Saccharomyces hybrids with improved oenological and aromatic properties. Microbial Biotechnology. https://doi.org/10.1111/1751-7915.14068

Pizarro, F.J., Jewett, M.C., Nielsen, J., Agosin, E., 2008. Growth Temperature Exerts Differential Physiological and Transcriptional Responses in Laboratory and Wine Strains of *Saccharomyces cerevisiae*. Appl Environ Microbiol 74, 6358–6368. https://doi.org/10.1128/AEM.00602-08

Procopio, S., Qian, F., Becker, T., 2011. Function and regulation of yeast genes involved in higher alcohol and ester metabolism during beverage fermentation. European Food Research and Technology 233, 721–729. https://doi.org/10.1007/s00217-011-1567-9

QUAIN, D.E., 1985. A metabolic function for higher alcohol production in yeast. Proceedings of the 20th European Brewery Convention Congress 307–314.

Saerens, S.M.G., Delvaux, F., Verstrepen, K.J., Van Dijck, P., Thevelein, J.M., Delvaux, F.R., 2008. Parameters Affecting Ethyl Ester Production by Saccharomyces cerevisiae during Fermentation. Applied and Environmental Microbiology 74, 454–461. https://doi.org/10.1128/AEM.01616-07

Stöckmann, C., Losen, M., Dahlems, U., Knocke, C., Gellissen, G., Büchs, J., 2003. Effect of oxygen supply on passaging, stabilising and screening of recombinant Hansenula polymorpha production strains in test tube cultures. FEMS Yeast Res 4, 195–205. https://doi.org/10.1016/S1567-1356(03)00147-8

Vázquez-Lima, F., Silva, P., Barreiro, A., Martínez-Moreno, R., Morales, P., Quirós, M., González, R., Albiol, J., Ferrer, P., 2014. Use of chemostat cultures mimicking different phases of wine fermentations as a tool for quantitative physiological analysis. Microbial Cell Factories 13, 85. https://doi.org/10.1186/1475-2859-13-85

Verduyn, C., Postma, E., Scheffers, W.A., van Dijken, J.P.Y. 1990, 1990. Physiology of Saccharomyces Cerevisiae in Anaerobic Glucose-Limited Chemostat Cultures. Microbiology 136, 395–403. https://doi.org/10.1099/00221287-136-3-395

Verstrepen, K.J., Derdelinckx, G., Dufour, J.-P., Winderickx, J., Thevelein, J.M., Pretorius, I.S., Delvaux, F.R., 2003a. Flavor-active esters: Adding fruitiness to beer. Journal of Bioscience and Bioengineering 96, 110–118. https://doi.org/10.1016/S1389-1723(03)90112-5

Verstrepen, K.J., Van Laere, S.D.M., Vanderhaegen, B.M.P., Derdelinckx, G., Dufour, J.-P., Pretorius, I.S., Winderickx, J., Thevelein, J.M., Delvaux, F.R., 2003b. Expression levels of the yeast alcohol acetyltransferase genes ATF1, Lg-ATF1, and ATF2 control the formation of a broad range of volatile esters. Appl. Environ. Microbiol. 69, 5228–5237.

Vidal, E.E., de Billerbeck, G.M., Simões, D.A., Schuler, A., François, J.M., de Morais, M.A., 2013. Influence of nitrogen supply on the production of higher alcohols/esters and expression of flavour-related genes in cachaça fermentation. Food Chem 138, 701–708. https://doi.org/10.1016/j.foodchem.2012.10.147

Vidal, E.E., Morais, M.A. de, François, J.M., Billerbeck, G.M. de, 2015. Biosynthesis of higher alcohol flavour compounds by the yeast Saccharomyces cerevisiae: impact of oxygen availability and responses to glucose pulse in minimal growth medium with leucine as sole nitrogen source. Yeast 32, 47–56. https://doi.org/10.1002/yea.3045

Chapter 3 - Restoring fertility in yeast hybrids: breeding and quantitative genetics of beneficial traits

Samina Naseeb[1,§], **Federico Visinoni**[1,§], Yue Hu[2], Alex J. Hinks Roberts[2], Agnieszka Maslowska[2], Thomas Walsh[2], Katherine A. Smart[3], Edward. J. Louis[2,*], Daniela Delneri[1,*]

[1] *Manchester Institute of Biotechnology, University of Manchester, Manchester, UK*

[2] *Department of Genetics & Genome Biology, University of Leicester, Leicester, UK*

[3] *Department of Chemical Engineering and Biotechnology, University of Cambridge, Cambridge, UK.*

[§] *these authors contributed equally to the study*

3.1 Foreword

The work in this chapter has been published in Proceedings of the National Academy of Sciences 118.38 (2021): e2101242118. doi: 10.1073/pnas.2101242118. The final version of the publication is presented here with the supplementary methods consolidated with the information on material and methods to avoid further repetitions. References used within the manuscript are presented at the end of the chapter.

Author contributions: EJL and DD designed research and supervised the study; SN generated and screened the library of *S. cerevisiae* x *S. kudriavzevii* and *S. cerevisiae* x *S. kudriavzevii* hybrids while AJHR and AM generated and screened the *S. cerevisiae* x *S. eubayanus* and the *S. cerevisiae* x *S. uvarum* hybrids; TW and YH carried out the bioinformatic analysis; FV carried out the phenotypic screening of the F12 *S. cerevisiae* x *S. kudriavzevii* spores harbouring *S. cerevisiae* mitotype, the SWIFT analysis and performed the *in vivo* validation. FV analysed the QTL data with the contribution of AJHR; All the authors contributed to the data interpretation and analysis; FV, SN, YH, EJL and DD wrote the manuscript with the input of KAS.

Detailed FV contributions: I worked alongside SN and contributed to the following section of this manuscript: *i.* the data analysis of Figure 3-2 and data acquisition of Figure 3-2C, *ii.* all the QTL data analysis outlined in the chapters 3.4.3, 3.4.4, and 3.4.5 and in Figure 3-3 and Figure 3-4, *iii.* all the data of chapters 3.4.6 and 3.4.7 and of Figure 3-5.

3.2 Abstract

Hybrids between species can harbour a combination of beneficial traits from each parent and may exhibit hybrid vigour, more readily adapting to new harsher environments. Inter-species hybrids are also sterile and therefore an evolutionary dead-end unless fertility is restored, usually via auto-polyploidisation events. In the *Saccharomyces* genus, hybrids are readily found in nature and in industrial settings, where they have adapted to severe fermentative conditions. Due to their hybrid sterility, the development of new commercial yeast strains has so far been primarily conducted via selection methods rather than via further breeding. In this study, we overcame infertility by creating tetraploid intermediates of *Saccharomyces* inter-species hybrids, to allow continuous multigenerational breeding. We incorporated nuclear and mitochondrial genetic diversity within each parental species, allowing for quantitative genetic analysis of traits exhibited by the hybrids, and for nuclear-mitochondrial interactions to be assessed. Using pooled F12 generation segregants of different hybrids with extreme phenotype distributions, we identified QTLs for tolerance to high and low temperatures, high sugar concentration, high ethanol concentration, and acetic acid levels. We identified QTLs that are species specific, that are shared between species, as well as hybrid specific, where the variants do not exhibit phenotypic differences in the original parental species. Moreover, we could distinguish between mitochondria-type dependent and independent traits. This study tackles the complexity of the genetic interactions and traits in hybrid species, bringing hybrids into the realm of full genetic analysis of diploid species, and paves the road for the biotechnological exploitation of yeast biodiversity.

3.3 Introduction

Hybridization is important evolutionarily, as well as industrially, as it may offer advantageous gene combinations and traits of interest to the newly formed hybrids. Hybrids between species are commonly found in both natural and domestic situations with as many as 25% of plant species and 10% of animal species hybridizing naturally (Mallet 2007). The genus *Saccharomyces* encompasses eight species, included the newly discovered *S. jurei* (Naseeb et al. 2018; Naseeb et al. 2017), which all readily hybridize among them. In the *Saccharomyces* yeasts there are many examples of hybrids from both natural (wild) as well as fermentation sources, and indeed as many as 10% of all yeast isolates are hybrids (Liti, Barton, and Louis 2006; Liti et al. 2005;

Liti and Louis 2005). The stringent condition of beer and wine fermentations in particular, represent a fertile ground for hybrids, influencing their creation, stabilisation, and phenotypic and genetic makeup (Gonzalez, Barrio, and Querol 2008; Lopandic 2018). Indeed, *S. pastorianus* (synonym *S. carlsbergensis*), a *S. cerevisiae/S. eubayanus* hybrid, has been employed in beermaking since the 15th century (Dunn and Sherlock 2008; Libkind et al. 2011). *S. cerevisiae/S. kudriavzevii hybrids* have also been isolated from wine, beer and cider fermentations along with *S. cerevisiae*/*S. uvarum* hybrids, and the triple hybrid between *S. cerevisiae*, *S. uvarum* and *S. kudriavzevii* as well as *S. cerevisiae*, *S. uvarum* and *S. eubayanus* (Gonzalez et al. 2006; Gallone et al. 2019). Moreover, examples of hybrids between the closely related species *S. cerevisiae* and *S. paradoxus* have been isolated from wild environments (Barbosa et al. 2016). Interspecies hybrids of *Saccharomyces* species have therefore been used as model organisms for studying natural evolution, speciation and fitness adaptation to different environments.

Recently, much work has gone into the generation of *de novo* yeast hybrids, exploiting their potential for the production of biofuels (Snoek et al. 2015), brewing (Krogerus et al. 2015; Mertens et al. 2015), and winemaking (Garcia-Rios et al. 2018). Inter-species hybrids are not only selected for their capability to combine the advantageous traits of the parent strains, as the genomes from both parents undergo chromosomal rearrangements, mutations, widespread transcriptional changes (Hewitt et al. 2020; Lairon-Peris et al. 2020), gene loss and gene duplications which also impact the nature of protein complexes formed (Piatkowska et al. 2013). Hence, new and improved phenotypes can arise thanks to heterosis or hybrid vigour (Lopandic et al. 2016).

A great deal has been learned on the acquired properties of particular hybrids from comparative genomics and molecular studies. However, to date, no thorough genome-wide analysis of genetic contributions to traits of industrial interest has been possible. The sterility of the inter-species yeast hybrids is in fact hindering the application of both predictive quantitative approaches and any attempt of strain improvement via breeding. A previous study by Greig et al. (Greig et al. 2002) showed that sterility of inter-species yeast hybrids can be overcome by creating tetraploids, using a MAT-locus deletion strategy. The engineered tetraploid hybrids were able to produce viable diploid progeny after undergoing meiosis (Greig et al. 2002). Another study by Schwartz et al. (Schwartz et al. 2012) demonstrated the ability to mate a hybrid for quantitative trait loci (QTL) analysis using expression of *HO* to switch a diploid non-

mater to a mater. QTL mapping in particular has shown to be a powerful tool for understanding the genetic basis of various complex traits and has been similarly applied in industrial and medical applications (Zimmer et al. 2014; Steinmetz et al. 2002). Nonetheless, QTL analysis and understanding of hybrid genetics remains poor and limited to a single generation of meiosis in these studies, due to the sterility of *Saccharomyces* hybrids.

In this study, we used two different approaches to bring *de novo* yeast hybrids into the realm of genetic analysis and improvement by breeding. A large set of *de novo* hybrids was engineered by crossing geographically distinct *Saccharomyces* strains of different species. We were able to generate genetically and phenotypically diverse populations through multiple rounds of interbreeding. Diploid F2 and F12 progeny were phenotyped for several traits, and two approaches towards genotyping pools of phenotypic extremes were used to map genetic variation in both parental genomes responsible for the phenotypes selected. For 3 sets of hybrids, F12 diploid hybrid progeny were arrayed and phenotyped under several different conditions. For each hybrid, two versions were assessed, one each with each parental species mitochondrion. The top 20 and bottom 20 from an array of 384 were pooled for sequencing and the frequencies of segregating SNPs in the two parental species genomes were compared to identify QTL involved in the traits. For one of these hybrids (2 mitochondrial versions), strong selection was applied to a population of 10^8 F12 progeny resulting in fewer than 10^6 survivors whose pooled genomic DNA was compared to the pool prior to selection, for several conditions. We demonstrate *Saccharomyces* hybrids are now amenable to all the tools available for yeast, including breeding and utilisation of the vast genetic diversity available. We show that there are QTL both unique to one parent species or shared by both, QTL dependent and independent of the mitochondrial origin, and QTL that are specific to the hybrid and not to the parent species where the variants are segregating.

3.4 Results

3.4.1 Construction of tetraploid yeast hybrids from a variety of parental strains leads to restoration of fertility

We constructed yeast hybrid tetraploid lines combining four different genomes of strains coming from two separate species belonging to the *Saccharomyces* genus. To construct such fertile tetraploid hybrids, we employed two different strategies (Figure

3-1). First *inter-species* diploid hybrids were constructed using stable haploids after deletion of *HO* (5 for *S. cerevisiae/S. jurei* and 10 for *S. cerevisiae/S. kudriavzevii*, Table A-1, Appendix A), followed by reciprocal deletion of the MAT locus, and subsequent crossing of the two diploid mater hybrids. In the second strategy *intra-species* diploid strains were first constructed by crossing diverged populations of the same species, again using stable haploids after deletion of *HO* (10 *S. cerevisiae*, 6 *S. uvarum* and 2 *S. eubayanus* intra-species crossings, Table A-2, Appendix A), followed by reciprocal deletion of the MAT locus, and subsequent hybridization of the two diploid maters. Tetraploid lines of *S. cerevisiae*/*S. kudriavzevii* (Sc/Sk) and *S. cerevisiae*/*S. jurei* (Sc/Sj) hybrids were created with this first strategy while *S. cerevisiae*/*S. uvarum*, and *S. cerevisiae*/*S. eubayanus* were constructed using the second approach.

Hybrids between *Saccharomyces* species are homoplasmic and tend to carry mitochondrial DNA from only one parent. The natural hybrid *S. pastorianus* (hybridized from *S. cerevisiae* and *S. eubayanus*) carries the *S. eubayanus* mitochondria (Okuno et al. 2016; Baker et al. 2015), while other industrial hybrids of *Saccharomyces* species used in wine and cider production have retained *S. cerevisiae* mitochondrial genome (Masneuf et al. 1998). It has also recently been shown that the type of mitochondria inherited affects the phenotype (Albertin et al. 2013; Baker et al. 2019; Li et al. 2019) and the transcriptional network (Hewitt et al. 2020) in hybrids. Therefore, here, each of the tetraploid hybrids constructed were also selected for different mitotypes. Throughout the paper, in the hybrid nomenclature, a subscripted $_m$ following the initial of the species, represents the particular mitochondria inheritance of that hybrid (*i.e.,* Sc_m/Sj is tetraploid hybrid containing Sc mitochondria, Sc/Sj_m is tetraploid hybrid containing Sj mitochondria).

A total of 226 tetraploid hybrids were created and each hybrid had four unique parental strains and a unique mitochondrion contributing to the genome (Dataset S1, Naseeb et al 2021). All the constructed tetraploids were fertile as they had a homologous set of chromosomes to align in meiosis. While diploid hybrids between species of *Saccharomyces* genus are reproductively isolated (Naseeb et al. 2017; Liti, Barton, and Louis 2006), the tetraploid hybrids constructed here, were fertile and exhibited spore viability as high as 98% (Table A-3, Appendix A) as has previously been reported for tetraploids (Greig et al. 2002). Ultimately, the diploid F1 spores obtained from the tetraploid hybrids were sequentially randomly mated and

sporulated eleven times until the F12 generation (Figure 3-1). From the F12 generation around 384 spores for each were isolated for further studies.

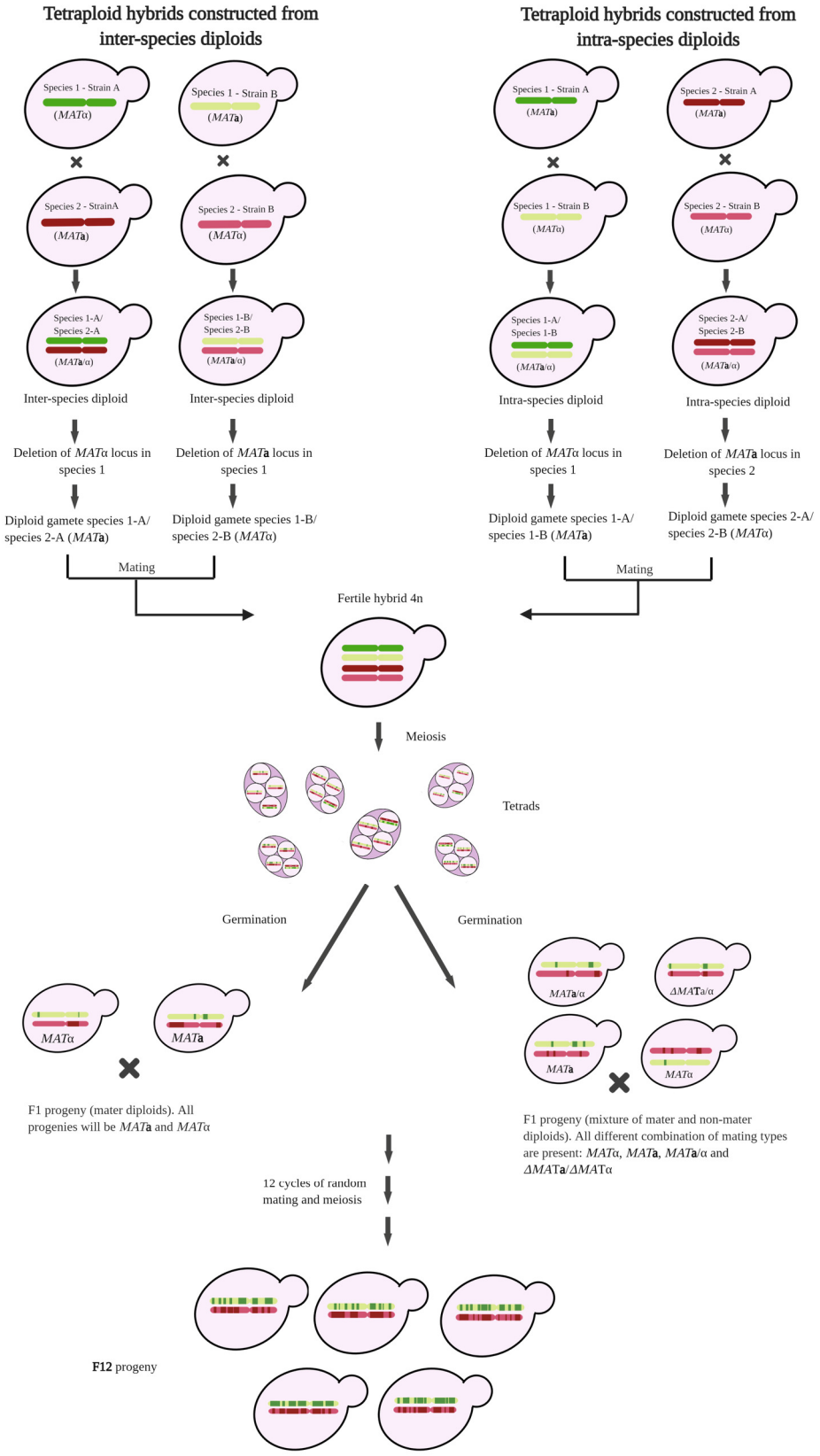

Figure 3-1 | Construction of fertile hybrids. The tetraploid hybrids were constructed using two different strategies. In the first strategy, two different *Saccharomyces* species were crossed to obtain 2n inter-species diploid hybrids (species 1 and species 2 are represented in shade of green and red, respectively). Two different of such hybrids were made to behave as gametes by deleting either the MATa or α locus in one species and subsequently crossed to make the fertile tetraploid hybrid (4n). In the second strategy, two diverged populations (A and B) of the same species were crossed to construct the 2n intra-species hybrids. Two different intra-species lines were also made to behave as gametes by deleting the MATa from species 1 and MATα from species 2, and subsequently these were crossed to construct the 4n hybrids. The tetraploid hybrids were sporulated and germinated to obtain the diploid F1 progeny which were randomly mated and sporulated several times until a F12 generation with a high level of scrambled genomes.

3.4.2 Meiotic offspring of tetraploid hybrids exhibit broad phenotypic diversity

Inter-crossing different populations of *Saccharomyces* species over many generations reduces linkage disequilibrium by increasing recombination. To assess whether the fitness traits are associated with genetic linkage, we assessed the phenotypic landscape of F1 and F12 diploid generations in up to 12 conditions encompassing different growth temperatures, carbon sources and stressors. An example of phenotypic divergence between F1 diploid segregants of tetraploid Sc/Sj ($Sc^{OS3}/Sj^{D5088}/Sc^{OS104}/Sj^{D5095}$) and Sc/Sk ($Sc^{OS253}/Sk^{OS575}/Sc^{OS104}/Sk^{IFO1802}$) harbouring different mitotypes is reported in Figure A-1 (Appendix A). Significant fitness differences were seen in all the segregant lines with a dispersion up to 0.33 (quartile coefficient of dispersion, Table A-4, Appendix A), with some progeny being fitter than any of the parents (Figure A-2, Appendix A) and some being less fit (transgressive variation) in virtually all cases.

When colony size is normalised within each specific condition, to allow the teasing apart of fitness differences between spores derived from the same tetraploid line, F12 segregants of Sc_m/Sj, Sc/Sj_m, Sc_m/Sk, and Sc/Sk_m again exhibited a large phenotypic variation in all the tested conditions (Figure 3-2).

Given that the tetraploid lines are composed of *S. cerevisiae* combined with genomes of other *Saccharomyces* species with different levels of phylogenetic distance, we investigated whether such differences in genome divergence have an impact on phenotypic plasticity in any given condition. By analysing the un-normalised fitness data, to tease apart differences in the colony size range between progeny from

separate tetraploid lines, no striking differences were found in either range or dispersion between different hybrids (Figure A-3, Appendix A). Therefore, the different levels of divergence of the genomes present did not impact significantly on phenotypic range and plasticity in the progeny in the hybrid lines generated.

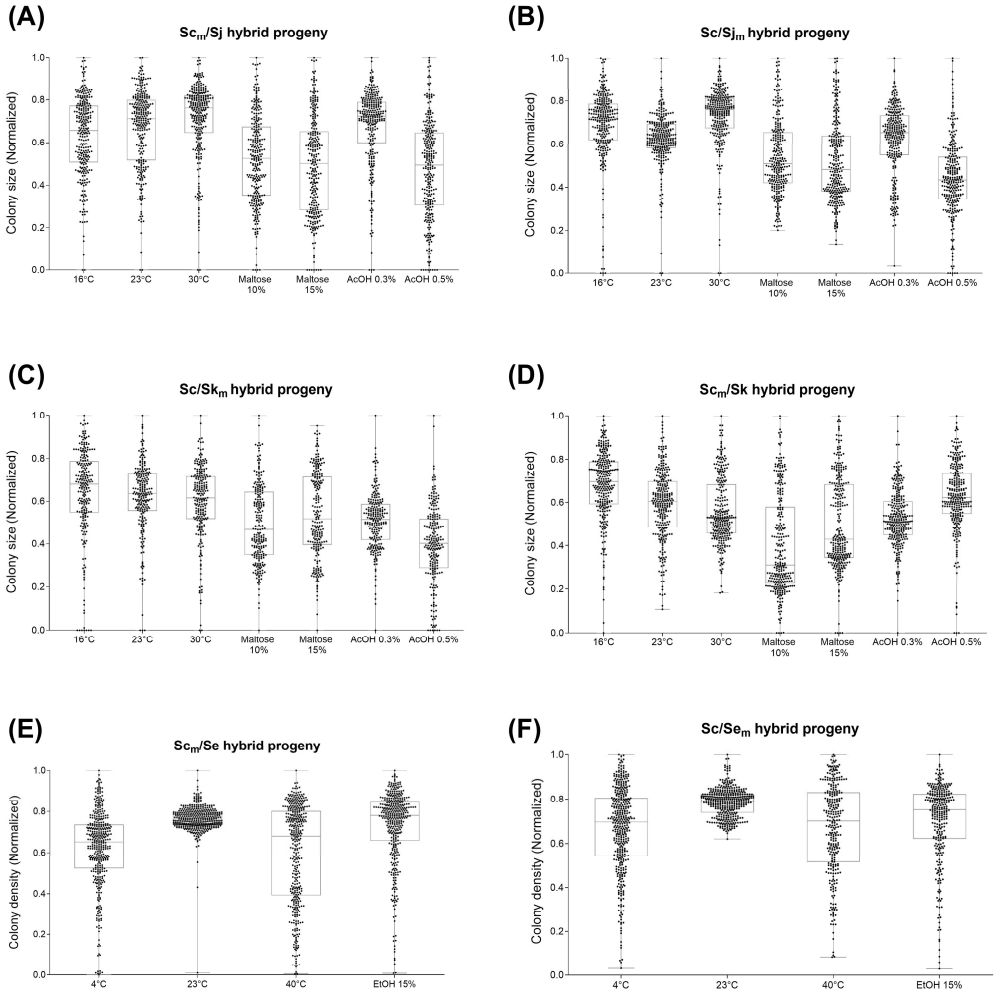

Figure 3-2 | Box plot of the fitness of F12 diploid progeny for *S. cerevisiae/S. jurei* (Sc_m/Sj and Sc/Sj_m) and *S. cerevisiae/S. kudriavzevii* (Sc_m/Sk and Sc/Sk_m) and *S. cerevisiae/S. eubayanus* (Sc_m/Se and Sc/Se_m) hybrids. For Sc_m/Sj (panel A), Sc/Sj_m (panel B), Sc_m/Sk (Panel C) and Sc/Sk_m (Panel D), the normalised colony size was used as proxy of fitness (see Material and Methods) and was scored in YPD at different temperatures 16ºC, 23ºC, and 30ºC, in YP- Maltose (10% and 15%), and in YPD with 0.3% and 0.5% acetic acid (AcOH). For Sc_m/Se (Panel E) and Sc/Se_m (Panel F) the colony optical density was used as proxy of fitness (see Material and Methods) and was scored in YPD at different temperature 4ºC, 23ºC, and 40ºC, and in YPD with 15% Ethanol (EtOH). Each black dot represents a different F12 diploid hybrid. The upper and lower error bars represent the minimum and maximum values.

3.4.3 Phenotypic diversity of tetraploid hybrids is underpinned by the presence of QTL

To identify the genetic basis underlying the observed phenotypic diversity we performed QTL analysis on selected segregant pools of Sc/Sj, Sc/Sk, Sc/Se and Sc/Su hybrids. Two different methods for QTL analysis were employed. The Multipool technique, pioneered by (Edwards and Gifford 2012), was used to analyse the F12 generation of Sc/Sj, Sc/Sk, and in Sc/Se hybrids, while the Pooled Selection method (Ehrenreich et al. 2010; Parts et al. 2011) was applied to Sc/Se and Sc_m/Su hybrids. Both approaches proved successful in mapping QTL regions in a variety of conditions for all hybrids, however a higher number of QTLs and more consistent results across the conditions tested were obtained using the Multipool approach (Table A-5, Appendix A). A comprehensive list of the QTL intervals mapped, including coordinates of the regions, LOD scores and gene content is presented in Dataset S2 available on the published version of the paper (Naseeb et al. 2021).

For the Multipool the top 20 and bottom 20 individuals of 384 arrayed were pooled for each condition for comparison. Sc/Sj and Sc/Sk hybrids were selected at low temperature (16 ºC), in 15% maltose and in 0.3% acetic acid, while Se/Sc hybrids were selected in 10% ethanol and low and high temperatures (4 ºC and 40 ºC). Such conditions are relevant to fermentation industries. Low temperature is required for the storage of brewing yeast and for fermentation of lager beer. Maltose is one of the key wort sugars and the high concentration of this sugar mimics the osmotic pressure exerted upon yeast in high gravity wort (Gibson et al. 2007). Acetic acid is found in grape must, and wine producing yeasts are known to require the resistance to this stress (Belloch et al. 2008; Gibson et al. 2007). Ethanol is the major stressor for both the production of fermented beverages and bioethanol (Gibson et al. 2007).

From segregants generated from the tetraploids Sc_m/Sj and Sc/Sj_m, a total of 56 QTLs were identified in the *S. cerevisiae* genomes with an average length of 19.4 kb (Table A-6, Appendix A). Despite the high similarity between the two *S. jurei* parental strains (Naseeb et al. 2018), we were able to map 62 QTL regions in the genome of this species. However, with an average length of 35.5 kb, the QTL mapping intervals were the longest observed in the hybrids generated due to the lower density of segregating markers in the two genomes of this species.

An even higher number of QTL was mapped from the progeny of Sc_m/Sk and Sc/Sk_m tetraploids with up to 155 and 128 regions mapped in *S. cerevisiae* and *S. kudriavzevii*,

respectively (Table A-6, Appendix A). Here, the QTL intervals were narrower than those seen in the *S. jurei* genome, with only 15.6 kb average length on *S. cerevisiae* alleles and 18.6 kb on *S. kudriavzevii* ones as there is a higher density of segregating markers in these genomes.

Similar results were obtained in Sc_m/Se and Sc/Se_m hybrids analysed for their fitness in high ethanol concentration and at high and low temperatures (40°C and 4°C) (Table A-6, Appendix A). Here, we were able to identify 111 and 64 QTLs regions in *S. cerevisiae* and *S. eubayanus*, respectively, with an average length of 18.5 kb and 21.82 kb.

A total of 28 genes mapped in different QTLs in Sc/Sj and Sc/Sk hybrids were classified as potential causal genes, as their role in the selection condition was already confirmed by previous published work (Cherry et al. 2012) (Table A-7, Appendix A). For example, one of the acetic acid QTL detected in *S. cerevisiae* chromosome III (52-97 kb) in Sc_mSj hybrids contains variant alleles of *LEU2*. The gene encodes for a β-isopropyl-malate dehydrogenase and null mutants are reported as sensitive to acetic acid while its overexpression increase acetic acid resistance (Hueso et al. 2012).

Amongst the genes identified, a total of 43 genes with segregating alleles found in low temperature QTL were previously identified in large-scale competition studies carried out in *S. cerevisiae* at 16°C, with an additional 5 being described as cold favouring by thermodynamic model predictions (Table A-7, Appendix A) (Paget, Schwartz, and Delneri 2014).

Thanks to the abundance of data on heat and ethanol sensitivity in *S. cerevisiae* (Teixeira et al. 2009; Sinha et al. 2008; Cubillos et al. 2013; Parts et al. 2011), a high number of potential causal genes with segregating variation were identified in the QTL regions of Sc/Se hybrids. Thus, we were able to identify up to 38 genes in the 44 QTL regions for the *Sc* alleles that likely promote a fitness advantage while growing at 40°C (Table A-7, Appendix A). Amongst these, *IRA1*, a regulator of the RAS pathway, was previously validated as a heat-QTL in OS3/OS104 crosses (Parts et al. 2011). Moreover, two additional genes involved in the RAS/cAMP signalling pathway (*ESB1* and *GPB2*) were mapped in heat QTLs, supporting its involvement in mediating heat resistance as previously suggested by Parts et al. (Parts et al. 2011).

The potential causal genes detected in *S. cerevisiae* genomes in Sc/Sj, Sc/Sk, and Sc/Se hybrids may contain amino-acid variants that are affecting protein function. Hence, we analysed these genes through SIFT analysis (Sorting Intolerant From Tolerant), to

identify non-synonimous SNPs underlying the observed phenotypic difference between alleles (Kumar, Henikoff, and Ng 2009; Bergstrom et al. 2014). SIFT analysis was carried out on the 82 predicted *S. cerevisae* causal genes. A strong effect on the protein function was detected in 23% of potential causal genes due to amino acid differences between the *S. cerevisiae* parental strains (Table A-8, Appendix A), while ca. 38% of mutations were inferred as tolerated and for the remaining 39% no non-synonymous SNPs at the protein-coding region were detected.

GO analysis did not help to narrow down choices of potential causal gene candidates, since the enrichment GO terms were at broad level only generally associated with intracellular membrane bound organelle, cytoplasm, catalytic activity, and cellular processes in all the conditions.

In total 14, 22 and 11 pleiotropic QTLs were mapped in Sc/Sj, Sc/Sk and Sc/Se hybrids, respectively (Dataset S3, Naseeb et al. 2021). A 7 kb region on the *S. cerevisiae* chromosome XIII was common across all conditions tested for $ScSj_m$ hybrids, but, interestingly, it was not detected for Sc_mSj in any condition tested. This region contains the genes *CLU1* (a subunit of eIF3), *ANY1* (a protein involved in phospholipid flippase) and *HXT2* (a high-affinity glucose transporter). It is possible that the phenotypic effect of variation in these genes depends solely on mitochondrial-nuclear interactions, independent of the condition. *CLU1* is known to play a role in mitochondrial distribution and morphology but *Δclu1 strains* maintain their respiratory function and inheritance (Fields, Conrad, and Clarke 1998; Dimmer et al. 2002). The *Δclu1* mutants possess a more condensed mitochondrial mass found at one side of the cell (Fields, Conrad, and Clarke 1998). They are haplo-insufficient in nutrient limited media (Fields, Conrad, and Clarke 1998; Pir et al. 2012) and haplo-proficient in phosphorus limited media (Delneri et al. 2008).

In parallel to the comparison of small pools performed with Multipool, pooled selection experiments were performed on Sc_m/Se and Sc/Se_m, Sc_m/Su segregants. For the selected pools, the strength of selection was chosen such that approximately 0.1% of the population survived the selective condition which was then pooled for comparison to the unselected population. Specifically, Sc_m/Se and Sc/Se_m were selected for a variety of selectable traits of industrial relevance, spanning from high maltose and glucose concentrations (35%), to H_2O_2 treatment (4 mM), and very low temperature (4°C); while the Sc_mSu hybrid progeny were selected in YPD at high temperature (40°C) and YPD with levulinic acid (50 mM), acetic acid (0.35%) at 23°C.

The linkage analysis on the pooled selection segregants yielded narrow intervals, averaging at 18.1 kb and 20 kb in Sc/Se and Sc_m/Su hybrids, respectively. However, only a limited number of QTL was identified, except for YP-Maltose (Table A-5, Appendix A). No QTL were found among segregating *S. uvarum* alleles (Table A-9, Appendix A).

Thirtyfive of the 41 QTL regions detected in Sc_m/Se and Sc/Se_m segregants were present in hybrids with a fitness advantage in high maltose concentrations (Table A-9, Appendix A). However, it was unexpected that only one QTL was identified when selection took place at 4°C, given that in the multipool analysis in the same condition, 45 QTLs were identified. Characteristics such as growth at low temperature, which, albeit selectable, do not show extremes phenotypes, are better discriminated using the Multipool approach as it exploits the richness of fitness data acquired through individual phenotyping. Growth at 4ºC may not be strong enough selection, *i.e.* doesn't kill the majority of individuals in the population, resulting in less discrimination in the pooled selection approach.

Similarly, pooled selection of Sc_m/Su segregants yielded only 9 intervals of interest, all mapping to *S. cerevisiae* alleles across the four conditions tested. These regions included a single interval conferring tolerance to acetic acid, four conferring selective advantage at high temperature, and four giving tolerance in an environment containing levulinic acid. As mentioned above none were found in the *S. uvarum* genome.

As with Multipool QTLs, we identified several genes, which had already been reported as having a phenotypic effect or a function closely linked to the condition tested. For Sc_m/Se and Sc/Se_m hybrids, we detected in the Pooled Segregants in high maltose concentrations 8 genes where deletion was reported to cause osmotic stress sensitivity (Table A-10, Appendix A). Among these, *SKO1*, a basic leucine zipper transcription factor, mapped in *S. eubayanus* alleles of Sc/Se_m segregants, has been described having a major role in mediating HOG pathway-dependent osmotic regulation (Rep et al. 2001).

Overall, our results indicate that the Multipool approach with individuals at each extreme of a phenotype distribution is more efficient than a highly selected pool approach. However, the highly selected pool approach can identify rare genotypes of linked recombinant variants that are too rare to be in the arrays used to choose individuals for the Multipool approach.

3.4.4 Different types of mitochondria have a profound effect on the QTL landscape

Mitochondrial-nuclear interactions have been reported as having a major role in phenotypic variation both in intra-species and inter-species yeast hybrids (Lee et al. 2008; Baker et al. 2019; Hewitt et al. 2020; Li et al. 2019), affecting respiration (Albertin et al. 2013) fermentation properties (Hewitt et al. 2020; Solieri et al. 2008), progeny fitness (Zeyl 2006; Zeyl, Andreson, and Weninck 2005), reproductive isolation (Lee et al. 2008) and nuclear transcription (Hewitt et al. 2020). Given the complexity and the diversity of the hybrid background, thorough mapping of the epistasis in genome-wide studies has been a challenge. Here, in order to evaluate how the mitochondria inherited may affect the QTL landscape, we compared QTL regions mapped in diploid hybrid progeny derived from tetraploid lines harbouring different mitochondria but the same parental nuclear inputs.

Interestingly, the majority of QTL detected via the Multipool method were exclusive to a specific mitotype (Figure 3-3). In fact, in all of the conditions analysed, only ca. 2.45% QTL regions (the mean percentage for all hybrids in all the conditions) were in common among the segregants from tetraploid hybrids with different mitochondria. This difference in the QTL landscape between the same yeast hybrid cross, differing only for the mitotype, is consistent with the idea that mitochondrial-nuclear interactions have a genome-wide effect and are important in the context of evolution, as already demonstrated by several studies both in yeast (Lee et al. 2008; Wolters et al. 2018) and in other organisms (Ellison, Niehuis, and Gadau 2008; Mossman et al. 2016; Wernick et al. 2019).

The experiments carried out via Pooled Selection also demonstrated mitotype-specific QTLs. Only one QTL region was in common in the Sc/Se hybrids with different mitochondria: a 21 kb region on chromosome I, containing the genes *FLO1* and *PHO11* where specific Sc alleles are associated with an increase in fitness at high maltose concentrations. Given these are located in a subtelomeric region, known to be highly variable in copy number and location in addition to sequence, as well as difficult to assemble (Liti et al. 2009; Louis and Becker 2014), the causal genetic variation may be an unknown sequence linked to the *FLO1* and *PHO11* genes, as these regions are not assembled in all of the genomes utilized here.

Amongst the QTLs shared between Sc_mSj and $ScSj_m$ segregants, a major maltose QTL near the telomeric regions of chromosome II of *S. cerevisiae* (780 – 795 kb) was detected with a high LOD score (> 17). The recurrence of this QTL and its high LOD score could be ascribed to the *MAL3* multigene complex in the sub-telomeric region and the natural variation in copy number, location, and sequence of this complex (Liti et al. 2009). Furthermore, this maltose QTL is also mapped on the *S. cerevisiae* alleles of both Sc_m/Sk and Sc/Sk_m hybrid pointing to a more general effect of these allelic variants rather than a strain background dependent one.

3.4.5 Overlap of QTL regions between different hybrids facilitates the identification of causal genes

One way to help to identify relevant genes within QTL regions, at least for QTL not specific to a particular hybrid combination, is to investigate overlapping QTL regions detected in different hybrids. Such an approach can lead to the unambiguous identification of genes underlying the phenotypic effect observed. Twelve overlapping intervals, shared by at least three hybrid genomes, were mapped in low temperature-, high maltose-, and high ethanol-QTLs, while an additional 52 intervals were overlapping between two hybrids (Dataset S4, Naseeb et al. 2021). Within acetic acid-QTLs, only 12 overlapping intervals were detected with no region shared between more than two species, suggesting a greater diversity of variants connected with the phenotype. Amongst these intervals, we identified several candidates with biological functions closely linked to the selection condition. For instance, a low temperature-QTL mapped both in *S. cerevisia*e and *S. kudriavzevii* includes *OSH6* (Figure 3-4 A), related to sterol metabolism and, as such, membrane fluidity, often considered a feature of low-temperature adaptation (Buzzini et al. 2012). Similarly, an acetic acid-QTL mapped in both Sc/Sj_m and Sc_mSk hybrids includes *NQM1*, a nuclear transaldolase involved in oxidative stress response, known to be induced by acetic acid stresses (Michel et al. 2015) (Figure 3-4 B).

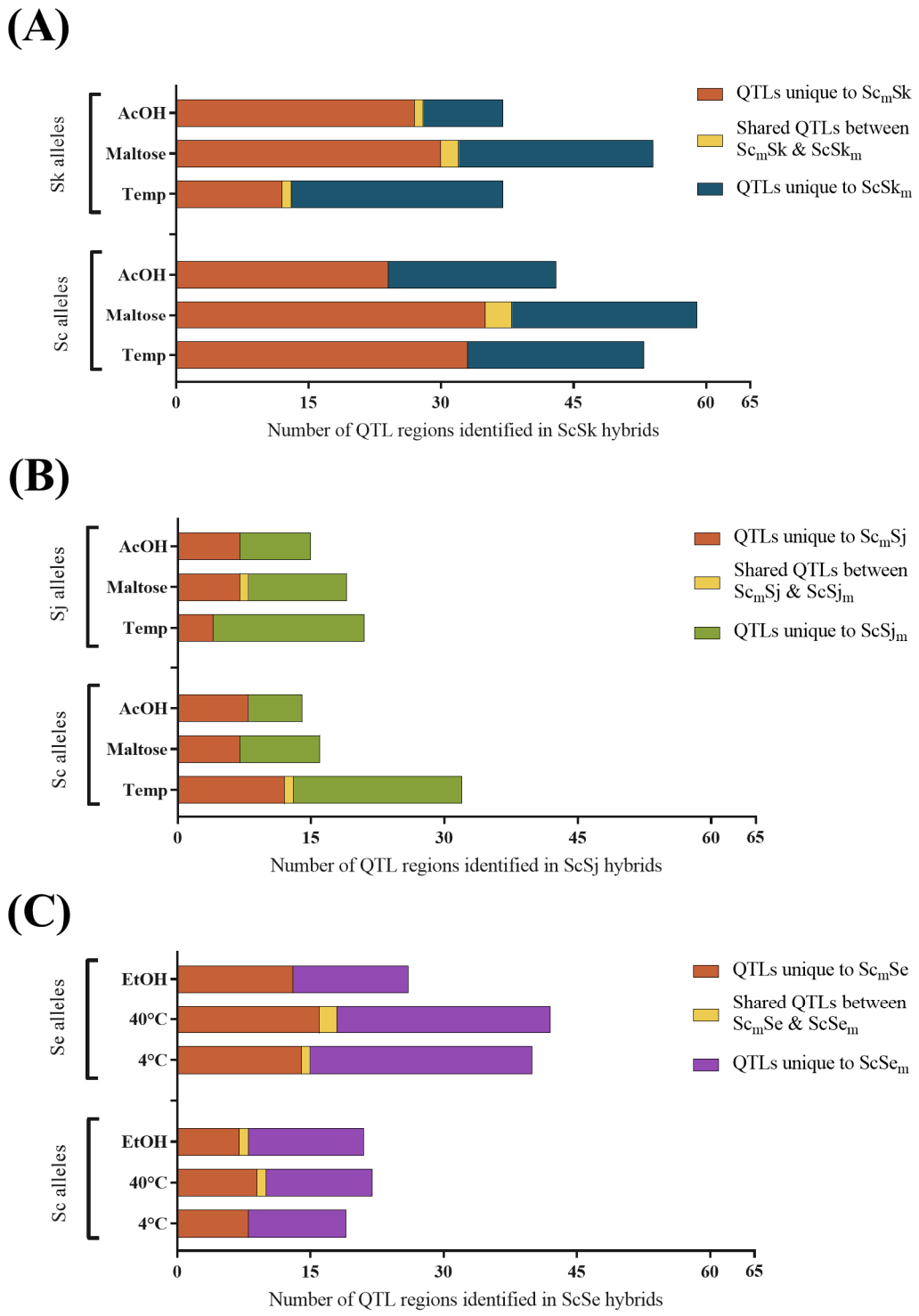

Figure 3-3 | Hybrids with different mitotype exhibit a different QTL landscape. Boxplot of the distribution of QTLs in *S. cerevisiae/S. kudriavzevii* (Panel A), *S. cerevisiae/S. jurei* (Panel B) and *S. cerevisiae/S. eubayanus* hybrids (Panel C). The QTL regions are grouped first by the alleles and then by growth condition in which they were identified: acetic acid (AcOH), high maltose concentrations (Maltose), low temperature (16°C or 4°C), heat and ethanol (EtOH). The small proportion of QTLs shared between mitotypes of the same hybrid is represented in yellow.

Ethanol- and high temperature-QTLs were analysed only in Sc/Se hybrids, limiting the outcomes compared to the other traits. Nonetheless, we found 3 overlapping ethanol-QTLs with a major region mapped on chromosome XV shared between genomes (Figure 3-4 C). Moreover, this region included the genes *PAC1*, *VPH1* and *MOD5* where null mutations are linked to a decreased fitness in ethanol supplemented media (van Voorst et al. 2006; Yoshikawa et al. 2009).

A major overlap was detected in the sub-telomeric region of chromosome II, with a maltose-QTL shared between the *S. cerevisiae* allele of all Sc/Sj and Sc/Sk hybrids and the *S. jurei* alleles of Sc/Sj$_m$. The QTL contains a causal gene, *MAL33*, a MAL-activator protein, and two transporter *CTP1* and *PHO89*, involved in the transport of citrate and phosphate, respectively, which are key metabolites for the glycolytic pathway (Figure 3-4E). Remarkably, two low temperature-QTLs regions were mapped in at least one mitotype of all tetraploid hybrids analysed through Multipool. The overlapping regions resulted in both cases in a single-gene intersection with *COQ6* (Figure 3-4F) and *PEP3* (Figure 3-4D) identified in 4 and 5 different intervals, respectively. *COQ6* is a mitochondrial monooxygenase which, in addition to its known role in mitochondrial respiration, is involved in fatty acid β-oxidation (Awad et al. 2018). *PEP3*, instead, is a component of the CORVET membrane tethering complex, and its role at cold temperature was previously suggested by large-scale competition studies (Paget, Schwartz, and Delneri 2014). Moreover, SIFT analysis performed with mutfunc (Wagih et al. 2018) predicted a strong deleterious effect of the SNP in the OS253 *PEP3* variant, due to a substitution in a conserved region.

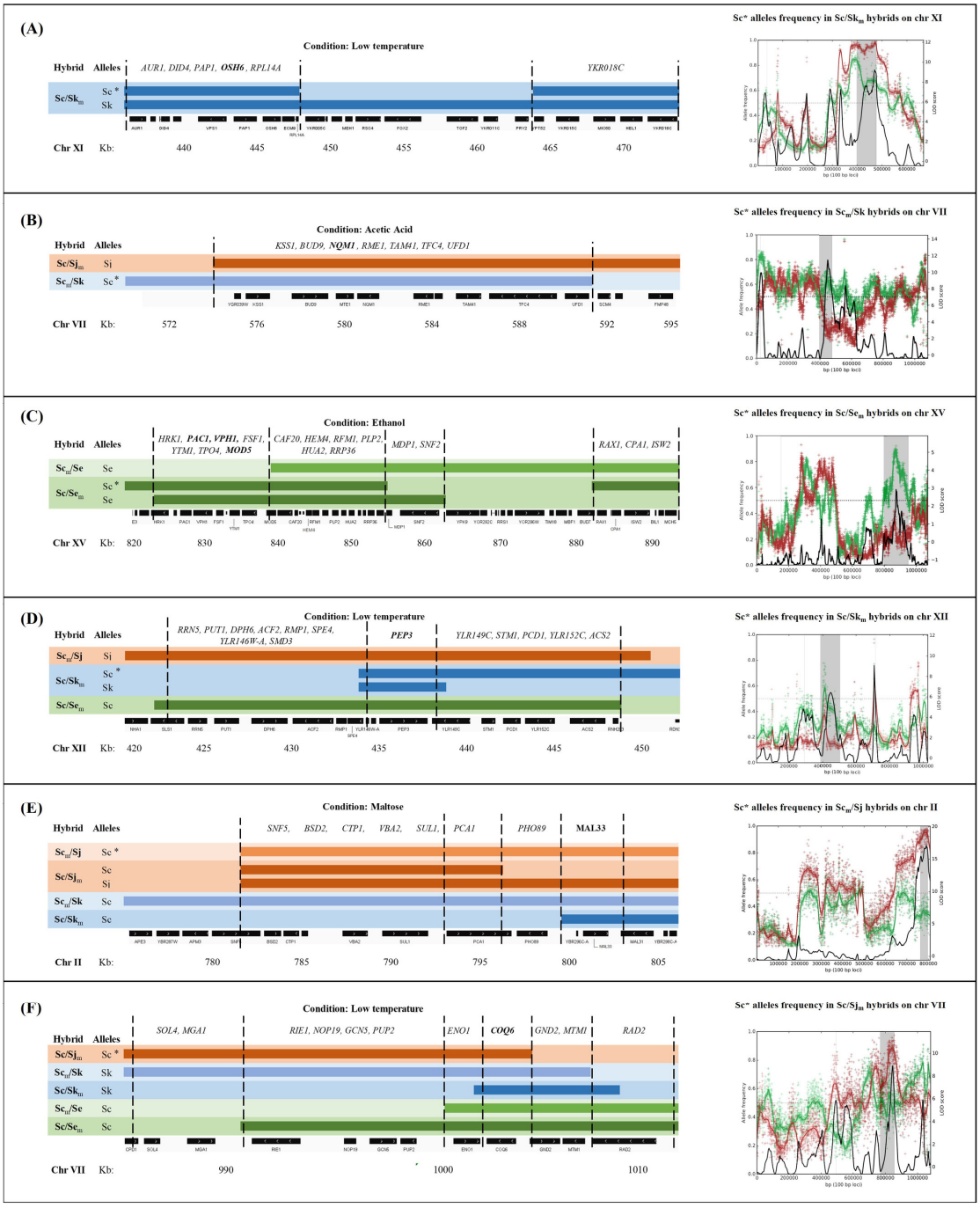

Figure 3-4 | Example of inter-species QTLs detected in *S. cerevisiae/S. jurei*, *S. cerevisiae/S. kudriavzevii* and *S. cerevisiae/S. eubayanus* hybrids. The QTL regions, represented by coloured bars, are mapped onto *S. cerevisiae* chromosomes to identify the overlapping QTL intervals and the genes shared between different species and hybrids. The parental species alleles for each hybrid are stated and the genes in bold denotes potential causal genes. The QTL plots represents the frequency of *S. cerevisiae* alleles, marked in the figure with an asterisk, from different hybrid pool lines. The red and green lines represent the alternative allele frequency of high and

low fitness pools using the Sc^{OS104} genome as reference. Black line indicates the LOD score and grey area is the 90% credible interval of the significance. The dash line is the threshold of LOD considered in this study.

3.4.6 Validation of QTL via reciprocal hemizygosis analysis

The narrow mapping intervals identified in the Sc/Sk_m hybrid allowed single-gene studies to validate the effect of candidate alleles, which were not strongly identified as causal genes. The fitness of the allelic variants was tested with reciprocal-hemizygosity analysis (RHA) (Steinmetz et al. 2002) performed on *ASI2*, *FUS3* and *GIT1*, which are candidate QTLs in acetic acid, low temperature (16ºC) and high maltose, respectively (Figure 3-5, Panel A, Table A-11, Appendix A). Amongst the genes included in the acetic acid-QTLs, *ASI2*, part of the Asi ubiquitinase complex, was defined as a potential candidate gene as its null mutant was previously described as sensitive to oxidative stress in systematic studies (Higgins et al. 2002). *FUS3*, a MAPK protein, was previously described as haplo-insufficient in large-scale competition studies at 16ºC (Paget, Schwartz, and Delneri 2014). Lastly, we selected the plasma membrane permease *GIT1* included in a high LOD QTL region in chromosome III identified at high maltose concentrations, along *HMRA1*, *HMRA2*, *CDC39*, *CDC50* and *OCA4*. *GIT1* was deemed the most promising candidate as it is involved in phosphate and glycerol-3-phospate transport, important metabolites of the glycolytic pathway (Popova et al. 2010).

The phenotypic effect of *ASI2*, *FUS3* and *GIT1* alleles were validated via RHA performed on the hemizygote tetraploid parents ($Sc^{OS253}/Sk^{OS575}/Sc^{OS104}/Sk^{IFO1802}$) in YPD + 0.3% acetic acid at 30°C, YPD at 10°C and YP-maltose (15%) at 25°C, respectively (Figure 3-5, Panel B, C, D, Table A-12, Appendix A). We observed a significant difference of the growth curve integral area (Table A-12, Appendix A) between the performance of the allelic variants in all the three genes tested confirming their impact in the selection condition and validating them as having causal variant alleles. The $FUS3^{OS253}$ and $GIT1^{OS104}$ alleles performed better than the $FUS3^{OS104}$ and $GIT1^{OS253}$ alleles in terms of specific growth rate (p value = 0.0010 and 0.0335, respectively) and integral area (p value = 0.0047, 0.0435, respectively) (Table A-12, Appendix A), mirroring what we have seen in our multipool QTL screening. For the *ASI2* gene, the $ASI2^{OS253}$ was the allele prevalent in the high-fitness pool exposed to high concentration of acetic acid.

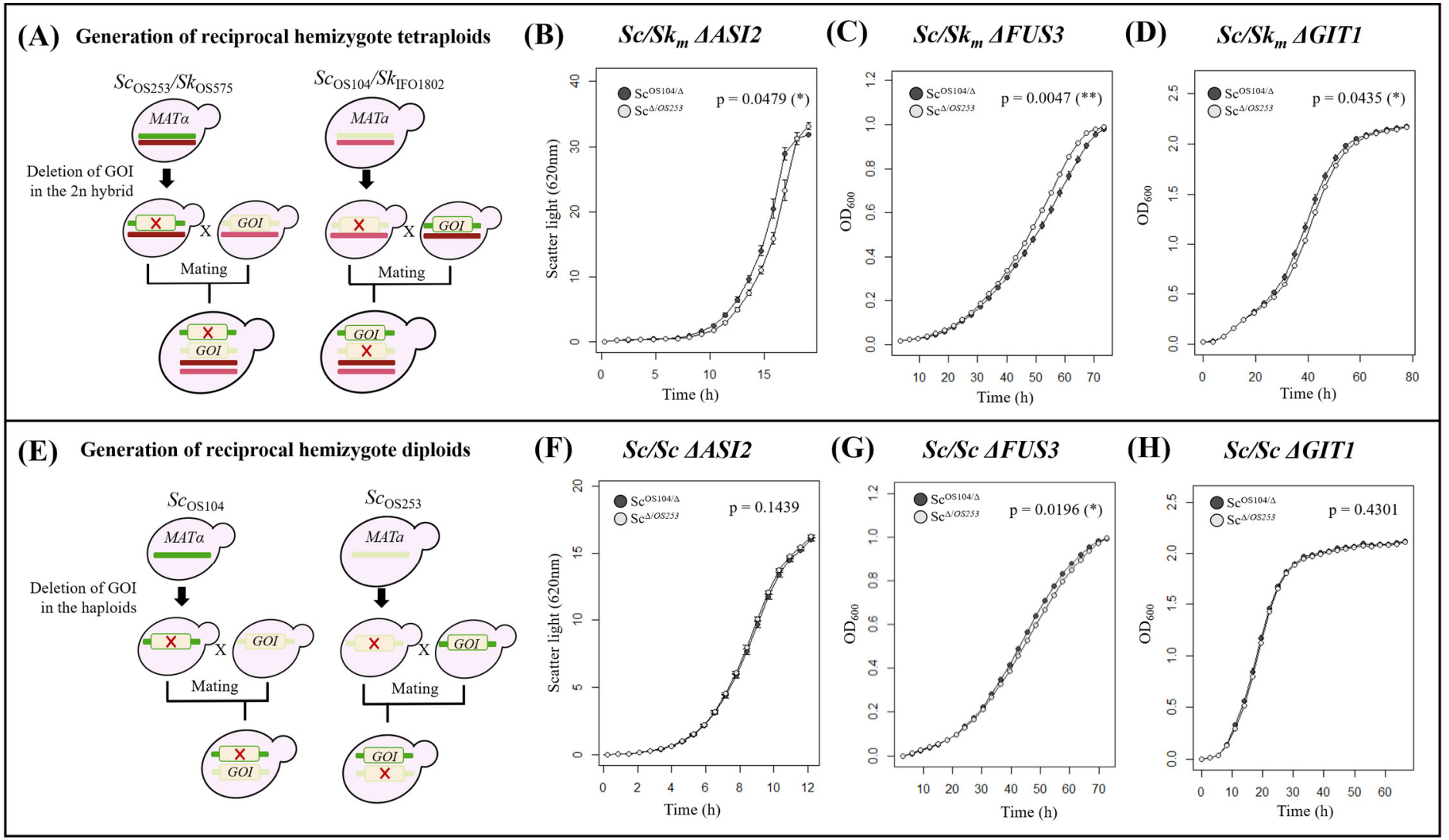
(A) Generation of reciprocal hemizygote tetraploids
Sc_OS253/Sk_OS575
Sc_OS104/Sk_IFO1802
MATα
MATa
Deletion of GOI in the 2n hybrid
GOI
X
Mating
(B) Sc/Sk_m ΔASI2
(C) Sc/Sk_m ΔFUS3
(D) Sc/Sk_m ΔGIT1
Sc^OS104/Δ
Sc^Δ/OS253
p = 0.0479 (*)
p = 0.0047 (**)
p = 0.0435 (*)
Scatter light (620nm)
OD600
Time (h)
(E) Generation of reciprocal hemizygote diploids
Sc_OS104
Sc_OS253
Deletion of GOI in the haploids
(F) Sc/Sc ΔASI2
(G) Sc/Sc ΔFUS3
(H) Sc/Sc ΔGIT1
p = 0.1439
p = 0.0196 (*)
p = 0.4301

Figure 3-5 | Validation of the phenotypic effect of candidate genes in inter- and intra-species hybrid background. Diagram of the construction of the reciprocal hemizygote $ScSk_m$ tetraploid strains (Panel A). The gene of interest (GOI) was first deleted from the respective ScSk diploid hybrids. The engineered 2n hybrids were crossed to construct the reciprocal hemizygote tetraploid strains. Growth curves of $ScSk_m$ reciprocal hemizygotes for the *ASI2*, *FUS3* and *GIT1* genes are shown in Panels B, C and D, respectively. Diagram of the construction of the reciprocal hemizygote diploid strains (Panel E). The gene of interest (GOI) was deleted from Sc_{OS104} and Sc_{OS253}. The engineered haploid strains were crossed to construct the hemizygote diploids. Growth curves of Sc OS104/OS253 reciprocal hemizygotes for the *ASI2*, *FUS3* and *GIT1* are shown in Panels F, G and H respectively. Fitness assays were performed in YPD supplemented with 0.3% acetic acid (B, F), YPD at 10°C (C, G) and YP + maltose 15% (D, H) as outlined in Material and Methods. Significance difference between the integral area of the reciprocal hemizygotes is shown as p-value assessed by t-test.

In the phenotypic validation the $ASI2^{OS253}$ variant performed worse than the $ASI2^{OS104}$ in terms of integral area (p value = 0.0479) and T_{mid} (p value = 0.0182) but it reached a higher maximum biomass (p value = 0.0001). Although the growth parameters for these two alleles are clearly different, it is more ambiguous whether their fitness performance overlaps with that one detected in the QTL study where the $ASI2^{OS253}$ was the allele prevalent in the high-fitness pool. This discrepancy could be due to other genes in the close proximity masking its effect or to the difference in the phenotypic screening employed, as the F12 segregants were assayed for their growth in solid media. Many of yeast QTLs have shown to be environment and background dependent and have linked sets of quantitative trait nucleotides (QTN) (Cubillos et al. 2011; Liti and Louis 2012; Sinha et al. 2006). In fact, it has been shown that sporulation efficiency in yeast is controlled by four QTNs (Gerke, Lorenz, and Cohen 2009).

3.4.7 Inter-species hybrids generate new QTLs not present in parental intra-species crosses.

Finally, we investigated whether the phenotypic effect of the *ASI2*, *FUS3* and *GIT1*, allelic variants was exclusive to the inter-species hybrid background. If the QTLs are hybrid-dependent, then they should not be present in crosses involving only strains belonging to the same species. Hence, we evaluated the presence of QTLs involving different *S. cerevisiae* alleles in intra-specific crosses between the two relevant *S. cerevisiae* strains (Figure 3-5, Panel E, F, G, H). Specifically, the validation was performed through RHA on *S. cerevisiae*

Sc^{OS104}/Sc^{OS253} diploids. No significant difference in fitness between the allelic variants was observed for both *ASI2* and *GIT1* alleles, indicating that such QTLs are exclusive to inter-species hybrid background (Table A-12, Appendix A). In the Sc^{OS104}/Sc^{OS253} diploids, *FUS3* alleles showed a significant difference in the integral area of the curve (p value = 0.0196; Table A-12, Appendix A) and growth rate (p value = 0.0014, Table A-12, Appendix A). This phenotypic variation is however opposite to that one observed in Sc/Sk_m tetraploids, suggesting that also in this case the allelic differences are influenced by the inter-species hybrid genomes. Moreover, a temperature-QTL including *FUS3* was also mapped in Sc/Sj_m hybrids suggesting that the phenotypic effect may be indeed hybrid background independent.

3.5 Discussion

Hybrid sterility can be overcome by doubling the genome of the hybrid. Such fertility restored hybrids, known as amphidiploids, are commonly found in plants and represent the majority of major evolutionary events in angiosperms (Wang et al. 2011; Zhang et al. 2016). Tetraploidisation, resulting in amphidiploids, can also restore fertility in yeast hybrids (Greig et al. 2002). *Saccharomyces* yeast hybrids have now entered the realm of classical genetic analysis as well as molecular genetic analysis. Previous studies have created variants of many inter-species hybrids and some even have been able to complete one round of meiotic recombination allowing some linkage analysis of genetic variants associated with traits of interest. Here we take this one step further by overcoming hybrid sterility in ways that allow continuous sequential crossing resulting in advanced intercross lines that bring in the full power of breeding genetics and quantitative genetic analysis of hybrid traits. We demonstrate that multiple traits of interest can be analysed with the same sensitivity and resolution as performed for intra-species studies. Moreover, we compare different QTL analysis approaches and can advise that the Multipool approach is more efficient for detecting most QTL than pools of highly selected subpopulations. The multipool approach will not resolve tightly linked sets of QTN within a QTL, such as the *ASI2* alleles likely to be linked to other alleles of opposite phenotypic effect. In such cases the highly selected pool can identify these complex situations by enriching for rare recombinant haplotypes in the region (Liti and Louis 2012). The identification of overlapping QTL regions among progeny from different tetraploid hybrids allowed us to focus on the genes that are more likely to be responsible for the phenotypic variation. Such an approach can also identify alleles which exert a background-independent effect.

With the sterility of hybrids overcome, we have shown that the hybrid situation is even more complex than the complex trait analysis within a species.

Firstly, the type of mitochondria inherited affects the QTL landscape. We were able to compare QTL regions mapped in diploid hybrid progeny derived from tetraploid parental lines with different mitochondria. Interestingly, the majority of QTL detected were exclusive to a specific mitotype, and only a small number of QTL regions were in common among the segregants from tetraploid hybrids with different mitochondria. Although the extent of the mitochondrial-nuclear epistasis cannot be easily extrapolated from these data, these results reinforce the idea that genetic interactions between the mitochondrial and nuclear genome are important. Studies on inter-species yeast hybrids in the lab have shown a correlation between the origin of the mitochondrial genome and the higher stability of one of the nuclear genomes (Antunovics et al. 2005; Peris et al. 2020). Moreover, several mitochondrial-nuclear incompatibilities leading to respiratory deficiencies have been identified in yeast hybrids (Lee et al. 2008), and some are associated with the splicing of mitochondrial intron cox1I3β (Spirek et al. 2014). The incompatibility of the *S. uvarum* mitochondrion with the *S. cerevisiae* nucleus was reinforced by the transplacement of mitochondria isolated from *S. uvarum* (Osusky, Kissova, and Kovac 1997; Spirek et al. 2000). A recent study on *S.cerevisiae*/*S. uvarum* hybrids has also shown that selective mitochondria retention is influenced by its contribution to hybrid fitness in different environments, and the type of mitochondria inherited affect the nuclear transcription at alleles level (Hewitt et al. 2020). In yeast, mitochondrial-nuclear epistasis also contributes to coadaptation to changing environmental conditions (Paliwal, Fiumera, and Fiumera 2014; Zeyl, Andreson, and Weninck 2005; Wolters et al. 2018; De Chiara et al. 2020). These mitochondrial-nuclear interactions are examples of the growing number of Bateson–Dobzhansky–Müller (B-D-M) incompatibilities affecting the function of certain processes and fitness, but are not directly leading to inviability/infertility, so called speciation genes, which are quite rare in *Saccharomyces* (Dujon and Louis 2017). Mitochondrial-nuclear epistasis has been shown to affect phenotypes in several taxa. In insects, such as *Drosophila* and *Callosobruchus*, exchange of mtDNA variant has led to decreased metabolic rate (Dowling, Abiega, and Arnqvist 2007) and shortened life span (Zhu, Ingelmo, and Rand 2014). In mice it is known to affect cognition and respiratory functions (Roubertoux et al. 2003; Betancourt et al. 2014). Interactions between mitochondrial and nuclear genomes can result in cytoplasmic male sterility in plants (Hu et al. 2014) and impact ageing and longevity in humans (Tranah 2011).

Secondly, and even more profound, new QTLs are generated in hybrids. This is allelic

variation that has no phenotypic consequences in a parent species but has phenotypic consequences in the hybrid. Reciprocal-hemizygosity analysis (Steinmetz et al. 2002) on *ASI2*, *FUS3* and *GIT1*, was carried out to assess the fitness the Sc^{OS253} and Sc^{OS104} alleles in inter-specific tetraploid hybrid ($Sc^{OS253}/Sk^{OS575}/Sc^{OS104}/Sk^{IFO1802}$) and in *S. cerevisiae* intra-specific diploid hybrid (Sc^{OS104}/Sc^{OS253}) and we showed that these QTLs are exclusive to inter-species hybrid background. The potential, therefore, for exploiting natural genetic variation in developing new hybrids, is greater than expected and bodes well for future advances in yeast breeding for improvement.

3.6 Materials and Methods

3.6.1 Strains, growth conditions and sporulation

The complete list of diploid strains used in this study is shown in Dataset S5 (Naseeb et al. 2021). These strains were chosen for the creation of *de novo* inter-species and intra-species hybrids. Yeast strains were routinely cultured in YPD medium (1% yeast extract, 2% peptone, and 2% glucose, Formedium, Norfolk, UK). To select for the drug resistance markers, YPD medium was supplemented either with 300 µg/ml geneticin, 300 µg/ml hygromycin B, 100 µg/ml nourseothricin or 10 µg/mL bleomycin.

3.6.2 Construction of genetically stable haploid strains

All the haploid strains used in this study are listed in Table A-13 (Appendix A). Genetically stable haploid *S. cerevisiae* strains used to make the hybrids were obtained from the Louis lab (Cubillos, Louis, and Liti 2009) and from derivatives of these (Louvel et al. 2014). *S. jurei* haploid strain was constructed previously in Delneri lab (Naseeb et al. 2017). *S. uvarum*, *S. eubayanus* and *S. kudriavzevii* haploid strains were engineered in this study, by deleting the HO gene. The plasmids and the primers used for the gene deletion and verification are listed in Table A-14 (Appendix A) and Dataset S6 (Naseeb et al. 2021), respectively. Prototrophic diploid strains were made heterothallic by knocking out the *HO* gene using standard PCR-mediated gene deletion strategy containing drug resistance cassettes (Guldener et al. 1996). The marker cassettes were amplified from plasmids listed in Table A-14 (Appendix A). Plasmids pAG32, pZC1, pZC2 and pZC4 were used to create stable haploids, pS30 pFA6-KanMX4 was used to create diploid maters in *S. eubayanus* and *S. uvarum* strains, whilst pFP18 was used to this effect in *S. cerevisiae* strains. A standard PEG/LiAc heat-shock protocol was used for transformation (Gietz and Schiestl 2007). The *HO* gene deletion was verified by diagnostic colony PCR using gene specific and cassette-specific primers. The primers used

for amplification of gene knock-out cassettes and for verification of gene deletions are listed in Dataset S6 (Naseeb et al. 2021). The heterozygote *HO/ho*Δ diploid strains were sporulated and tetrads were dissected to obtain stable *Mat***a** and *Matα ho*Δ haploid strains.

3.6.3 Generating Tetraploid Hybrids and Sporulation

Mass mating, sporulation and tetrad dissection were conducted by following standard protocols (Sherman and Hicks 1991). The sporulation of the strains was carried out in sporulation medium (potassium acetate 1%, agar 2%) for five days at 21ºC. Two approaches to generating tetraploids of hybrids were used (Figure 3-1). One, developed by Greig et al. (Greig et al. 2002) started with diploid hybrids between *S. cerevisiae* and other *Saccharomyces* species (inter-species diploids). In these the *S. cerevisiae* copy of the *MAT* locus was deleted creating a diploid that behaved as a haploid. In the study of Greig et al. (Greig et al. 2002) these were *HO*, so they switched and mated creating tetraploids with the two remaining MAT loci coming from the non-cerevisiae parent. Here we used *ho*Δ haploids to start with and created two versions of diploid hybrids where in one the *S. cerevisiae* parent had one mating type while the other had the opposite. In addition, two different *S. cerevisiae* strains and two of the other parent species were used to incorporate genetic diversity in each tetraploid. The *S. cerevisiae MAT* locus in each was deleted in the same way as in Greig et al. (Greig et al. 2002) and the resultant mating diploid hybrids were mated generating tetraploids, heterozygous for many SNPs across both genomes. In this method every meiotic spore will be a diploid hybrid that can mate, allowing further rounds of mating and meiosis. The second method started with heterozygous diploids of each species (intra-species diploids). Here one of the two *MAT* loci is deleted, and species diploids of opposite mating type are mated generating tetraploids, also heterozygous for many SNPs across both genomes. In this case, meiotic spores will all be diploid hybrids but will be a mixture of non-maters and maters, still allowing for continuous rounds of mating and meiosis. In generating the various combinations of diploids to start with, the *MAT* locus was analyzed by the PCR method described previously (Huxley, Green, and Dunham 1990). The species of diploid spores was determined by species specific PCR (Muir, Harrison, and Wheals 2011). The primers used are listed in supplementary Dataset S6 (Naseeb et al. 2021). The cycling condition of the PCR reaction to amplify both regions are as follows: 3 min at 95°C for the first cycle, then 1 min at 95°C, 1 min at 55°C, 3 min at 72°C for 35 cycle, and 5 min at 72°C for the last cycle.

3.6.4 Multigenerational advanced intercross lines

Tetraploids were subjected to sporulation and tetrads were isolated for dissection to assess the spore viability and phenotypic variation and to prepare the spores for further rounds of mating. After 5-7 days of sporulation, tetrads were isolated for dissection (as above) for assessing spore viability and phenotypic variation or random spore generation for further rounds of mating. For random spores, asci were washed from the sporulation plate with the help of glass beads and water. Suspended asci were pipetted into Eppendorf tubes and washed once with water and resuspended in 0.5ml water. 0.5ml of di-ethyl ether was added and the mixture vortexed for 10 minutes to kill any vegetative, unsporulated cells (Dawes and Hardie 1974). These were then microfuged and the supernatant removed. The spore pellets were washed twice in water and resuspended in dissection buffer and treated with Zymolyase 20T (1/10 volume of 10mg/ml solution) at 37^{o}C for 30 minutes before washing and plating onto YPD media to allow germination and mating. After growth for 24 hours, the lawn of cells is replica plated onto new sporulation media and the cycle starts again. In method one, all cells that can sporulate in subsequent rounds are tetraploids generating diploid hybrid progeny. In method two, approximately 1/3 of the sporulating cells will be diploid non-mating hybrids from the previous round and their spores will be non-viable and not enter the next round. The rest of the sporulating cells will be tetraploids generating the same mixture of mater and non-mater diploid hybrid progeny.

3.6.5 Analysis of mitochondrial origin in hybrids

For each diploid mater, a petite version was generated by exposure to ethidium bromide (EtBr) (Goldring, Grossman, and Marmur 1971). Isolates were seeded at an approximate density of 300 individuals per plate. A 3µl drop of EtBr (10 mg/ml) was spotted onto the centre of each plate. A ring around the spot formed where all cells were killed due to the toxic effects of EtBr. Surrounding this kill zone, a ring of petite colonies form. Loss of mitochondria enables petites to grow faster than colonies with functional mitochondria, in the presence of EtBr. These individuals were confirmed as petites by their inability to grow on YPD plates containing ethanol and glycerol, non-fermentable carbon sources (Day 2013). The specific mitotype was identified by amplifying the *COX2* and *COX3* genes through colony PCR as described previously (Hewitt et al. 2020). The primers used for the amplification of these genes are listed in Dataset S6 (Naseeb et al. 2021).

3.6.6 Phenotypic Assays

A high-throughput spot assay was performed using Singer ROTOR HDA robot (Singer Instruments, UK) as mentioned previously (Naseeb et al. 2018). The fitness of ~384 hybrid spores was assessed at five different temperatures *i.e.* 10°C, 16°C, 23°C, 30°C and 37°C, under different carbon sources at 30°C *i.e.* YPA + 10% & 15% maltose, YPA + 10% & 15% fructose, YPA + 10% & 15% sucrose, YPA + 10% & 15% galactose, YPA + 30% & 35% glucose and under different environmental stressors at 30°C *i.e.* YPAD + 6% & 10% ethanol, YPAD + 0.3% & 0.5% acetic acid, YPAD + 4 mM hydrogen peroxide, YPAD + 50 mM levulinic acid and YPA + 10% & 15% glycerol.

Fitness analysis was done following two different strategies. In strategy one, high-resolution images of phenotypic plates were taken using Phenobooth after 3 days of incubation (Singer Instruments, UK). The colony sizes were calculated in pixels using Phenosuite software (Singer Instruments, UK) and the heat maps of the phenotypic behaviours were constructed using a in-house R shiny app[1]. In strategy two, phenotyping was performed using the PHENOS platform (Barton et al. 2018). Change in absorbance (600 nm) was measured using the FLUOstar Omega plate reader (BMG Labtech). Prior to seeding cells on selection plates, a blank reading was taken, with values subtracted from each time course reading. Plates were incubated at 30°C (except for temperature selection plates) and absorbance was measured every 20 minutes over the course of three days. Individuals were ranked by the maximum change in absorbance, after normalisation for the maximum change in absorbance under control conditions.

3.6.7 Sequencing, Mapping and Variant Calling

Each parental genome in the hybrid was sequenced previously (Naseeb et al. 2018) or in this study at the Earlham Institute or at the GTCF of the University of Manchester. Two different pooling strategies were followed for Multipool and Pooled selection, respectively. In strategy one, from each selective media plate the top twenty performing F12 individuals, with the highest fitness, and the twenty lowest performing F12 individuals were picked for pooling. In second strategy, a pool of $1 * 10^8$ F12 cells were seeded onto each selection condition as well as the YPD control. Selection conditions were prepared so that only the top 0.1 – 1 % of

[1] https://kobchai- 180 shinyapps01.shinyapps.io/heatmap_construction/

the pool would be capable of growth. The sequencing was done to 100-120X coverage on the Illumina platform.

Paired-end raw Illumina sequence reads were quality checked through FastQC 0.11.5 (Andrews 2010) and trimmed through Trimmomatic 0.36 (Bolger, Lohse, and Usadel 2014). Alignments to reference genomes were then applied for founder sequences and hybrids pool sequences using bwa/0.7.16a (Li and Durbin 2009). For each cross of parental species, reference genome was selected from one of the founder species (*S. cerevisiae* OS104 (Yue et al. 2017), *S. eubayanus* OS578 (Libkind et al. 2011), *S. jurei* D5088 (Naseeb et al. 2018), and *S. kudriavzevii* IFO 1802 assembled by using SPAdes assembler 3.9.0). The sequencing reads of alternative founder for each cross of parental species is mapped to reference founder parental genomes. For hybrid pool sequences, reads are mapped to a combined reference genome with *S. cerevisiae* YP128 concatenated with *S. eubayanus* CBS12357 / *S. jurei* D5088 / *S. kudriavzevii* IFO1802. Assembly quality was assessed through QUAST/4.3. Local realignment was then performed to minimise the number of mismatching bases through RealignerTargetCreator and IndelRealigner using GATK 3.8. The MarkDuplicates tool was then used with picard /2.6.0 for removing the optical duplicates to control the alignment quality for variant analysis. Samtools was applied for sorting and indexing (Li et al. 2009). Variant calling was then applied on the aligned reads using freebayes/1.0.2 (Garrison E 2012) with ploidy setting at 1 with the combined reference as well as the following parameters --min-mapping-quality 30 --min-base-quality 20 --no-mnps. The bi-allele markers for each cross founder species were identified for the variants sites that differed between the parents. Reads depths below 10 were excluded. Pool SNPs were extracted for the variants sites with allele depth counts and variant positions to reference genome which were further compared to the bi-allele marker sets among the founders through an R script. This variant calling pipeline is displayed in Figure A-4 (Appendix A).

Based on the counts of each bi-allele markers, reads depths at each allele is recorded and allele frequency can be determined. Absolute allele frequency differences were calculated for each experiment. Each experiment consists of two pools for comparison.

3.6.8 QTL mapping

Multipool analysis: 384 diploid hybrid spores from each F12 tetraploid population were arrayed on plates for phenotyping. For each condition tested the best and worst performers were chosen and DNA was prepared from each individually. Concentrations of DNA were adjusted so that the pool of 20 had equal contributions from each individual. These were then

sequenced as described above and allele frequencies of segregating SNPs compared as follows: read counts for the allele positions of each pool were used to compute LOD scores using the MULTIPOOL method (Edwards and Gifford 2012) with the "contrast" mode, bin size of 100 bp and centimorgan length at 3300 CM for yeast average as suggested. N=20 and N=150 are run for each comparison. According to Treusch et al. (Treusch et al. 2015), the n parameter only affects the magnitude of LOD scores and not their overall shape. To assess statistical significance, LOD thresholds were set at 0 for N=20 and 5 for N=150 (Treusch et al. 2015) with 1-LOD drop from the peak LOD bin as the QTL interval region. For N of these sizes there is a basal minimum LOD that is less than 0 which is why a threshold of 0 can be used. For N=20 in the *S. cerevisiae x S. eubayanus* data analysis, the basal minimum is -1.3 while for the N=150 analyses the minimum is -0.43. In order to assure ourselves that we were not overestimating QTLs for the N=20 analyses, we looked at the distribution of LOD values for each bin generated to see where the values of selected QTLs fall. All are above the upper range limits (1.5 *IQR + Q3) where the lowest value is -0.58 for very low temperature group and highest value is -0.22 for ethanol. This means that we expect LOD scores less than the -0.58 for low temperature under the pool size of 20 occur by chance and the threshold of 0 can filter these out. Moreover, to further validate the significance of the results, 1000 permutation re-samplings were tested for each comparison. We applied multipool QTL to pair the high and low fitness for each experiment and shuffled the data to break any relationship between the two. Any "QTL" in such comparisons must be due to technical or biological noise as they are randomly resampled. The maximum LOD score is then recorded on each permutation which represents the highest LOD score generated by random chance. Under 95% percentile (significance level 5%), the thresholds generated range from -0.0928 with an estimated FDR for threshold 0 of 0.0465 for high temperature, to -0.6617 with an estimated FDR for threshold 0 of 0.002 for very low temperature. The overall threshold generated is -0.2962 with an estimated FDR for threshold 0 of 0.02423 (Brion, Lutz, and Albert 2020). We are therefore satisfied that the use of threshold 0 to select significantly associated QTLs.

Selected pool analysis: Absolute allele frequency differences between the control and treatment pools are calculated and continuous curves were fitted with the smoothing method with geom_smooth() which is similar to the method described in Huang et al. 2020 (Huang et al. 2020). Under the null hypothesis that the allele frequencies are the same between the unselected pool and selected pool, the larger the absolute value of the allele frequency difference, the more significance there should be accounted for by the markers. Based on this identification, the peak QTL is decided by the absolute allele frequency difference more than

0.2 along with a p-value based on a Fisher exact test. A maximum of one peak per chromosome if significant was chosen for analysis.

QTL regions associated with the phenotype were identified by analyzing the changes in frequencies of SNP alleles across the genomes.

3.6.9 Gene ontology and SIFT analysis

Gene ontology (GO) terms were determined using the GO Term Finder tool of *Saccharomyces* Genome Database (SGD) with the Bonferroni correction for multiple hypothesis and a p-value cutoff of 0.01.

Potential causal genes were analysed with the Sorting Intolerant from Tolerant (SIFT) algorithm to assess if amino-acids variants were predicted to influence the protein function. SIFT analysis were conducted using data from Bergstrom et al. (Bergstrom et al. 2014) on the *S. cerevisiae* strains OS3, OS104 and OS253, and the tool mutfunc (Wagih et al. 2018).

3.6.10 Validation of candidate genes through reciprocal hemizygosity analysis

The candidate genes selected for reciprocal-hemizygosity analysis (RHA) were chosen based on their LOD score and on gene ontology studies carried out with YeastMine (Balakrishnan et al. 2012) and Funspec (Robinson et al. 2002) to prioritize terms connected to the phenotypic trait tested.

To dissect the mapped QTL regions and confirm the effect of candidate genes in determining the phenotypic fitness, we performed reciprocal-hemizygosity analysis (Steinmetz et al. 2002) on selected candidate genes: *ASI2*, *FUS3* and *GIT1*. PCR mediated deletion of the target genes was performed in the engineered *S. cerevisiae/S. kudriavzevii* hybrid (Sc^{OS253}/Sk^{OS575} and $Sc^{OS104}/Sk^{IF01802}$), to delete each *S. cerevisiae* allele. The transformants were then mass mated together to construct the reciprocal hemizygotes hybrid and selected in triple drug plates (300 µg/ml geneticin, 100 µg/ml nourseothricin and 10 µg/mL bleomycin) (Figure 3-5A, Table A-15, Appendix A).

To investigate if the effect of the allelic variants was exclusive to the inter-species hybrid background rather than to the intra-species strain, PCR-mediated deletion was used to generate null mutants of the parental *S. cerevisiae* haploid strains (Sc^{OS253} and Sc^{OS104}) for the candidate genes. The transformed haploid strains were them mass mated together to construct the reciprocal hemizygotes hybrids and selected in SD +ura +leu with 100 µg/ml nourseothricin or 300 µg/ml geneticin (Table A-15, Appendix A). Successful gene deletions

were confirmed by PCR. All the primers used for the construction of the strains are listed in Dataset S6 (Naseeb et al. 2021).

The fitness of the *S. cerevisiae* allelic variants of *FUS3*, *GIT1* and *ASI2* was assessed both in the hemizygous *S. cerevisiae* / *S. kudriavzevii* tetraploids and in the hemizygous *S. cerevisiae* diploids. The *FUS3* and *GIT1* allelic variants was assessed with a BMG FLUOstar OPTIMA Microplate 466 Reader as previously described (Naseeb and Delneri 2012) in YPD at 10°C, and at 25°C in YPD + 15% maltose, respectively. The fitness of *ASI2* hemizygous hybrids was assessed with the BioLector (m2p Labs, GmbH). A 48-well flowerplate with transparent glass bottom was inoculated with overnight cultures at a starting OD_{600} of 0.1. Every culture was run in triplicates in 1.5 ml of YPD + 0.3% acetic acid. The flowerplate was incubated at 30°C in the BioLector with orbital shaking of 800 rpm and oxygenation was maintained at 20%. Scatter light readings, to measure the cell density, were taken from the bottom of each well every 8 min with a gain of 15 and 25. The growth characteristics of the plate reader experiments were assessed with the R package Growthcurver using K as maximum biomass, *r* as maximum growth rate, *auc_l* as integral area (Sprouffske and Wagner 2016) and T_{mid} as the time at which the population density reaches *1/K*.

3.6.11 Data availability

The sequencing data generated in this study was deposited on the European Nucleotide Archive (ENA) (Project PRJEB44105). The datasheets referred as Dataset S1-6 throughout the paper are available from the published version of the paper at doi: 10.1073/pnas.210124211.

3.7 Acknowledgments

The authors wish to thank Gianni Liti, Chris Powell, Philippe Malcorps and Stewart Wilkinson for useful discussions, and Ian Donaldson for initial bioinformatic support. Sequencing was done through Genomic Services at the Earlham Institute and Genomic Technologies Core Facility at the University of Manchester. This work was funded by a BBSRC grant to EJL (BB/L022508/1) and DD (BB/L021471/1) in collaboration with SAB-Miller and AB-InBev; FV is supported by H2020-MSCA-ITN-2017 grant to DD (764364; https://cordis.europa.eu/project/id/764364). AHR has been supported by BBSRC-CASE studentship to EJL (BB/L017229/1). Strains were obtained from various culture collections as referenced. The *S. eubayanus* type strain, CBS12357, was obtained from CBS-KNAW (Westerdijk Fungal Biodiversity Institute) under MTA for academic research use. The Chinese strains LZSP32.1, CDFM212.1 and 48BYC-4 were obtained from Prof Fen-Yang Bai

and the China General Microbiological Culture Collection Center (CGMCC) under MTA for academic research use.

3.8 References

Albertin, W., T. da Silva, M. Rigoulet, B. Salin, I. Masneuf-Pomarede, D. de Vienne, D. Sicard, M. Bely, and P. Marullo. 2013. 'The mitochondrial genome impacts respiration but not fermentation in interspecific Saccharomyces hybrids', *PLoS One*, 8: e75121.

Andrews, S. 2010. 'FastQC A Quality Control Tool for High Throughput Sequence Data'.

Antunovics, Z., H. V. Nguyen, C. Gaillardin, and M. Sipiczki. 2005. 'Gradual genome stabilisation by progressive reduction of the Saccharomyces uvarum genome in an interspecific hybrid with Saccharomyces cerevisiae', *FEMS Yeast Res*, 5: 1141-50.

Awad, A. M., M. C. Bradley, L. Fernandez-Del-Rio, A. Nag, H. S. Tsui, and C. F. Clarke. 2018. 'Coenzyme Q10 deficiencies: pathways in yeast and humans', *Essays Biochem*, 62: 361-76.

Baker, E. P., D. Peris, R. V. Moriarty, X. C. Li, J. C. Fay, and C. T. Hittinger. 2019. 'Mitochondrial DNA and temperature tolerance in lager yeasts', *Sci Adv*, 5: eaav1869.

Baker, E., B. Wang, N. Bellora, D. Peris, A. B. Hulfachor, J. A. Koshalek, M. Adams, D. Libkind, and C. T. Hittinger. 2015. 'The Genome Sequence of Saccharomyces eubayanus and the Domestication of Lager-Brewing Yeasts', *Mol Biol Evol*, 32: 2818-31.

Balakrishnan, R., J. Park, K. Karra, B. C. Hitz, G. Binkley, E. L. Hong, J. Sullivan, G. Micklem, and J. M. Cherry. 2012. 'YeastMine--an integrated data warehouse for Saccharomyces cerevisiae data as a multipurpose tool-kit', *Database (Oxford)*, 2012: bar062.

Barbosa, R., P. Almeida, S. V. Safar, R. O. Santos, P. B. Morais, L. Nielly-Thibault, J. B. Leducq, C. R. Landry, P. Goncalves, C. A. Rosa, and J. P. Sampaio. 2016. 'Evidence of Natural Hybridization in Brazilian Wild Lineages of Saccharomyces cerevisiae', *Genome Biol Evol*, 8: 317-29.

Barton, D. B. H., D. Georghiou, N. Dave, M. Alghamdi, T. A. Walsh, E. J. Louis, and S. S. Foster. 2018. 'PHENOS: a high-throughput and flexible tool for microorganism growth phenotyping on solid media', *BMC Microbiol*, 18: 9.

Belloch, C., S. Orlic, E. Barrio, and A. Querol. 2008. 'Fermentative stress adaptation of hybrids within the Saccharomyces sensu stricto complex', *Int J Food Microbiol*, 122: 188-95.

Bergstrom, A., J. T. Simpson, F. Salinas, B. Barre, L. Parts, A. Zia, A. N. Nguyen Ba, A. M. Moses, E. J. Louis, V. Mustonen, J. Warringer, R. Durbin, and G. Liti. 2014. 'A high-definition view of functional genetic variation from natural yeast genomes', *Mol Biol Evol*, 31: 872-88.

Betancourt, A. M., A. L. King, J. L. Fetterman, T. Millender-Swain, R. D. Finley, C. R. Oliva, D. R. Crowe, S. W. Ballinger, and S. M. Bailey. 2014. 'Mitochondrial-nuclear genome interactions in non-alcoholic fatty liver disease in mice', *Biochem J*, 461: 223-32.

Bolger, A. M., M. Lohse, and B. Usadel. 2014. 'Trimmomatic: a flexible trimmer for Illumina sequence data', *Bioinformatics*, 30: 2114-20.

Brion, C., S. M. Lutz, and F. W. Albert. 2020. 'Simultaneous quantification of mRNA and protein in single cells reveals post-transcriptional effects of genetic variation', *Elife*, 9.

Buzzini, P., E. Branda, M. Goretti, and B. Turchetti. 2012. 'Psychrophilic yeasts from worldwide glacial habitats: diversity, adaptation strategies and biotechnological potential', *FEMS Microbiol Ecol*, 82: 217-41.

Cherry, J. M., E. L. Hong, C. Amundsen, R. Balakrishnan, G. Binkley, E. T. Chan, K. R. Christie, M. C. Costanzo, S. S. Dwight, S. R. Engel, D. G. Fisk, J. E. Hirschman, B. C. Hitz, K. Karra, C. J. Krieger, S. R. Miyasato, R. S. Nash, J. Park, M. S. Skrzypek, M. Simison, S. Weng, and E. D. Wong. 2012. 'Saccharomyces Genome Database: the genomics resource of budding yeast', *Nucleic Acids Res*, 40: D700-5.

Cubillos, F. A., E. Billi, E. Zorgo, L. Parts, P. Fargier, S. Omholt, A. Blomberg, J. Warringer, E. J. Louis, and G. Liti. 2011. 'Assessing the complex architecture of polygenic traits in diverged yeast populations', *Mol Ecol*, 20: 1401-13.

Cubillos, F. A., E. J. Louis, and G. Liti. 2009. 'Generation of a large set of genetically tractable haploid and diploid Saccharomyces strains', *FEMS Yeast Res*, 9: 1217-25.

Cubillos, F. A., L. Parts, F. Salinas, A. Bergstrom, E. Scovacricchi, A. Zia, C. J. Illingworth, V. Mustonen, S. Ibstedt, J. Warringer, E. J. Louis, R. Durbin, and G. Liti. 2013. 'High-resolution mapping of complex traits with a four-parent advanced intercross yeast population', *Genetics*, 195: 1141-55.

Dawes, I. W., and I. D. Hardie. 1974. 'Selective killing of vegetative cells in sporulated yeast cultures by exposure to diethyl ether', *Mol Gen Genet*, 131: 281-9.

Day, M. 2013. 'Yeast petites and small colony variants: for everything there is a season', *Adv Appl Microbiol*, 85: 1-41.

De Chiara, M., A. Friedrich, B. Barre, M. Breitenbach, J. Schacherer, and G. Liti. 2020. 'Discordant evolution of mitochondrial and nuclear yeast genomes at population level', *BMC Biol*, 18: 49.

Delneri, D., D. C. Hoyle, K. Gkargkas, E. J. Cross, B. Rash, L. Zeef, H. S. Leong, H. M. Davey, A. Hayes, D. B. Kell, G. W. Griffith, and S. G. Oliver. 2008. 'Identification and characterization of high-flux-control genes of yeast through competition analyses in continuous cultures', *Nat Genet*, 40: 113-7.

Dimmer, K. S., S. Fritz, F. Fuchs, M. Messerschmitt, N. Weinbach, W. Neupert, and B. Westermann. 2002. 'Genetic basis of mitochondrial function and morphology in Saccharomyces cerevisiae', *Mol Biol Cell*, 13: 847-53.

Dowling, D. K., K. C. Abiega, and G. Arnqvist. 2007. 'Temperature-specific outcomes of cytoplasmic-nuclear interactions on egg-to-adult development time in seed beetles', *Evolution*, 61: 194-201.

Dujon, B. A., and E. J. Louis. 2017. 'Genome Diversity and Evolution in the Budding Yeasts (Saccharomycotina)', *Genetics*, 206: 717-50.

Dunn, B., and G. Sherlock. 2008. 'Reconstruction of the genome origins and evolution of the hybrid lager yeast Saccharomyces pastorianus', *Genome Res*, 18: 1610-23.

Edwards, M. D., and D. K. Gifford. 2012. 'High-resolution genetic mapping with pooled sequencing', *BMC Bioinformatics*, 13 Suppl 6: S8.

Ehrenreich, I. M., N. Torabi, Y. Jia, J. Kent, S. Martis, J. A. Shapiro, D. Gresham, A. A. Caudy, and L. Kruglyak. 2010. 'Dissection of genetically complex traits with extremely large pools of yeast segregants', *Nature*, 464: 1039-42.

Ellison, C. K., O. Niehuis, and J. Gadau. 2008. 'Hybrid breakdown and mitochondrial dysfunction in hybrids of Nasonia parasitoid wasps', *J Evol Biol*, 21: 1844-51.

Fields, S. D., M. N. Conrad, and M. Clarke. 1998. 'The S. cerevisiae CLU1 and D. discoideum cluA genes are functional homologues that influence mitochondrial morphology and distribution', *J Cell Sci*, 111 (Pt 12): 1717-27.

Gallone, B., J. Steensels, S. Mertens, M. C. Dzialo, J. L. Gordon, R. Wauters, F. A. Thesseling, F. Bellinazzo, V. Saels, B. Herrera-Malaver, T. Prahl, C. White, M. Hutzler, F. Meussdoerffer, P. Malcorps, B. Souffriau, L. Daenen, G. Baele, S. Maere, and K. J. Verstrepen. 2019. 'Interspecific hybridization facilitates niche adaptation in beer yeast', *Nat Ecol Evol*, 3: 1562-75.

Garcia-Rios, E., A. Guillen, R. de la Cerda, L. Perez-Traves, A. Querol, and J. M. Guillamon. 2018. 'Improving the Cryotolerance of Wine Yeast by Interspecific Hybridization in the Genus Saccharomyces', *Front Microbiol*, 9: 3232.

Garrison E, Marth G. 2012. 'Haplotype-based variant detection from short-read sequencing', *arXiv*, 2012;1207.3907.

Gerke, J., K. Lorenz, and B. Cohen. 2009. 'Genetic interactions between transcription factors cause natural variation in yeast', *Science*, 323: 498-501.

Gibson, B. R., S. J. Lawrence, J. P. Leclaire, C. D. Powell, and K. A. Smart. 2007. 'Yeast responses to stresses associated with industrial brewery handling', *FEMS Microbiol Rev*, 31: 535-69.

Gietz, R. D., and R. H. Schiestl. 2007. 'High-efficiency yeast transformation using the LiAc/SS carrier DNA/PEG method', *Nat Protoc*, 2: 31-4.

Goldring, E. S., L. I. Grossman, and J. Marmur. 1971. 'Petite mutation in yeast. II. Isolation of mutants containing mitochondrial deoxyribonucleic acid of reduced size', *J Bacteriol*, 107: 377-81.

Gonzalez, S. S., E. Barrio, J. Gafner, and A. Querol. 2006. 'Natural hybrids from Saccharomyces cerevisiae, Saccharomyces bayanus and Saccharomyces kudriavzevii in wine fermentations', *FEMS Yeast Res*, 6: 1221-34.

Gonzalez, S. S., E. Barrio, and A. Querol. 2008. 'Molecular characterization of new natural hybrids of Saccharomyces cerevisiae and S. kudriavzevii in brewing', *Appl Environ Microbiol*, 74: 2314-20.

Greig, D., R. H. Borts, E. J. Louis, and M. Travisano. 2002. 'Epistasis and hybrid sterility in Saccharomyces', *Proc Biol Sci*, 269: 1167-71.

Guldener, U., S. Heck, T. Fielder, J. Beinhauer, and J. H. Hegemann. 1996. 'A new efficient gene disruption cassette for repeated use in budding yeast', *Nucleic Acids Res*, 24: 2519-24.

Hewitt, S. K., K. Duangrattanalert, T. Burgis, L. A. H. Zeef, S. Naseeb, and D. Delneri. 2020. 'Plasticity of Mitochondrial DNA Inheritance and its Impact on Nuclear Gene Transcription in Yeast Hybrids', *Microorganisms*, 8.

Higgins, V. J., N. Alic, G. W. Thorpe, M. Breitenbach, V. Larsson, and I. W. Dawes. 2002. 'Phenotypic analysis of gene deletant strains for sensitivity to oxidative stress', *Yeast*, 19: 203-14.

Hu, J., W. Huang, Q. Huang, X. Qin, C. Yu, L. Wang, S. Li, R. Zhu, and Y. Zhu. 2014. 'Mitochondria and cytoplasmic male sterility in plants', *Mitochondrion*, 19 Pt B: 282-8.

Huang, L., W. Tang, S. Bu, and W. Wu. 2020. 'BRM: a statistical method for QTL mapping based on bulked segregant analysis by deep sequencing', *Bioinformatics*, 36: 2150-56.

Hueso, G., R. Aparicio-Sanchis, C. Montesinos, S. Lorenz, J. R. Murguia, and R. Serrano. 2012. 'A novel role for protein kinase Gcn2 in yeast tolerance to intracellular acid stress', *Biochem J*, 441: 255-64.

Huxley, C., E. D. Green, and I. Dunham. 1990. 'Rapid assessment of S. cerevisiae mating type by PCR', *Trends Genet*, 6: 236.

Krogerus, K., F. Magalhaes, V. Vidgren, and B. Gibson. 2015. 'New lager yeast strains generated by interspecific hybridization', *J Ind Microbiol Biotechnol*, 42: 769-78.

Kumar, P., S. Henikoff, and P. C. Ng. 2009. 'Predicting the effects of coding non-synonymous variants on protein function using the SIFT algorithm', *Nat Protoc*, 4: 1073-81.

Lairon-Peris, M., L. Perez-Traves, S. Muniz-Calvo, J. M. Guillamon, J. M. Heras, E. Barrio, and A. Querol. 2020. 'Differential Contribution of the Parental Genomes to a S. cerevisiae x S. uvarum Hybrid, Inferred by Phenomic, Genomic, and Transcriptomic Analyses, at Different Industrial Stress Conditions', *Front Bioeng Biotechnol*, 8: 129.

Lee, H. Y., J. Y. Chou, L. Cheong, N. H. Chang, S. Y. Yang, and J. Y. Leu. 2008. 'Incompatibility of nuclear and mitochondrial genomes causes hybrid sterility between two yeast species', *Cell*, 135: 1065-73.
Li, H., and R. Durbin. 2009. 'Fast and accurate short read alignment with Burrows-Wheeler transform', *Bioinformatics*, 25: 1754-60.
Li, H., B. Handsaker, A. Wysoker, T. Fennell, J. Ruan, N. Homer, G. Marth, G. Abecasis, R. Durbin, and Subgroup Genome Project Data Processing. 2009. 'The Sequence Alignment/Map format and SAMtools', *Bioinformatics*, 25: 2078-9.
Li, X. C., D. Peris, C. T. Hittinger, E. A. Sia, and J. C. Fay. 2019. 'Mitochondria-encoded genes contribute to evolution of heat and cold tolerance in yeast', *Sci Adv*, 5: eaav1848.
Libkind, D., C. T. Hittinger, E. Valerio, C. Goncalves, J. Dover, M. Johnston, P. Goncalves, and J. P. Sampaio. 2011. 'Microbe domestication and the identification of the wild genetic stock of lager-brewing yeast', *Proc Natl Acad Sci U S A*, 108: 14539-44.
Liti, G., D. B. Barton, and E. J. Louis. 2006. 'Sequence diversity, reproductive isolation and species concepts in Saccharomyces', *Genetics*, 174: 839-50.
Liti, G., D. M. Carter, A. M. Moses, J. Warringer, L. Parts, S. A. James, R. P. Davey, I. N. Roberts, A. Burt, V. Koufopanou, I. J. Tsai, C. M. Bergman, D. Bensasson, M. J. O'Kelly, A. van Oudenaarden, D. B. Barton, E. Bailes, A. N. Nguyen, M. Jones, M. A. Quail, I. Goodhead, S. Sims, F. Smith, A. Blomberg, R. Durbin, and E. J. Louis. 2009. 'Population genomics of domestic and wild yeasts', *Nature*, 458: 337-41.
Liti, G., and E. J. Louis. 2005. 'Yeast evolution and comparative genomics', *Annu Rev Microbiol*, 59: 135-53.
——— 2012. 'Advances in quantitative trait analysis in yeast', *PLoS Genet*, 8: e1002912.
Liti, G., A. Peruffo, S. A. James, I. N. Roberts, and E. J. Louis. 2005. 'Inferences of evolutionary relationships from a population survey of LTR-retrotransposons and telomeric-associated sequences in the Saccharomyces sensu stricto complex', *Yeast*, 22: 177-92.
Lopandic, K. 2018. 'Saccharomyces interspecies hybrids as model organisms for studying yeast adaptation to stressful environments', *Yeast*, 35: 21-38.
Lopandic, K., W. P. Pfliegler, W. Tiefenbrunner, H. Gangl, M. Sipiczki, and K. Sterflinger. 2016. 'Genotypic and phenotypic evolution of yeast interspecies hybrids during high-sugar fermentation', *Appl Microbiol Biotechnol*, 100: 6331-43.
Louis, E. J., and M. M. Becker. 2014. *Subtelomeres* (Springer Berlin Heidelberg: Berlin, Heidelberg).
Louvel, H., A. Gillet-Markowska, G. Liti, and G. Fischer. 2014. 'A set of genetically diverged Saccharomyces cerevisiae strains with markerless deletions of multiple auxotrophic genes', *Yeast*, 31: 91-101.
Mallet, J. 2007. 'Hybrid speciation', *Nature*, 446: 279-83.
Masneuf, I., J. Hansen, C. Groth, J. Piskur, and D. Dubourdieu. 1998. 'New hybrids between Saccharomyces sensu stricto yeast species found among wine and cider production strains', *Appl Environ Microbiol*, 64: 3887-92.
Mertens, S., J. Steensels, V. Saels, G. De Rouck, G. Aerts, and K. J. Verstrepen. 2015. 'A large set of newly created interspecific Saccharomyces hybrids increases aromatic diversity in lager beers', *Appl Environ Microbiol*, 81: 8202-14.
Michel, S., M. A. Keller, M. M. Wamelink, and M. Ralser. 2015. 'A haploproficient interaction of the transaldolase paralogue NQM1 with the transcription factor VHR1 affects stationary phase survival and oxidative stress resistance', *BMC Genet*, 16: 13.
Mossman, J. A., J. G. Tross, N. Li, Z. Wu, and D. M. Rand. 2016. 'Mitochondrial-Nuclear Interactions Mediate Sex-Specific Transcriptional Profiles in Drosophila', *Genetics*, 204: 613-30.

Muir, A., E. Harrison, and A. Wheals. 2011. 'A multiplex set of species-specific primers for rapid identification of members of the genus Saccharomyces', *FEMS Yeast Res*, 11: 552-63.
Naseeb, S., H. Alsammar, T. Burgis, I. Donaldson, N. Knyazev, C. Knight, and D. Delneri. 2018. 'Whole Genome Sequencing, de Novo Assembly and Phenotypic Profiling for the New Budding Yeast Species Saccharomyces jurei', *G3 (Bethesda)*, 8: 2967-77.
Naseeb, S., and D. Delneri. 2012. 'Impact of chromosomal inversions on the yeast DAL cluster', *PLoS One*, 7: e42022.
Naseeb, S., S. A. James, H. Alsammar, C. J. Michaels, B. Gini, C. Nueno-Palop, C. J. Bond, H. McGhie, I. N. Roberts, and D. Delneri. 2017. 'Saccharomyces jurei sp. nov., isolation and genetic identification of a novel yeast species from Quercus robur', *Int J Syst Evol Microbiol*, 67: 2046-52.
Okuno, M., R. Kajitani, R. Ryusui, H. Morimoto, Y. Kodama, and T. Itoh. 2016. 'Next-generation sequencing analysis of lager brewing yeast strains reveals the evolutionary history of interspecies hybridization', *DNA Res*, 23: 67-80.
Osusky, M., J. Kissova, and L. Kovac. 1997. 'Interspecies transplacement of mitochondria in yeasts', *Curr Genet*, 32: 24-6.
Paget, C. M., J. M. Schwartz, and D. Delneri. 2014. 'Environmental systems biology of cold-tolerant phenotype in Saccharomyces species adapted to grow at different temperatures', *Mol Ecol*, 23: 5241-57.
Paliwal, S., A. C. Fiumera, and H. L. Fiumera. 2014. 'Mitochondrial-nuclear epistasis contributes to phenotypic variation and coadaptation in natural isolates of Saccharomyces cerevisiae', *Genetics*, 198: 1251-65.
Parts, L., F. A. Cubillos, J. Warringer, K. Jain, F. Salinas, S. J. Bumpstead, M. Molin, A. Zia, J. T. Simpson, M. A. Quail, A. Moses, E. J. Louis, R. Durbin, and G. Liti. 2011. 'Revealing the genetic structure of a trait by sequencing a population under selection', *Genome Res*, 21: 1131-8.
Peris, D., W. G. Alexander, K. J. Fisher, R. V. Moriarty, M. G. Basuino, E. J. Ubbelohde, R. L. Wrobel, and C. T. Hittinger. 2020. 'Synthetic hybrids of six yeast species', *Nat Commun*, 11: 2085.
Piatkowska, E. M., S. Naseeb, D. Knight, and D. Delneri. 2013. 'Chimeric protein complexes in hybrid species generate novel phenotypes', *PLoS Genet*, 9: e1003836.
Pir, P., A. Gutteridge, J. Wu, B. Rash, D. B. Kell, N. Zhang, and S. G. Oliver. 2012. 'The genetic control of growth rate: a systems biology study in yeast', *BMC Syst Biol*, 6: 4.
Popova, Y., P. Thayumanavan, E. Lonati, M. Agrochao, and J. M. Thevelein. 2010. 'Transport and signaling through the phosphate-binding site of the yeast Pho84 phosphate transceptor', *Proc Natl Acad Sci U S A*, 107: 2890-5.
Rep, M., M. Proft, F. Remize, M. Tamas, R. Serrano, J. M. Thevelein, and S. Hohmann. 2001. 'The Saccharomyces cerevisiae Sko1p transcription factor mediates HOG pathway-dependent osmotic regulation of a set of genes encoding enzymes implicated in protection from oxidative damage', *Mol Microbiol*, 40: 1067-83.
Robinson, M. D., J. Grigull, N. Mohammad, and T. R. Hughes. 2002. 'FunSpec: a web-based cluster interpreter for yeast', *BMC Bioinformatics*, 3: 35.
Roubertoux, P. L., F. Sluyter, M. Carlier, B. Marcet, F. Maarouf-Veray, C. Cherif, C. Marican, P. Arrechi, F. Godin, M. Jamon, B. Verrier, and C. Cohen-Salmon. 2003. 'Mitochondrial DNA modifies cognition in interaction with the nuclear genome and age in mice', *Nat Genet*, 35: 65-9.
Schwartz, K., J. W. Wenger, B. Dunn, and G. Sherlock. 2012. 'APJ1 and GRE3 homologs work in concert to allow growth in xylose in a natural Saccharomyces sensu stricto hybrid yeast', *Genetics*, 191: 621-32.

Sherman, F., and J. Hicks. 1991. 'Micromanipulation and dissection of asci', *Methods Enzymol*, 194: 21-37.
Sinha, H., L. David, R. C. Pascon, S. Clauder-Munster, S. Krishnakumar, M. Nguyen, G. Shi, J. Dean, R. W. Davis, P. J. Oefner, J. H. McCusker, and L. M. Steinmetz. 2008. 'Sequential elimination of major-effect contributors identifies additional quantitative trait loci conditioning high-temperature growth in yeast', *Genetics*, 180: 1661-70.
Sinha, H., B. P. Nicholson, L. M. Steinmetz, and J. H. McCusker. 2006. 'Complex genetic interactions in a quantitative trait locus', *PLoS Genet*, 2: e13.
Snoek, T., M. Picca Nicolino, S. Van den Bremt, S. Mertens, V. Saels, A. Verplaetse, J. Steensels, and K. J. Verstrepen. 2015. 'Large-scale robot-assisted genome shuffling yields industrial Saccharomyces cerevisiae yeasts with increased ethanol tolerance', *Biotechnol Biofuels*, 8: 32.
Solieri, L., O. Antunez, J. E. Perez-Ortin, E. Barrio, and P. Giudici. 2008. 'Mitochondrial inheritance and fermentative : oxidative balance in hybrids between Saccharomyces cerevisiae and Saccharomyces uvarum', *Yeast*, 25: 485-500.
Spirek, M., A. Horvath, J. Piskur, and P. Sulo. 2000. 'Functional co-operation between the nuclei of Saccharomyces cerevisiae and mitochondria from other yeast species', *Curr Genet*, 38: 202-7.
Spirek, M., S. Polakova, K. Jatzova, and P. Sulo. 2014. 'Post-zygotic sterility and cytonuclear compatibility limits in S. cerevisiae xenomitochondrial cybrids', *Front Genet*, 5: 454.
Sprouffske, K., and A. Wagner. 2016. 'Growthcurver: an R package for obtaining interpretable metrics from microbial growth curves', *BMC Bioinformatics*, 17: 172.
Steinmetz, L. M., H. Sinha, D. R. Richards, J. I. Spiegelman, P. J. Oefner, J. H. McCusker, and R. W. Davis. 2002. 'Dissecting the architecture of a quantitative trait locus in yeast', *Nature*, 416: 326-30.
Teixeira, M. C., L. R. Raposo, N. P. Mira, A. B. Lourenco, and I. Sa-Correia. 2009. 'Genome-wide identification of Saccharomyces cerevisiae genes required for maximal tolerance to ethanol', *Appl Environ Microbiol*, 75: 5761-72.
Tranah, G. J. 2011. 'Mitochondrial-nuclear epistasis: implications for human aging and longevity', *Ageing Res Rev*, 10: 238-52.
Treusch, S., F. W. Albert, J. S. Bloom, I. E. Kotenko, and L. Kruglyak. 2015. 'Genetic mapping of MAPK-mediated complex traits Across S. cerevisiae', *PLoS Genet*, 11: e1004913.
van Voorst, F., J. Houghton-Larsen, L. Jonson, M. C. Kielland-Brandt, and A. Brandt. 2006. 'Genome-wide identification of genes required for growth of Saccharomyces cerevisiae under ethanol stress', *Yeast*, 23: 351-9.
Wagih, O., M. Galardini, B. P. Busby, D. Memon, A. Typas, and P. Beltrao. 2018. 'A resource of variant effect predictions of single nucleotide variants in model organisms', *Mol Syst Biol*, 14: e8430.
Wang, X., H. Wang, J. Wang, R. Sun, J. Wu, S. Liu, Y. Bai, J. H. Mun, I. Bancroft, F. Cheng, S. Huang, X. Li, W. Hua, J. Wang, X. Wang, M. Freeling, J. C. Pires, A. H. Paterson, B. Chalhoub, B. Wang, A. Hayward, A. G. Sharpe, B. S. Park, B. Weisshaar, B. Liu, B. Li, B. Liu, C. Tong, C. Song, C. Duran, C. Peng, C. Geng, C. Koh, C. Lin, D. Edwards, D. Mu, D. Shen, E. Soumpourou, F. Li, F. Fraser, G. Conant, G. Lassalle, G. J. King, G. Bonnema, H. Tang, H. Wang, H. Belcram, H. Zhou, H. Hirakawa, H. Abe, H. Guo, H. Wang, H. Jin, I. A. Parkin, J. Batley, J. S. Kim, J. Just, J. Li, J. Xu, J. Deng, J. A. Kim, J. Li, J. Yu, J. Meng, J. Wang, J. Min, J. Poulain, J. Wang, K. Hatakeyama, K. Wu, L. Wang, L. Fang, M. Trick, M. G. Links, M. Zhao, M. Jin, N. Ramchiary, N. Drou, P. J. Berkman, Q. Cai, Q. Huang, R. Li, S. Tabata, S. Cheng, S. Zhang, S. Zhang, S. Huang, S. Sato, S. Sun, S. J. Kwon, S. R. Choi, T. H. Lee, W. Fan, X. Zhao, X. Tan, X. Xu, Y. Wang, Y. Qiu, Y. Yin, Y. Li, Y. Du, Y. Liao, Y. Lim, Y. Narusaka, Y. Wang, Z. Wang, Z. Li, Z. Wang, Z. Xiong, Z. Zhang, and Consortium Brassica rapa Genome Sequencing

Project. 2011. 'The genome of the mesopolyploid crop species Brassica rapa', *Nat Genet*, 43: 1035-9.
Wernick, R. I., S. F. Christy, D. K. Howe, J. A. Sullins, J. F. Ramirez, M. Sare, M. J. Penley, L. T. Morran, D. R. Denver, and S. Estes. 2019. 'Sex and Mitonuclear Adaptation in Experimental Caenorhabditis elegans Populations', *Genetics*, 211: 1045-58.
Wolters, J. F., G. Charron, A. Gaspary, C. R. Landry, A. C. Fiumera, and H. L. Fiumera. 2018. 'Mitochondrial Recombination Reveals Mito-Mito Epistasis in Yeast', *Genetics*, 209: 307-19.
Yoshikawa, K., T. Tanaka, C. Furusawa, K. Nagahisa, T. Hirasawa, and H. Shimizu. 2009. 'Comprehensive phenotypic analysis for identification of genes affecting growth under ethanol stress in Saccharomyces cerevisiae', *FEMS Yeast Res*, 9: 32-44.
Yue, J. X., J. Li, L. Aigrain, J. Hallin, K. Persson, K. Oliver, A. Bergstrom, P. Coupland, J. Warringer, M. C. Lagomarsino, G. Fischer, R. Durbin, and G. Liti. 2017. 'Contrasting evolutionary genome dynamics between domesticated and wild yeasts', *Nat Genet*, 49: 913-24.
Zeyl, C. 2006. 'Experimental evolution with yeast', *FEMS Yeast Res*, 6: 685-91.
Zeyl, C., B. Andreson, and E. Weninck. 2005. 'Nuclear-mitochondrial epistasis for fitness in Saccharomyces cerevisiae', *Evolution*, 59: 910-4.
Zhang, X., T. Liu, X. Li, M. Duan, J. Wang, Y. Qiu, H. Wang, J. Song, and D. Shen. 2016. 'Interspecific hybridization, polyploidization, and backcross of Brassica oleracea var. alboglabra with B. rapa var. purpurea morphologically recapitulate the evolution of Brassica vegetables', *Sci Rep*, 6: 18618.
Zhu, C. T., P. Ingelmo, and D. M. Rand. 2014. 'GxGxE for lifespan in Drosophila: mitochondrial, nuclear, and dietary interactions that modify longevity', *PLoS Genet*, 10: e1004354.
Zimmer, A., C. Durand, N. Loira, P. Durrens, D. J. Sherman, and P. Marullo. 2014. 'QTL dissection of Lag phase in wine fermentation reveals a new translocation responsible for Saccharomyces cerevisiae adaptation to sulfite', *PLoS One*, 9: e86298.

Chapter 4 – Identification of genetic markers of antifungal drug resistance in *Saccharomyces* hybrids via QTL mapping

Federico Visinoni[1], Rachel Scholey[2], Soukaina Timouma[1], Yue Hu[3], Leo Zeef[2], Daniela Delneri[1]

[1] *Manchester Institute of Biotechnology, University of Manchester, Manchester, UK*

[2] *Bioinformatics Core Facility, University of Manchester, Manchester, UK.*

[3]*Department of Genetics and Genome Biology, University of Leicester, Leicester, UK.*

4.1 Foreword

The work in this chapter is a further investigation of the work presented in chapter 3 and refers to an ongoing project on the identification of complex traits related to antifungal resistance in *Saccharomyces* hybrids. References used within the manuscript are presented at the end of the chapter.

Author contributions: FV and DD conceived the study; FV performed the phenotypic screening, analysed the QTL data, and selected the candidate genes for validation; RS performed the QTL mapping with assistance from ST. DD and LZ supervised the study. FV wrote the manuscript with the input of DD and RS.

4.2 Abstract

The emergence of antifungal drug resistance amongst invasive species represents one of the major causes for failures in the treatment of fungal infections. Moreover, the development of new classes of antifungal has been hindered by the eukaryotic nature of fungal pathogens and the toolset available to treat fungal infection remains limited. Thus, it is of the foremost importance to understand the evolutionary pathways driving the development of antifungal resistance and detect the genetic traits responsible for the phenotype. Here we exploited recent advances in the breeding of *Saccharomyces* hybrid to study how hybridisation may affect antifungal resistance and identify the genes responsible for the phenotype. A library of mutigenerational *Saccharomyces cerevisiae* x *S. kudriavzevii* hybrids was screened at sub-lethal concentrations of six antifungal agents, revealing a broad phenotypic diversity in the conditions tested. Moreover, through quantitative trait locus (QTL) analysis, we were able to detect the genetic region responsible for fluconazole, micafungin, and flucytosine resistance in the hybrid strains, and identified numerous potential causal genes. The result of this screening will help identify new genes and pathway contributing to drug resistance, will

accelerate the development of new antifungal, and the understanding of how allelic variations, hybridisation and evolution may affect antifungal resistance in fungi.

4.3 Introduction

The tally of life-threatening infections associated with fungal pathogens was recently estimated to be on the same scale as tuberculosis and malaria with 13 million infections and a mortality of 1.5 million (Bongomin et al., 2017; Fisher et al., 2018). The severity of fungal infection has been exacerbated by the diffusion of immunocompromising conditions such as cancer, human immunodeficiency virus (HIV) disease, tuberculosis and by the coronavirus disease 2019 (COVID-19) (Gold et al., 2022). Moreover, the emergence of antifungal resistance in clinical strains, similarly to antibacterial resistance, has highlighted the need to expand our current toolset against the main fungal pathogens such as *Candida*, *Aspergillus* and *Cryptococcus* species. However, the development of new antifungal agents is hindered by the eukaryotic nature of fungi, limiting the number of molecular targets which can uniquely affect fungal pathogens without harming the human host. As a consequence, only four classes of compounds are routinely used: azoles, polyenes, pyrimidine analogues and echinocandins (Lee et al., 2021). Amongst these, azoles, such as fluconazole and miconazole, are the most commonly prescribed for the treatment of *Candida* and *Cryptococcus* infections (Berkow and Lockhart, 2017; Lee et al., 2021). Azoles acts as strong inhibitors of the lanosterol demethylase (encoded by *ERG11*), disrupting ergosterol biosynthesis, an essential component of fungal membrane, and leading to the accumulation of toxic sterol intermediates (Heimark et al., 2002). Similarly, polyenes, disrupt membrane functions by acting on ergosterol. Polyenes are thought to act as "sterol sponges", sequestering sterol from the lipid bilayers to form extra-membranous aggregates (Anderson et al., 2014) . Albeit the development of fungal resistance to polyenes, such as amphotericin B, is very rare, the administration of such compounds is often disfavoured, due to a high toxicity to the host (Anderson et al., 2014). Amongst the pyrimidine analogues, flucytosine has been employed as an antifungal drug since 1968 (Delma et al., 2021). Flucytosine is first converted *in vivo* in 5-fluorouridine by a cytosine deaminase and then phosphorylated to 5-fluoro-uridine-triophosphate (5-F-UTP) or reduced to 5-fluoro-deoxyuridine-monophosphate (5-F-dUMP). As 5-F-UTP the drug is incorporated into RNA, leading to the inhibition of protein synthesis. Instead, as 5-F-dUMP the antifungal act as an inhibitor of thymidylate synthase and, as a consequence, of purine and DNA synthesis (Campoy and Adrio, 2017; Delma et al., 2021). The last class of antifungal

introduced for clinical use is the echinocandins, lipopeptides which act through a non-competitive binding of the enzyme β-D-glucan synthase complex in both *Candida* and *Aspergillus spp.*. Echinocandins, such as caspofungin and micafungin, inhibit the biosynthesis of β-D-glucan, a crucial component of the fungal cell wall, leading to osmotic stress and cell death (Denning, 2002). The known molecular mechanisms of fungal resistance are often linked to mutations in the target gene or in the pathway affected by the drug. As a case in point, *Candida spp.* are known to develop resistance to fluconazole by the overexpression of the target gene, *ERG11*, or by the accumulation of point mutations which alter the structure of the molecular target. Similarly, mutations in the key enzymes of the pyrimidine biosynthetic pathway can lead to increased resistance to flucytosine (Delma et al., 2021; Zhang and Xu, 2018). However, the high-level of resistance of clinical isolates can rarely be ascribed to the effect of single mutations, which, instead, is often attributable to a combination of traits and a gradual adaptation to the stressor (Berkow et al., 2020; Berkow and Lockhart, 2017). Thus, for a throughout investigation of the genes and pathways associated with antifungal resistance, it is of the utmost importance to carry out genome-wide investigations to sample the breadth of the cellular response to antifungal agents. In recent years, a growing number of high-throughput and -omics studies have been successfully applied to the study of antifungal resistance and pathogenicity in both model systems and pathogenic species (Ehrenreich et al., 2010; Homann et al., 2009; Phadke et al., 2018; Vogan et al., 2016; Zhang et al., 2002; Zhou et al., 2013). However, such studies are often limited by the use of laboratory strains which precludes in-depth analysis into the mechanisms developing through adaptation and evolution mechanisms in nature. Here we applied the pipeline recently described in Naseeb et al. 2021 (Naseeb et al., 2021) for the study of QTL in multigenerational yeast hybrids, containing a combination of four genomes, to unpick allelic variants associated with antifungal resistance. We screened a diverse library of hybrids spores derived from crossing of different strains belonging to *S. cerevisiae* and *S. kudriavzevii* and propagated for 12 meiotic generations (F12) in media containing sub-lethal concentrations of six antifungal agents. The hybrid spores revealed a broad phenotypic diversity in all the conditions tested. QTL studies through Multipool allowed to unpick the genetic basis underlying the phenotype observed and study how natural variations and hybridization could lead to a resistant phenotype. Moreover, through the application of state-of-the-art genome-wide studies we were able to sample the complexity of the traits associated with resistance to fluconazole, micafungin and flucytosine. The data generated represent a

valuable resource for the identification of new marker and predictors of antifungal resistance and for the development of new drugs and combinational therapies.

4.4 Result & Discussion

4.4.1 Phenotypic analysis

In a previous study, we generated a library of genotypically diverse F12 *S. cerevisiae* x *S. kudriavzevii* diploid hybrids (Naseeb et al., 2021). The strains were found to exhibit a broad phenotypic divergence in stressors connected with industrial processes, such as high osmolarity or high acid concentrations. Here, we exploited this strain library to study traits underpinning antifungal susceptibility and resistance. The hybrid spores were incubated with a variety of antifungal agents to assess their phenotypic diversity and their colony size, calculated in pixels, was used as a proxy of fitness. The pipeline followed for this study is outlined in Figure 4-1. The colony size of the spores was recorded after 72h of incubation in media containing compounds which inhibits ergosterol biosynthesis (fluconazole and miconazole), cell wall biogenesis (micafungin and caffeine) and nucleic acid biosynthesis (flucytosine and phleomycin) (Campoy and Adrio, 2017; Gebre et al., 2015). The hybrids exhibited a broad phenotypic divergence for all the six antifungals screened, comparable or higher to the one observed in YPD (Table 4-1, Figure 4-2A). The higher dispersion was recorded in media with 10 μg/ml of fluconazole with a IQR (quartile coefficient of dispersion) of 0.55, compared to 0.14 in YPD (Table 4-1). The antifungal drugs were added at sub-lethal concentrations in the media, according to Gebre et al. 2015 (Gebre et al., 2015), to allow for two-tailed selection, hence to be able to identify both high-performing and low-performing spores. Nonetheless, the analysis in miconazole and phleomycin were characterised by low cell viability (<99%), with only around 20% of the hybrids able to sustain the highest concentration tested (Table 4-1, Figure 4-2B). Interestingly, the highest growth recorded in phleomycin was that of the F1 *S. cerevisiae x S. kudriavzevii* tetraploid parent which was able to grow in each of the antifungal tested but in miconazole. The reduced cell viability of the progeny in these antifungal drugs might reflect a lower amount of allelic variants connected to the resistant phenotype in the F1 tetraploid parent.

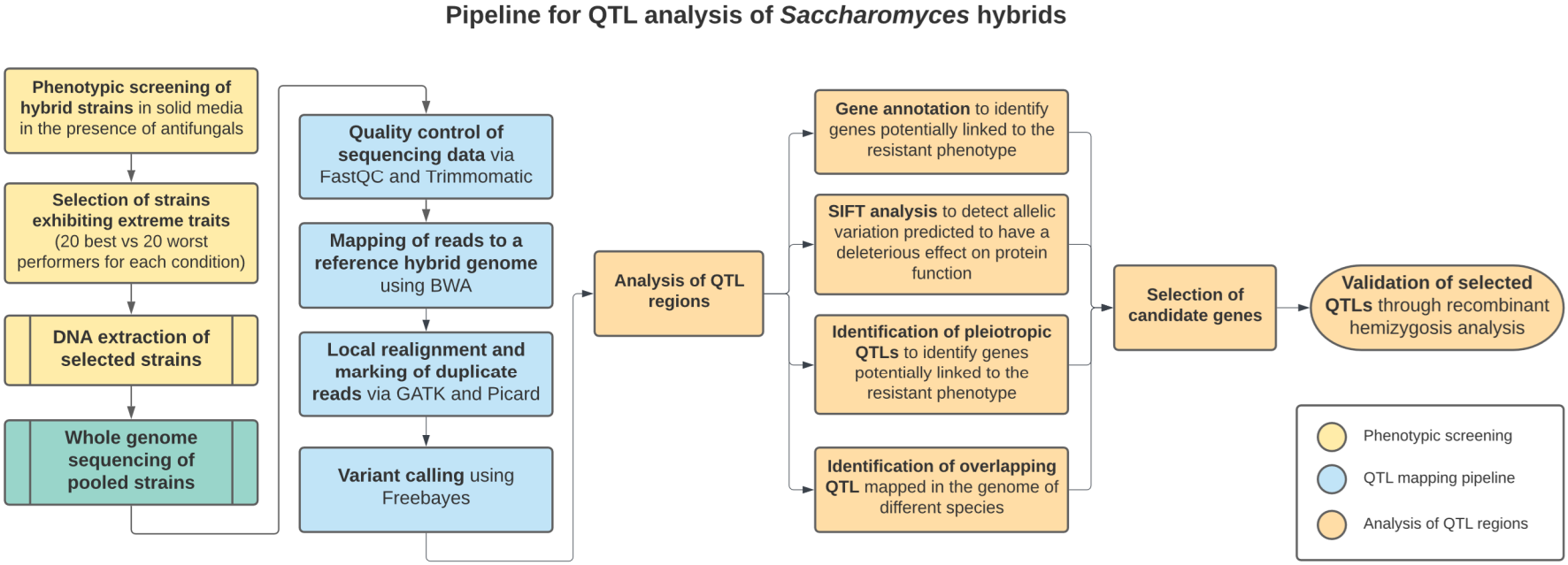

Figure 4-1 | Pipeline for the detection of QTL responsible for antifungal resistance of *Saccharomyces* hybris. A high-throughput phenotypic screening in solid media of a library of *S. cerevisiae x S. kudriavzevii* hybrids will allow the selection of a pool of the 20 best and the 20 worst hybrid strains in each condition tested. QTL analysis will allow to map the genetic regions underlying the phenotypic differences between the two pool and the data generated will be mined for the identification of candidate genes for further validation *in vivo*.

Table 4-1 | Descriptive statistics analysis of the colony size of F12 diploid progeny for *S. cerevisiae/S. kudriavzevii* hybrids after incubation with different concentrations of antifungal drugs: fluconazole (FCZ), miconazole (MCZ), caffeine (CAF), micafungin (MCF), flucytosine (FCY) and phleomycin (BLE).

	YPD	FCZ 5 µg/ml	FCZ 10 µg/ml	MCZ 10 µM	MCZ 20 µM	CAF 1 mg/ml	CAF 2.5 mg/ml	MCF 25 ng/ml	MCF 50 ng/ml	FCY 10 µg/ml	FCY 20 µg/ml	BLE 0.5 µg/ml	BLE 1 µg/ml
F1 tetraploid colony size	296	295	172	0	0	234	101	255	224	138	131	361	382.5
25% Percentile	270.6	149	42.13	0	0	243.1	127.3	290.8	296	151.3	132.1	4	0
Median	310.5	203.3	87	31.5	0	275.8	168	336.3	351.3	184	158.3	153	0
75% Percentile	358	258	145.9	111.4	0	298.9	198.4	366.9	380.9	217.9	183.9	256.8	0
IQR	0.14	0.27	0.55	1.00	0.00	0.10	0.22	0.12	0.13	0.18	0.16	0.97	0.00
Range	444.5	482.5	254.5	263	294	331	269	409.5	468	276	222.5	462.5	461
Viability	100.0%	99.6%	87.7%	64.5%	23.2%	100.0%	99.6%	100.0%	100.0%	100.0%	100.0%	75.4%	19.3%

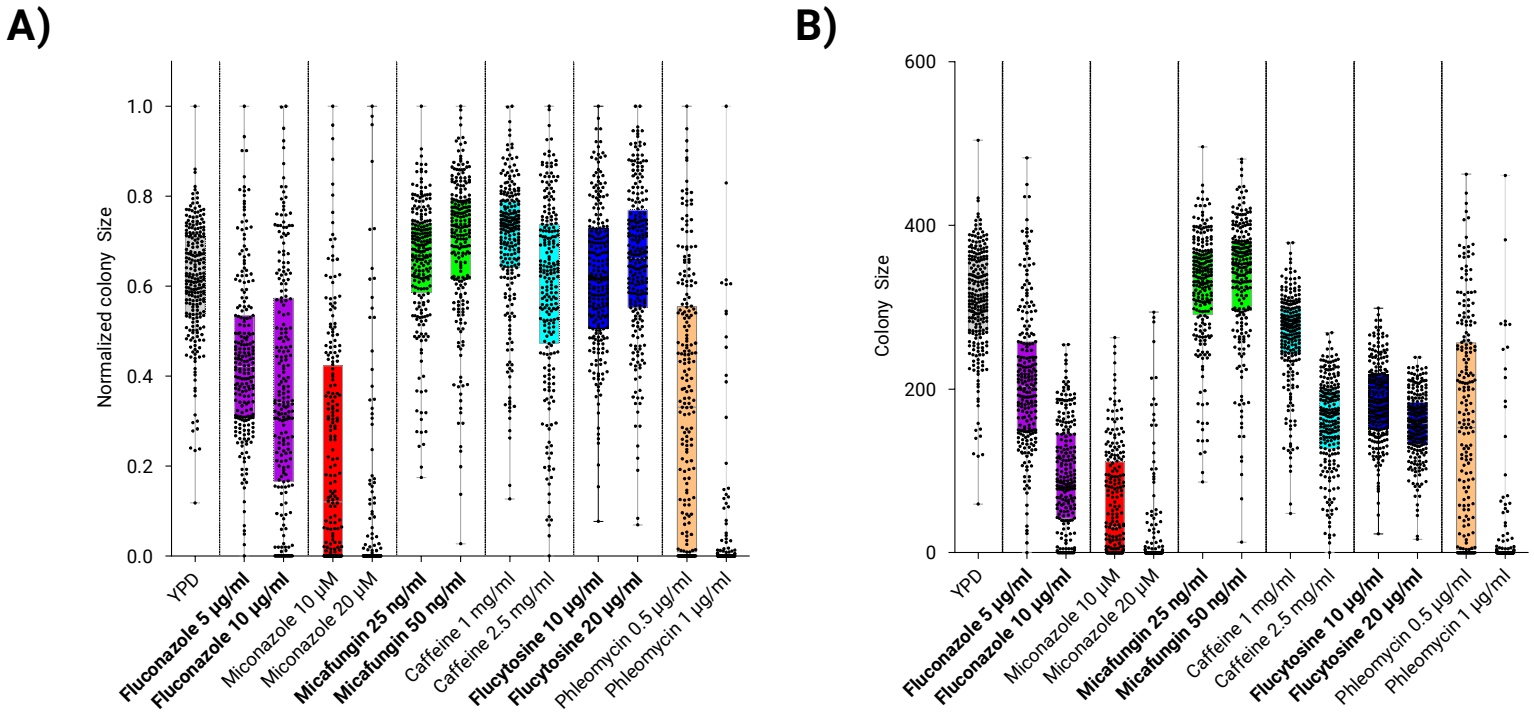

Figure 4-2 | Box plot of the fitness of F12 diploid progeny for *S. cerevisiae/S. kudriavzevii* hybrids after incubation with different concentrations of antifungal drugs expressed as normalized colony size (A), where 1 represents the highest value recorded in each condition and 0 equals to no growth, and colony size (B).

Unexpectedly, the spores incubated in media containing sub-lethal concentrations of micafungin showed a higher median colony size compared to growth in YPD (Table 4-1 and Figure 1A). Previous studies observed an abnormal morphology in yeast cell treated with micafungin, reportedly similar to *hoc1* and *mnn10* mutants, which correlated with an abnormally large morphology (Gebre et al., 2015; Jorgensen et al., 2002). Thus, the high colony size recorded after incubation in micafungin might be a correlated to an increase in cell size instead of cells number and, as such, be an artifact of the screening procedure in solid media.

4.4.2 QTL analysis

To identify the genetic traits underlying antifungal resistance in the hybrid progeny, we sequenced a pool of the 20 best and of the 20 worst performing strains for three antifungals acting on different biological processes: fluconazole, micafungin and flucytosine. The resulting genomic data was analysed with Multipool to map for QTL loci where allele frequencies significantly differed between the pools of spores exhibiting diametric phenotypes for each antifungal. QTL analysis identified 101 and 89 different QTL regions in the *S. cerevisiae* and in the *S. kudriavzevii* genome of the hybrid spores, respectively (Table 4-2). The results were comparable in terms on numbers of QTL mapped to previous analysis of the same crossing in metabolic stresses (Naseeb et al., 2021). Thus, these results suggest that while antifungal targets a particular enzyme or metabolic process, drugs resistance is governed by multiple quantitative traits. In particular, QTL regions identified in flucytosine accounted for over half of the total regions mapped (51.6%) in all conditions with 47 and 51 QTL regions identified in *S. cerevisiae* and *S. kudriavzevii*, respectively. Flucytosine is known to affect both RNA and DNA biosynthesis in fungi (Vermes et al., 2000). Thus, the higher number of QTL associated with the trait might be resulting from a higher complexity of the flucytosine-resistance trait. The difference in the mechanism of action of these antifungal resulted in a high number of drug trait-specific QTLs (99%), with only three pleiotropic regions shared across condition (Table 4-3). A small region in the chromosome V of *S. cerevisiae*, encompassing genes encoding for *Pab1p*, *Dnf1p* and *Bck2p*, was mapped in all conditions. This locus was not identified in previous QTL studies of the hybrid progeny in maltose, acetic acid and low temperature (Naseeb et al., 2021), ruling out a general growth effect of the enclosed alleles and rather pointing to a more specific role in drug resistance of these genes. Further validation studies *in vivo* will be needed to pinpoint the allelic variations

responsible for the phenotypic effect in each of the antifungal tested. *Bck2p*, a protein involved in the regulation of the cell cycle, might be partially responsible for the phenotypic effect observed in the three antifungals. In fact, Δ*BCK2* strains were found to affect sensitivity to cell wall stressors such as caffeine and echinocandin, and to phleomycin, an antifungal affecting DNA synthesis (Kapitzky et al., 2010). Moreover, deletion of *DNF1*, a flippase, resulted in increased fitness in phleomycin in *S. cerevisiae* and thus the gene might contribute to the phenotypic effect in flucytosine which is similarly involved in DNA and RNA synthesis (Kapitzky et al., 2010).

Table 4-2 | Number of QTL regions detected, and genes encoded in the QTL region in *S. cerevisiae*/*S. kudriavzevii* F12 segregants via Multipool strategies. Sc = *S. cerevisiae*, Sk = *S. kudriavzevii*

	Number of QTL regions detected		Number of genes within the QTL regions	
Genome	**Sc**	**Sk**	**Sc**	**Sk**
Micafungin	25	17	93	48
Fluconazole	29	21	212	107
Flucytosine	47	51	175	279

Four QTL regions were "reciprocally" identified in both *S. cerevisiae* and *S. kudriavzevii* genome affecting the hybrid fitness in flucytosine (Table 4-4), while, in the QTLs of hybrid treated with fluconazole and micafungin, no regions were "reciprocally" detected in the genomes of both species. Amongst the genes mapped in the shared flucytosine-QTLs we were able to identify potential causal genes which were previously linked to DNA synthesis and maintenance or to drugs sensitivity. In particular, *ENV11* and *TRR1* deletions were found to affect sensitivity to phleomycins (Kapitzky et al., 2010; Krol et al., 2015), while *ALD2* null mutants had increased sensitivity to floxuridine, a pyrimidine analogue which inhibits DNA and RNA synthesis similarly to flucytosine (Lum et al., 2004). Moreover, *MLH1* is an ATPase involved in meiotic mismatch repair in mitosis and meiosis (Kramer et al., 1989) while *PFU1* overexpression was found to exacerbate UV radiation toxicity in overexpression studies (Chakrabortee et al., 2016). Thus, the dissection and the validation of the QTL regions outlined in Table 4-4 may reveal new loci for antifungal resistance.

Table 4-3 | List of pleiotropic QTLs in *S. cerevisiae* x *S. kudriavzevii* hybrid diploid progeny. The coordinates of the pleiotropic intervals are reported along with the species and the selection condition in which they were identified.

	Chromosome	Start (bp)	End (bp)	Selection conditions	Genes in QTL interval
***S. cerevisiae* genome**	IV	730300	740100	Fluconazole Micafungin	*MKC7, TAF12, SWI5, EKI1*
	V	506200	519700	Fluconazole Flucytosine Micafungin	*PAB1, DNF1, BCK2*
	XV	592700	602600	Fluconazole Flucytosine	*LSC1, THI80, ELG1, PNO1*

Table 4-4. | List of QTLs intervals identified in both *S. cerevisiae* and S. *kudriavzevii* genome. For each interval shared, the position and the peak of the individual QTL is specified. Sc = *S. cerevisiae*, Sk = *S. kudriavzevii*

Condition	Chromosome	Genome	QTL Peak	Genes shared within QTL region
Flucytosine	XIII	Sc Sk	583400 602300	*MME1, MLH1, CEP3, ALD3, ALD2*
	IV	Sc Sk	1033900 1021600	PFU1
	IV	Sc Sk	1200700 1105600	*YPQ2, TRR1*
	VII	Sc Sk	612000 622000	*ENV11*

A total of 75 genes within the QTL regions mapped were deemed as potential causal genes as their phenotypic effect in the presence of the antifungal was previously described in classical genetic (Cherry et al., 2012) or transcriptome studies (Zhang et al., 2002) in *S. cerevisiae* (Table 4-5). Moreover, in micafungin-QTLs, we identified four orthologues of *Schizosaccharomyces pombe* genes associated with micafungin resistance (Zhou et al., 2013). Amongst these, *TOR1*, a protein kinase involved in signal transduction, cell growth and autophagy, was found similarly involved in the development of resistance to caffeine, a cell wall stressors, in both *S. cerevisiae* and *C. albicans* (Homann et al., 2009). Additionally, 56 genes in the QTL regions mapped were found interacting with the drug target (*e.g.,* with *ERG11* in fluconazole-QTLs) or with cellular processes closely linked to the drug mechanism of action (*e.g.,* nucleotide biosynthetic processes for flucytosine-QTLs or β-glucan metabolism for micafungin-QTLs) (Table 4-5).

Potential causal genes identified in *S. cerevisiae* genome were further analysed using the SIFT (Sorting Intolerant from Tolerant) algorithm to identify non-synonymous SNPs between the parental strains which could affect protein function (Bergstrom et al., 2014; Kumar et al., 2009). Around 60% of the 83 potential causal genes identified within *S. cerevisiae* genome had one or more SNPs between the parental strains. Amongst these, 11 alleles were found to carry SNPs predicted to cause a strong deleterious effect on the protein function (13.25%) while 38 were inferred to have tolerated mutations (45.8%) (Table 4-6).

Table 4-5 | List of potential causal genes identified in *S. cerevisiae* x *S. kudriavzevii* hybrids. The genes are clustered by their function or by the phenotype reported in genetic studies in SGD(Cherry et al., 2012), if not specified otherwise.

Causal genes identified in Fluconazole QTLs		
	***S. cerevisiae* alleles**	***S. kudriavzevii* alleles**
Increased resistance to fluconazole	*PPZ1, SLY41, YAP1, ARP8, DEG1, HST4, ERV25, RAD17, ISW2, HAP5, ERG6, MRT4, SNU66, ADR1, GYP1, DST1, PSP2, MSA1, ANY1, NUP42, MRX16, TAF12, UBP6, CDC5, ITT1, UPC2, ALG8, PDE2, NDD1, COM2, HSC82, SWI5, COQ4, LDB19, VTS1, PRT1*	*SSK1, PUB1, RDH54, KES1, VPS27, CSE2, ACS2, ARK1, CBF2, HDA1, SOL1*
Ergosterol bio-metabolism	*ERG6, HEM2, UPC2*	*ARE2*
Reported physical interaction with *ERG11*	*PPZ1, ERV25, ERG6, LAC1*	*ASI3, KES1*
Reported genetic interaction with *ERG11*	*DOP1, TAF12, CBS2, SPC19, RAV2, RAD9, UBC6, RNA15, UBX2, SGS1, RPL36A, GYP1, HEM4, PLP2, DGK1, FAA1, PDE2, MRS6*	*NOC3, RPS10B, PET8, ASI3, LRO1, DBP6, PRP46*
Causal genes identified in Flucytosine QTLs		
	***S. cerevisiae* alleles**	***S. kudriavzevii* alleles**
Resistance to flucytosine	*BCH2, LSM6, ATO3, NKP1, ATP17, XRS2*	*PEX8, RRT2, BUB3, ROM1, NOC2, STP3, BFR1, MAK21, RRP46, PAC10, HMS1*
DNA Damage Repair	*RDH54, ESC2, POL1, RAD3, MLH1*	*DDR48, EXO1, IES4, MLH1*
Resistance to phleomycin	*CPR5, DNF1, HXK1, HNT3, BCK2, ENV11*	*SCL1, AIM34*

Drug resistance	*PDR15, RDS2* (Jung et al., 2015)	*PDR10*
Nucleotide biosynthetic processes	*ADE8, ADK2*	*DUT1, ADE16, CDD1*
DE genes and paralogs after flucytosine treatment in *S. cerevisiae* (Zhang et al., 2002)	*RPL12B, ADE8, PDR15*	*MMT1, SPT21, CTL1, SER1, RPL9B, RPL15A*
Causal genes identified in Micafungin QTLs		
	***S. cerevisiae* alleles**	***S. kudriavzevii* alleles**
Resistance to caspofungin	*AKR1, MEH1*	*FEN2, MSN5, YSP2*
Resistance to echinocandin	*BCK2*	
Beta glucan bio-metabolism	*EXG2*	
Cell wall stress	*BCK2*	*RQC1, CNB1*
Resistance to caffeine	*IPK1, BCK2, TOR1*	*DPH2, DCG1, CNB1*
Orthologues of *S. pombe* genes associated with micafungin resistance (Zhou et al., 2013)	*MKC7, TOR1, HEL1, YTA6*	

Table 4-6. | List of potential causal genes identified in the *S. cerevisiae* genome of *S. cerevisiae x S. kudriavzevii* hybrids with non-synonymous SNPs predicted to be tolerated or deleterious by SIFT analysis (Bergstrom et al., 2014)

Condition	SIFT analysis	
	Tolerated	Deleterious
Fluconazole	*UBC6, COM2, LAC1, UBP6, MRX16, TAF12, HST4, NUP42, CBS2, RNA15, YAP1, PPZ1, PSP2, ITT1, HSC82, MSA1, ALG8, GYP1, HEM4, SLY41, SNU66, VTS1, NDD1*	*DEG1, UPC2, ADR1, RAD9, UBX2, SGS1, FAA1*
Flucytosine	*RDH54, ESC2, XRS2, NKP1, ADE8, MLH1, HNT3, RDS2, BCK2, ENV11*	*DNF1, BCH2, PDR15, POL1*
Micafungin	*BCK2, MEH1, EXG2, IPK1, TOR1, YTA6*	

4.4.3 Selection of candidate genes for further validation studies

Three candidate genes for each antifungal drug were chosen based on the LOD score of the QTL region, prioritizing potential causal genes with allelic variants highlighted by SIFT analysis (Table 4-6). The candidate genes selected are presented in Table 4-7 alongside a description of their function and the QTL coordinates. The genes *UPC2* and *ADR1*, enclosed in a 57kb fluconazole-QTL in chromosome IV of *S. cerevisiae*, were predicted to have deleterious SNPs between *S. cerevisiae* parental strains by SIFT analysis (Bergstrom et al., 2014). Moreover, the transcription factors *UPC2* and *ADR1* were previously described as affecting fluconazole resistance in classical genetic studies (Marie et al., 2008) and in overexpression studies (Chakrabortee et al., 2016), respectively. Thus, the genes were selected as prime candidates for the validation studies of fluconazole-QTLs alongside *NBP2*, a gene encoding for a protein involved in cell wall integrity. While NBP2 was not previously linked to fluconazole resistance, the gene was enclosed in a tight high-LOD QTL of 10kb in chromosome IV and SIFT analysis predicted a deleterious mutation.

The genes *PDR15* and *MLH1* were chosen as candidates for further validations of flucytosine-QTLs. The former, a multidrug transporter, was highlighted by SIFT with a deleterious SNP and found down-regulated after treatment with flucytosine in *S. cerevisiae* (Zhang et al., 2002). *MLH1*, instead, was shortlisted as the most promising candidate of a QTL between *S. cerevisiae* and *S. kudriavzevii* genome, due to its role in mismatch repair (Table 4-5). Amongst the pleiotropic QTL identified in chromosome V in the three antifungal tested, *DNF1* was selected as candidate for flucytosine-QTLs and *BCK2* for micafungin due to their links to phleomycin and echinocandin C derivative resistance (Hoepfner et al., 2014; Kapitzky et al., 2010). The validation of the effect of these genes in all the antifungal tested will allow to dissect the alleles underlying the pleiotropic QTL and identify possible new markers of antifungal resistance. Lastly, within micafungin-QTLs, *IPK1* and the aforementioned *TOR1* were selected as previously linked to caffeine resistance in genetic studies (Homann et al., 2009; Kapitzky et al., 2010) and as 8 and 4 SNPs were present between the parental allelic variants of the two genes, respectively.

The validations are scheduled to be carried out in Delneri's lab in the near future through reciprocal hemizygosis analysis on the hemizygote tetraploid hybrids, as depicted in Naseeb et al. 2021 (Naseeb et al., 2021). In short, a knockout of the candidate gene will be performed through PCR-mediated deletion in the parental diploids (Sc^{OS253}/Sk^{OS575} and $Sc^{OS104}/Sk^{IFO1802}$). The strains generated will be mass mated to generate reciprocal hemizygote tetraploids carrying only one *S. cerevisiae* allele of the candidate gene. Lastly, the fitness of the generated strains will be assessed after incubation in the presence of the antifungal to determine the effect of each allele on the phenotypic fitness.

Table 4-7 | List of *S. cerevisiae* QTL regions selected for RHA validation. The coordinates of the QTL regions are indicated alongside the genes annotated within the QTL region. The selected candidate genes are highlighted in bold.

Selection condition	Chr	Start (kb)	End (kb)	LOD	Genes within the QTL region	Gene function
Fluconazole	IV	825.7	882.7	15.8	RVB1, HST4, NUP42, MSS116, REF2, CAB5, CBS2, RKM2, VPS64, SPC19, RAV2, COQ4, MSC2, EBS1, UME6, MSS4, GCD6, TCP1, **UPC2,** AHA1, **ADR1**, RAD9, SPR28, MFB1	*Upc2* is a transcription factor which induces sterol biosynthetic genes
	IV					*Adr1* is a transcription factor which activate the expression of genes involved in ethanol, glycerol and fatty acid utilization
	IV	763.1	773.1	16.73	*SSY1, ACL4,* ***NBP2,*** *CWC15, SEC1*	*Nbp2* is a protein adapter involved in osmosensory signalling and cell wall integrity pathway
Flucytosine	IV	1234.4	1268.8	8.16	*DIT2, DIT1, RPB7, MRP20,* ***PDR15,*** *TRS120, ADE8, SIZ1, STE14, DFM1, RRP17, ERD1, YDR415C, SYF1, RPL12B, RAD30*	*Pdr15* is a multidrug transporter implicated in cellular detoxification
	V	506.2	529.6	5.98	*PAB1,* ***DNF1****, BCK2, CCA1, RPH1, ADK2, RAD3*	*Dnf1* is a flippase involved in phospholipids translocation
	XIII	566.3	586.5	20.33	*INP2, MSS11, PAH1, MME1,* ***MLH1****, CEP3, ALD3, ALD2*	*Mlh1* is an ATPase required for mismatch repair in mitosis and meiosis
Micafungin	IV	1048.9	1084.6	8.76	*TFB1, SSF2, PIB1, RAD34,* ***IPK1,*** *OMS1, HIM1, MCM21, YFT2, SWA2, DAD4, ASP1, TIM11, MRPL35, PEP7*	*Ipk1* is an inositol pentakisphosphate 2-kinase involved in the biosynthesis of inositol phosphate
	V	505.6	519.7	9.26	*PAB1, DNF1,* ***BCK2***	*Bck2* is a protein involved in the G1/S transition of the cell cycle
	X	530.6	546	9.25	*NTA1, RPA12, CCT5, ARP3,* **TOR1**, YAE1	*Tor1* is a kinase involved in cell growth and autophagy

4.5 Conclusions and future work

In this study we have successfully applied the platform developed by Naseeb et al. (2021) (Naseeb et al., 2021) for the dissection of complex traits in *Saccharomyces* hybrids to the identification of QTLs associated with antifungal resistance. The F12 progeny of a tetraploid hybrid between geographically distant strains of *S. cerevisiae* and *S. kudriavzevii* revealed a broad phenotypic diversity when screened in media containing sub-lethal concentrations of antifungal agents. This approach allowed to dissect complex trait linked with resistance and susceptibility to a diverse range of antifungal: from azole (fluconazole) to pyrimidine analogue (flucytosine), and echinocandins (micafungin). Moreover, the study of interspecies hybrids from natural sources allowed to study how natural variation, developing outside of clinical samples, and hybrid vigour may affect the evolutionary pathway leading to a resistant phenotype.

The wealth of information provided by the QTL study will further advance the field of antifungal drug development, facilitating the identification of new pathway and metabolic targets which could be exploited in the generation of new drugs. Moreover, through RHA, we will be able to validate the phenotypic effect of the candidate genes and determine allelic variations which could represent markers of antifungal resistance. This will accelerate the development of new screening methods to predict antifungal resistance of clinical strains and guide the choice of treatment. In particular, the dissection of a pleiotropic QTL in chromosome V of *S. cerevisiae* present in all the antifungal tested could allow the identification of new strong predictors of drug resistance. Application of this approach using human pathogens, such as *Candida* and *Cryptococcus spp.*, where hybridisation is commonplace (Samarasinghe et al., 2020), will further enhance the field, allowing to quickly identify markers of resistance for new screening procedures and study the evolution pathways responsible for antifungal adaptation in nature.

4.6 Material and methods

4.6.1 Strains used in the study

The F1 parental tetraploid *S. cerevisiae* x *S. kudriavzevii* hybrid ($Sc^{OS253}/Sk^{OS575}/Sc^{OS104}/Sk^{IF01802}$) harbouring *S. kudriavzevii* mitochondria and 228 F12 *S. cerevisiae x S. kudriavzevii* diploid progeny with *S. kudriavzevii* mitochondria generated in Naseeb et al. 2021 were used in this study. Yeast strains were maintained in YPD medium (1% yeast extract, 2% peptone, 2% glucose, Formedium, UK) in 96 well-plates, and in PlusPlates (Singer Instruments, UK) with YPD + 2% agar incubated at 30°C.

4.6.2 Phenotypic tests

Diploid spores of *S. cerevisiae* x *S. kudriavzevii* hybrids were grown in YPDA at 30°C and then inoculated into 100 µL YPD in a 96 well microtiter plate alongside the parental tetraploid ($Sc^{OS253}/Sk^{OS575}/Sc^{OS104}/Sk^{IF01802}$). The strains were incubated for 96 hours at 30°C and then sub-cultured in 384 well microtiter plate containing 70 µL YPD using the Singer Rotor HAD (Signer Instruments, Somerset, UK), prepared with four technical replicates of each strain.

For the fitness analysis of *S. cerevisiae* x *S. kudriavzevii* spores, the liquid cultures were grown to saturation at 30°C and stamped in solid media plates at a density of 384 strains per plate. The spores were grown at 30°C in: YPDA, YPDA + 5 µg/ml and 10 µg/ml of fluconazole, 10 µM and 20 µM of miconazole, 1 mg/ml and 2.5 mg/ml of caffeine, 25 ng/ml and 50 ng/ml of micafungin, 10 µg/ml and 20 µg/ml of flucytosine, 0.5 µg/ml and 1 µg/ml of bleomycin.

The plates were imaged with the PhenoBooth Colony Counter (Singer Instruments, UK) after 72 hours of incubation and the size of the individual colonies, calculated in pixels with the Phenosuite software (Singer Instruments, UK), was used as a proxy for fitness.

4.6.3 DNA Extraction and sequencing

Diploid spores of *S. cerevisiae* x *S. kudriavzevii* hybrids were inoculated in 1.5 mL of YPD and incubated overnight at 30°C, shaking. Total DNA was purified using Epicentre Masterpure™ Yeast DNA Purification Kit (Lucigen, USA) and resuspended in 50 µL of

RNase-free water. To remove any RNA contamination present in the sample, the purified DNA was incubated for 30 minutes at 37°C with 1 µL of 5 µg/µL RNase A.
The quality of the purified DNA was assessed through gel electrophoresis on a 0.8% agarose gel and a Thermo Scientific™ NanoDrop Lite spectrophotometer (Thermo Scientific, UK). The DNA in each sample was quantified with a Qubit 4 Fluorometer (Thermo Scientific, UK).

4.6.4 QTL mapping

The unmapped paired-end sequences from an Illumina HiSeq 4000 sequencer were quality assessed by FastQC (S. Andrews, 2010). Sequence adapters were removed, and reads were quality trimmed (to quality score q20) using Trimmomatic_0.36 (Bolger et al., 2014). The mapping, variant calling and Multipool analysis was performed as previously described (Naseeb et al., 2021). Briefly, the reads were mapped against a reference hybrid genome containing the reference sequence for each founder species (*S. cerevisiae* OS104 (Yue et al., 2017) and *S. kudriavzevii* IF0 1802T Ultra-Scaffolds assembly (Scannell et al., 2011) using BWA-MEM (Li and Durbin, 2009) (bwa_ 0.7.15). Local realignment was performed with GATK_3.8.0 (DePristo et al., 2011) and duplicates were marked with Picard Toolkit_2.1.0 ("Picard Toolkit," 2019). The alignment quality was assessed with Qualimap_2.2.1 (García-Alcalde et al., 2012). For each sample, variant calling was performed individually using Freebayes_1.1.0 (Garrison E, 2012) with ploidy setting at 1 and including the following parameters --minmapping-quality 30 --min-base-quality 20 --no-mnps. The resultant VCF files were filtered for 'type=SNP' variants and processed using R. Unique bi-allele markers for each founder species were identified. Reads depths below 10 were excluded. The parental allele counts in each F12 pool were then calculated by matching reference (RO) and alternate (AO) alleles to the bi-allele marker sets among the founders. The allele counts were provided to Multipool (Edwards and Gifford, 2012) and $\log_{10}$ likelihood ratios (LOD scores) were calculated across each chromosome. QTLs were identified and reported with an LOD support interval of 1, in regions where a minimum LOD score of 5 extended across at least 20kb. The identified QTLs were annotated using the available annotation from *S. cerevisiae* OS104. Annotation for the *S.*

kudriavzevii IF0 1810T ultra-scaffolds assembly was performed using HybridMine (Timouma et al., 2020).

4.6.5 Data analysis

Potential causal genes were analysed with the Sorting Intolerant from Tolerant (SIFT) algorithm to assess if amino-acids variants were predicted to influence the protein function. SIFT analysis were conducted using data from Bergstrom et al. 2014 (Bergstrom et al., 2014) on the *S. cerevisiae* strains OS104 and OS253.

4.7 Acknowledgments

We thank Yue Hue for the support on establishing the QTL mapping pipeline and the Genomic Technologies Core Facility (GTCF) of the University of Manchester for the sequencing. This work was supported by the Facilitating Excellence Fund awarded to DD and FV. FV and ST were supported by H2020-MSCA-ITN-2017 grant to DD (764364; https://cordis.europa.eu/project/id/764364).

4.8 References

Anderson, T.M., Clay, M.C., Cioffi, A.G., Diaz, K.A., Hisao, G.S., Tuttle, M.D., Nieuwkoop, A.J., Comellas, G., Maryum, N., Wang, S., Uno, B.E., Wildeman, E.L., Gonen, T., Rienstra, C.M., Burke, M.D., 2014. Amphotericin forms an extramembranous and fungicidal sterol sponge. Nat Chem Biol 10, 400–406. https://doi.org/10.1038/nchembio.1496

Bergstrom, A., Simpson, J.T., Salinas, F., Barre, B., Parts, L., Zia, A., Nguyen Ba, A.N., Moses, A.M., Louis, E.J., Mustonen, V., Warringer, J., Durbin, R., Liti, G., 2014. A high-definition view of functional genetic variation from natural yeast genomes. Molecular biology and evolution 31, 872–88. https://doi.org/10.1093/molbev/msu037

Berkow, E.L., Lockhart, S.R., 2017. Fluconazole resistance in Candida species: a current perspective. Infect Drug Resist 10, 237–245. https://doi.org/10.2147/IDR.S118892

Berkow, E.L., Lockhart, S.R., Ostrosky-Zeichner, L., 2020. Antifungal Susceptibility Testing: Current Approaches. Clin Microbiol Rev 33, e00069-19. https://doi.org/10.1128/CMR.00069-19

Bolger, A.M., Lohse, M., Usadel, B., 2014. Trimmomatic: a flexible trimmer for Illumina sequence data. Bioinformatics 30, 2114–2120. https://doi.org/10.1093/bioinformatics/btu170

Bongomin, F., Gago, S., Oladele, R.O., Denning, D.W., 2017. Global and Multi-National Prevalence of Fungal Diseases—Estimate Precision. Journal of Fungi 3, 57. https://doi.org/10.3390/jof3040057

Campoy, S., Adrio, J.L., 2017. Antifungals. Biochemical Pharmacology, Antibiotics - Meeting the Challenges of 21st Century Health Care: Part I 133, 86–96. https://doi.org/10.1016/j.bcp.2016.11.019

Chakrabortee, S., Byers, J.S., Jones, S., Garcia, D.M., Bhullar, B., Chang, A., She, R., Lee, L., Fremin, B., Lindquist, S., Jarosz, D.F., 2016. Intrinsically Disordered Proteins Drive Emergence and Inheritance of Biological Traits. Cell 167, 369-381.e12. https://doi.org/10.1016/j.cell.2016.09.017

Cherry, J.M., Hong, E.L., Amundsen, C., Balakrishnan, R., Binkley, G., Chan, E.T., Christie, K.R., Costanzo, M.C., Dwight, S.S., Engel, S.R., Fisk, D.G., Hirschman, J.E., Hitz, B.C., Karra, K., Krieger, C.J., Miyasato, S.R., Nash, R.S., Park, J., Skrzypek, M.S., Simison, M., Weng, S., Wong, E.D., 2012. Saccharomyces Genome Database: the genomics resource of budding yeast. Nucleic Acids Res. 40, D700-705. https://doi.org/10.1093/nar/gkr1029

Delma, F.Z., Al-Hatmi, A.M.S., Brüggemann, R.J.M., Melchers, W.J.G., de Hoog, S., Verweij, P.E., Buil, J.B., 2021. Molecular Mechanisms of 5-Fluorocytosine Resistance in Yeasts and Filamentous Fungi. J Fungi (Basel) 7, 909. https://doi.org/10.3390/jof7110909

Denning, D.W., 2002. Echinocandins: a new class of antifungal. Journal of Antimicrobial Chemotherapy 49, 889–891. https://doi.org/10.1093/jac/dkf045

DePristo, M.A., Banks, E., Poplin, R., Garimella, K.V., Maguire, J.R., Hartl, C., Philippakis, A.A., del Angel, G., Rivas, M.A., Hanna, M., McKenna, A., Fennell, T.J., Kernytsky, A.M., Sivachenko, A.Y., Cibulskis, K., Gabriel, S.B., Altshuler, D., Daly, M.J., 2011. A framework for variation discovery and genotyping using next-generation DNA sequencing data. Nat Genet 43, 491–498. https://doi.org/10.1038/ng.806

Edwards, M.D., Gifford, D.K., 2012. High-resolution genetic mapping with pooled sequencing. BMC Bioinformatics 13 Suppl 6, S8. https://doi.org/10.1186/1471-2105-13-S6-S8

Ehrenreich, I.M., Torabi, N., Jia, Y., Kent, J., Martis, S., Shapiro, J.A., Gresham, D., Caudy, A.A., Kruglyak, L., 2010. Dissection of genetically complex traits with extremely large pools of yeast segregants. Nature 464, 1039–1042. https://doi.org/10.1038/nature08923

Fisher, M.C., Hawkins, N.J., Sanglard, D., Gurr, S.J., 2018. Worldwide emergence of resistance to antifungal drugs challenges human health and food security. Science 360, 739–742. https://doi.org/10.1126/science.aap7999

García-Alcalde, F., Okonechnikov, K., Carbonell, J., Cruz, L.M., Götz, S., Tarazona, S., Dopazo, J., Meyer, T.F., Conesa, A., 2012. Qualimap: evaluating next-generation sequencing alignment data. Bioinformatics 28, 2678–2679. https://doi.org/10.1093/bioinformatics/bts503

Garrison E, M.G., 2012. Haplotype-based variant detection from short-read sequencing. arXiv 2012;1207.3907.

Gebre, A.A., Okada, H., Kim, C., Kubo, K., Ohnuki, S., Ohya, Y., 2015. Profiling of the effects of antifungal agents on yeast cells based on morphometric analysis. FEMS Yeast Research 15, fov040. https://doi.org/10.1093/femsyr/fov040

Gold, J.A.W., Ahmad, F.B., Cisewski, J.A., Rossen, L.M., Montero, A.J., Benedict, K., Jackson, B.R., Toda, M., 2022. Increased Deaths From Fungal Infections During the Coronavirus Disease 2019 Pandemic—National Vital Statistics System, United States, January 2020–December 2021. Clinical Infectious Diseases ciac489. https://doi.org/10.1093/cid/ciac489

Heimark, L., Shipkova, P., Greene, J., Munayyer, H., Yarosh-Tomaine, T., DiDomenico, B., Hare, R., Pramanik, B.N., 2002. Mechanism of azole antifungal activity as determined by liquid chromatographic/mass spectrometric monitoring of ergosterol biosynthesis. J Mass Spectrom 37, 265–269. https://doi.org/10.1002/jms.280

Hoepfner, D., Helliwell, S.B., Sadlish, H., Schuierer, S., Filipuzzi, I., Brachat, S., Bhullar, B., Plikat, U., Abraham, Y., Altorfer, M., Aust, T., Baeriswyl, L., Cerino, R., Chang, L., Estoppey, D., Eichenberger, J., Frederiksen, M., Hartmann, N., Hohendahl, A., Knapp, B., Krastel, P., Melin, N., Nigsch, F., Oakeley, E.J., Petitjean, V., Petersen, F., Riedl, R., Schmitt, E.K., Staedtler, F., Studer, C., Tallarico, J.A., Wetzel, S., Fishman, M.C., Porter, J.A., Movva, N.R., 2014. High-resolution chemical dissection of a model eukaryote reveals targets, pathways and gene functions. Microbiological Research 169, 107–120. https://doi.org/10.1016/j.micres.2013.11.004

Homann, O.R., Dea, J., Noble, S.M., Johnson, A.D., 2009. A Phenotypic Profile of the Candida albicans Regulatory Network. PLOS Genetics 5, e1000783. https://doi.org/10.1371/journal.pgen.1000783

Jorgensen, P., Nishikawa, J.L., Breitkreutz, B.-J., Tyers, M., 2002. Systematic Identification of Pathways That Couple Cell Growth and Division in Yeast. Science 297, 395–400. https://doi.org/10.1126/science.1070850

Jung, K.-W., Yang, D.-H., Maeng, S., Lee, K.-T., So, Y.-S., Hong, J., Choi, J., Byun, H.-J., Kim, H., Bang, S., Song, M.-H., Lee, J.-W., Kim, M.S., Kim, S.-Y., Ji, J.-H., Park, G., Kwon, H., Cha, S., Meyers, G.L., Wang, L.L., Jang, J., Janbon, G., Adedoyin, G., Kim, T., Averette, A.K., Heitman, J., Cheong, E., Lee, Y.-H., Lee, Y.-W., Bahn, Y.-S., 2015. Systematic functional profiling of transcription factor networks in Cryptococcus neoformans. Nat Commun 6, 6757. https://doi.org/10.1038/ncomms7757

Kapitzky, L., Beltrao, P., berens, T.J., Gassner, N., Zhou, C., Wüster, A., Wu, J., Babu, M.M., Elledge, S.J., Toczyski, D., Lokey, R.S., Krogan, N.J., 2010. Cross-species chemogenomic profiling reveals evolutionarily conserved drug mode of action. Molecular Systems Biology 6, 451. https://doi.org/10.1038/msb.2010.107

Kramer, B., Kramer, W., Williamson, M.S., Fogel, S., 1989. Heteroduplex DNA correction in Saccharomyces cerevisiae is mismatch specific and requires functional PMS genes. Molecular and Cellular Biology 9, 4432–4440. https://doi.org/10.1128/mcb.9.10.4432-4440.1989

Krol, K., Brozda, I., Skoneczny, M., Bretne, M., Skoneczna, A., 2015. A Genomic Screen Revealing the Importance of Vesicular Trafficking Pathways in Genome Maintenance and Protection against Genotoxic Stress in Diploid Saccharomyces cerevisiae Cells. PLOS ONE 10, e0120702. https://doi.org/10.1371/journal.pone.0120702

Kumar, P., Henikoff, S., Ng, P.C., 2009. Predicting the effects of coding non-synonymous variants on protein function using the SIFT algorithm. Nat Protoc 4, 1073–81. https://doi.org/10.1038/nprot.2009.86

Lee, Y., Puumala, E., Robbins, N., Cowen, L.E., 2021. Antifungal Drug Resistance: Molecular Mechanisms in Candida albicans and Beyond. Chem Rev 121, 3390–3411. https://doi.org/10.1021/acs.chemrev.0c00199

Li, H., Durbin, R., 2009. Fast and accurate short read alignment with Burrows-Wheeler transform. Bioinformatics 25, 1754–60. https://doi.org/10.1093/bioinformatics/btp324

Lum, P.Y., Armour, C.D., Stepaniants, S.B., Cavet, G., Wolf, M.K., Butler, J.S., Hinshaw, J.C., Garnier, P., Prestwich, G.D., Leonardson, A., Garrett-Engele, P., Rush, C.M., Bard, M., Schimmack, G., Phillips, J.W., Roberts, C.J., Shoemaker, D.D., 2004. Discovering Modes of Action for Therapeutic Compounds Using a Genome-Wide Screen of Yeast Heterozygotes. Cell 116, 121–137. https://doi.org/10.1016/S0092-8674(03)01035-3

Marie, C., Leyde, S., White, T.C., 2008. Cytoplasmic localization of sterol transcription factors Upc2p and Ecm22p in S. cerevisiae. Fungal Genetics and Biology 45, 1430–1438. https://doi.org/10.1016/j.fgb.2008.07.004

Naseeb, S., Visinoni, F., Hu, Y., Roberts, A.J.H., Maslowska, A., Walsh, T., Smart, K.A., Louis, E.J., Delneri, D., 2021. Restoring fertility in yeast hybrids: Breeding and quantitative genetics of beneficial traits. PNAS 118. https://doi.org/10.1073/pnas.2101242118

Phadke, S.S., Maclean, C.J., Zhao, S.Y., Mueller, E.A., Michelotti, L.A., Norman, K.L., Kumar, A., James, T.Y., 2018. Genome-Wide Screen for Saccharomyces cerevisiae Genes Contributing to Opportunistic Pathogenicity in an Invertebrate Model Host. G3 Genes|Genomes|Genetics 8, 63–78. https://doi.org/10.1534/g3.117.300245

Picard Toolkit, 2019. Broad Institute, GitHub repository. https://broadinstitute.github.io/picard/

S. Andrews, 2010. FastQC A Quality Control Tool for High Throughput Sequence Data.

Samarasinghe, H., You, M., Jenkinson, T.S., Xu, J., James, T.Y., 2020. Hybridization Facilitates Adaptive Evolution in Two Major Fungal Pathogens. Genes 11, 101. https://doi.org/10.3390/genes11010101

Scannell, D.R., Zill, O.A., Rokas, A., Payen, C., Dunham, M.J., Eisen, M.B., Rine, J., Johnston, M., Hittinger, C.T., 2011. The Awesome Power of Yeast Evolutionary Genetics: New Genome Sequences and Strain Resources for the Saccharomyces sensu stricto Genus. G3 (Bethesda) 1, 11–25. https://doi.org/10.1534/g3.111.000273

Timouma, S., Schwartz, J.-M., Delneri, D., 2020. HybridMine: A Pipeline for Allele Inheritance and Gene Copy Number Prediction in Hybrid Genomes and Its Application to Industrial Yeasts. Microorganisms 8, 1554. https://doi.org/10.3390/microorganisms8101554

Vermes, A., Guchelaar, H.-J., Dankert, J., 2000. Flucytosine: a review of its pharmacology, clinical indications, pharmacokinetics, toxicity and drug interactions. Journal of Antimicrobial Chemotherapy 46, 171–179. https://doi.org/10.1093/jac/46.2.171

Vogan, A.A., Khankhet, J., Samarasinghe, H., Xu, J., 2016. Identification of QTLs Associated with Virulence Related Traits and Drug Resistance in Cryptococcus neoformans. G3 (Bethesda) 6, 2745–2759. https://doi.org/10.1534/g3.116.029595

Yue, J.-X., Li, J., Aigrain, L., Hallin, J., Persson, K., Oliver, K., Bergström, A., Coupland, P., Warringer, J., Lagomarsino, M.C., Fischer, G., Durbin, R., Liti, G., 2017. Contrasting evolutionary genome dynamics between domesticated and wild yeasts. Nat Genet 49, 913–924. https://doi.org/10.1038/ng.3847

Zhang, L., Zhang, Y., Zhou, Yiming, Zhao, Y., Zhou, Yuxiang, Cheng, J., 2002. Expression profiling of the response of Saccharomyces cerevisiae to 5-fluorocytosine using a DNA microarray. International Journal of Antimicrobial Agents 20, 444–450. https://doi.org/10.1016/S0924-8579(02)00201-7

Zhang, Y., Xu, J., 2018. Molecular Mechanisms of Fungal Adaptive Evolution, in: Rampelotto, P.H. (Ed.), Molecular Mechanisms of Microbial Evolution, Grand Challenges in Biology and Biotechnology. Springer International Publishing, Cham, pp. 409–435. https://doi.org/10.1007/978-3-319-69078-0_15

Zhou, X., Ma, Y., Fang, Y., Gerile, W., Jaiseng, W., Yamada, Y., Kuno, T., 2013. A Genome-Wide Screening of Potential Target Genes to Enhance the Antifungal Activity of Micafungin in Schizosaccharomyces pombe. PLOS ONE 8, e65904. https://doi.org/10.1371/journal.pone.0065904

Chapter 5 - Biotechnological exploitation of Saccharomyces jurei and its hybrids in craft beer fermentation uncovers new aroma combinations

Konstantina Giannakou[1, 2], **Federico Visinoni[1]**, Penghan Zhang[3], Nishan Nathoo[1], Paul Jones[2], Mark Cotterrell[2], Urska Vrhovsek[3] and Daniela Delneri[1]

[1]*Manchester Institute of Biotechnology, University of Manchester, 131 Princess Street Manchester M1 7DN, UK*

[2]*Cloudwater Brew Co, 7-8 Piccadilly Trading Estate, Manchester M1 2NP, UK*

[3]*Foundation Edmund Mach, Via Edmund Mach 1, 38010 San Michele all'Adige TN, Italy*

5.1 Foreword

The work in this chapter has been published in *Food Microbiol.* (2021) **100**: 103838 (DOI: 10.1016/j.fm.2021.103838). Here, the manuscript has been revised to maintain a coherent style with the rest of the thesis. References used within the manuscript are presented at the end of the chapter.

Author contributions: DD conceived the study; DD and UV supervised the genetic and phenotypic experiments, and the GC-GC-MS analysis, respectively. MC and PJ supervised the pilot-scale fermentation. KG carried out the experimental work with the input of FV. NN contributed to the construction of five hybrids. KG and FV analysed the genetic and physiological data and KG, FV and PZ performed and analysed the GCxGC-MS volatile compounds spectra. KG, FV and DD wrote the manuscript with input of MC, PZ, UV. All authors contributed to the article and approved the submitted version.

Detailed FV contribution: I worked alongside KG and directly contributed to the following section of this manuscript: *i.* the data of Fig. 5-1 in relation to Sc-200, Sj-95, H1, H2 and H3; *ii.* all the data in Figure 5-2; *iii.* acquisition and initial data normalisation for Table 5-1; iv. all data for Fig. 5-5.

5.2 Abstract

Hybridization is an important evolutionary mechanism to generate novel phenotypes and can produce new hybrids harbouring advantageous combinations of relevant traits. *Saccharomyces jurei* is a recently discovered species in the *Saccharomyces* genus and its biotechnological potential has yet to be fully explored. *S. jurei* exhibited several traits of industrial interest, such as sustained growth in wort and at low temperature, which suggest possible applications in the production of fermented beverages.

Here, we analysed the fermentation capabilities and aroma profile of *S. jurei* D5095 in pilot scale beer fermentations. Moreover, we generated novel non-GMO hybrids between *S. jurei* and a *S. cerevisiae* ale yeast. Through hybridisation we combined the good fermentation performances of the ale parent strain with *S. jurei* cold-tolerance, while eliminating unwanted traits such as sugar hyper-attenuation and high production of 4-vinyl guaiacol. Moreover, we were able to generate strains displaying novel, complex aroma profile of great interest for the craft brewing and beverage industry. This study exploits the genetic diversity of *Saccharomyces* yeasts and proves how inter-specific hybridisation and clone selection can be effectively used in brewing to introduce novel products and to eliminate or increase specific traits.

5.3 Introduction

The brewer's yeast is often synonymous with *S. cerevisiae*, the predominant species in beer and wine fermentations (Gallone et al., 2016). *S. cerevisiae* offers outstanding fermentation capability together with the ability to consume most of the available sugars in wort and must (Mortimer et al, 2000). Moreover, the *S. cerevisiae* strains employed in the production of fermented beverages underwent centuries of domestication and diverged from wild isolates for their performances in industrial settings and for their aroma profile. For instance, wild strains often possess traits which impart unusual, often unwanted, notes to the aroma, such as the production of the so-called phenolic off flavours (Gallone et al., 2016).

However, the role of *Saccharomyces* species in the production of fermented beverages is not limited to that of *S. cerevisiae* alone. In particular, natural hybrids between *S. cerevisiae* and at least three other species, namely *S. eubayanus*, *S. uvarum*, and *S. kudriavzevii*, were also isolated from brewing and wine-making processes (Alsammar and Delneri, 2020) (García-Ríos et al., 2019) (Krogerus et al., 2018). In fact, hybridization represents an important tool to bridge the gap between domestic and wild species, allowing the addition of traits of industrial relevance, such as cold tolerance and flocculation, to the *S. cerevisiae* backbone (Giannakou et al., 2020). A clear example of hybridization industrial potential is represented by *S. pastorianus*, a *S. cerevisiae* and *S. eubayanus* hybrid, employed in the production of lager beers (Mertens et al., 2015, Monerawela and Bond, 2018). Albeit less common, *S. cerevisiae* hybrids with *S. uvarum* or *S. kudriavzevii* have been associated with wine and cider fermentations while *S. cerevisiae* x *S. kudriavzevii* and *S. cerevisiae x S. uvarum* interspecific hybrids have also been isolated from brewing and winemaking fermentative environments (Krogerus et al., 2018, García-Ríos et al., 2019). Recently, much work has gone in the generation of novel hybrids, both to improve the fitness in industrial conditions and to diversify the aroma profile of industrial strains (Bellon et al. 2013; Krogerus et al 2017). The recent years have seen a considerable growth in the craft beer market, stemming from consumers demands for new, innovative beer styles and flavours (Jaeger et al., 2020). More complex and stronger flavours in fermented beverages can be achieved with the addition of unconventional ingredients or the application of unconventional yeast strains with a diverse aroma profile. Recently, a new species in the genus, *S. jurei*, was discovered from *Quercus robur* bark in France. Phenotypic assays revealed *S. jurei* to possess attractive traits for industrial application. The strains characterized were resistant to a variety of stressors, from osmo-tolerance to high sugar concentrations, while presenting a relatively high fitness at low temperature (Naseeb et al., 2017; 2018). Moreover, *S. jurei* possible application and performance in baking were assessed together with other cryotolerant species of the *Saccharomyces* genus, opening new avenues for its application in the food market (Magalhães et al., 2021).

Here, we evaluate *S. jurei* potential in the production of fermented beverages, outlining its performance in wort media and providing a comprehensive characterization of its aroma profile through GCxGC-MS analysis. Moreover, we constructed non-GMO hybrids

between *S. jurei* and a *S. cerevisiae* ale strain harbouring different combination of allelic traits through spore-to-spore mating. The novel hybrids were tested in pilot beer fermentation and displayed optimal sugar attenuation while producing a broad and different spectrum of flavours. This study shows the efficacy of inter-specific hybridisation as a tool for strain development and its potential to generate strains for industrial applications.

5.4 Results and Discussion

5.4.1 Constructions of diploid non-GMO hybrids between S. jurei D5095, D5088 and ale strains S. cerevisiae OYL200 and OYL500

A previous study highlighted *S. jurei* capability to consume maltose, the main sugar found in wort, on solid media (Naseeb et al., 2017). To further assess *S. jurei* potential as a brewer strain, we determined the growth kinetics of *S. jurei* in liquid media containing maltose or maltotriose, as sole carbon source and compared its fitness to *S. cerevisiae* lab (Sc-505), wild (Sc-96-2) and ale strains (Sc-20). All strains were able to utilise maltose and maltotriose, although at different rates, with *S. cerevisiae* ale and lab strains outperforming *S. jurei* and *S. cerevisiae* wild isolates (Figure B-1, Appendix B). Sj-95 performed consistently better than Sj-88 in both sugar sources, while both *S. jurei* strains reached a higher final biomass than *S. cerevisiae* wild strain. Next, we investigated if the different rates of maltose and maltotriose utilization observed in the two *S. jurei* strains could be explained by allelic variation of maltose and maltotriose related genes. We annotated *S. jurei* genome using HybridMine to determine one-to-one orthologues between *S. cerevisiae* and *S. jurei* (Timouma et al, 2020). Both *S. jurei* strains were found to have 100% identical *MAL13*, *MTT1* and *AGT1* genes. However, *MAL61*, *MAL33* and *MAL32* are diverged between the two strains both at nucleotide and protein level (Table B-1, Appendix B), potentially explaining the phenotypic differences observed in the maltose and maltotriose uptake.

While *S. jurei* performances in maltose were not comparable to the one of the industrial *S. cerevisiae* strain, its ability to ferment both maltose and maltotriose is a unique trait in

wild *Saccharomyces* species. Therefore, *S. jurei* was deemed an interesting candidate for the generation of interspecific hybrids with commercial *S. cerevisiae* strains of biotechnology importance. We attempted to obtain meiotic offspring from 16 different *S. cerevisiae* industrial strains which could be crossed with *S. jurei* strains. Two strains, Sc-200 and Sc-500, displayed the highest sporulation efficiency amongst the strain tested, with 100% viability, and thus were chosen for the crossings (Table B-2, Appendix B). We created eight non-GMO hybrids via spore-to-spore mating (H1-8): H1-3 from crossing Sc-200 x Sj-95, and H4-8 from crossing Sc-500 x Sj-88. The hybridisation technique was chosen to exploit the parental strain heterozygosity and generate hybrids harbouring different combinations of traits and thus phenotypic variations. The hybrid nature of the spores was validated via species-specific PCR (Figure B-2, Appendix B). The diploid nature of the hybrids H1-3 was further confirmed via FACS (Figure B-3, Appendix B). Moreover, we carried out a species-specific chromosome-specific PCR to check for the presence of both parental chromosome sets in the hybrids. All 16 chromosomes of *S. cerevisiae* and *S. jurei* were present in the hybrids, thus ruling out chromosomal loss (Figure B-4, Appendix B). Finally, meiosis was triggered in the hybrids to check the spore viability. As expected for an inter-specific diploid hybrid there were no viable spores (*i.e.* aneuploid hybrid would produce some viable spores; data not shown).

5.4.2 Physiological characterisation of the hybrids

The growth of the hybrids was tested in liquid medium in presence of the main wort sugars: glucose, maltose, and maltotriose, and compared to the one of the parents (Figure 5-1 and Table B-3, Appendix B). In both YP + 2% maltose and YP + 2% maltotriose the hybrids outpaced the *S. jurei* parent achieving a higher growth rate and maximum biomass over the course of the fermentation (Figure 5-1A, Table B-3, Appendix B). Moreover, H1 exhibited similar fermentation kinetics to the industrial *S. cerevisiae* parent (Sc-200) in YP + 2% maltose, while H2 mirrored Sc-200 in YP + 2% maltotriose. In YP + 2% glucose, all strains behaved similarly with no significant difference in growth rates. Interestingly, H3 fermentations resulted in the highest final biomass recorded from all strains in all three sugar sources (Figure 5-1A, Table B-3, Appendix B). The results obtained suggests that H1 and H2 inherited different traits from the parental strains in

relation to the efficient utilisation of the different brewing sugars, resulting in diverging phenotypes in different carbon sources.

Regarding the family of hybrids resulting from the cross between Sj-88 x Sc-500, different patterns emerged. In YP + 2% maltose, hybrids H4 and H8 presented the highest specific growth rate and performed significantly better than the ale parent Sc-500 (Table B-3, Appendix B). Similarly, in YPD, hybrid H8, alongside H5 and H7, reached a higher specific growth rate than the ale strain Sc-500. In YP + 2% maltotriose, however, the growth rate of the hybrids was lower than both parents, indicating an impaired maltotriose assimilation. Overall H4 was the best performing hybrid from this family in both maltose and maltotriose and may thus represent a good candidate for further studies.

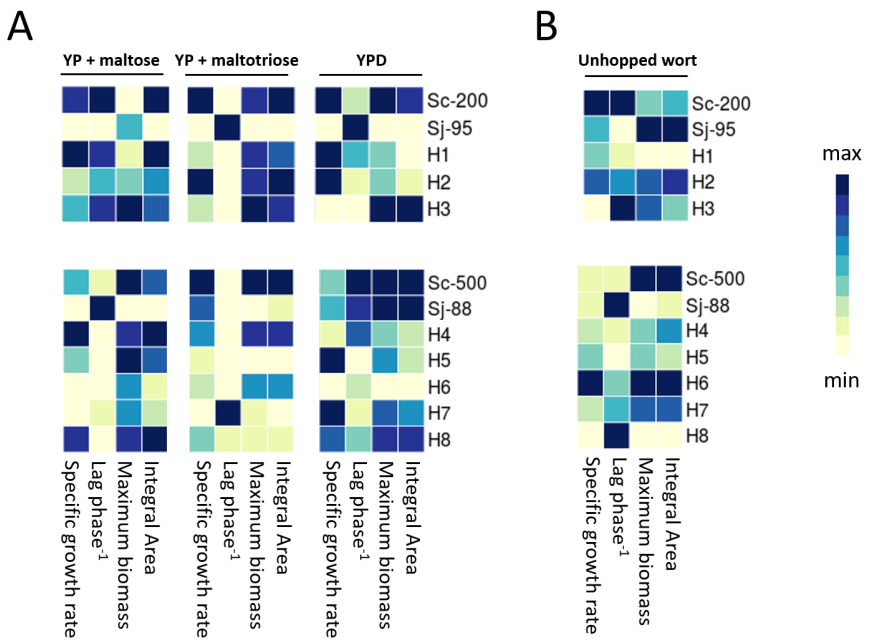

Figure 5-1 | Heat map of growth parameters of Sj-95, Sj-88, Sc-200, Sc-500 and H1-8 hybrids. Growth parameters were assessed in YPD, YP + 2% maltose an YP + 2% maltotriose at 16°C (A) and in unhopped wort at 20°C (B). For each parameter, min and max represent the lowest and highest value reported for each hybrid cross in a specific medium. Lag phase is expressed as $(\text{lag phase})^{-1}$, thus a darker colour corresponds to the lowest lag phase observed.

Next, we evaluated the resistance of the hybrid strains to the hyperosmotic stress derived by the high sugar concentration present in wort and their performance in a mixed sugar medium through micro-fermentation in malt extract (Figure 5-1B). All the strains generated were able to grow and cope with the ever-changing fermentation environment resulting from the consumption of different sugars, lowering pH and ethanol accumulation. In malt extract, H2 presented the fastest growth among the hybrids resulting from the cross between Sj-95 x Sc 200. As for the cross Sj-88 x Sc 500, the hybrid progeny H4, H5 and H6 reached a significantly higher specific growth rate than the parent strains (Table B-3, Appendix B). Unexpectedly, H8 was the worst performing strain in unhopped wort despite the high growth recorded in YP + maltose, suggesting that the strain might not be adapted to the stressors of the brewing process.

Next, we examined the fitness of all strains in solid media contaning glucose or maltose at different temperatures. As *S. jurei* is described as a cold-tolerant species within the *Saccharomyces* genus (Naseeb et al., 2017), we tested the phenotypes of the hybrids at a broad range of temperatures used in brewing fermentations: 22ºC, 16ºC and 8ºC. Strains from crossings between Sj-95 x Sc-200 in YPD at 22 ºC and 16 ºC showed a similar growth pattern (Figure 5-2A, 5-2C), while at 8ºC Sj-95, H1 and H2 grew considerably better compared to the other strains, indicating that the hybrids inherited the cold tolerance traits from *S. jurei* (Figure 5-2E). Moreover, H1 grew visibly better than the other strains in YP-maltose at 8ºC presenting a clear example of hybrid vigour (Figure 5-2F). Similarly, to what we previously observed in liquid medium, all the strains grew marginally better than Sj-95 in YP + maltose at 22ºC and 16ºC (Figure 5-2B, 5-2D).

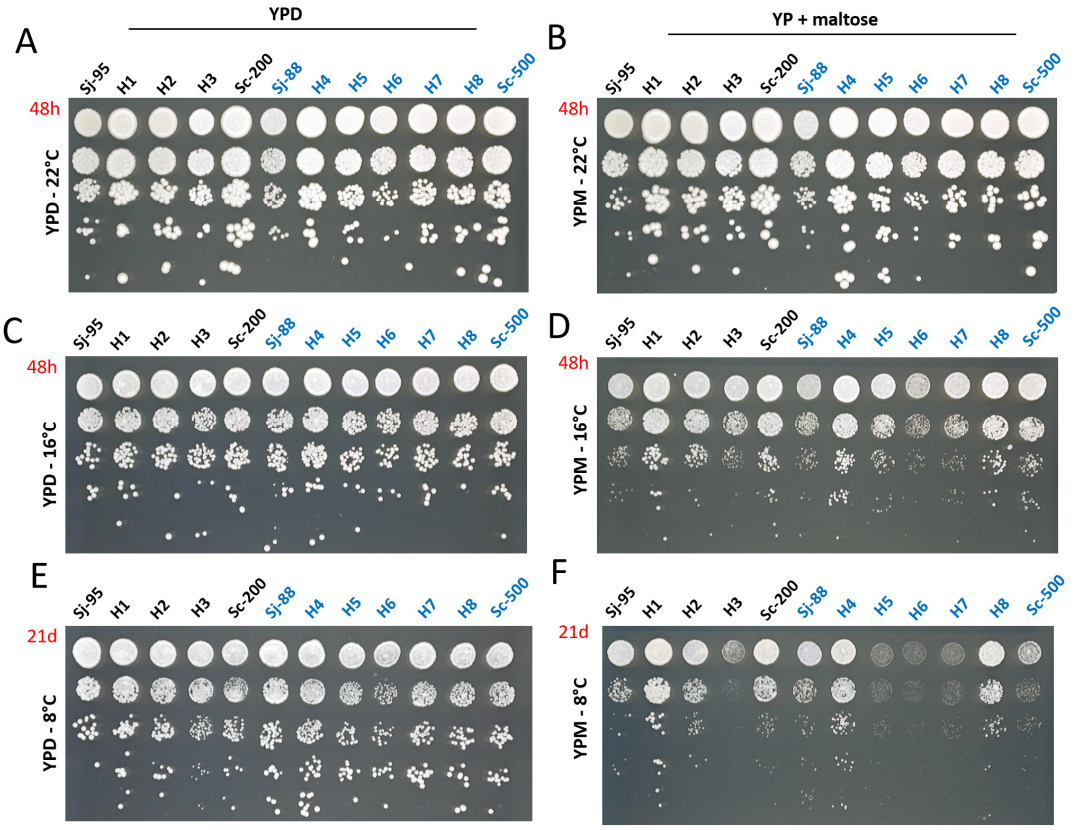

Figure 5-2 | Spot test assay of Sj-95, Sj-88, Sc-200, Sc-500 and H1-8 hybrids at different temperatures. Each strain was spotted in YPD at 22°C (A), 16°C (C) and 8°C (E) and YP + 2% maltose at 22°C (B), 16°C (D) and 8°C (F) and incubated for 48h (A, B, C, D) and 21 days (E, F).

As for the Sc-500 x Sj-88 hybrids (H4-H8), we observed good growth for all strains in YPD at 22ºC and 16ºC (Figure 5-2A, 5-2C). However, at 8ºC, H4 and H8 showed considerably better performances compared to both parental strains and the other hybrids (Figure 5-2E). Similarly, in YP-Maltose, H4 and H8 have the highest growth and colony formation among all strains at 8°C (Figure 5-2F). At 22°C we could not detect any difference between strains fitness in both glucose and maltose, except a slower growth of the parental Sj-88, while at 16ºC, H4 and H8 grow better than the other hybrids (Figure 5-2B, 5-2D).

Overall, H1 (crossing Sj-95 x Sc-200) and H8 (crossing Sj-88 x Sc-500) inherited the efficient maltose assimilation from the *S. cerevisiae* ale strain, and cold tolerance from the

parental *S. jurei* (Figure 5-2). The hybrid progenies of the cross Sj-95 x Sc-200 (H1-3) were selected for further studies in pilot scale fermentations based on the performance in unhopped wort of the specific *S. jurei* parent (Sj-95 is growing better than Sj-88 as shown in Figure B-1, Appendix B) and the relative hybrids.

5.4.3 Pilot-scale beer fermentation in 10L vessels

In beer fermentation, sugar attenuation and cell viability at the end of the process are key parameters for a successful fermentation (Sanchez et al., 2012). In brewing terms, attenuation describes the level of wort carbohydrates assimilated during fermentation (Vidgren et al., 2009). Generally, the desired level of attenuation is around 70-80% as the leftover sugars contribute to the flavour of the final product, conferring a desirable sweetness and body composition. Certain *S. cerevisiae* strains are characterized by their ability to secrete a glucoamylase (*STA1*), an enzyme that catalyses the digestion of starch and complex oligosaccharides. This amylolytic activity can lead to hyper-attenuation, as it allows the consumption of the complex sugars in the wort which are otherwise non-fermentable, and excess carbon dioxide formation in bottles, cans or kegs (Meier-Dörnberg et al., 2018) (Yamashita et al., 1985). We conducted 10L beer fermentation experiments to evaluate the sugar attenuation and cell viability of all strains of the Sj-95 x Sc-200 family and analyse their performances in pilot scale fermentations (Figure 5-3). Sc-200 was found to over-attenuate the beer, with a decrease of 92% of the original gravity. The poor performance of Sj-95 observed in micro-fermentations was mirrored in pilot scale fermentations, with a total decrease in gravity of only 23% across 14 days. All the hybrids showed improved fermentation ability compared to Sj-95, having inherited from Sc-200 the necessary traits to sustain the stressors of industrial fermentation and efficiently utilize the wort sugars. In particular, H3 behaved similarly to Sc-200, over attenuating the beer (89%), while H1 and H2 attenuated the beer to 70% of the original gravity, a desirable characteristic for different beer styles. The gravity remained stable after the 14th day indicating that no further fermentation took place. All the strains were stained with methylene blue to estimate cell viability at the end of the fermentation, which allows to reuse the yeast in a practice known as re-pitching. No significant difference in viability across strains was detected (*i.e.* approximately 50% viable cells at

the end of the fermentation process). End point fermentation samples were analysed via HPLC to estimate the sugars consumed and ethanol produced by the different strains (Figure 5-4). The consumed sugars detected at the end of the fermentation confirmed the attenuation observed in the gravity data (Figure 5-3). Sj-95 showed the highest amount of residual sugars and the lowest production of ethanol compared to the Sc-200 and the generated hybrids. The ethanol produced (% ABV) varied between all strains, reflecting the different sugar consumption: 6.6% (Sc-200), 6.4% (H3), 5.2% (H2), 4.5% (H1) and 1.8% (Sj-95).

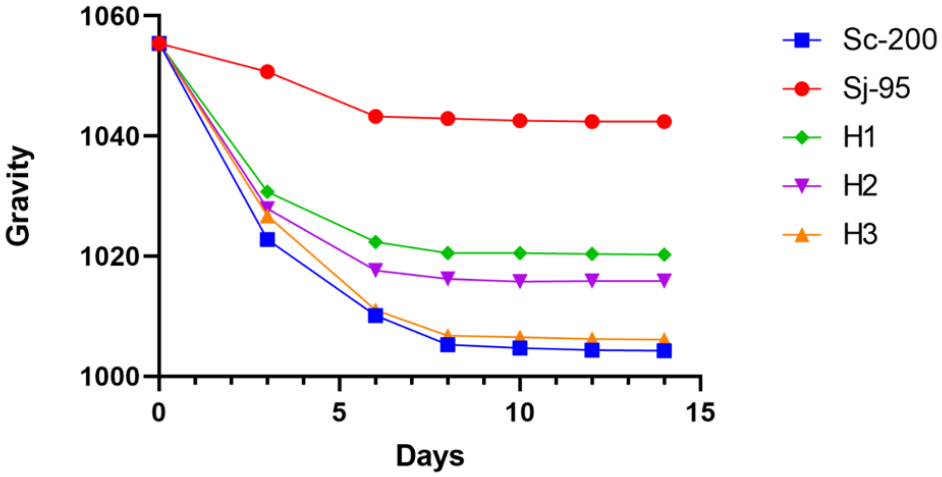

Figure 5-3 | Fermentation kinetics of strains Sj-95, Sc-200 and the generated hybrids H1-3 in pale wort media of initial OG 1055.4. The consumption of sugars throughout the process is displayed by the specific gravity of the media, measured with a density meter.

Based on the hyper-attenuation characteristic observed in the fermentation profiles of Sc-200, we tested for the presence of the *STA1* gene in the newly made hybrids via PCR (Yamauchi et al., 1998). The PCR results showed that only the ale parent strain Sc-200 and H3 possess the *STA1* gene, while H1, H2 and Sj-95 do not, as confirmed by the available genomic data on *S. jurei* (Naseeb et al., 2018) (Figure B-5, Appendix B). Therefore, it is likely that Sc-200 is heterozygotic for the *STA1* gene, and thus the undesirable trait could be effectively eliminated via spore-to-spore mating, as in the case for H1 and H2.

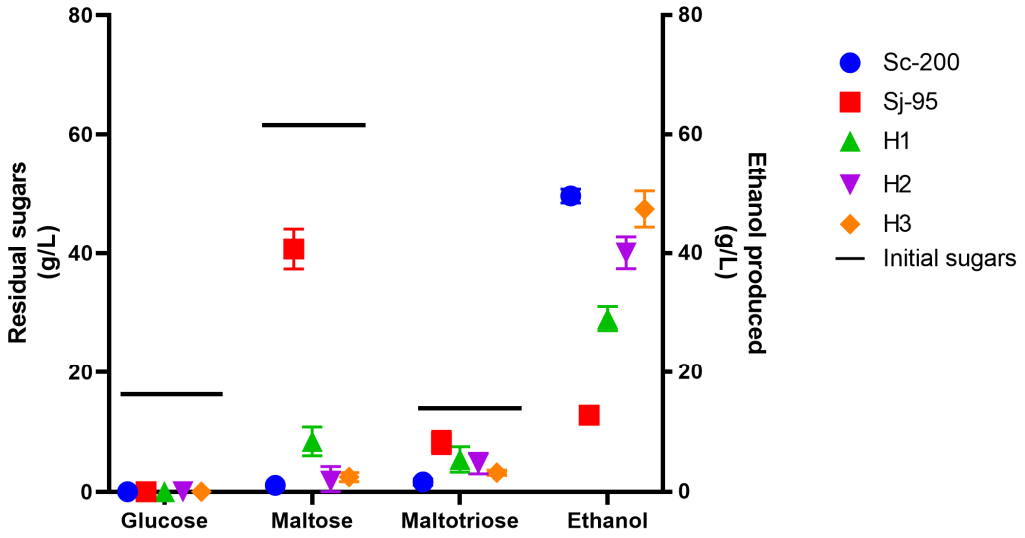

Figure 5-4 | Sugar content and production of ethanol in final beer samples analysed via HPLC. The residual wort sugars and the ethanol production at the end of fermentation from strains Sc-200, Sj-95, H1, H2, and H3 was quantified by HPLC. Error bars display the standard deviation of technical replicates.

5.4.4 Aroma profiling of generated hybrids reveals different aroma compounds from both *S. jurei* and *S. cerevisiae* parents

Identification of volatile aromatic compounds for all strains was carried out at the end of the beer fermentation using GCxGC-MS. In total, 18 esters, 11 alcohols and 33 volatile compounds including acids, terpenes, aldehydes, ketones, and phenolic compounds were identified (Table 5-1).

As expected, the levels of volatile compounds varied significantly between the parent strains. A strong tropical and fruity character was detected in Sc-200, due to the greater production of esters and isohexanoic acid (Table 5-1 and Figure 5-5). Instead, Sj-95 had low levels of esters, but produced a significant amount of spice/clove and alcoholic aromas deriving from phenolic compounds and fusel alcohols, respectively. The phenotypic difference observed in the hybrid strains was reflected in differences between their aroma profiles, as the strain inherited different flavour notes from the parental

strains. For instance, high level of ethyl hexanoate, a compound with a sweet fruity/apple aroma, was achieved only in H2 and in Sc-200 fermentations, while H2 and H3 mirrored the parental Sj-95 with little to no production of this compound. On the other hand, 4-vinyl-guaiacol, a spicy phenolic aroma, was detected in Sj-95 and inherited only in H1 and H2, albeit in lower concentrations.

Table 5-1 | Target volatile metabolites of beer samples after 14 days of fermentation with Sj-95, Sc-200, H1, H2 and H3.

Esters						
		Peak Area x 10^6				
Compound name	**Flavour description**	**Sj-95**	**H1**	**H2**	**H3**	**Sc-200**
Ethyl Acetate	Fruity, pear	0.10	14.07	n.d	2.17	20.55
Isoamyl acetate	fruity, banana	113.09	118.07	113.51	33.91	195.70
Isobutyl acetate	Fruity	1.34	3.08	0.80	1.24	2.47
Phenylethyl Acetate	floral, roses	n.d	n.d	49.89	73.73	204.76
Ethyl hexanoate	fruity, apple	n.d	139.98	0.63	n.d	182.91
Ethyl benzoate	medicinal	0.10	n.d	0.83	0.13	1.31
Propyl acetate	fruity, pear	9.16	30.06	17.27	46.10	13.12
Ethyl Propionate	fruity, pineapple	5.91	12.57	5.93	16.99	5.79
Ethyl heptanoate	fruity, grape	9.52	14.08	23.08	8.11	16.54
Ethyl octanoate	fruity, wine, sweet	122.15	384.92	341.67	91.09	256.04
Isopentyl isobutyrate	fruity, apricot, banana	7.12	10.87	8.37	7.30	n.d
Ethyl decanoate	sweet, apple, grape	n.d	135.00	20.73	2.73	9.26
Ethyl isobutyrate	fruity	0.65	0.82	0.55	1.46	0.79
Methyl Phenylacetate	honey	3.28	3.75	3.31	3.60	3.13

cis-Carvyl acetate	minty	n.d	n.d	0.91	0.75	0.75
Propyl octanoate	coconut, cacao	0.12	5.47	0.50	n.d	0.10
Alcohols						
		Peak Area x 10^6				
Compound name	**Flavour description**	**Sj-95**	**H1**	**H2**	**H3**	**Sc-200**
Isoamyl alcohol	fusel, alcoholic, fruity	775.86	523.41	615.71	0.58	1.67
Phenylethyl alcohol	floral, rose, honey	n.d	141.54	102.47	n.d	199.83
Butanol	solvent, fusel	4.22	4.79	4.55	5.62	17.69
Propanol	solvent, fusel	58.09	113.88	0.27	84.11	40.09
Isobutanol	etheral, wine	31.05	35.44	18.22	27.29	31.40
Furfuryl alcohol	Sweet	n.d	3.13	1.44	2.83	1.67
Hexanol	pungent, fusel, fruity	19.07	23.32	17.57	22.85	19.38
Methionol	meaty, onion	0.59	0.63	n.d	0.81	0.98
Acids						
		Peak Area x 10^6				
Compound name	**Flavour description**	**Sj-95**	**H1**	**H2**	**H3**	**Sc-200**
Hexanoic Acid	sour, cheesy	114.68	191.37	110.19	171.14	126.50
Butanoic Acid	acidic, unpleasant	11.08	3.88	7.04	5.46	5.81
Isovaleric Acid	cheesy	12.92	10.76	9.12	17.20	9.96
Isohexanoic acid	Fruity	n.d	0.08	0.03	0.69	0.42
Propanoic acid	pungent, acidic	2.07	5.02	3.94	8.40	1.64
Acetic Acid	sour, acidic	32.58	0.68	19.70	n.d	0.68
Octanoic Acid	rancid, cheesy	n.d	315.80	173.67	186.57	116.58
Terpenes and other volatile compounds						

		Peak Area x 10^6				
Compound name	**Flavour description**	**Sj-95**	**H1**	**H2**	**H3**	**Sc-200**
1-alpha-Terpinyl acetate	herbal	3.70	4.44	2.16	4.61	2.91
Hop ether	floral, woody	11.40	10.06	10.93	14.16	8.13
Myrcene	woody, spicy	3.79	14.06	13.58	9.78	10.76
Linalool	citrus, floral, waxy	97.57	n.d	n.d	107.32	n.d
4-vinyl guaiacol	clove, spicy, smoke	1.95	2.30	1.36	n.d	n.d
2-4-di-tert-butylphenol	phenolic	3.16	3.84	2.94	3.52	3.46
Alpha-Phellandrene	citrusy, peppery	0.56	0.63	0.58	0.58	0.68
o-Cymene	Spicy	9.48	9.30	8.54	10.72	7.83
Dehydro-p-cymene	fresh, citrus	0.46	0.56	0.32	n.d	0.39
Nonanol	Citrus	17.61	14.38	48.42	23.02	n.d
Limonene	citrus, fresh, sweet	0.61	0.16	0.90	n.d	0.27
2-Acetylfuran	sweet, nutty	n.d	1.31	n.d	1.54	1.24
2-Hexanone	acetone like	0.03	0.06	0.04	n.d	0.06
Terpinolene	pine	0.27	n.d	0.29	0.41	0.42
Camphene	fresh, herbal, woody	0.04	0.04	0.02	0.05	n.d
(E)-2,6-Dimethylocta-1,5,7-trien-3-ol	camphoreous, lime	1.73	2.29	1.17	2.01	2.44
Nonanal	citrus	0.31	0.54	0.55	n.d	0.54
Ocimene	fruity	13.09	11.71	9.43	n.d	9.77
Pinene	woody, pine	n.d	2.16	n.d	17.93	2.16
1-Decene	sweet	0.29	5.06	7.55	n.d	5.79

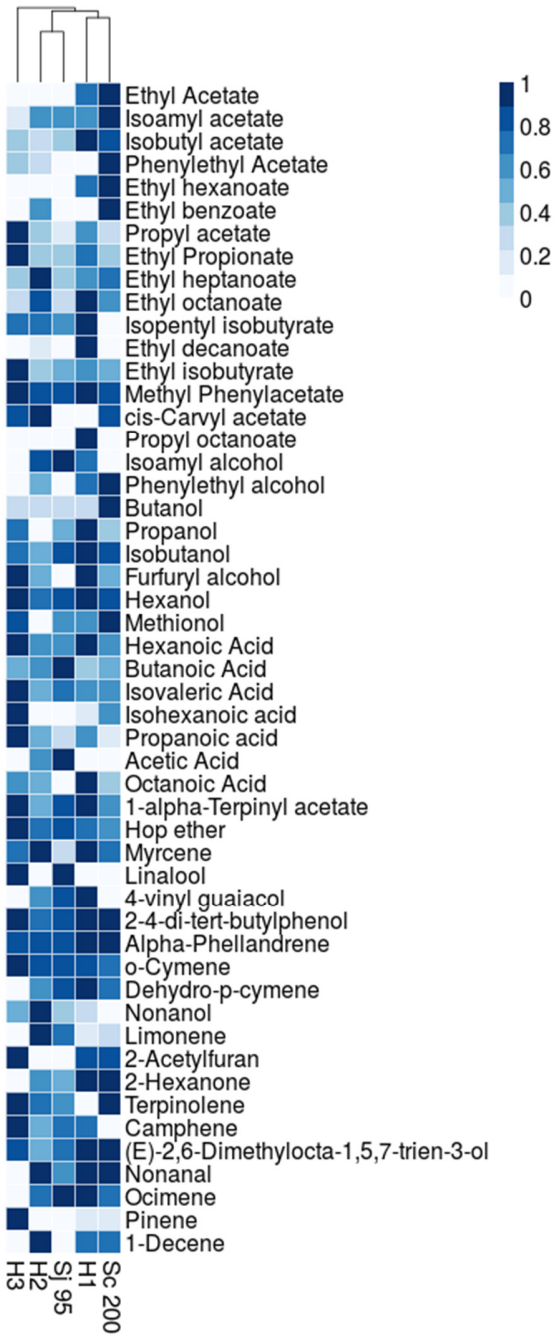

Figure 5-5 | Clustering and heatmap visualization of aroma profiling. Normalized values per detected volatile compound across 14 days fermentation beer samples with Sj-95, Sc-200, H1, H2 and H3. For each compound, 1 and 0 represent the lowest and highest value reported across all strains tested.

Interestingly, the hybrids achieved a higher production of specific compounds, such as ethyl propionate and α-terpinyl-acetate compared to the parental strains, perhaps as a result of an additive effect between parental genes. As a case in point, H1 outperformed both parental strains in the production of propyl acetate and ethyl isobutyrate, esters imparting a fruity aroma. Different parental allele inheritance in the hybrids allowed both the diversification of aroma characteristics in the beer by strengthening or weakening specific features, and the generation of new aroma profiles. In fact, clustering of the samples according to the GCxGC-MS data showed H1 and H2 aroma profiles resembled those of Sc-200 and Sj-95, respectively (Figure 5-5). However, H3 did not clearly cluster with any of the two parents for its flavour profile.

Transcription levels of the genes responsible for the decarboxylation of ferulic acid to 4-vinyl guaiacol (*PAD1* and *FDC1)* were quantified via RT-PCR to determine if differential expression of the two genes in the hybrids was responsible for the different levels 4-vinyl guaiacol recorded. (Mukai et al., 2010). All hybrids expressed the *S. cerevisiae* allele of *PAD1* at lower levels than the parent Sc-200. In contrast, the *S. jurei* allele was only significantly different from the parent Sj-95 in the hybrid H3 (Figure 5-6A). As for the *FDC1* gene, similar levels of expression of the *S. jurei* allele were detected in H1, H2, H3 and Sj-95, but a lower expression of the *S. cerevisiae* allele was observed in all hybrids when compared to the Sc-200 parent (Figure 5-6B). Therefore, the undetectable levels of 4-vinyl-guaiacol in H3 could be due to the lower expression of *PAD1* and *FDC1* for both *S. cerevisiae* and *S. jurei* alleles recorded in that strain. A sensory evaluation of the final beers was carried out at Cloudwater Brew Co (Figure 5-7; Table B-4, Appendix B). Finished beers made with H1 and H2 were found to possess a likable estery character with predominant hits of apple, banana, and pear. Instead, the beer fermented with strain Sc-200 was characterized by a predominant estery profile, as observed via GCxGC-MS, which contributed to fruity characteristics and an astringent character and dry after taste, deriving from the sugars over-attenuation. A clove/phenolic character was present in different intensities in Sj-95, H1 and H2 beers likely resulting from the presence of 4-vinyl-guaiacol in the samples. Beer made from H3 was described as fruity and tropical, with notes of peach and berries, with a marked astringent and light sour character when compared to H1 and H2, and with a minimal phenolic content. H2 aroma and flavour

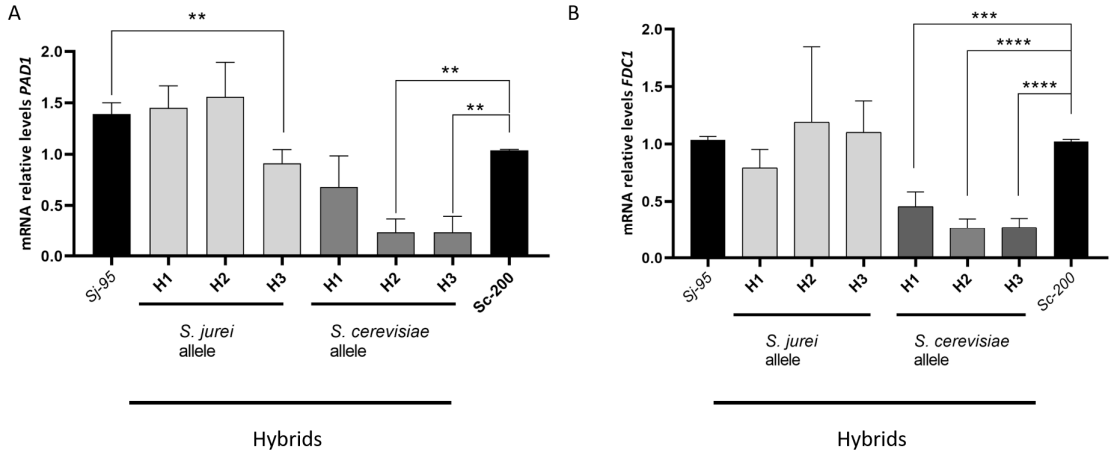

Figure 5-6 | Relative PAD1 and FDC1 expression in all strains. The mRNA levels of *PAD1* (A) and *FDC1* (B) normalized to *ACT1* were determined by RT-qPCR. Sj-alleles in H1-3 (light gray) are compared with Sj-95. Sc-allele in H1-3 (dark gray) are compared with Sc-95. ** indicate $p<0.005$, *** indicate $p<0.0005$, **** indicate $p<0.0001$ upon ANOVA.

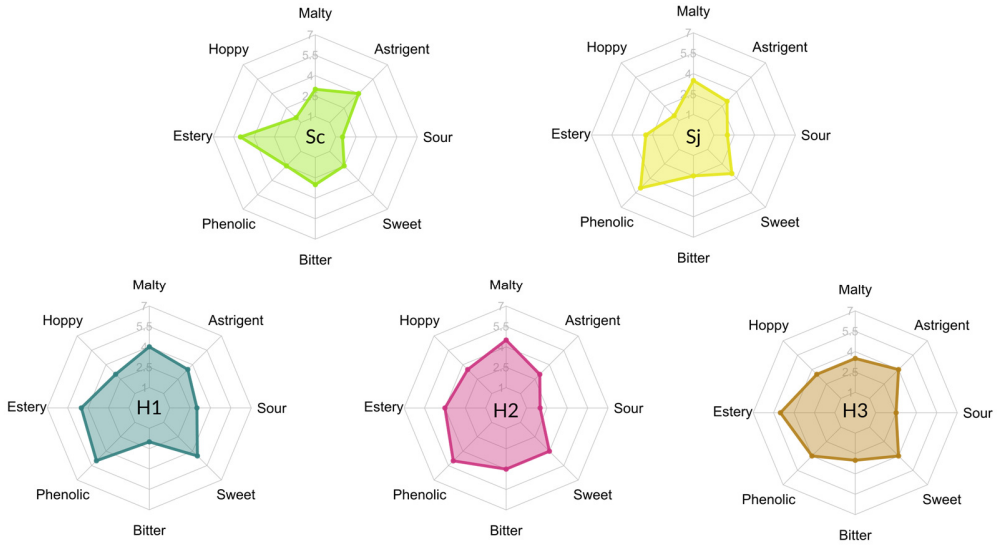

Figure 5-7 | Spider chart of descriptive sensory analysis. The intensity of eight different descriptors in the aroma of Final samples from 10L beer fermentation with Sc-200 (Sc), Sj-95 (Sj) and hybrids 1-3 were scored by a sensory panel.

profile was considered the most balanced, with a nice sweetness and soft body characteristics. Following the sensory evaluation, H1 and H2 were selected by Cloudwater Brew Co. for the production of beer in in 200L barrels.

5.5 Conclusion

Recent years have brought a remarkable increase in the demand of craft beer as consumers demand unique recipes and flavours beyond the traditional and well-known beer styles. As a result, interspecific hybridisation between yeast species has gained increased relevance as a way to generate new, complex aroma profiles through the combination of traits from different parental species.

In this study, we evaluated the beer fermentation performances and aroma profiles of *S. jurei* and of novel S. *cerevisiae x S. jurei* hybrids generated through non-GM techniques. *S. jurei* is a prime candidate for a brewing strain as it is able to utilize maltose efficiently and sustain growth at the low temperatures which characterise both ale and lager beer fermentations. Moreover, we found that *S. jurei* is able to assimilate maltotriose, a sugar present in malt, a rare trait in the *Saccharomyces* genus. It is our understanding that maltotriose uptake mechanisms and brewing potential of a novel *S. jurei* strain isolated from *Fraxinus excelsior*, Bavaria, Germany, have been the topic of a collaborative study involving VTT Technical Research Centre of Finland, TU Berlin, and TU Munich, and that this work will be reported shortly in *Frontiers in Microbiology* (Hutzler et al. 2021). An intriguing outcome of this work has also been the observation that *S. jurei* has the ability to utilize maltotriose and may, under the right conditions, or with appropriate evolutionary engineering, serve as a brewing strain in its own right. Our study, however, shows that, *S. jurei* fermentation ability is limited when compared with a *S. cerevisiae* ale strain. Thus, we constructed hybrids between the two different species through spore-to-spore mating to combine the parental traits contributing to beneficial phenotypes, such as cold tolerance and efficient utilization of malt sugars. Moreover, the ability of both parents to ferment maltose and maltotriose efficiently provides a fertile ground for the generation of hybrids possessing an allele combination that improves on the parental phenotype (heterosis; Bernardes et al., 2017).

Interestingly, the generated hybrids showed improved fermentation performance over the *S. jurei* parent, overcoming its inability to complete the fermentation in dry malt extract. This suggests that strain domestication in industrial settings from both parent strains is not essential to create successful hybrids for the brewing industry, paving the way for the application of other alternative *Saccharomyces*. Different allele inheritance in the generated hybrids also resulted in the elimination of the unwanted hyper-attenuation character of the *S. cerevisiae* ale parent. Thus, we suggest that Sc-200 is likely to be heterozygous for *STA1,* the gene, responsible for this trait. Similar results regarding the phenotypic influence of specific allele inheritance in the generated hybrids were also observed in the 4-vinyl guaiacol production derived from the activity of *PAD1/FDC1* genes. For example, the hybrid H3 exhibited a lower expression of the inherited genes, compared to the parental strains, resulting in undetectable levels of 4-vinyl guaiacol. Therefore, breeding techniques and meiotic segregation proved as an efficient tool for the elimination of *STA1+*/*POF+* traits and hold a great potential for further applications in the brewing industry (Krogerus et al., 2017, Nikulin et al., 2018, Tubb et al., 1981).

In this study we analysed the aroma profile of beers fermented by a selection of hybrids generated through spore-to-spore mating between *S. jurei* and a *S. cerevisiae* ale strain. Moreover, we described for the first time the aroma profile of *S. jurei* in beer products which resulted characterised by a strong clove/phenolic aroma. The complementary aroma profiles of the parental strains granted a desirable combination of tropical and floral character in the hybrid strains. The three hybrids presented different concentrations and intensities of various flavour compounds resulting in an increased concentrations of selected aroma compounds compared to the parents, as observed in the case of H3 propyl acetate production. Moreover, through spore to spore mating, we were able to eliminate the *S. jurei* genes responsible for 4-vinyl guaiacol production, which is generally considered to be an off-flavour and its removal is a signature of domestication in brewing yeast (Gonçalves et al., 2016, Gallone et al., 2016) These results indicate that mixed or intermediary flavour profiles between parental strains can arise through hybridisation and thus breeding techniques can facilitate yeast selection for specific beer styles or new recipes.

Applying classical breeding to ale strains can be challenging as strains often suffer from poor sporulation ability and efficiency (Codon et al., 1995). Nonetheless, interspecific hybridisation is an efficient tool to create new yeast strains harbouring beneficial characteristics from different species without recurring to GM techniques (Krogerus et al., 2018, 2019, Mertens et al., 2015). Recent studies demonstrated that hybridisation played an important role in the domestication of beer and wine yeast strains (Gallone et al., 2018, 2019, Giannakou et al., 2020, González et al., 2008). Here, we show that hybridisation with a brewing strain can effectively ease the introduction of natural strains in the *Saccharomyces* genus in industrial processes and generated novel products, catering to consumer demands for complex flavour.

5.6 Materials and Methods

5.6.1 Yeast strains

The strains used in this study are the *S. cerevisiae* ale strains OYL200 (Tropical IPA; Omega Yeast lab; Sc-200) and OYL500 (Saisonstein's monster, Omega Yeast Lab, Sc-500), *S. jurei* D5088 (NCYC 3947; Sj-88) and D5095 (NCYC 3962; Sj-95)(Naseeb et al., 2017), the *S. cerevisiae* lab strain NCYC505 (Sc-505) (Martini and Kurtzman, 1985), the *S. cerevisiae* wild isolate 96.2 (Sc-96.2) (Paget et al., 2014) and the *S. cerevisiae* x *S. kudriavzevii* allotetraploid hybrid PB7 (Morard et al, 2020).

5.6.2 Hybridisation and hybrids confirmation

Sj-95 was crossed with ale strain Sc-200, while Sj-88 was crossed with strain Sc-500. Strains were forced to sporulate by growth in pre-sporulation media (yeast extract 0.8%, bacto-peptone 0.3% and glucose 10%, VWR, UK) at 30ºC for 16 h followed by incubation on minimal sporulation medium (1% Potassium acetate, 0.125 % yeast extract, 0.1% glucose and 2% bacto-agar, VWR,UK) at 20ºC for 7–10, until tetrad formation. Tetrad dissection and spore to spore mating were performed in fresh YPD plates (1% yeast extract, 2% peptone, 2% agar, 2% glucose, VWR, UK) using a 400MSM micromanipulator (Singer Instruments, UK). The plates were incubated at 30ºC until colony formation. Then, the colonies were spread plated in fresh YPM plates (1% yeast extract, 2% peptone,

2% agar, 2% maltose, Sigma Aldrich, UK) and a single colony was used for DNA extraction. Yeast DNA was extracted from overnight cultures by using the standard phenol/chloroform method described previously (Fujita and Hashimoto, 2000) with modifications described in (Naseeb et al., 2018). The hybrid nature of potential hybrids was confirmed by species-specific PCR. The primers pairs used for the species-specific multiplex PCR are specified in Table B-5 (Appendix B). The PCR conditions were as follows: 2 min at 94°C, 35 cycles of 1 min at 94°C, 1 min at 55°C, and 30 s at 72°C, followed by a final cycle of 3 min at 72°C and subsequent cooling to room temperature. The hybrid status of the newly generated strains was confirmed by the presence of both parental bands in the gel. Hybrids confirmed via PCR were streaked another six times in YPM plates to ensure strain purity and genome stability. The ploidy of the hybrids was estimated by flow cytometry (Haase and Reed, 2002) using Amnis ImageStream X (ISX MKII,) multispectral imaging flow cytometer. Furthermore, species-specific, chromosome-specific primers sets were designed for all the 16 chromosomes present in *S. cerevisiae* and *S. jurei*, respectively (Table B-5, Appendix B) and PCR was performed to confirm the presence of both chromosomes sets in the hybrids. The hybrids were sporulated to ensure no viable spores were detected.

5.6.3 Micro-fermentations and culture conditions

Growth kinetics in YPD, YP+ 2% maltose and YP+2% maltotriose were generated using BMG LabTech Omega series Microplate Readers. Growth was monitored for 72h in 96 well plates with 4 biological replicates at an initial OD_{600} of 0.1 in 200µl of working volume. Growth was recorded via optical density at 600nm by measuring the absorbance every 10 minutes.

Micro-fermentations in unhopped wort were carried out using a BioLector® I system (m2p Labs, Germany) with a 48 well FlowerPlate® (MTP-48-B, m2p Labs, Germany) for 72h. Unhopped wort, with starting gravity (OG) of 1037, was made by using 104 g/L DME (Dry Malt Extract, Browland,UK) and boiled for 1 hour. The media was filtered to remove any undiluted powder. The following BioLector settings were used: filter: biomass (gain 15), humidity: on (>85% using ddH2O), temperature: 20°C, oxygen supply: 20.85% (atmospheric air), agitation speed: 800 rpm. The total volume of each well was 1500 µL,

initial OD_{600} was 0.1. Scatter light at 620nm was measured every 7.29 min and logged by the BioLector®. The R package grofit was used to analyse the growth curve data of plate reader and micro-fermentation experiments (Kahm et al., 2010). Heat maps of the growth parameters were constructed using a in house R shiny app[2] using min-max column scaling.

The 10L scale beer fermentations were carried out for 14 days in home brewing equipment (plastic fermentor, lid and airlock) using pale wort OG 1055.4 according to the Cloudwater Brew Co. in-house recipe (Table B-6, Appendix B). The gravity (OG) was measured daily to evaluate the fermentation rate using a density meter (DMA 48, Anton Paar). End point fermentation samples were collected on the 14th day and stored at -20°C for GCxGC–MS and HPLC analysis.

5.6.4 *PAD1* and *FDC1* transcript analysis by RT-qPCR

Overnight cultures were grown in YP-glucose 2% and used to inoculate a 12°P unhopped wort to a starting OD_{600} of 0.1. Cultures were incubated overnight at 20°C until an OD_{600} of 6-8 after which RNA was isolated from pelleted yeast using RNeasy Mini Kit (Qiagen, Germany) The lysis was performed by enzymatic digestion of cell wall followed by lysis of spheroplasts. Between 0.25 to 0.5 micrograms of total RNA was transcribed into cDNA in a 20 µL reaction mix using QuantiTect Reverse Transcription Kit (Qiagen, Germany) according to the manufacturer's protocol. The resulting cDNA was diluted 5-fold and 2 µL of diluted cDNA (corresponding to 10 ng of total RNA) was used as template in 10 µL qPCR reactions. The qPCR reactions were prepared with 5 µl of iTAq Universal SYBR Green super Mix 2X and 0.3 µM of gene-specific primers (Table B-6, Appendix B). The qPCR reactions were performed on a LightCycler® 480 II instrument (Roche Diagnostics, Basel, Switzerland) in 3 technical replicates on the reverse-transcribed RNA isolated from 3 biological replicates. The following programme was used: initial denaturation (95 °C for 3 min), amplification cycle (95°C for 15s, 55°C for 30s, 72°C for 30s) repeated 45 times,

[2] https://kobchai-shinyapps01.shinyapps.io/heatmap_construction/

melting curve programme (65–97°C with continuous fluorescence measurement), and a cooling step to 10°C. The relative expression of *PAD1* and *FDC1* was calculated using the ΔΔCT method by normalizing gene expression to that of the *ACT1* gene. Statistical analysis and plots were produced using GraphPad prism.

5.6.5 Phenotypic assay test

Cells were incubated in YPD and YP-maltose agar plates at 22°C, 16°C and 8°C, to determine fitness at different growth temperatures and carbon sources. The range of temperatures was selected according to temperatures used in the brewing industry. Strains were grown overnight in liquid YPD and 5 µl of 10-fold serial dilutions were spotted to plates starting with an initial OD_{600} of 0.4.

5.6.6 HPLC and Headspace – SPME GCxGC–TOF-MS

Substrate consumption and alcohol production in pilot scale fermentations was determined by ion-exchange HPLC using a 1269 Infinity II LC system equipped with a Refractive Index detector (Agilent). A 300x7.8 mm Hi-Plex HPLC Column (Agilent) was equilibrated with 5 mM H_2SO_4 in HPLC grade water at 60° at a 0.8 mL/min flow rate. The samples were filtered prior to HPLC analysis (pore size 0.45 µm) and 10 µL of the sample was injected. Sugars and ethanol were quantified using calibration curves generated from authentic standards.

Aroma composition of the final beer products was determined by HS-SPME-GCxGC-TOF-MS. as previously described (Carlin et al., 2016). A Gerstel MultiPurpose Sampler autosampler (Gerstel GmbH & Co. Mülheim an der Ruhr Germany) with an agitator and SPME fibre was used to extract the volatiles from the sample vial headspace. The GCxGC system consisted of an Agilent 7890 A (Agilent Technologies, Santa Clara, CA) equipped with a Pegasus IV time-of-flight mass spectrometer (Leco Corporation, St. Joseph, MI). A VF-Wax column was used as first-dimension (1D) column, and a RTX-200MS-column was used as a second-dimension (2D) column. The GC system was equipped with a secondary column oven and non-moving quadjet dual-stage thermal modulator. The injector/ transfer line was maintained at 250°C. Oven temperature programme conditions were as follows: initial temperature of 40°C for 4 min, programmed at 6°C min^{-1} up to 250°C,

where it remained for 5 min. The secondary oven was kept 5°C above the primary oven throughout the chromatographic run. The modulator was offset by +15°C in relation to the secondary oven; the modulation time was 7s and 1.4s of hot pulse duration. Helium was used as carrier gas at a constant flow of 1.2 mL min-1. The MS parameters included electron ionisation at 70 eV with ion source temperature at 230 °C, detector voltage of 1317 V, mass range of m/z 35–450 and acquisition rate of 200 spectra s-1. SPME extraction was carried as follows: 5 mL of beer, sonicated for 2 min to remove the foam, were put into 20 mL glass headspace vials, 1.5 g of NaCl were added, the samples were spiked with 50 µl of alcoholic solution of 2-octanol at 2.13 mg L-1 (99%, Sigma-Aldrich) as internal standard. Samples were kept at 35°C for 5 min and then extracted for 30 min at 35°C. The headspace was sampled using 2-cm DVB/CAR/PDMS 50/30 lm fibre. The volatile and semi-volatile compounds were desorbed in the GC inlet at 250°C for 4 min in splitless mode and the fibre was reconditioned for 7 min at 270°C prior to each analysis. Aroma profiles were visualized using the R shiny app for heatmap construction.

5.6.7 Data processing and peak annotation

GCxGC-MS data acquisition and processing were achieved with LECO ChromaTOF (Version 4.71). The processing consisted of peak picking, peak annotation, and statistic confirmation. During the peak picking, only signals which were above the noise were considered (baseline offset = 1). The minimal expected peak width (on 2nd dimension) for deconvolution was 0.8 s. A peak was defined when at least 5 ions, whose signal to noise ratio was above 100 (Stefanuto et al., 2017), can be grouped. A picked peak was annotated by matching its mass spectrum (MS) to the reference spectrum in the database. In this study, the MS databases used were NIST/EPA/NIH 11, Wiley 8 and the FFNSC 2. The MS similarity threshold for the peak annotation was 700. Each sample was analysed with three technical replicates. Inter-measurements peak alignment was performed based on the retention times (both 1st and 2nd dimensions) and the mass spectrum. A minimal MS similarity of 600 was required. Analytes were further examined, only if they could be detected in all the technical replicates. An inter-class comparison was performed between sample class and blank class. Fisher ratio threshold was used to eliminate artifact compounds (sorbent bleeding, column bleeding and other possible interferences). The

applied significance level was 0.05. Peak identification was then completed by checking the linear temperature programmed retention index (LTPRI), which is available in the NIST RI database.

5.6.8 Sensory evaluation of beer products

Sensory analysis were carried out at Cloudwater Brew Co. by brewing experts trained on beer sensory analysis and on the detection off-flavours. Beers from the 10L scale fermentation were tasted by a panel of 6 assessors to evaluate the differences and/or similarities between their aroma, flavour, taste/mouthfeel and to record overall impressions. The samples were blind-coded by using 3-digit codes and presented to the trained assessors in random order and duplicates. Palate cleansers were provided and recommended throughout the sensory testing. The panel was asked to score the intensity of different characters present in beer, and to provide any descriptive profiling of the flavours presented in the samples. A list of the following descriptors was provided beforehand to the panel: malty, astringent, sour, sweet, bitter, phenolic, estery, hoppy.

5.7 Acknowledgments

We thank Silvia Carlin for the assistance during the GCxGC-MS analysis, Laura Natalia Balarezo Cisneros for the help with RNA extraction and RT-qPCR, Soukaina Timouma for help with gene annotations and Daniel Schindler for providing the Omega yeast collection. We thank the production team of Cloudwater Brew Co. for helpful advice on the brew making and diastaticus yeast. This work was supported by Innovate-UK grant between the DD at University of Manchester and PJ at Cloudwater Brew. FV and PZ are supported by H2020-MSCA-ITN-2017 (764364) awarded to DD and UV, respectively.

5.8 References

Alsammar, H., Delneri, D., 2020. An update on the diversity, ecology and biogeography of the *Saccharomyces* genus. FEMS Yeast Res. https://doi.org/10.1093/femsyr/foaa013

Baker, E.C.P., Hittinger, C.T., 2019. Evolution of a novel chimeric maltotriose transporter in Saccharomyces eubayanus from parent proteins unable to perform this function. PLoS Genet. 15, e1007786. https://doi.org/10.1371/journal.pgen.1007786

Bellon, J.R., Schmid, F., Capone, D.L., Dunn, B.L., Chambers, P.J., 2013. Introducing a New Breed of Wine Yeast: Interspecific Hybridisation between a Commercial *Saccharomyces cerevisiae* Wine Yeast and *Saccharomyces mikatae*. PLoS One 8, e62053. https://doi.org/10.1371/journal.pone.0062053

Bernardes, J.P., Stelkens, R.B., Greig, D., 2017. Heterosis in hybrids within and between yeast species. J. Evol. Biol. 30, 538–548. https://doi.org/10.1111/jeb.13023

Carlin, S., Vrhovsek, U., Franceschi, P., Lotti, C., Bontempo, L., Camin, F., Toubiana, D., Zottele, F., Toller, G., Fait, A., Mattivi, F., 2016. Regional features of northern Italian sparkling wines, identified using solid-phase micro extraction and comprehensive two-dimensional gas chromatography coupled with time-of-flight mass spectrometry. Food Chem. 208, 68–80. https://doi.org/10.1016/j.foodchem.2016.03.112

Codon, A.C., Gasent-Ramirez, J.M., Benitez, T., 1995. Factors which affect the frequency of sporulation and tetrad formation in *Saccharomyces cerevisiae* baker's yeasts. Appl. Environ. Microbiol. 61, 630–638. https://doi.org/10.1128/aem.61.2.630-638.1995

Fujita, S.I., Hashimoto, T., 2000. DNA fingerprinting patterns of *Candida* species using HinfI endonuclease. Int. J. Syst. Evol. Microbiol. 50, 1381–1389. https://doi.org/10.1099/00207713-50-3-1381

Gallone, B., Mertens, S., Gordon, J.L., Maere, S., Verstrepen, K.J., Steensels, J., 2018. Origins, evolution, domestication and diversity of *Saccharomyces* beer yeasts. Curr. Opin. Biotechnol. 49, 148–155. https://doi.org/10.1016/j.copbio.2017.08.005

Gallone, B., Steensels, J., Mertens, S., Dzialo, M.C., Gordon, J.L., Wauters, R., Theßeling, F.A., Bellinazzo, F., Saels, V., Herrera-Malaver, B., Prahl, T., White, C., Hutzler, M., Meußdoerffer, F., Malcorps, P., Souffriau, B., Daenen, L., Baele, G., Maere, S., Verstrepen, K.J., 2019. Interspecific hybridization facilitates niche adaptation in beer yeast. Nat. Ecol. Evol. 3, 1562–1575. https://doi.org/10.1038/s41559-019-0997-9

Gallone, B., Steensels, J., Prahl, T., Soriaga, L., Saels, V., Herrera-Malaver, B., Merlevede, A., Roncoroni, M., Voordeckers, K., Miraglia, L., Teiling, C., Steffy, B., Taylor, M., Schwartz, A., Richardson, T., White, C., Baele, G., Maere, S., Verstrepen, K.J., 2016. Domestication and Divergence of *Saccharomyces cerevisiae* Beer Yeasts. Cell 166, 1397-1410.e16. https://doi.org/10.1016/j.cell.2016.08.020

García-Ríos, E., Guillén, A., De La Cerda, R., Pérez-Través, L., Querol, A., Guillamón, J.M., 2019. Improving the cryotolerance of wine yeast by interspecific hybridization in the genus *Saccharomyces*. Front. Microbiol. 10, 1–12. https://doi.org/10.3389/fmicb.2018.03232

Giannakou, K., Cotterrell, M., Delneri, D., 2020. Genomic Adaptation of *Saccharomyces* Species to Industrial Environments. Front. Genet. 11, 916. https://doi.org/10.3389/fgene.2020.00916

Gonçalves, M., Pontes, A., Almeida, P., Barbosa, R., Serra, M., Libkind, D., Hutzler, M., Gonçalves, P., Sampaio, J.P., 2016. Distinct Domestication Trajectories in Top-Fermenting Beer Yeasts and Wine Yeasts. Curr. Biol. 26, 2750–2761. https://doi.org/10.1016/j.cub.2016.08.040

González, S.S., Barrio, E., Querol, A., 2008. Molecular characterization of new natural hybrids of *Saccharomyces cerevisiae* and *S. kudriavzevii* in brewing. Appl. Environ. Microbiol. 74, 2314–2320. https://doi.org/10.1128/AEM.01867-07

Haase, S.B., Reed, S.I., 2002. Improved flow cytometric analysis of the budding yeast cell cycle. Cell Cycle 1, 117–121. https://doi.org/10.4161/cc.1.2.114

Hutzler, M., Michel, M., Kunz, O., Kuusisto, T., Magalhães, F., Krogerus, K. and Gibson, B., 2021. Unique brewing-relevant properties of a strain of *Saccharomyces jurei* isolated from ash (Fraxinus excelsior). Front. Microbiol, 12, p.645271. https://doi.org/10.3389/fmicb.2021.645271

Jaeger, S.R., Worch, T., Phelps, T., Jin, D., Cardello, A. V., 2020. Preference segments among declared craft beer drinkers: Perceptual, attitudinal and behavioral responses underlying craft-style vs. traditional-style flavor preferences. Food Qual. Prefer. 82, 103884. https://doi.org/10.1016/j.foodqual.2020.103884

Kahm, M., Hasenbrink, G., Lichtenberg-Fraté, H., Ludwig, J., Kschischo, M., 2010. Grofit: Fitting biological growth curves with R. J. Stat. Softw. 33, 1–21. https://doi.org/10.18637/jss.v033.i07

Krogerus, K., Preiss, R., Gibson, B., 2018. A Unique *Saccharomyces cerevisiae* × *Saccharomyces uvarum* Hybrid Isolated From Norwegian Farmhouse Beer: Characterization and Reconstruction. Front. Microbiol. 9. https://doi.org/10.3389/fmicb.2018.02253

Krogerus, K., Seppänen-Laakso, T., Castillo, S., Gibson, B., 2017. Inheritance of brewing-relevant phenotypes in constructed *Saccharomyces cerevisiae*×*Saccharomyces eubayanus* hybrids. Microb. Cell Fact. 16, 1–22. https://doi.org/10.1186/s12934-017-0679-8

Magalhães, F., Calton, A., Heiniö, R.L., Gibson, B., 2021. Frozen-dough baking potential of psychrotolerant Saccharomyces species and derived hybrids. Food Microbiol. 94, 103640. https://doi.org/10.1016/j.fm.2020.103640

Martini, A. V., Kurtzman, C.P., 1985. Deoxyribonucleic acid relatedness among species of the genus *Saccharomyces* sensu stricto. Int. J. Syst. Bacteriol. 35, 508–511. https://doi.org/10.1099/00207713-35-4-508

Meier-Dörnberg, T., Kory, O.I., Jacob, F., Michel, M., Hutzler, M., 2018. *Saccharomyces cerevisiae* variety *diastaticus* friend or foe?—spoilage potential and brewing ability of different *Saccharomyces cerevisiae* variety *diastaticus* yeast isolates by genetic, phenotypic and physiological characterizati. FEMS Yeast Res. 18. https://doi.org/10.1093/femsyr/foy023

Mertens, S., Steensels, J., Saels, V., De Rouck, G., Aerts, G., Verstrepen, K.J., 2015. A large set of newly created interspecific *Saccharomyces* hybrids increases aromatic diversity in lager beers. Appl. Environ. Microbiol. 81, 8202–8214. https://doi.org/10.1128/AEM.02464-15

Monerawela, C., Bond, U., 2018. The hybrid genomes of *Saccharomyces pastorianus*: A current perspective. Yeast 35, 39–50. https://doi.org/10.1002/yea.3250

Morard, M., Benavent-Gil, Y., Ortiz-Tovar, G., Pérez-Través, L., Querol, A., Toft, C. and Barrio, E., 2020. Genome structure reveals the diversity of mating mechanisms in Saccharomyces cerevisiae x Saccharomyces kudriavzevii hybrids, and the genomic instability that promotes phenotypic diversity. *Microbial genomics*, *6*(3).

Mukai, N., Masaki, K., Fujii, T., Kawamukai, M., Iefuji, H., 2010. PAD1 and FDC1 are essential for the decarboxylation of phenylacrylic acids in Saccharomyces cerevisiae. J. Biosci. Bioeng. 109, 564–569. https://doi.org/10.1016/j.jbiosc.2009.11.011

Naseeb, S., Alsammar, H., Burgis, T., Donaldson, I., Knyazev, N., Knight, C., Delneri, D., 2018. Whole genome sequencing, de novo assembly and phenotypic profiling for the new budding yeast species *Saccharomyces jurei*. G3 Genes, Genomes, Genet. 8, 2967–2977. https://doi.org/10.1534/g3.118.200476

Naseeb, S., James, S.A., Alsammar, H., Michaels, C.J., Gini, B., Nueno-Palop, C., Bond, C.J., McGhie, H., Roberts, I.N., Delneri, D., 2017. *Saccharomyces jurei* sp. nov., isolation and genetic identification of a novel yeast species from Quercus robur. Int. J. Syst. Evol. Microbiol. 67, 2046–2052. https://doi.org/10.1099/ijsem.0.002013

Nikulin, J., Krogerus, K., Gibson, B., 2018. Alternative *Saccharomyces* interspecies hybrid combinations and their potential for low-temperature wort fermentation. Yeast 35, 113–127. https://doi.org/10.1002/yea.3246

Paget, C.M., Schwartz, J.M., Delneri, D., 2014. Environmental systems biology of cold-tolerant phenotype in *Saccharomyces* species adapted to grow at different temperatures. Mol. Ecol. 23, 5241–5257. https://doi.org/10.1111/mec.12930

Sanchez, R.G., Solodovnikova, N., Wendland, J., 2012. Breeding of lager yeast with *Saccharomyces cerevisiae* improves stress resistance and fermentation performance. Yeast 29, 343–355. https://doi.org/10.1002/yea.2914

Stefanuto, P.H., Perrault, K.A., Dubois, L.M., L'Homme, B., Allen, C., Loughnane, C., Ochiai, N., Focant, J.F., 2017. Advanced method optimization for volatile aroma profiling of beer using two-dimensional gas chromatography time-of-flight mass spectrometry. J. Chromatogr. A 1507, 45–52. https://doi.org/10.1016/j.chroma.2017.05.064

Timouma, S., Schwartz, J.M. and Delneri, D., 2020. HybridMine: A Pipeline for Allele Inheritance and Gene Copy Number Prediction in Hybrid Genomes and Its Application to Industrial Yeasts. *Microorganisms*, *8*(10), p.1554.

Tubb, R.S., Searle, B.A., Goodey, A.R., Brown, A.J.P., 1981. Rare mating and transformation for construction of novel brewing yeasts. Proc. 18th Congr. Eur. Brew. Conv. 487–496.

Vidgren, V., Huuskonen, A., Virtanen, H., Ruohonen, L., Londesborough, J., 2009. Improved fermentation performance of a lager yeast after repair of its *AGT1* maltose and maltotriose transporter genes. Appl. Environ. Microbiol. 75, 2333–2345. https://doi.org/10.1128/AEM.01558-08

Yamashita, I., Suzuki, K., Fukui, S., 1985. Nucleotide sequence of the extracellular glucoamylase gene *STA1* in the yeast *Saccharomyces diastaticus*. J. Bacteriol. 161, 567–573. https://doi.org/10.1128/jb.161.2.567-573.1985

Chapter 6 – General conclusions and future work

6.1 Conclusions

Products in the food and beverage industry will need to quickly adapt to changes in both the climate and in customer demands, requiring the development of new strains and processes (Donadini and Porretta, 2017; Jones et al., 2005; Marín et al., 2021). However, breakthroughs in the field are hindered by the genetic complexity of the commercial yeast strains, which are typically sterile hybrids, and by the limited knowledge of the production of aroma compounds and their physiological impact in yeast. In this study, I applied a combination of genomics and metabolomics tools to tackle these challenges and advance the field, revealing new strategies for both strain and process development. First, I shed new lights on how yeast physiology may drive aroma compound production in yeast. As outlined in chapter 2, I uncovered a correlation between yeast growth and aroma production in *S. cerevisiae* using carbon-limited continuous fermentations in anaerobic conditions. In particular, the production of two higher alcohols (isobutanol and isoamyl alcohol) was found to decrease at higher growth rate, while ethyl octanoate and

acetaldehyde titres increased. Guided by the results obtained in chemostats I designed a feeding profile to limit yeast growth to study the extent aroma compound production could be manipulated by nutrients availability. The final concentration of seven out of ten volatile compound resulted significantly different between fed-batch fermentations, where growth was artificially limited, and batch. Consistently with the chemostat results, higher alcohols concentrations increased by 60% in fed-batch, while the concentrations of selected esters, such as ethyl decanoate, decreased. The results obtained revealed the high potential of the application of feeding profiles for the manipulation of volatile compounds production in yeast and provided new, important insights in the link between aroma and yeast physiology.

The body of work presented in chapter 3 expanded the toolset available to study *Saccharomyces* hybrids, bringing multigenerational hybrids into the realm of quantitative genetics. In collaboration with Dr. Naseeb, I was able to restore fertility in hybrid spores through rare mating, generating a library of F12 diploid hybrids between different *Saccharomyces* species. The unique makeup of the hybrids studied, derived by an allotetraploid hybrid from geographically distant strains, allowed to study the effect of natural variation and hybridisation on several traits of biotechnological interest. The hybrids spores generated displayed a broad phenotypic diversity in all the conditions tested and provided fertile grounds for genome-wide studies. Through quantitative genetics techniques I identified species-specific and hybrid-specific features responsible for industrial traits such as maltose, low temperature, and acetic acid tolerance. Furthermore, I revealed a strong genome wide-effect of mito-nuclear incompatibilities on the QTL landscape, by comparing QTL regions mapped in hybrid progeny derived from parental lines with different mitochondria.

The incredible potential of the pipeline developed for the study of complex traits in *Saccharomyces* hybrids was further explored in the work presented in chapter 4. A library of F12 *S. cerevisiae* x *S. kudriavzevii* hybrids was screened in sub-lethal concentrations of six antifungal agents to allow the dissection of complex traits linked with antifungal resistance. QTL mapping of genetic traits contributing to resistance to fluconazole, micafungin, and flucytosine revealed the high degree of complexity underlying these

traits and allowed the identification of several potential causal genes. The wealth of genetic data generated from the QTL studies presented in chapter 3 and 4 will help identify new genes and pathway linked to traits of biotechnological interest to accelerate the development of new products and strains. Moreover, it will allow further studies on nuclear-nuclear and mito-nuclear interactions arising in interspecies hybrids to untangle the genomic complexity of industrial hybrid strains.

Lastly, in chapter 5, I contributed to explore the potential of spore-to-spore mating between natural and industrial strains to generate novel brewing yeast with new and diverse aroma profiles. First, in collaboration with K. Giannakou, I assessed the brewing potential of *S. jurei* strains isolated from nature, in lab-scale and pilot-scale fermentations. The strains were found able to consume the main sugar presents in wort, maltose and maltotriose, a rare trait in *Saccharomyces,* and were thus deemed strong candidates for further applications. However, *S. jurei* fermentation capabilities were limited when compared to selected *S. cerevisiae* ale strains, in particular when screened in wort media and in industrial settings. Thus, to accelerate the development of new brewing strains harbouring *S. jurei* backbone without resorting to GMO techniques, Giannakou hybridised *S. jurei* with *S. cerevisiae* industrial strains using classical breeding techniques. I tested three hybrids generated in this study which consistently outperformed the parental *S. jurei*, combining beneficial traits from both parents such as the efficient sugar consumption of *S. cerevisiae* and *S. jurei* cold tolerance. Moreover, through hybridisation novel aroma profiles of great interest for the craft beer market were generated. In fact, the complementary aroma profiles of the parental strains gave rise to a desirable combination of tropical and floral notes in the hybrids, while eliminating undesirable traits such as the high production of 4-vinyl guaiacol of the *S. jurei* parent.

To conclude, the results of this thesis successfully tackled the main challenges arising in the food and beverage industry applying a combination of metabolic and genomic techniques to untangle the complexity of the fermentation processes. In particular, I expanded the tools available to study *Saccharomyces* hybrids and studied how yeast physiological state affects the final aroma. Moreover, new strains of industrial interest

were generated through spore-to-spore mating accelerating the introduction of new, complex aroma profiles into novel products.

6.2 Future Work

Volatile aroma compound production is affected by growth rate in *S. cerevisiae*. In the work presented we uncovered a correlation between growth rate and volatile compound production in the *S. cerevisiae* type strain NCYC505 which was exploited to increase higher alcohol production. Further studies should be directed to understand if the correlation observed is strain- or species-specific and evaluate how conserved are the mechanisms underlying the link observed. Previous studies, highlighted how differences in the acetate metabolism between *S. cerevisiae* strains CBS 8066 and H1022 led to significant differences in ethanol yields, in anaerobic glucose-limited chemostats (Verduyn et al., 1990). Thus, I would suggest expanding the study to a broader range of strains and species, and, in particular, to *S. cerevisiae* and *S. pastorianus* strains which are commonly employed in brewing processes. In this study, I have shown that a controlled feeding profile can increase the concentrations of higher alcohols by 60% in synthetic media. Further studies in wort-media and in industrial-scale fermentations will allow to define the potentiality of the implementation of feeding profiles to artificially regulate growth and manipulate aroma compound productions in fermentation processes.

Restoring fertility in yeast hybrids: breeding and quantitative genetics of beneficial traits. The wealth of data generated by the QTL analysis on *Saccharomyces* hybrids represents an important resource to study mito-nuclear and nuclear-nuclear interactions in hybrids. Further studies should be directed on the dissection of pleiotropic QTLs such as the one detected in maltose, acetic acid and low temperature in chromosome XIII of *S. cerevisiae* in *S. cerevisiae x S. jurei* hybrids harbouring *S. jurei* mitochondria. Allelic variation in the *CLU1* gene, in particular, may uncover a negative epistatic effect of the *S. cerevisiae* allele which may be background-specific. In fact, the QTL was not mapped in *S. cerevisiae* x *S. jurei* hybrids with *S. cerevisiae* mitochondria nor in the other *Saccharomyces* hybrids tested. *CLU1* was described as affecting mitochondria morphology and distribution in *S. cerevisiae* strains (Fields et al., 1998). Thus, I

hypothesise that the *S. cerevisiae* alleles of *CLU1* may interact in a different manner with *S. jurei* mitochondria, leading to mito-nuclear interactions which could be underlying the phenotypic effect observed. Validation of *CLU1* through reciprocal hemizygosity analysis, coupled with fluorescence localization of mitochondria as described in Marobbio et al. (2003), will confirm the effect and lead to further study to dissect the molecular mechanisms of the mito-nuclear interaction.

Aside from genomic data, the framework described in this project to both generate and screen de-novo could be easily applied to a broader variety of stressors and to hybrids of different *Saccharomyces* species. In chapter 4, I have successfully applied the pipeline to the dissection of complex traits correlated with antifungal resistance, allowing to study how natural variations and hybridisation affect this trait. Expanding the phenotypic screening to industrial-relevant traits such as ethanol tolerance and growth at low pH will help identify new evolutionary pathways for strain development. Moreover, mito-nuclear incompatibilities are consistently detected more frequently in *Saccharomyces* hybrids when assayed in non-fermentable carbon sources (Szabo et al., 2020; Visinoni and Delneri, 2022; Wolters et al., 2018). Thus, a thorough screening in non-fermentable media, such as glycerol, could provide new insights on the role of the mitochondria in *Saccharomyces* hybrids.

Experimental evolution studies in industrial stressors on the best-performing strains selected for QTL studies will be able to capitalize on the incredible genetic diversity of the hybrid spores generated. Moreover, the application of mutagenesis protocols extensively described in literature could generate further instability and diversity from previously evolved strains (Bellon et al., 2011; Ekberg et al., 2013). Continuous culturing systems could also proven as a valuable tool to evolve and select populations of yeast hybrids, maintaining a finely tuned selective pressure. While applications of chemostat cultures have already been proven successful in improving *S. pastorianus* attenuation (Brickwedde et al., 2017), I believe turbidostat systems could replicate better the selection pressure yeast is subjected to during the brewing processes. Performing continuous culturing in turbidostat will allow to evolve cells in nutrient abundance while applying

an increasing selection pressure. This will facilitate adaptive evolution in a complex media, like wort, and better replicate industrial conditions.

Identification of genetic markers of antifungal drug resistance in *Saccharomyces* hybrids via QTL mapping. The analysis of the QTL regions linked to antifungal resistance identified in *S. cerevisiae* x *S. kudriavzevii* hybrids provided a large number of potential causal genes which could contribute to the phenotype observed. Reciprocal hemizygosity analysis will help define whether the candidate genes selected are responsible for the resistant phenotype and detect allelic variant which could be exploited in antifungal susceptibility screening. Moreover, a thorough dissection of the QTL detected will help identify novel pathways and genes which could be exploited for the generation of new antifungal drug or for the development of combination therapies.

Application of the pipeline for the study of hybrids between pathogenic species will further advance the field, allowing to monitor the evolutionary pathways leading to antifungal resistance. Interspecies hybrids of *Cryptococcus neoformans* and *Cryptococcus deneoformans* are frequently isolated in natural and clinical samples and were previously exploited for the QTL analysis (Samarasinghe et al., 2020; Vogan et al., 2016). However, similarly to *Saccharomyces* hybrids, the strains isolated are sterile and propagate only asexually. The platform presented in this thesis will allow to restore fertility in the hybrids allowing multigenerational crosses and reducing linkage disequilibrium by increasing recombination. The greater phenotypic and genomic diversity produced will provide fertile grounds to quantitative genetics studies on the evolutionary pathways leading to antifungal resistance and the role of hybridisation.

Biotechnological exploitation of *Saccharomyces jurei* and its hybrids in craft beer fermentation uncovers new aroma combinations. Previous studies highlighted the role of the mitochondria in determining hybrid fitness in low temperature in *S. cerevisiae x S. uvarum* hybrids, as well as affecting the aroma profile in *S. cerevisiae* x *S. eubayanus* crosses (Hewitt et al., 2020; Li et al., 2019; Pérez et al., 2022). Thus, identification of the mitotype in the hybrid strains generated will help to further define the role of the mitochondria in determining the hybrid phenotype. Moreover, whole genome sequencing of the strains generated will help identify the molecular agents underlying

the phenotypical differences observed between the hybrids. In fact, spore-to-spore mating allows for a differential allele inheritance in the spores, leading to the broad range of aroma profiles and phenotypes observed. Dissection of genomic data, followed by validation *in vivo* in lab-scale, will complement the qPCR on the genes responsible for the production of aroma compounds and genes responsible for maltose and maltotriose consumption. Such studies will allow to dissect the alleles responsible for the phenotypes observed and allow further development of the strains.

The hybrids strains H4 and H8, derived from the crossing of Sj-88 x Sc-500, displayed high fitness in maltose at 8°C and 16°C in spot test assays, while H4 and H6 outperformed both parental strains in terms of specific growth rate in micro-fermentations in malt extract. However, due to time and equipment restraints, only the hybrids from the crossing of Sj-95 and Sc-200 were evaluated in pilot-scale fermentations. Further characterisation in industrial settings of the Sj-88 x Sc-500 hybrids generated in this study may lead to the identification of interesting new candidates and results in novel aromas and products.

Lastly, in this study we attempted to obtain meiotic offspring from sixteen different *S. cerevisiae* industrial strains identifying four strains exhibiting high sporulation, coupled with good spore viability, an unusual trait in ale strains (Table B-2) (Gallone et al., 2016). Here, spore-to-spore mating was successfully employed to generate novel hybrid strains with industrial potential and to remove unwanted parental traits such as the high sugar attenuation recorded in Sc-200. The *S. cerevisiae* ale strain Sc-200, Sc-500 may thus be exploited for further hybridisation studies to ease the introduction of other natural strains in the *Saccharomyces* genus in industrial processes.

Chapter 7 - References

Please note that the references associated with Chapter 2, 3, 4 and 5 are presented at the end of the relevant sections.

Albertin, W., da Silva, T., Rigoulet, M., Salin, B., Masneuf-Pomarede, I., de Vienne, D., Sicard, D., Bely, M., Marullo, P., 2013. The Mitochondrial Genome Impacts Respiration but Not Fermentation in Interspecific Saccharomyces Hybrids. PLoS One 8. https://doi.org/10.1371/journal.pone.0075121

Alexander, W.G., Peris, D., Pfannenstiel, B.T., Opulente, D.A., Kuang, M., Hittinger, C.T., 2016. Efficient engineering of marker-free synthetic allotetraploids of Saccharomyces. Fungal Genet. Biol. 89, 10–17. https://doi.org/10.1016/j.fgb.2015.11.002

Antunovics, Z., Nguyen, H.V., Gaillardin, C., Sipiczki, M., 2005. Gradual genome stabilisation by progressive reduction of the Saccharomyces uvarum genome in an interspecific hybrid with Saccharomyces cerevisiae. FEMS yeast research 5, 1141–50. https://doi.org/10.1016/j.femsyr.2005.04.008

Aritomi, K., Hirosawa, I., Hoshida, H., Shiigi, M., Nishizawa, Y., Kashiwagi, S., Akada, R., 2004. Self-cloning yeast strains containing novel FAS2 mutations produce a higher amount of ethyl caproate in Japanese sake. Biosci. Biotechnol. Biochem. 68, 206–214.

Baker, E. P., Peris, D., Moriarty, R.V., Li, X.C., Fay, J.C., Hittinger, C.T., 2019. Mitochondrial DNA and temperature tolerance in lager yeasts. Science advances 5, eaav1869. https://doi.org/10.1126/sciadv.aav1869

Baker, EmilyClare P., Peris, D., Moriarty, R.V., Li, X.C., Fay, J.C., Hittinger, C.T., 2019. Mitochondrial DNA and temperature tolerance in lager yeasts. Sci Adv 5, eaav1869. https://doi.org/10.1126/sciadv.aav1869

Barbosa, R., Almeida, P., Safar, S.V., Santos, R.O., Morais, P.B., Nielly-Thibault, L., Leducq, J.B., Landry, C.R., Goncalves, P., Rosa, C.A., Sampaio, J.P., 2016. Evidence of Natural Hybridization in Brazilian Wild Lineages of Saccharomyces cerevisiae. Genome Biol Evol 8, 317–29. https://doi.org/10.1093/gbe/evv263

Bartowsky, E.J., Henschke, P.A., 2004. The "buttery" attribute of wine--diacetyl--desirability, spoilage and beyond. Int. J. Food Microbiol. 96, 235–252. https://doi.org/10.1016/j.ijfoodmicro.2004.05.013

Baur, B., 1992. Hemmer, Helmut 1990. Domestication: the Decline of Environmental Appreciation (German edition 1983, translated into English by Neil Beckhaus). Cambridge University Press, Cambridge. ix + 208 pp. £45.00 H/b, $69.50. ISBN: 0-521-34178-7. Journal of Evolutionary Biology 5, 356–356. https://doi.org/10.1046/j.1420-9101.1992.5020356.x

Belloch, C., Perez-Torrado, R., Gonzalez, S.S., Perez-Ortin, J.E., Garcia-Martinez, J., Querol, A., Barrio, E., 2009. Chimeric Genomes of Natural Hybrids of Saccharomyces cerevisiae and Saccharomyces kudriavzevii. Applied and Environmental Microbiology 75, 2534–2544. https://doi.org/10.1128/AEM.02282-08

Bellon, J.R., Eglinton, J.M., Siebert, T.E., Pollnitz, A.P., Rose, L., de Barros Lopes, M., Chambers, P.J., 2011. Newly generated interspecific wine yeast hybrids introduce flavour and aroma diversity to wines. Appl. Microbiol. Biotechnol. 91, 603–612. https://doi.org/10.1007/s00253-011-3294-3

Bellon, J.R., Schmid, F., Capone, D.L., Dunn, B.L., Chambers, P.J., 2013. Introducing a New Breed of Wine Yeast: Interspecific Hybridisation between a Commercial Saccharomyces cerevisiae Wine Yeast and Saccharomyces mikatae. PLOS ONE 8, e62053. https://doi.org/10.1371/journal.pone.0062053

Bendixsen, D.P., Frazão, J.G., Stelkens, R., 2022. Saccharomyces yeast hybrids on the rise. Yeast 39, 40–54. https://doi.org/10.1002/yea.3684

Beran, K., 1968. Budding of Yeast Cells, their Scars and Ageing, in: Rose, A.H., Wilkinson, J.F. (Eds.), Advances in Microbial Physiology. Academic Press, pp. 143–171. https://doi.org/10.1016/S0065-2911(08)60261-1

Bergström, A., Simpson, J.T., Salinas, F., Barré, B., Parts, L., Zia, A., Nguyen Ba, A.N., Moses, A.M., Louis, E.J., Mustonen, V., Warringer, J., Durbin, R., Liti, G., 2014. A high-definition view of functional genetic variation from natural yeast genomes. Mol. Biol. Evol. 31, 872–888. https://doi.org/10.1093/molbev/msu037

Bokulich, N.A., Bamforth, C.W., 2013. The Microbiology of Malting and Brewing. Microbiol. Mol. Biol. Rev. 77, 157–172. https://doi.org/10.1128/MMBR.00060-12

Borneman, A.R., Desany, B.A., Riches, D., Affourtit, J.P., Forgan, A.H., Pretorius, I.S., Egholm, M., Chambers, P.J., 2011. Whole-Genome Comparison Reveals Novel Genetic Elements That Characterize the Genome of Industrial Strains of Saccharomyces cerevisiae. PLOS Genetics 7, e1001287. https://doi.org/10.1371/journal.pgen.1001287

Borneman, A.R., Forgan, A.H., Kolouchova, R., Fraser, J.A., Schmidt, S.A., 2016. Whole Genome Comparison Reveals High Levels of Inbreeding and Strain Redundancy Across the Spectrum of Commercial Wine Strains of Saccharomyces cerevisiae. G3 (Bethesda) 6, 957–971. https://doi.org/10.1534/g3.115.025692

Borneman, A.R., Pretorius, I.S., 2015. Genomic Insights into the Saccharomyces sensu stricto Complex. Genetics 199, 281–291. https://doi.org/10.1534/genetics.114.173633

Bornscheuer, U.T., 2018. Lipid Modification by Enzymes and Engineered Microbes. Elsevier.

Boulton, C., Quain, D., 2008. Brewing Yeast and Fermentation. John Wiley & Sons.

Breeden, L., Nasmyth, K., 1985. Regulation of the Yeast HO Gene. Cold Spring Harb Symp Quant Biol 50, 643–650. https://doi.org/10.1101/SQB.1985.050.01.078

Brickwedde, A., van den Broek, M., Geertman, J.-M.A., Magalhães, F., Kuijpers, N.G.A., Gibson, B., Pronk, J.T., Daran, J.-M.G., 2017. Evolutionary Engineering in Chemostat Cultures for Improved Maltotriose Fermentation Kinetics in Saccharomyces pastorianus Lager Brewing Yeast. Front. Microbiol. 8. https://doi.org/10.3389/fmicb.2017.01690

Bull, A.T., 2010. The renaissance of continuous culture in the post-genomics age. J Ind Microbiol Biotechnol 37, 993–1021. https://doi.org/10.1007/s10295-010-0816-4

Cheong, C., Wackerbauer, K., Beckmann, M., Kang, S.A., 2007. Influence of preserved brewing yeast strains on fermentation behavior and flocculation capacity. Nutr Res Pract 1, 260–265. https://doi.org/10.4162/nrp.2007.1.4.260

Cherry, J.M., Hong, E.L., Amundsen, C., Balakrishnan, R., Binkley, G., Chan, E.T., Christie, K.R., Costanzo, M.C., Dwight, S.S., Engel, S.R., Fisk, D.G., Hirschman, J.E., Hitz, B.C., Karra, K., Krieger, C.J., Miyasato, S.R., Nash, R.S., Park, J., Skrzypek, M.S., Simison, M., Weng, S., Wong, E.D., 2012. Saccharomyces Genome Database: the genomics resource of budding yeast. Nucleic Acids Res. 40, D700-705. https://doi.org/10.1093/nar/gkr1029

Chou, J.-Y., Hung, Y.-S., Lin, K.-H., Lee, H.-Y., Leu, J.-Y., 2010. Multiple Molecular Mechanisms Cause Reproductive Isolation between Three Yeast Species. PLoS Biol 8. https://doi.org/10.1371/journal.pbio.1000432

Colson, I., Delneri, D., Oliver, S.G., 2004. Effects of reciprocal chromosomal translocations on the fitness of Saccharomyces cerevisiae. EMBO Rep 5, 392–398. https://doi.org/10.1038/sj.embor.7400123

Cordente, A.G., Heinrich, A., Pretorius, I.S., Swiegers, J.H., 2009. Isolation of sulfite reductase variants of a commercial wine yeast with significantly reduced hydrogen sulfide production. FEMS Yeast Res. 9, 446–459. https://doi.org/10.1111/j.1567-1364.2009.00489.x

D'Amore, T., Russell, I., Stewart, G.G., 1989. Sugar utilization by yeast during fermentation. Journal of Industrial Microbiology 4, 315–323. https://doi.org/10.1007/BF01577355

David, M.H., Kirsop, B.H., 1972. The Varied Response of Brewing Yeasts to Oxygen and Sterol Treatment. Proceedings. Annual meeting - American Society of Brewing Chemists 30, 14–16. https://doi.org/10.1080/00960845.1972.12005950

DE DEKEN, R.H., 1966. The Crabtree Effect: A Regulatory System in Yeast. Microbiology 44, 149–156. https://doi.org/10.1099/00221287-44-2-149

Delneri, D., Hoyle, D.C., Gkargkas, K., Cross, E.J.M., Rash, B., Zeef, L., Leong, H.-S., Davey, H.M., Hayes, A., Kell, D.B., Griffith, G.W., Oliver, S.G., 2008. Identification and

characterization of high-flux-control genes of yeast through competition analyses in continuous cultures. Nature Genetics 40, 113–117. https://doi.org/10.1038/ng.2007.49

Donadini, G., Porretta, S., 2017. Uncovering patterns of consumers' interest for beer: A case study with craft beers. Food Research International 91, 183–198. https://doi.org/10.1016/j.foodres.2016.11.043

Driscoll, C.A., Macdonald, D.W., O'Brien, S.J., 2009. From wild animals to domestic pets, an evolutionary view of domestication. PNAS 106, 9971–9978. https://doi.org/10.1073/pnas.0901586106

Dunn, B., Paulish, T., Stanbery, A., Piotrowski, J., Koniges, G., Kroll, E., Louis, E.J., Liti, G., Sherlock, G., Rosenzweig, F., 2013. Recurrent Rearrangement during Adaptive Evolution in an Interspecific Yeast Hybrid Suggests a Model for Rapid Introgression. PLOS Genetics 9, e1003366. https://doi.org/10.1371/journal.pgen.1003366

Dzialo, M.C., Park, R., Steensels, J., Lievens, B., Verstrepen, K.J., 2017. Physiology, ecology and industrial applications of aroma formation in yeast. FEMS Microbiol Rev 41, S95–S128. https://doi.org/10.1093/femsre/fux031

Ehrlich, P., Bertheim, A., 1907. Über p-Aminophenylarsinsäure. Berichte der deutschen chemischen Gesellschaft 40, 3292–3297. https://doi.org/10.1002/cber.19070400397

Ekberg, J., Rautio, J., Mattinen, L., Vidgren, V., Londesborough, J., Gibson, B.R., 2013. Adaptive evolution of the lager brewing yeast Saccharomyces pastorianus for improved growth under hyperosmotic conditions and its influence on fermentation performance. FEMS Yeast Research 13, 335–349. https://doi.org/10.1111/1567-1364.12038

Ellison, C.K., Burton, R.S., 2010. Cytonuclear conflict in interpopulation hybrids: the role of RNA polymerase in mtDNA transcription and replication. Journal of Evolutionary Biology 23, 528–538. https://doi.org/10.1111/j.1420-9101.2009.01917.x

Ernandes, J.R., Williams, J.W., Russell, I., Stewart, G.G., 1993. Effect of Yeast Adaptation to Maltose Utilization on Sugar Uptake During the Fermentation of Brewer's Wort. Journal of the Institute of Brewing 99, 67–71. https://doi.org/10.1002/j.2050-0416.1993.tb01149.x

Etschmann, M.M.W., Bluemke, W., Sell, D., Schrader, J., 2002. Biotechnological production of 2-phenylethanol. Appl. Microbiol. Biotechnol. 59, 1–8. https://doi.org/10.1007/s00253-002-0992-x

Ferea, T.L., Botstein, D., Brown, P.O., Rosenzweig, R.F., 1999. Systematic changes in gene expression patterns following adaptive evolution in yeast. PNAS 96, 9721–9726. https://doi.org/10.1073/pnas.96.17.9721

Fields, S.D., Conrad, M.N., Clarke, M., 1998. The S. cerevisiae CLU1 and D. discoideum cluA genes are functional homologues that influence mitochondrial morphology and distribution. Journal of Cell Science 111, 1717–1727.

Fretz, C.B., Luisier, J.-L., Tominaga, T., Amadò, R., 2005. 3-Mercaptohexanol: An Aroma Impact Compound of Petite Arvine Wine. Am J Enol Vitic. 56, 407–410.

Fukuda, H., Kizaki, Y., Ishikawa, T., Takahashi, K., 2001. Sake brewing characteristics of a new type of cerulenin-resistant sake yeast mutant. Biotechnology Letters 23, 717–721. https://doi.org/10.1023/A:1010398818695

Fukuda, K., Watanabe, M., Asano, K., 1990. Altered Regulation of Aromatic Amino Acid Biosynthesis in β -Phenylethyl-alcohol-overproducing Mutants of *Sake* Yeast *Saccharomyces cerevisiae*. Agricultural and Biological Chemistry 54, 3151–3156. https://doi.org/10.1080/00021369.1990.10870488

Fukuda, N., Kaishima, M., Ishii, J., Kondo, A., Honda, S., 2016. Continuous crossbreeding of sake yeasts using growth selection systems for a-type and α-type cells. AMB Express 6, 45. https://doi.org/10.1186/s13568-016-0216-x

Gallone, B., Mertens, S., Gordon, J.L., Maere, S., Verstrepen, K.J., Steensels, J., 2018. Origins, evolution, domestication and diversity of Saccharomyces beer yeasts. Current Opinion in Biotechnology, Food biotechnology • Plant biotechnology 49, 148–155. https://doi.org/10.1016/j.copbio.2017.08.005

Gallone, B., Steensels, J., Mertens, S., Dzialo, M.C., Gordon, J.L., Wauters, R., Theßeling, F.A., Bellinazzo, F., Saels, V., Herrera-Malaver, B., Prahl, T., White, C., Hutzler, M., Meußdoerffer, F., Malcorps, P., Souffriau, B., Daenen, L., Baele, G., Maere, S., Verstrepen, K.J., 2019. Interspecific hybridization facilitates niche adaptation in beer yeast. Nat Ecol Evol 3, 1562–1575. https://doi.org/10.1038/s41559-019-0997-9

Gallone, B., Steensels, J., Prahl, T., Soriaga, L., Saels, V., Herrera-Malaver, B., Merlevede, A., Roncoroni, M., Voordeckers, K., Miraglia, L., Teiling, C., Steffy, B., Taylor, M., Schwartz, A., Richardson, T., White, C., Baele, G., Maere, S., Verstrepen, K.J., 2016. Domestication and Divergence of Saccharomyces cerevisiae Beer Yeasts. Cell 166, 1397-1410.e16. https://doi.org/10.1016/j.cell.2016.08.020

Godtfredsen, S.E., Ottesen, M., 1982. Maturation of beer with α-acetolactate decarboxylase. Carlsberg Res. Commun. 47, 93–102. https://doi.org/10.1007/BF02914029

Goffeau, A., Barrell, B.G., Bussey, H., Davis, R.W., Dujon, B., Feldmann, H., Galibert, F., Hoheisel, J.D., Jacq, C., Johnston, M., Louis, E.J., Mewes, H.W., Murakami, Y., Philippsen, P., Tettelin, H., Oliver, S.G., 1996. Life with 6000 Genes. Science 274, 546–567. https://doi.org/10.1126/science.274.5287.546

Gonzalez, S.S., Barrio, E., Gafner, J., Querol, A., 2006. Natural hybrids from Saccharomyces cerevisiae, Saccharomyces bayanus and Saccharomyces kudriavzevii in wine fermentations. FEMS yeast research 6, 1221–34. https://doi.org/10.1111/j.1567-1364.2006.00126.x

Gorter de Vries, A.R., Voskamp, M.A., van Aalst, A.C.A., Kristensen, L.H., Jansen, L., van den Broek, M., Salazar, A.N., Brouwers, N., Abeel, T., Pronk, J.T., Daran, J.-M.G., 2019.

Laboratory Evolution of a Saccharomyces cerevisiae × S. eubayanus Hybrid Under Simulated Lager-Brewing Conditions. Front Genet 10, 242. https://doi.org/10.3389/fgene.2019.00242

Greig, D., Borts, R.H., Louis, E.J., Travisano, m., 2002. Epistasis and hybrid sterility in *Saccharomyces*. Proc. R. Soc. Lond. B 269, 1167–1171. https://doi.org/10.1098/rspb.2002.1989

Gresham, D., Desai, M.M., Tucker, C.M., Jenq, H.T., Pai, D.A., Ward, A., DeSevo, C.G., Botstein, D., Dunham, M.J., 2008. The repertoire and dynamics of evolutionary adaptations to controlled nutrient-limited environments in yeast. PLoS Genet. 4, e1000303. https://doi.org/10.1371/journal.pgen.1000303

Gresham, D., Dunham, M.J., 2014. The Enduring Utility of Continuous Culturing in Experimental Evolution. Genomics 104, 399–405. https://doi.org/10.1016/j.ygeno.2014.09.015

Gresham, D., Hong, J., 2015. The functional basis of adaptive evolution in chemostats. FEMS Microbiol Rev 39, 2–16. https://doi.org/10.1111/1574-6976.12082

Gunge, N., Nakatomi, Y., 1972. Genetic Mechanisms of Rare Matings of the Yeast SACCHAROMYCES CEREVISIAE Heterozygous for Mating Type. Genetics 70, 41.

Haber, J.E., 2012. Mating-Type Genes and MAT Switching in Saccharomyces cerevisiae. Genetics 191, 33–64. https://doi.org/10.1534/genetics.111.134577

Hanson, S.J., Wolfe, K.H., 2017. An Evolutionary Perspective on Yeast Mating-Type Switching. Genetics 206, 9–32. https://doi.org/10.1534/genetics.117.202036

Harada, M., Ueda, Y., Iwata, T., 1985. Purification and Some Properties of Alcohol Acetyltransferase from Banana Fruit. Plant Cell Physiol 26, 1067–1074. https://doi.org/10.1093/oxfordjournals.pcp.a077002

Hazelwood, L.A., Daran, J.-M., Maris, A.J.A. van, Pronk, J.T., Dickinson, J.R., 2008. The Ehrlich Pathway for Fusel Alcohol Production: a Century of Research on Saccharomyces cerevisiae Metabolism. Appl. Environ. Microbiol. 74, 2259–2266. https://doi.org/10.1128/AEM.02625-07

Herskowitz, I., 1988. Life cycle of the budding yeast Saccharomyces cerevisiae. Microbiol Rev 52, 536–553.

Hewitt, S.K., Duangrattanalert, K., Burgis, T., Zeef, L.A.H., Naseeb, S., Delneri, D., 2020. Plasticity of Mitochondrial DNA Inheritance and Its Impact on Nuclear Gene Transcription in Yeast Hybrids. Microorganisms 8, 494. https://doi.org/10.3390/microorganisms8040494

Hochholdinger, F., Hoecker, N., 2007. Towards the molecular basis of heterosis. Trends Plant Sci. 12, 427–432. https://doi.org/10.1016/j.tplants.2007.08.005

Hornsey, I.S., 2003. A History of Beer and Brewing. Royal Society of Chemistry.

Jansen, M.L.A., Daran-Lapujade, P., Winde, J.H. de, Piper, M.D.W., Pronk, J.T., 2004. Prolonged Maltose-Limited Cultivation of Saccharomyces cerevisiae Selects for Cells with Improved Maltose Affinity and Hypersensitivity. Appl. Environ. Microbiol. 70, 1956–1963. https://doi.org/10.1128/AEM.70.4.1956-1963.2004

Jansen, M.L.A., Winde, J.H.D., Pronk, J.T., 2002. Hxt-Carrier-Mediated Glucose Efflux upon Exposure of Saccharomyces cerevisiae to Excess Maltose. Appl. Environ. Microbiol. 68, 4259–4265. https://doi.org/10.1128/AEM.68.9.4259-4265.2002

Jiranek, V., Langridge, P., Henschke, P.A., 1995. Regulation of hydrogen sulfide liberation in wine-producing Saccharomyces cerevisiae strains by assimilable nitrogen. Appl. Environ. Microbiol. 61, 461–467.

Jones, G.V., White, M.A., Cooper, O.R., Storchmann, K., 2005. Climate Change and Global Wine Quality. Climatic Change 73, 319–343. https://doi.org/10.1007/s10584-005-4704-2

Kincaid, H.L., 1993. Selective Breeding and Domestication, in: Cloud, J.G., Thorgaard, G.H. (Eds.), Genetic Conservation of Salmonid Fishes, NATO ASI Series. Springer US, Boston, MA, pp. 307–309. https://doi.org/10.1007/978-1-4615-2866-1_27

Kitagaki, H., Kitamoto, K., 2013. Breeding Research on Sake Yeasts in Japan: History, Recent Technological Advances, and Future Perspectives. Annu. Rev. Food Sci. Technol. 4, 215–235. https://doi.org/10.1146/annurev-food-030212-182545

Klinke, H.B., Thomsen, A.B., Ahring, B.K., 2004. Inhibition of ethanol-producing yeast and bacteria by degradation products produced during pre-treatment of biomass. Appl Microbiol Biotechnol 66, 10–26. https://doi.org/10.1007/s00253-004-1642-2

Krogerus, K., Gibson, B.R., 2013a. 125th Anniversary Review: Diacetyl and its control during brewery fermentation. Journal of the Institute of Brewing 119, 86–97. https://doi.org/10.1002/jib.84

Krogerus, K., Gibson, B.R., 2013b. Influence of valine and other amino acids on total diacetyl and 2,3-pentanedione levels during fermentation of brewer's wort. Appl Microbiol Biotechnol 97, 6919–6930. https://doi.org/10.1007/s00253-013-4955-1

Krogerus, K., Holmström, S., Gibson, B., 2018. Enhanced Wort Fermentation with De Novo Lager Hybrids Adapted to High-Ethanol Environments. Applied and Environmental Microbiology 84, 20.

Krogerus, K., Magalhães, F., Vidgren, V., Gibson, B., 2017a. Novel brewing yeast hybrids: creation and application. Appl Microbiol Biotechnol 101, 65–78. https://doi.org/10.1007/s00253-016-8007-5

Krogerus, K., Magalhães, F., Vidgren, V., Gibson, B., 2015. New lager yeast strains generated by interspecific hybridization. J Ind Microbiol Biotechnol 42, 769–778. https://doi.org/10.1007/s10295-015-1597-6

Krogerus, K., Seppänen-Laakso, T., Castillo, S., Gibson, B., 2017b. Inheritance of brewing-relevant phenotypes in constructed Saccharomyces cerevisiae × Saccharomyces eubayanus hybrids. Microbial Cell Factories 16. https://doi.org/10.1186/s12934-017-0679-8

Kruis, A.J., Levisson, M., Mars, A.E., van der Ploeg, M., Garcés Daza, F., Ellena, V., Kengen, S.W.M., van der Oost, J., Weusthuis, R.A., 2017. Ethyl acetate production by the elusive alcohol acetyltransferase from yeast. Metabolic Engineering 41, 92–101. https://doi.org/10.1016/j.ymben.2017.03.004

Kucharczyk, K., Tuszyński, T., 2015. The effect of pitching rate on fermentation, maturation and flavour compounds of beer produced on an industrial scale. Journal of the Institute of Brewing 121, 349–355. https://doi.org/10.1002/jib.242

Kusunoki, K., Ogata, T., 2012. Construction of self-cloning bottom-fermenting yeast with low vicinal diketone production by the homo-integration of ILV5. Yeast 29, 435–442. https://doi.org/10.1002/yea.2922

Lambrechts, M.G., Pretorius, I.S., 2000. Yeast and its Importance to Wine Aroma - A Review. S. Afr. J. Enol. Vitic. 21, 33.

Lancaster, S.M., Payen, C., Heil, C.S., Dunham, M.J., 2019. Fitness benefits of loss of heterozygosity in Saccharomyces hybrids. Genome Res. 29, 1685–1692. https://doi.org/10.1101/gr.245605.118

Le Jeune, C., Lollier, M., Demuyter, C., Erny, C., Legras, J.-L., Aigle, M., Masneuf-PomarÃ¨de, I., 2007. Characterization of natural hybrids of *Saccharomyces cerevisiae* and *Saccharomyces bayanus* var. *uvarum*. FEMS Yeast Research 7, 540–549. https://doi.org/10.1111/j.1567-1364.2007.00207.x

Lee, H.-Y., Chou, J.-Y., Cheong, L., Chang, N.-H., Yang, S.-Y., Leu, J.-Y., 2008. Incompatibility of Nuclear and Mitochondrial Genomes Causes Hybrid Sterility between Two Yeast Species. Cell 135, 1065–1073. https://doi.org/10.1016/j.cell.2008.10.047

Lei, H., Li, H., Mo, F., Zheng, L., Zhao, H., Zhao, M., 2013. Effects of Lys and His supplementations on the regulation of nitrogen metabolism in lager yeast. Appl. Microbiol. Biotechnol. 97, 8913–8921. https://doi.org/10.1007/s00253-013-5137-x

Lentz, M., 2018. The Impact of Simple Phenolic Compounds on Beer Aroma and Flavor. Fermentation 4, 20. https://doi.org/10.3390/fermentation4010020

Li, X.C., Peris, D., Hittinger, C.T., Sia, E.A., Fay, J.C., 2019. Mitochondria-encoded genes contribute to evolution of heat and cold tolerance in yeast. Science advances 5, eaav1848. https://doi.org/10.1126/sciadv.aav1848

Lilly, M., Bauer, F.F., Styger, G., Lambrechts, M.G., Pretorius, I.S., 2006. The effect of increased branched-chain amino acid transaminase activity in yeast on the production of higher alcohols and on the flavour profiles of wine and distillates. FEMS Yeast Res. 6, 726–743. https://doi.org/10.1111/j.1567-1364.2006.00057.x

Lilly, M., Lambrechts, M.G., Pretorius, I.S., 2000. Effect of increased yeast alcohol acetyltransferase activity on flavor profiles of wine and distillates. Appl. Environ. Microbiol. 66, 744–753.

Lin, F., Ferguson, K.L., Boyer, D.R., Lin, X.N., Marsh, E.N.G., 2015. Isofunctional enzymes PAD1 and UbiX catalyze formation of a novel cofactor required by ferulic acid decarboxylase and 4-hydroxy-3-polyprenylbenzoic acid decarboxylase. ACS Chem. Biol. 10, 1137–1144. https://doi.org/10.1021/cb5008103

Linderholm, A., Dietzel, K., Hirst, M., Bisson, L.F., 2010. Identification of MET10-932 and Characterization as an Allele Reducing Hydrogen Sulfide Formation in Wine Strains of Saccharomyces cerevisiae. Appl. Environ. Microbiol. 76, 7699–7707. https://doi.org/10.1128/AEM.01666-10

Linderholm, A.L., Findleton, C.L., Kumar, G., Hong, Y., Bisson, L.F., 2008. Identification of Genes Affecting Hydrogen Sulfide Formation in Saccharomyces cerevisiae. Appl. Environ. Microbiol. 74, 1418–1427. https://doi.org/10.1128/AEM.01758-07

Lucca, M., Spencer, J., de Figueroa, L., 2002. Glycerol and arabitol production by an intergeneric hybrid, PB2, obtained by protoplast fusion between Saccharomyces cerevisiae and Torulaspora delbrueckii. Appl Microbiol Biotechnol 59, 472–476. https://doi.org/10.1007/s00253-002-1025-5

Malcorps, P., Dufour, J.P., 1992. Short-chain and medium-chain aliphatic-ester synthesis in Saccharomyces cerevisiae. Eur. J. Biochem. 210, 1015–1022.

Marín, D., Armengol, J., Carbonell-Bejerano, P., Escalona, J. m., Gramaje, D., Hernández-Montes, E., Intrigliolo, D. s., Martínez-Zapater, J. m., Medrano, H., Mirás-Avalos, J. m., Palomares-Rius, J. e., Romero-Azorín, P., Savé, R., Santesteban, L. g., de Herralde, F., 2021. Challenges of viticulture adaptation to global change: tackling the issue from the roots. Australian Journal of Grape and Wine Research 27, 8–25. https://doi.org/10.1111/ajgw.12463

Marobbio, C.M.T., Agrimi, G., Lasorsa, F.M., Palmieri, F., 2003. Identification and functional reconstitution of yeast mitochondrial carrier for S-adenosylmethionine. The EMBO Journal 22, 5975–5982. https://doi.org/10.1093/emboj/cdg574

Mason, A.B., Dufour, J.P., 2000. Alcohol acetyltransferases and the significance of ester synthesis in yeast. Yeast 16, 1287–1298. https://doi.org/10.1002/1097-0061(200010)16:14<1287::AID-YEA613>3.0.CO;2-I

Meilgaard, M.C., 1975. Flavor chemistry of beer. I. Flavor interaction between principal volatiles. Tech Q Mast Brew Assoc Am.

Mendes-Ferreira, A., Mendes-Faia, A., Leão, C., 2004. Growth and fermentation patterns of Saccharomyces cerevisiae under different ammonium concentrations and its implications in winemaking industry. J. Appl. Microbiol. 97, 540–545. https://doi.org/10.1111/j.1365-2672.2004.02331.x

Mertens, S., Steensels, J., Saels, V., De Rouck, G., Aerts, G., Verstrepen, K.J., 2015. A Large Set of Newly Created Interspecific Saccharomyces Hybrids Increases Aromatic Diversity in Lager Beers. Applied and Environmental Microbiology 81, 8202–8214. https://doi.org/10.1128/AEM.02464-15

Molimard, P., Spinnler, H.E., 1996. Review: Compounds Involved in the Flavor of Surface Mold-Ripened Cheeses: Origins and Properties. Journal of Dairy Science 79, 169–184. https://doi.org/10.3168/jds.S0022-0302(96)76348-8

Monerawela, C., Bond, U., 2018. The hybrid genomes of Saccharomyces pastorianus: A current perspective. Yeast 35, 39–50. https://doi.org/10.1002/yea.3250

Monod, J., 1949. The Growth of Bacterial Cultures. Annual Review of Microbiology 3, 371–394. https://doi.org/10.1146/annurev.mi.03.100149.002103

Montanari, L., Floridi, S., Marconi, O., Tironzelli, M., Fantozzi, P., 2005. Effect of mashing procedures on brewing. Eur Food Res Technol 221, 175–179. https://doi.org/10.1007/s00217-005-1166-8

Morgenstern, M., Stiller, S.B., Lübbert, P., Peikert, C.D., Dannenmaier, S., Drepper, F., Weill, U., Höß, P., Feuerstein, R., Gebert, M., Bohnert, M., van der Laan, M., Schuldiner, M., Schütze, C., Oeljeklaus, S., Pfanner, N., Wiedemann, N., Warscheid, B., 2017. Definition of a High-Confidence Mitochondrial Proteome at Quantitative Scale. Cell Reports 19, 2836–2852. https://doi.org/10.1016/j.celrep.2017.06.014

Naseeb, S., James, S.A., Alsammar, H., Michaels, C.J., Gini, B., Nueno-Palop, C., Bond, C.J., McGhie, H., Roberts, I.N., Delneri, D., 2017. Saccharomyces jurei sp. nov., isolation and genetic identification of a novel yeast species from Quercus robur. International Journal of Systematic and Evolutionary Microbiology 67, 2046–2052. https://doi.org/10.1099/ijsem.0.002013

Nguyen, T.H.M., Sondhi, S., Ziesel, A., Paliwal, S., Fiumera, H.L., 2020. Mitochondrial-nuclear coadaptation revealed through mtDNA replacements in Saccharomyces cerevisiae. BMC Evolutionary Biology 20, 128. https://doi.org/10.1186/s12862-020-01685-6

Nordström, K., 1966. Formation of Esters from Acids by Brewer's Yeast: Formation from Unsaturated Acids. Nature 210, 99–100. https://doi.org/10.1038/210099a0

Nordström, K., 1964. Formation of Esters from Alcohols by Brewer's Yeast. Journal of the Institute of Brewing 70, 328–336. https://doi.org/10.1002/j.2050-0416.1964.tb01999.x

Novick, A., Szilard, L., 1950. Description of the Chemostat. Science 112, 715–716. https://doi.org/10.1126/science.112.2920.715

Oba, T., Nomiyama, S., Hirakawa, H., Tashiro, K., Kuhara, S., 2005. Asp578 in LEU4p is one of the key residues for leucine feedback inhibition release in sake yeast. Biosci. Biotechnol. Biochem. 69, 1270–1273.

Olaniran, A.O., Hiralal, L., Mokoena, M.P., Pillay, B., n.d. Flavour-active volatile compounds in beer: production, regulation and control. Journal of the Institute of Brewing 123, 13–23. https://doi.org/10.1002/jib.389

O'neill, J.P.J., 1960. Lautering method and apparatus. US2948661A.

Origone, A.C., Rodríguez, M.E., Oteiza, J.M., Querol, A., Lopes, C.A., 2018. Saccharomyces cerevisiae × Saccharomyces uvarum hybrids generated under different conditions share similar winemaking features. Yeast 35, 157–171. https://doi.org/10.1002/yea.3295

Paliwal, S., Fiumera, A.C., Fiumera, H.L., 2014. Mitochondrial-Nuclear Epistasis Contributes to Phenotypic Variation and Coadaptation in Natural Isolates of Saccharomyces cerevisiae. Genetics 198, 1251–1265. https://doi.org/10.1534/genetics.114.168575

Park, S.-H., Kim, S., Hahn, J.-S., 2014. Metabolic engineering of Saccharomyces cerevisiae for the production of isobutanol and 3-methyl-1-butanol. Appl Microbiol Biotechnol 98, 9139–9147. https://doi.org/10.1007/s00253-014-6081-0

Payne, K.A.P., White, M.D., Fisher, K., Khara, B., Bailey, S.S., Parker, D., Rattray, N.J.W., Trivedi, D.K., Goodacre, R., Beveridge, R., Barran, P., Rigby, S.E.J., Scrutton, N.S., Hay, S., Leys, D., 2015. New cofactor supports α,β-unsaturated acid decarboxylation via 1,3-dipolar cycloaddition. Nature 522, 497–501. https://doi.org/10.1038/nature14560

Pérez, D., Denat, M., Pérez-Través, L., Heras, J.M., Guillamón, J.M., Ferreira, V., Querol, A., 2022. Generation of intra- and interspecific Saccharomyces hybrids with improved oenological and aromatic properties. Microbial Biotechnology. https://doi.org/10.1111/1751-7915.14068

Pérez-Través, L., Lopes, C.A., Barrio, E., Querol, A., 2012. Evaluation of different genetic procedures for the generation of artificial hybrids in Saccharomyces genus for winemaking. International Journal of Food Microbiology 156, 102–111. https://doi.org/10.1016/j.ijfoodmicro.2012.03.008

Peris, D., Alexander, W.G., Fisher, K.J., Moriarty, R.V., Basuino, M.G., Ubbelohde, E.J., Wrobel, R.L., Hittinger, C.T., 2020. Synthetic hybrids of six yeast species. Nature Communications 11, 1–11. https://doi.org/10.1038/s41467-020-15559-4

Peris, D., Moriarty, R.V., Alexander, W.G., Baker, E., Sylvester, K., Sardi, M., Langdon, Q.K., Libkind, D., Wang, Q.-M., Bai, F.-Y., Leducq, J.-B., Charron, G., Landry, C.R., Sampaio, J.P., Gonçalves, P., Hyma, K.E., Fay, J.C., Sato, T.K., Hittinger, C.T., 2017.

Hybridization and adaptive evolution of diverse Saccharomyces species for cellulosic biofuel production. Biotechnology for Biofuels 10, 78. https://doi.org/10.1186/s13068-017-0763-7

Pfeiffer, T., Morley, A., 2014. An evolutionary perspective on the Crabtree effect. Front. Mol. Biosci. 1. https://doi.org/10.3389/fmolb.2014.00017

Picazo, C., Gamero-Sandemetrio, E., Orozco, H., Albertin, W., Marullo, P., Matallana, E., Aranda, A., 2015. Mitochondria inheritance is a key factor for tolerance to dehydration in wine yeast production. Letters in Applied Microbiology 60, 217–222. https://doi.org/10.1111/lam.12369

Preiss, R., Tyrawa, C., Krogerus, K., Garshol, L.M., van der Merwe, G., 2018. Traditional Norwegian Kveik Are a Genetically Distinct Group of Domesticated Saccharomyces cerevisiae Brewing Yeasts. Front. Microbiol. 9. https://doi.org/10.3389/fmicb.2018.02137

Quain, D.E., 1986. DIFFERENTIATION OF BREWING YEAST. Journal of the Institute of Brewing 92, 435–438. https://doi.org/10.1002/j.2050-0416.1986.tb04436.x

Querol, A., Fernández-Espinar, M.T., del Olmo, Marcel. lí, Barrio, E., 2003. Adaptive evolution of wine yeast. International Journal of Food Microbiology, 23rd International Specialized Symposium on Yeasts (ISSY-23) 86, 3–10. https://doi.org/10.1016/S0168-1605(03)00244-7

Replansky, T., Koufopanou, V., Greig, D., Bell, G., 2008. Saccharomyces sensu stricto as a model system for evolution and ecology. Trends in Ecology & Evolution 23, 494–501. https://doi.org/10.1016/j.tree.2008.05.005

Romagnoli, G., Knijnenburg, T.A., Liti, G., Louis, E.J., Pronk, J.T., Daran, J.-M., 2015. Deletion of the Saccharomyces cerevisiae ARO8 gene, encoding an aromatic amino acid transaminase, enhances phenylethanol production from glucose. Yeast 32, 29–45. https://doi.org/10.1002/yea.3015

Saerens, S.M.G., Delvaux, F., Verstrepen, K.J., Van Dijck, P., Thevelein, J.M., Delvaux, F.R., 2008. Parameters Affecting Ethyl Ester Production by Saccharomyces cerevisiae during Fermentation. Applied and Environmental Microbiology 74, 454–461. https://doi.org/10.1128/AEM.01616-07

Samarasinghe, H., You, M., Jenkinson, T.S., Xu, J., James, T.Y., 2020. Hybridization Facilitates Adaptive Evolution in Two Major Fungal Pathogens. Genes 11, 101. https://doi.org/10.3390/genes11010101

Sheltzer, J.M., Blank, H.M., Pfau, S.J., Tange, Y., George, B.M., Humpton, T.J., Brito, I.L., Hiraoka, Y., Niwa, O., Amon, A., 2011. Aneuploidy Drives Genomic Instability in Yeast. Science 333, 1026–1030. https://doi.org/10.1126/science.1206412

Shen, L., Nishimura, Y., Matsuda, F., Ishii, J., Kondo, A., 2016. Overexpressing enzymes of the Ehrlich pathway and deleting genes of the competing pathway in Saccharomyces

cerevisiae for increasing 2-phenylethanol production from glucose. Journal of Bioscience and Bioengineering 122, 34–39. https://doi.org/10.1016/j.jbiosc.2015.12.022

Shull, G.H., 1948. What Is "Heterosis"? Genetics 33, 439–446.

Sipiczki, M., 2008. Interspecies hybridization and recombination in Saccharomyces wine yeasts. FEMS Yeast Res 8, 996–1007. https://doi.org/10.1111/j.1567-1364.2008.00369.x

Smits, G.J., van den Ende, H., Klis, F.M., 2001. Differential regulation of cell wall biogenesis during growth and development in yeast. Microbiology (Reading, Engl.) 147, 781–794. https://doi.org/10.1099/00221287-147-4-781

Snoek, T., Nicolino, M.P., Bremt, S.V. den, Mertens, S., Saels, V., Verplaetse, A., Steensels, J., Verstrepen, K.J., 2015. Large-scale robot-assisted genome shuffling yields industrial Saccharomyces cerevisiae yeasts with increased ethanol tolerance. Biotechnology for Biofuels 8, 32. https://doi.org/10.1186/s13068-015-0216-0

Spirek, M., Polakova, S., Jatzova, K., Sulo, P., 2014. Post-zygotic sterility and cytonuclear compatibility limits in S. cerevisiae xenomitochondrial cybrids. Frontiers in genetics 5, 454. https://doi.org/10.3389/fgene.2014.00454

Steensels, J., Meersman, E., Snoek, T., Saels, V., Verstrepen, K.J., 2014a. Large-Scale Selection and Breeding To Generate Industrial Yeasts with Superior Aroma Production. Appl. Environ. Microbiol. 80, 6965–6975. https://doi.org/10.1128/AEM.02235-14

Steensels, J., Snoek, T., Meersman, E., Nicolino, M.P., Voordeckers, K., Verstrepen, K.J., 2014b. Improving industrial yeast strains: exploiting natural and artificial diversity. FEMS Microbiol Rev 38, 947–995. https://doi.org/10.1111/1574-6976.12073

Stratford, M., Plumridge, A., Archer, D.B., 2007. Decarboxylation of Sorbic Acid by Spoilage Yeasts Is Associated with the PAD1 Gene. Applied and Environmental Microbiology. https://doi.org/10.1128/AEM.01246-07

Strathern, J.N., Klar, A.J., Hicks, J.B., Abraham, J.A., Ivy, J.M., Nasmyth, K.A., McGill, C., 1982. Homothallic switching of yeast mating type cassettes is initiated by a double-stranded cut in the MAT locus. Cell 31, 183–192. https://doi.org/10.1016/0092-8674(82)90418-4

Szabo, A., Antunovics, Z., Karanyicz, E., Sipiczki, M., 2020. Diversity and Postzygotic Evolution of the Mitochondrial Genome in Hybrids of Saccharomyces Species Isolated by Double Sterility Barrier. Frontiers in microbiology 11, 838. https://doi.org/10.3389/fmicb.2020.00838

Takahashi, T., Ohara, Y., Sawatari, M., Sueno, K., 2017. Isolation and characterization of sake yeast mutants with enhanced isoamyl acetate productivity. Journal of Bioscience and Bioengineering 123, 71–77. https://doi.org/10.1016/j.jbiosc.2016.07.002

Tezuka, H., Mori, T., Okumura, Y., Kitabatake, K., Tsumura, Y., 1992. Cloning of a Gene Suppressing Hydrogen Sulfide Production by Saccharomyces Cerevisiae and its Expression in a Brewing Yeast. Journal of the American Society of Brewing Chemists 50, 130–133. https://doi.org/10.1094/ASBCJ-50-0130

Tretter, H., 1989. Whirlpool for coarse sludge separation in brewing of beer. US4836097A.

Van Mulders, S.E., Ghequire, M., Daenen, L., Verbelen, P.J., Verstrepen, K.J., Delvaux, F.R., 2010. Flocculation gene variability in industrial brewer's yeast strains. Appl Microbiol Biotechnol 88, 1321–1331. https://doi.org/10.1007/s00253-010-2843-5

van Solingen, P., van der Plaat, J.B., 1977. Fusion of yeast spheroplasts. J Bacteriol 130, 946–947.

Vanbeneden, N., Gils, F., Delvaux, F., Delvaux, F.R., 2008. Formation of 4-vinyl and 4-ethyl derivatives from hydroxycinnamic acids: Occurrence of volatile phenolic flavour compounds in beer and distribution of Pad1-activity among brewing yeasts. Food Chemistry 107, 221–230. https://doi.org/10.1016/j.foodchem.2007.08.008

Vanderhaegen, B., Neven, H., Verachtert, H., Derdelinckx, G., 2006. The chemistry of beer aging – a critical review. Food Chemistry 95, 357–381. https://doi.org/10.1016/j.foodchem.2005.01.006

Verduyn, C., Postma, E., Scheffers, W.A., van Dijken, J.P.Y. 1990, 1990. Physiology of Saccharomyces Cerevisiae in Anaerobic Glucose-Limited Chemostat Cultures. Microbiology 136, 395–403. https://doi.org/10.1099/00221287-136-3-395

Verstrepen, K.J., Van Laere, S.D.M., Vanderhaegen, B.M.P., Derdelinckx, G., Dufour, J.-P., Pretorius, I.S., Winderickx, J., Thevelein, J.M., Delvaux, F.R., 2003. Expression levels of the yeast alcohol acetyltransferase genes ATF1, Lg-ATF1, and ATF2 control the formation of a broad range of volatile esters. Appl. Environ. Microbiol. 69, 5228–5237.

Vidal, E.E., de Billerbeck, G.M., Simões, D.A., Schuler, A., François, J.M., de Morais, M.A., 2013. Influence of nitrogen supply on the production of higher alcohols/esters and expression of flavour-related genes in cachaça fermentation. Food Chem 138, 701–708. https://doi.org/10.1016/j.foodchem.2012.10.147

Vidal, E.E., Morais, M.A. de, François, J.M., Billerbeck, G.M. de, 2015. Biosynthesis of higher alcohol flavour compounds by the yeast Saccharomyces cerevisiae: impact of oxygen availability and responses to glucose pulse in minimal growth medium with leucine as sole nitrogen source. Yeast 32, 47–56. https://doi.org/10.1002/yea.3045

Visinoni, F., Delneri, D., 2022. Mitonuclear interplay in yeast: from speciation to phenotypic adaptation. Current Opinion in Genetics & Development 76, 101957. https://doi.org/10.1016/j.gde.2022.101957

Vogan, A.A., Khankhet, J., Samarasinghe, H., Xu, J., 2016. Identification of QTLs Associated with Virulence Related Traits and Drug Resistance in Cryptococcus neoformans. G3 (Bethesda) 6, 2745–2759. https://doi.org/10.1534/g3.116.029595

Wenger, J.W., Piotrowski, J., Nagarajan, S., Chiotti, K., Sherlock, G., Rosenzweig, F., 2011. Hunger Artists: Yeast Adapted to Carbon Limitation Show Trade-Offs under Carbon Sufficiency. PLoS Genet 7. https://doi.org/10.1371/journal.pgen.1002202

Weusthuis, R.A., Pronk, J.T., van den Broek, P.J., van Dijken, J.P., 1994. Chemostat cultivation as a tool for studies on sugar transport in yeasts. Microbiol Rev 58, 616–630.

Wolters, J.F., Charron, G., Gaspary, A., Landry, C.R., Fiumera, A.C., Fiumera, H.L., 2018. Mitochondrial Recombination Reveals Mito-Mito Epistasis in Yeast. Genetics 209, 307–319. https://doi.org/10.1534/genetics.117.300660

Wu, X., Haber, J.E., 1996. A 700 bp cis-acting region controls mating-type dependent recombination along the entire left arm of yeast chromosome III. Cell 87, 277–285.

Yin, S., Lang, T., Xiao, X., Liu, L., Sun, B., Wang, C., 2015. Significant enhancement of methionol production by co-expression of the aminotransferase gene ARO8 and the decarboxylase gene ARO10 in Saccharomyces cerevisiae. FEMS Microbiol Lett 362. https://doi.org/10.1093/femsle/fnu043

Yuan, J., Mishra, P., Ching, C.B., 2017. Engineering the leucine biosynthetic pathway for isoamyl alcohol overproduction in Saccharomyces cerevisiae. J Ind Microbiol Biotechnol 44, 107–117. https://doi.org/10.1007/s10295-016-1855-2

Zhang, Z., Bendixsen, D.P., Janzen, T., Nolte, A.W., Greig, D., Stelkens, R., 2020. Recombining Your Way Out of Trouble: The Genetic Architecture of Hybrid Fitness under Environmental Stress. Mol Biol Evol 37, 167–182. https://doi.org/10.1093/molbev/msz211

Appendix A – Supplementary information of Chapter 3

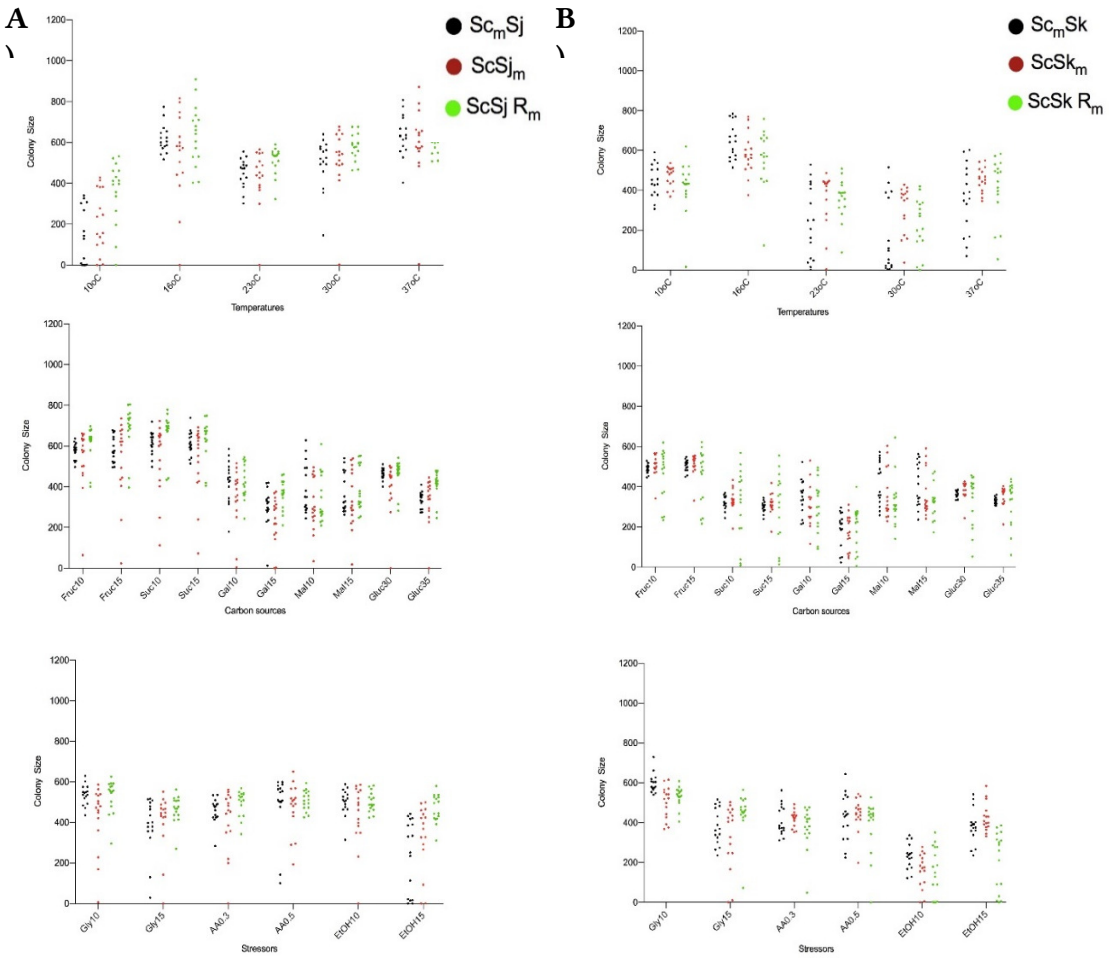

Figure A-1 | Scatter plots of fitness of F1 diploid progeny for *S. cerevisiae/S. jurei* and *S. cerevisiae/S. kudriavzevii* hybrids. The dot plots represent the colony sizes of *S. cerevisiae/S. jurei* (A) and *S. cerevisiae* × *S. kudriavzevii* (B) hybrids at different temperatures, carbon sources and stressors. Each dot represents the fitness of a F2 progeny. Different mitotypes are represented in black for *S. cerevisiae*, in red for the other parental species and in green for recombinant mitotypes.

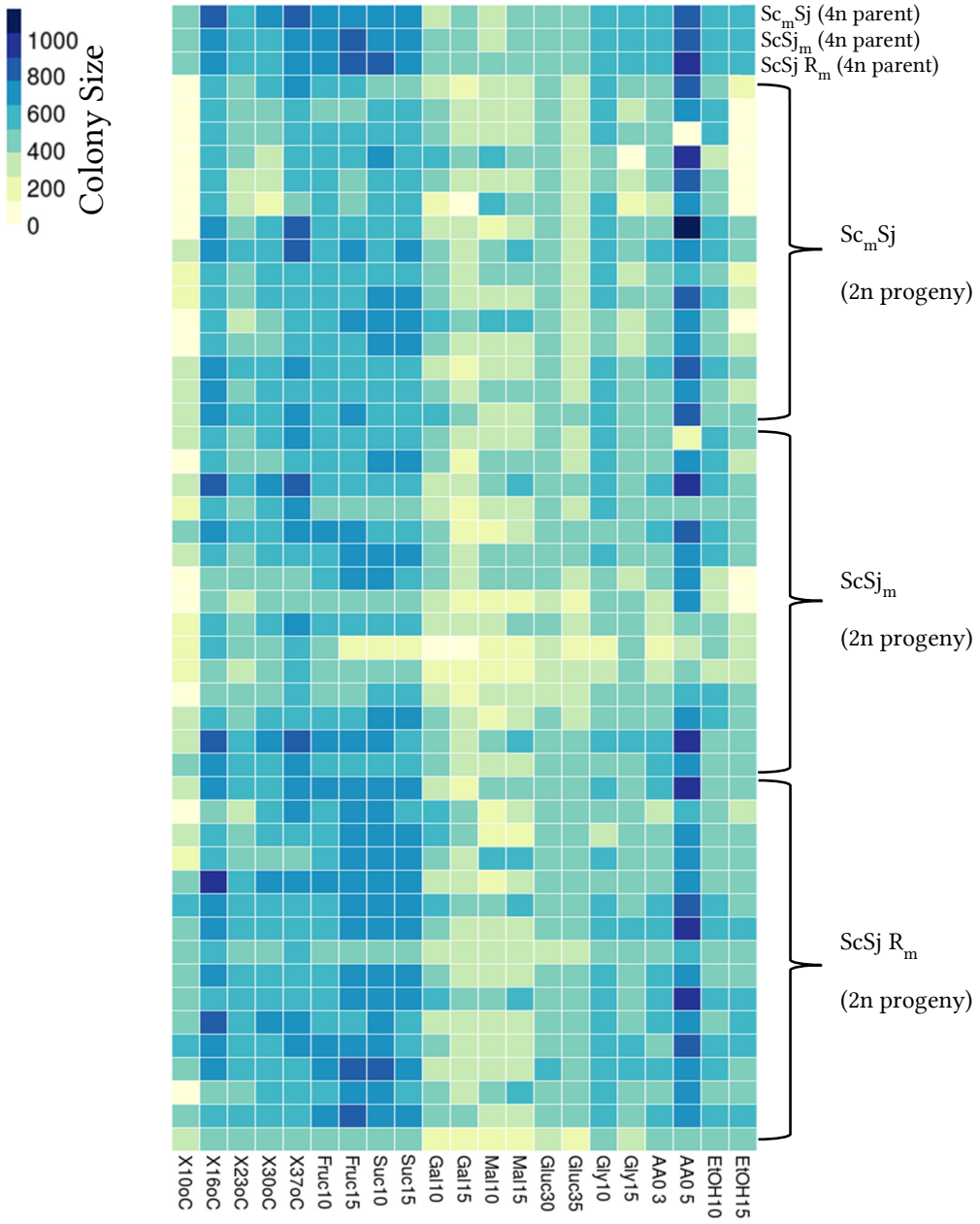

Figure A-2| Heat map representing phenotypic fitness of F1 diploid progeny for *S. cerevisiae/S. jurei* hybrids. Fitness was scored at five different temperatures and in response to different environmental stressors at 30°C for 4n hybrid parents Sc/Sj carrying different mitochondria and their diploid progeny. Phenotypes are represented with colony sizes calculated as pixels and coloured according to the scale, with light yellow and dark blue colours representing the lowest and highest growth respectively.

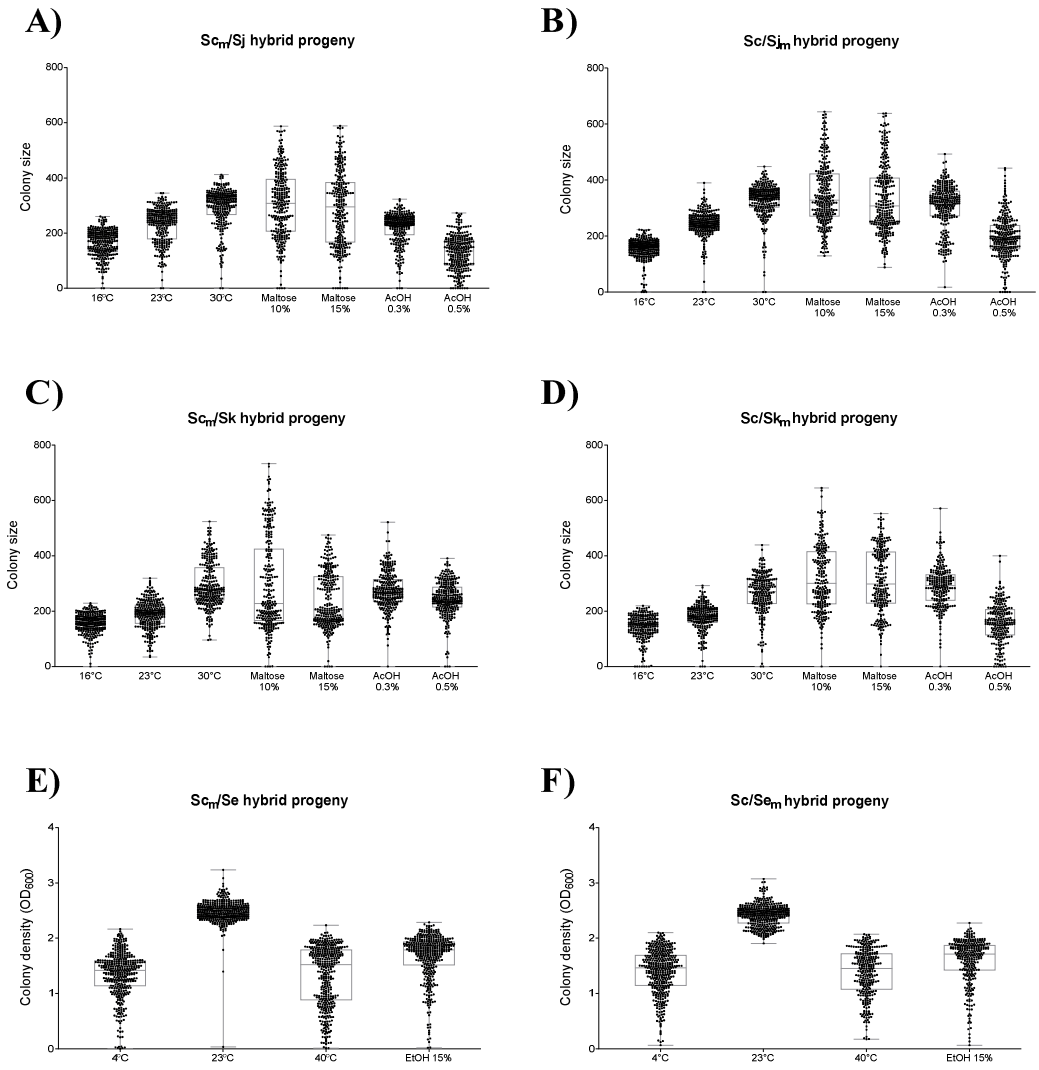

Figure A-3 | Scatter plots of fitness of F12 diploid progeny for *S. cerevisiae/S. jurei, S. cerevisiae/S. kudriavzevii* and S. *cerevisiae/S. eubayanus* hybrids. The dot plots represent the colony sizes of *S. cerevisiae/S. jurei* (A and B), *S. cerevisiae* × *S. kudriavzevii* (C and D) and *S. cerevisiae/S. eubayanus* (E and F) hybrids at different temperatures, carbon sources and stressors. Each dot represents the fitness of a F12 progeny.

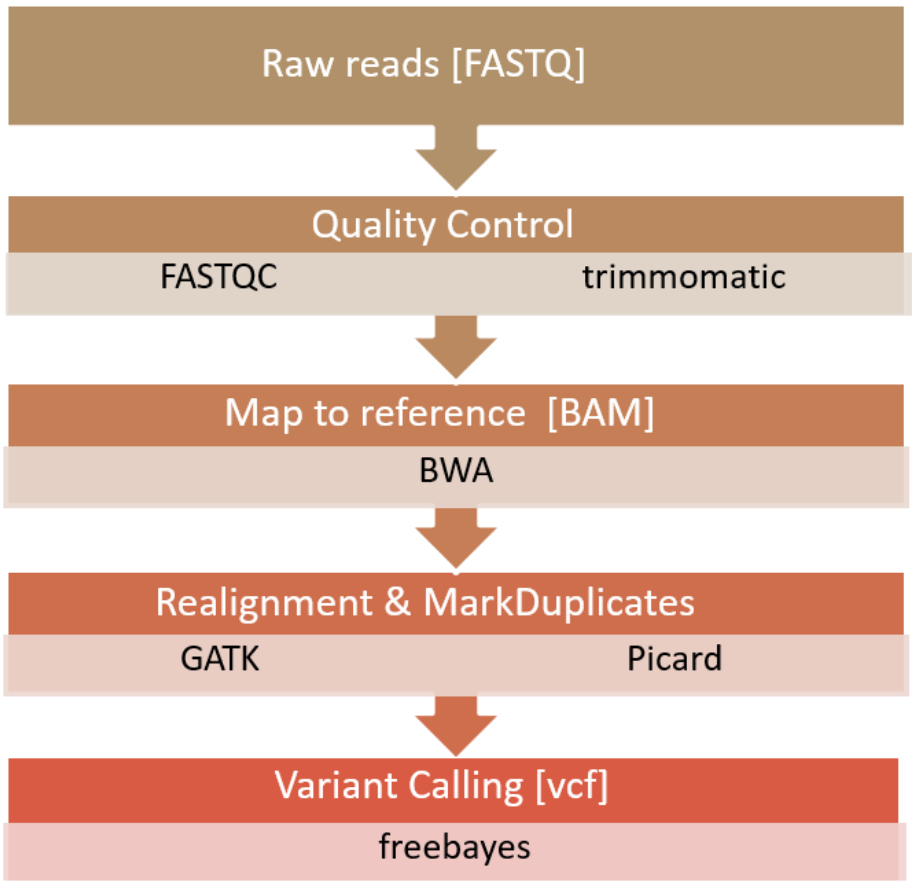

Figure A-4 | Variant calling pipeline

Table A-1 | Interspecies diploid hybrids constructed

Species	Strains crossed
S. cerevisiae × *S. jurei*	OS3 × D5088
	OS60 × D5095
	OS253 × D5095
	OS3 × D5095
	OS104 × D5095
S. cerevisiae × *S. kudriavzevii*	OS104 × OS575
	OS253 × OS575
	OS3 × OS575
	OS278 × OS575
	OS3 × IFO1802
	OS104 × IFO1802
	OS3 x ITD3
	OS60 x ITD3
	OS104 x ITD3
	OS253 x ITD3

Table A-2| Intraspecies diploid hybrids constructed

Species	Strains Crossed
S. cerevisiae	OS3 x OS60
	OS3 x OS104
	OS3 x OS253
	OS3 x OS278
	OS60 x OS104
	OS60 x OS278
	OS104 x OS253
	OS104 x OS278
	OS253 x OS278
	OS274 x OS388
S. uvarum	OS274 x OS449
	OS274 x OS471
	OS388 x OS449
	OS388 x OS471
	OS449 x OS471
	OS578 x OS626
S. eubayanus	OS578 x OS627
	OS626 x OS627
S. kudriavzevii	OS575 x IFO1802
	OS575 x OS393
	OS393 x IFO1802
	CAIII x IFO1802
	CAIII x OS393
	CAIII x ITD3

Table A-3 | Spore viability of constructed tetraploid lines

Tetraploids	Strains making up the 4n genome	Spore viability (%)
S. cerevisiae/S. kudriavzevii	OS253/OS575/OS104/IFO1802	90
	OS104/OS575/OS3/IFO1802	89
	OS253/OS575/OS3/IFO1802	93
S. cerevisiae/S. jurei	OS3/D5088/OS104/D5095	87
	OS3/D5088/OS104/D5095	92
S. cerevisiae/S. uvarum	OS388/OS471/OS3/OS253	75
	OS388/OS471/OS104/OS253	78.8
	OS388/OS449/OS3/OS104	92.5
	OS274/OS449/OS3/OS253	77.5
	OS449/OS471/OS3/OS104	73.8
	OS388/OS449/OS3/OS253	81.3
	OS388/OS449/OS3/OS104	88.8
	OS388/OS449/OS104/OS253	66.3
S. cerevisiae/S. eubayanus	OS578/OS626/OS3/OS253	86.5
	OS578/OS626/OS3/OS253	81.7
	OS578/OS626/OS104/OS253	89
	OS578/OS626/OS3/OS253	81.7
	OS578/OS626/OS3/OS103	81.7
	OS578/OS626/OS104/OS253	87.5
	OS578/OS627/OS3/OS253	80.8
	OS578/OS627/OS60/OS103	78.8
	OS578/OS627/OS3/OS103	98
	OS578/OS627/OS60/OS103	88

Table A-4| Quartile coefficient of dispersion of the F1 and F12 segregants colony size by condition. Mal (maltose), AcOH (acetic acid)

Tetraploid		16°C	23°C	30°C	Mal 10%	Mal 15%	AcOH 0.3%	AcOH 0.5%	Average
F1	Sc_m/Sj	0.06	0.11	0.10	0.25	0.24	0.07	0.14	0.14
	Sc/Sj_m	0.23	0.16	0.13	0.31	0.34	0.19	0.27	0.23
	$Sc/Sj\ R_m$	0.16	0.06	0.07	0.29	0.25	0.10	0.10	0.15
	Sc_m/Sk	0.14	0.79	0.92	0.23	0.24	0.14	0.22	0.38
	Sc/Sk_m	0.10	0.19	0.33	0.26	0.24	0.06	0.14	0.19
	$Sc/Sk\ R_m$	0.17	0.14	0.40	0.16	0.12	0.12	0.24	0.19
F12	Sc_m/Sj	0.21	0.22	0.12	0.31	0.40	0.14	0.36	0.25
	Sc/Sj_m	0.12	0.09	0.09	0.22	0.25	0.14	0.22	0.16
	Sc_m/Sk	0.14	0.18	0.20	0.44	0.33	0.15	0.15	0.23
	Sc/Sk_m	0.18	0.14	0.16	0.30	0.29	0.17	0.29	0.22

Table A-5 | Total number of QTLs identified in the F12 segregants in all conditions using the Multipool and pooled selection strategies

Multipool analysis			
Diploid hybrid F12 progeny	**Sc alleles**	**Other parental alleles**	**Total**
Sc_m/Sj	19	28	47
Sc/Sj_m	37	35	72
Sc_m/Sk	95	71	166
Sc/Sk_m	63	59	122
Sc_m/Se	46	26	72
Sc/Se_m	65	38	103
Pooled selection analysis			
Diploid hybrid F12 progeny	**Sc alleles**	**Other parental alleles**	**Total**
Sc_m/Se	6	10	16
Sc/Se_m	19	6	25
Sc_m/Su	9	0	9

Table A-6 | Number of QTL regions detected in *S. cerevisiae/S. jurei*, *S. cerevisiae/S. kudriavzevii* and *S. cerevisiae/S. eubayanus* F12 segregants via Multipool strategies.

	Number of QTL regions detected				**Number of genes within the QTL regions**			
	Sc_mSj Hybrid		**$ScSj_m$ Hybrid**		**Sc_mSj Hybrid**		**$ScSj_m$ Hybrid**	
	Sc genome	Sj genome	Sc genome	Sj genome	Sc genome	Sj genome	Sc genome	Sj genome
Low T°C (16°C)	4	13	17	20	59	269	140	264
Maltose	8	7	12	9	89	80	111	131
Acetic acid	7	8	8	6	74	159	87	77
	Sc_mSk Hybrid		**$ScSk_m$ Hybrid**		**Sc_mSk Hybrid**		**$ScSk_m$ Hybrid**	
	Sc genome	Sk genome	Sc genome	Sk genome	Sc genome	Sk genome	Sc genome	Sk genome
Low T°C (16°C)	33	11	20	25	243	64	171	95
Maltose	38	32	24	24	243	192	233	120
Acetic acid	24	28	19	10	164	200	188	39
	Sc_mSe Hybrid		**$ScSe_m$ Hybrid**		**Sc_mSe Hybrid**		**$ScSe_m$ Hybrid**	
	Sc genome	Se genome	Sc genome	Se genome	Sc genome	Se genome	Sc genome	Se genome
Very low T°C (4°C)	13	8	13	11	188	83	212	121
High T°C (40°C)	18	10	26	13	82	76	137	173
Ethanol	15	8	26	14	137	120	232	173

Table A-7 | List of potential causal genes identified in hybrids analysed via Multipool. The genes are clustered by function or phenotype reported in case of deletion or expression on SGD (Cherry et al. 2012).

List of potential causal genes identified in temperature-QTLs in Sc/Sj, Sc/Sk and Sc/Se hybrids.				
		Gene function or described phenotype		
Hybrid	**Allele**	Cold sensitivity	Haploinsufficiency/proficiency at cold temperature*	Cold favouring reactions**
Sc_m/Sj	Sc	*ARC1*	*YDL199C*	-
	Sj	*PAC10, RIM101, BTS1*	*PSF1, PEP3, RBA50, RPI1, CBP2, CDC7, GUT1, YPL071C, UGA2*	*MTD1*
Sc/Sj_m	Sc	*BIK1*	*PDX1, RNQ1, FUS3*	-
	Sj	-	*HLJ1, YMR315W, MET2, TOF1, DNF3*	*GDH2, ADH3*
Sc_m/Sk	Sc	*CIN1, LTE1, CKS1, PET9*	*CBS2, APE3, OSW7, NAT3, URN1, DRS2, RIF1, RET2, PYK2, MRPS18*	*GDH2*
	Sk	-	*MNT2, TIM17, ELP2*	-
Sc/Sk_m	Sc	-	*SEC4, PEP3, PEX35, FUS3, PSD2*	-
	Sk	*CTR9*	*FOL1, PEP3, THO2*	*MTD1*
Sc_m/Se	Sc	*HOG1*	*UGA2*	-
	Se	-	*PEX25, ELG1, GDE1, RRG9*	-

Sc/Se_m	Sc	*SLT2, BRL1, BEM4*	*PEP3*	*PUT2*
	Se	-	*DIG1, CPR2, COX6*	-

* genes from large-scale competition experiment at 16°C (Paget, Schwartz, and Delneri 2014)

** reactions classified as cold favouring in thermodynamic-based analysis of a genome-scale metabolic model (Paget, Schwartz, and Delneri 2014)

List of potential causal genes identified in maltose-QTLs in Sc/Sj and Sc/Sk hybrids.

		Gene function or described phenotype	
Hybrid	**Allele**	Maltose metabolism	Osmotic stress sensitivity
Sc_m/Sj	Sc	-	-
	Sj	-	-
Sc/Sj_m	Sc	*MAL31*	-
	Sj	*MAL33*	-
Sc_m/Sk	Sc	-	*RIM15*
	Sk	*IMA5*	-
Sc/Sk_m	Sc	*MAL33*	*KSS1*
	Sk	-	-

List of potential causal genes identified in acetic acid-QTLs in Sc/Sj and Sc/Sk hybrids.

Gene function or described phenotype

Hybrid	Allele	Acetic acid metabolism	Sensitivity to acetic acid	Oxidative stress resistance
Sc_m/Sj	Sc	-	*LEU2*	-
	Sj	*CIT1*	*OAR1, RTS1, MRH1, NRG1*	-
Sc/Sj_m	Sc	-	-	*PAC10*
	Sj	-	-	-
Sc_m/Sk	Sc	-	-	-
	Sk	*ACH1*	-	-
Sc/Sk_m	Sc	-	*ARF2, ARO2*	-
	Sk	-	-	-

List of potential causal genes identified in heat-QTLs in Sc/Se hybrids.

Gene function or described phenotype

Hybrid	Allele	Heat sensitivity	Heat response	Validated heat growth QTLs*
Sc_m/Se	Sc	*NGG1, SWR1, HHT2, ATG36, GTR1, SSN8, ATG7, PMA1, ARG82, DGK1, NUP42, RQC1, CIA1, ECM1, IPK1*	*HSP78*	
	Se	*CAB4, DOA4*	*TPS2*	

Sc/Se_m	Sc	*RPB9, GCN5, BUD27, COQ4, PET9, RAD50, ALG2, YAP3, ALG1, AIM21, BRX1, BIL1, DGK1, COQ6, ADH4*	*FLO1, WSC2, WSC3*	*IRA2*
	Se		*CHL1*	

* genes previously validated through RHA (Parts et al. 2011; Cubillos et al. 2013)

List of potential causal genes identified in ethanol-QTLs in Sc/Se hybrids.

		Gene function or described phenotype	
Hybrid	**Allele**	Ethanol sensitivity	Ethanol stress response
Sc_m/Se	Sc	*GAL7*	-
	Se	*CPR1, HTS1*	*ATH1*
Sc/Se_m	Sc	*CYC3, SFP1, TUF1, GCR1, ATG29, HTS1*	-
	Se	*GCN5, AIM33, ARO7*	-

Table A-8 | List of potential causal genes identified in the *S. cerevisiae* genome of hybrids analysed via Multipool with non-synonymous SNPs predicted to be tolerated or deleterious by SIFT analysis.

Potential causal genes identified in temperature-QTLs in Sc/Sj, Sc/Sk and Sc/Se hybrids		
Hybrid	Tolerated	Deleterious
Sc_m/Sj	*ARC1*	*YDL199C*
Sc/Sj_m	*FUS3, BIK1, PDX1*	*RNQ1*
Sc_m/Sk	*OSW7, RET2, MRPS18, DRS2, GDH2, CBS2, CIN1, URN1*	*PYK2, RIF1*
Sc/Sk_m		*PEP3*
Sc_m/Se	*HOG1*	
Sc/Se_m	*PUT2, BRL1, BEM4*	*PEP3*
Potential causal genes identified in maltose-QTLs in Sc/Sj and Sc/Sk hybrids		
Hybrid	Tolerated	Deleterious
Sc_m/Sj		
Sc/Sj_m		*MAL31*
Sc_m/Sk		*RIM15*
Sc/Sk_m		*MAL33*
Potential causal genes identified in heat-QTLs in Sc/Se hybrids		
Hybrid	Tolerated	Deleterious
Sc_m/Se	*ECM1, IPK1, ALG2, HSP78, SWR1, PMA1, GTR1, SSN8, NUP42*	*ARG82, ATG7, ATG36*
Sc/Se_m	*ADH4, WSC2, COQ6, RAD50*	*FLO1, BUD27, AIM21, WSC3*
Potential causal genes identified in ethanol-QTLs in Sc/Se hybrids		

Hybrid	Tolerated	Deleterious
Sc_m/Se		*GAL7*
Sc/Se_m	*CYC3, SFP1*	*GCR1, HTS1*

Total number of potential causal genes identified in the *S. cerevisiae* genome of hybrids analysed via Multipool

Hybrid	Tolerated	Deleterious	Total potential causal genes
Low temperature	*16*	*6*	*33*
Maltose	*0*	*3*	*4*
Acetic acid	*0*	*0*	*4*
Heat	*13*	*7*	*34*
Ethanol	*2*	*3*	*7*
Total	***31***	***19***	***82***

Table A-9 | Number of QTL regions detected in *S. cerevisiae* / *S. eubayanus* and *S. cerevisiae*/*S. uvarum* F12 segregants via Pooled selection strategy

	Number of QTL regions detected		**Number of genes within the QTL regions**		**Number of QTL regions detected**		**Number of genes within the QTL regions**	
	Sc_mSe Hybrid		**$ScSe_m$ Hybrid**		**Sc_mSe Hybrid**		**$ScSe_m$ Hybrid**	
	Sc genome	Se genome	Sc genome	Se genome	Sc genome	Se genome	Sc genome	Se genome
Very Low temperature 4°C	0	0	0	1	-	-	-	9
High maltose concentration	5	10	15	5	27	54	91	45
High glucose concentration	0	0	4	0	-	-	37	-
Oxidative stress (H_2O_2)	1	0	0	0	3	-	-	-
	Sc_mSu Hybrid		**Sc_mSu Hybrid**					
	Sc genome	Su genome	Sc genome	Su genome				
Levulinic Acid	4	0	18	-				
High temperature (40°C)	4	0	33	-				
Acetic acid	1	0	12	-				

Table A-10 | List of potential causal genes identified in QTLs in Sc_mSu hybrids analysed via pooled selection. The genes are clustered by function or phenotype reported in case of deletion or overexpression on SGD (Cherry et al. 2012).

List of potential causal genes identified in very low temperature-QTLs in Sc/Se hybrids.

		Gene function or described phenotype	
Hybrid	**Allele**	Cold sensitivity	Haploinsufficiency/proficiency at cold temperature*
Sc_m/Se	Sc	-	-
	Se	-	-
Sc/Se_m	Sc	-	-
	Se	-	*RKM1*

* genes from large-scale competition experiment at 16°C (Paget, Schwartz, and Delneri 2014)

List of potential causal genes identified in maltose-QTLs in Sc/Se hybrids.

		Gene function or described phenotype
Hybrid	**Allele**	Osmotic stress sensitivity
Sc_m/Se	Sc	*STE20*
	Se	*ACT1*
Sc/Se_m	Sc	*YAP3, RIM15*
	Se	*KSS1, BUD9, STE20, YAP3, SKO1*

List of potential causal genes identified in heat-QTLs in Sc_mSu hybrids.

		Gene function or described phenotype	
Hybrid	**Allele**	Heat sensitivity	Heat response
Sc_m/Su	Sc	*SUP45, BLM10, CAB2*	*FLO1*
	Su	-	-

List of potential causal genes identified in acetic acid-QTLs in Sc_mSu hybrids.

		Gene function or described phenotype	
Hybrid	**Allele**	Acetic acid metabolism	Sensitivity to acetic acid
Sc_m/Su	Sc	*COX13*	*TPN1, HOS2*
	Su	-	-

Table A-11 | List of QTL regions identified in *S. cerevisiae*/*S. kudriavzevii* F12 segregants validated via reciprocal hemizygosity analysis

Selection condition	Strain	Chromosome	Start (kb)	End (kb)	LOD	Alleles
Acetic acid	*S. cerevisiae*	chrII	324	334.8	17.13	*YCK2 PGA1 GIM3 IGO1 NSG2 CUZ1 YGP1* ***ASI2***
Maltose	*S. cerevisiae*	chrIII	283.2	306.2	14.31	***GIT1*** *OCA4 HMRA2 HMRA1 CDC39 CDC50*
Temperature	*S. cerevisiae*	chrII	187.7	196	7.17	*ACH1* ***FUS3*** *RRN6*

The genes validated through RHA are represented in bold

Table A-12| Growth parameters of reciprocal hemizygotes for the *ASI2*, *FUS3* and *GIT1* genes in inter- and intra- species hybrid background. $ScSk_m$ and OS104/OS253 reciprocal hemizygotes were assessed in YPD supplemented with 0.3% acetic acid (*ASI2*), YPD at 10°C (*FUS3*) and YP + maltose 15% (*GIT1*) as outlined in Material and Methods. The table shows the mean and the standard error across replicates. Significance difference between the reciprocal hemizygotes was assessed by t-test (p-value < 0.05)

Strain background:	**$ScSk_m$ Δ*ASI2***		
	$Sc^{OS104/\Delta}$	**$Sc^{\Delta/OS253}$**	**p-value**
Specific growth rate (h^{-1})	0.24 ± 0.003	0.24 ± 0.004	0.4443
Maximum biomass (Scatter light 620nm)	17.84 ± 0.39	20.51 ± 1.40	0.0001 (***)
T_{mid}	15.22 ± 0.55	16.4 ± 0.75	0.0182 (*)
Integral area	176.4 ± 15.1	159.26 ± 16.52	0.0479 (*)
Strain background:	**ScSc Δ*ASI2***		
	$Sc^{OS104/\Delta}$	**$Sc^{\Delta/OS253}$**	**p-value**
Specific growth rate (h^{-1})	0.187 ± 0.002	0.187 ± 0.002	0.9857
Maximum biomass (Scatter light 620nm)	17.39 ± 0.22	17.48 ± 0.28	0.3733
T_{mid}	8.7 ± 0.25	8.6 ± 0.18	0.5607

Integral area	62.89 ± 3.7	64.66 ± 2.36	0.1439
Strain background:	**$ScSk_m$ Δ*FUS3***		
	$Sc^{OS104/\Delta}$	**$Sc^{\Delta/OS253}$**	**p-value**
Specific growth rate (h^{-1})	0.08 ± 0.01	0.09 ± 0.01	0.0010 (**)
Maximum biomass (OD_{600})	1.21 ± 0.09	1.12 ± 0.05	0.0001 (***)
T_{mid}	55.2 ± 5.61	50.45 ± 2.87	0.0005 (***)
Integral area	25.69 ± 3.16	27.86 ± 1.68	0.0047 (**)
Strain background:	**ScSc Δ*FUS3***		
	$Sc^{OS104/\Delta}$	**$Sc^{\Delta/OS253}$**	**p-value**
Specific growth rate (h^{-1})	0.98 ± 0.006	0.092 ± 0.002	0.0014 (**)
Maximum biomass (OD_{600})	1.06 ± 0.04	1.08 ± 0.03	0.243
T_{mid}	44.11 ± 1.67	46.02 ± 1.65	0.0489 (*)
Integral area	31.16 ± 1.1	29.92 ± 1.35	0.0196 (*)

Strain background:	**$ScSk_m$ Δ*GIT1***		
	$Sc^{OS104/Δ}$	**$Sc^{Δ/OS253}$**	**p-value**
Specific growth rate (h^{-1})	0.119 ± 0.006	0.113 ± 0.006	0.0335 (*)
Maximum biomass (OD_{600})	2.2 ± 0.02	2.21 ± 0.03	0.3176
T_{mid}	37.47 ± 2.16	39.25 ± 1.43	0.003067 (**)
Integral area	93.34 ± 4.72	89.84 ± 3.15	0.0435 (*)
Strain background:	**ScSc Δ*GIT1***		
	$Sc^{OS104/Δ}$	**$Sc^{Δ/OS253}$**	**p-value**
Specific growth rate (h^{-1})	0.227 ± 0.006	0.229 ± 0.012	0.7076
Maximum biomass (OD_{600})	2.07 ± 0.03	2.06 ± 0.05	0.652
T_{mid}	18.76 ± 0.52	18.44 ± 0.74	0.312749
Integral area	104.67 ± 2.79	103.58 ± 2.89	0.4301

Table A-13 | Haploid strains used to construct hybrids

Species	Strain Number	Genotype
S. cerevisiae	OS3	*MAT**a** ho::HYG ura3::KanMX- barcode[GGCCAT]*
		MATα ho::HYG ura3::KanMX- barcode[GGCCAT]
	OS60	*MAT**a** ho::HYG ura3::KanMX- barcode[GCTAGC]*
		MATα ho::HYG ura3::KanMX- barcode[GCTAGC]
	OS104	*MAT*a *ho::HYG ura3::KanMX- barcode[GGTACC]*
		MATα ho::HYG ura3::KanMX- barcode[GGTACC]
	OS253	*MAT**a** ho::HYG ura3::KanMX- barcode[GTCGAC]*
		MATα ho::HYG ura3::KanMX- barcode[GTCGAC]
	OS278	*MAT**a** ho::HYG ura3::KanMX- barcode[CCCGGG]*
		MATα ho::HYG ura3::KanMX- barcode[CCCGGG]
S. uvarum	OS274	*MAT**a** ho::HYG*
		MATα ho::HYG
	OS388	*MAT**a** ho::HYG*
		MATα ho::HYG
	OS449	*MAT**a** ho::HYG*
		MATα ho::HYG
	OS471	*MAT**a** ho::HYG*
		MATα ho::HYG
S. eubayanus	OS578	*MAT**a** ho::HYG*
		MATα ho::HYG
	OS626	*MAT**a** ho::HYG*
		MATα ho::HYG
	OS627	*MAT**a** ho::HYG*
		MATα ho::HYG
S. jurei	D5088	*MAT**a** ho::loxP-hphNT1-loxP*
		MATα ho::loxP Δura3:lox2272-natNT2-lox2272

	D5095	*MAT**a** ho::loxP Δura3:loxP-kanMx-loxP*
		MATα ho::loxP-hphNT1-loxP
S. kudriavzevii	OS575	*MAT**a** ho::loxP-hphNT1-loxP Δura3:loxP-kanMx-loxP*
		MATα ho::loxP-hphNT1-loxP Δura3:loxP-kanMx-loxP
	OS393	*MAT**a** ho::loxP-hphNT1-loxP*
		MATα ho::loxP-hphNT1-loxP
	IFO1802	*MATα ho::natMX ura3Δ0*
	ITD3	*MAT**a** ho::loxP Δura3:lox2272-natNT2-lox2272*
		MATα ho::loxP Δura3:lox2272-natNT2-lox2272
	CAIII	*MAT**a** ho::loxP-hphNT1-loxP*
		MATα ho::loxP-hphNT1-loxP Δura3:loxP-kanMx-loxP

Table A-14 | Plasmids used for strain construction

Plasmid	Alias	Description
pRED231	pS30 pFA6-KanMX4	Derived from pFA6 with KanMX cloned into the PmeI site. Confers resistance to Geneticin.
pRED460	pAG32	Derived from pRED231, with KanMX substituted by hph at the PmeI site. Confers resistance to hygromycin B.
pRED266	pFP18	Contains a URA3 gene flanked by the sequences of the X, W, and Z2 portions of the mating type locus.
pFA6a-loxP-hphNT1-loxP	pZC1	Derived from pUG6. Confers resistance to Hygromycin B.
pFA6a-loxP-natNT2-loxP	pZC2	Derived from pUG6. Confers resistance to Nourseothricin.
pFA6a-lox2272-natNT2-lox2272	pZC4	Derived from pUG6. Confers resistance to Nourseothricin.

Table A-15 | Strains used for reciprocal hemizygosity analysis

Hybrid	Strain Number	Deletion
S. cerevisiae x S. cerevisiae	OS104 x OS253	$fus3^{OS104}$::*natMX* $git1^{OS104}$::*natMX* $asi2^{OS104}$::*natMX* $fus3^{OS253}$::*kanMX* $git1^{OS253}$::*kanMX* $asi2^{OS253}$::*kanMX*
S. cerevisiae / S. kudriavzevii	(OS104 x IFO1802) x (OS253 x OS575)	$fus3^{OS104}$::*BLE* $git1^{OS104}$::*BLE* $asi2^{OS104}$::*BLE* $fus3^{OS253}$::*BLE* $git1^{OS253}$::*BLE* $asi2^{OS253}$::*BLE*

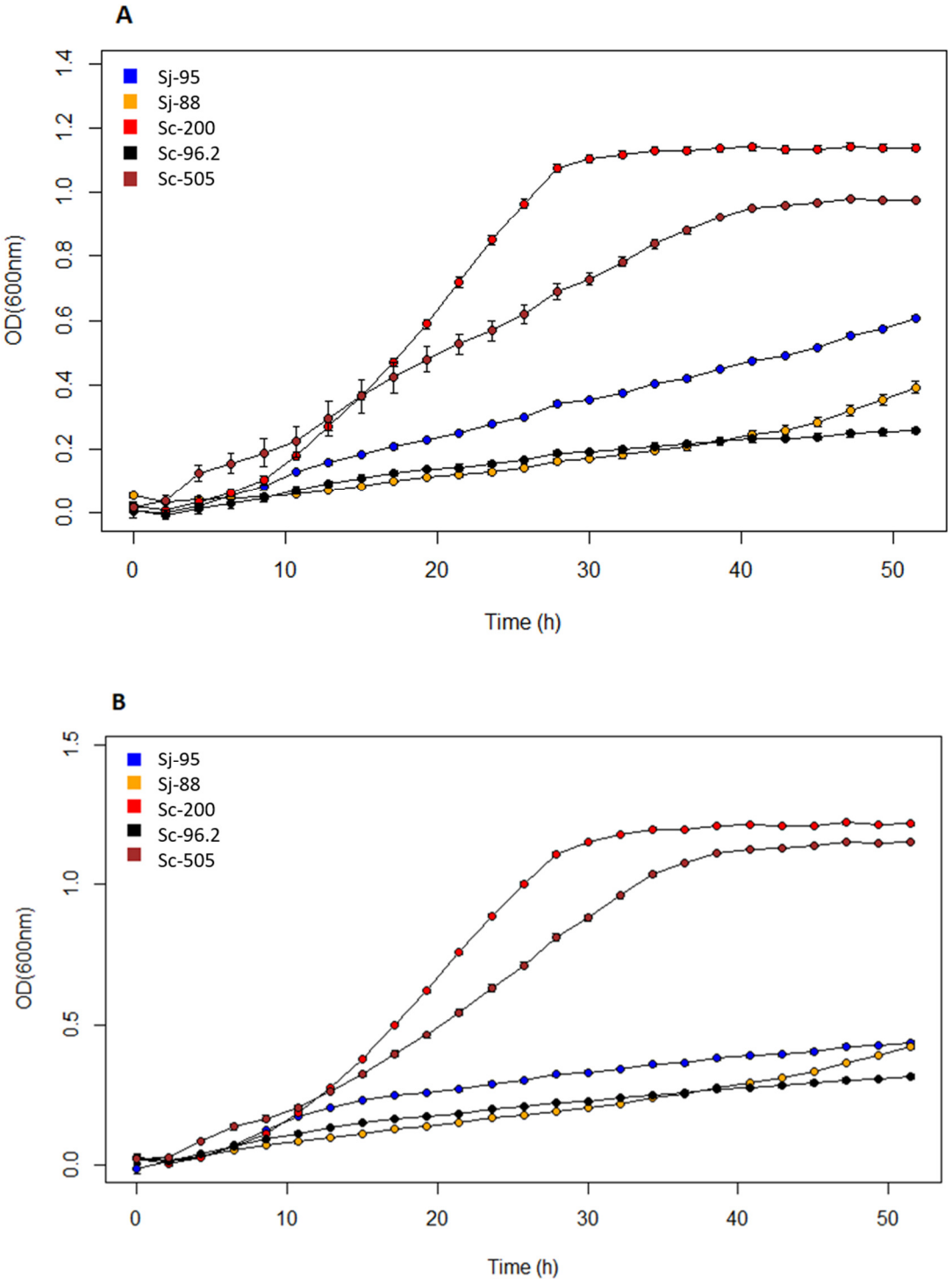

Figure B-1 | Growth kinetics of Sj-95, Sj-88, *S. cerevisiae* ale strain (Sc-200), type strain (Sc-505) and natural isolate (Sc-96.2). Strains were grown in YP + maltose (Panel A) and YP + maltotriose (Panel B). The standard error of biological replicates is represented by error bars at every timepoint.

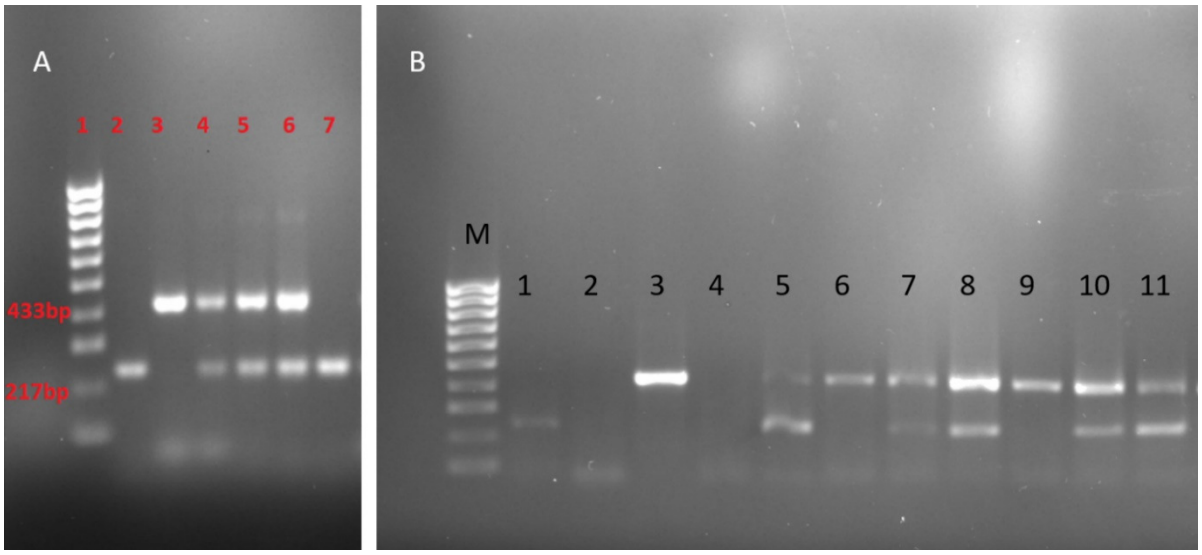

Figure B-2 | Species-specific PCR confirmation of successful hybrid construction in 1.5% agarose gel. (A) Lane 1: 100 bp ladder, lane 2: Sj-95, lane 3: Sc-200, lanes 4-6: Hybrids H1-3 (B): M: 100bp ladder, Lane 1: Sj-88, lane 2: negative control, lane 3: Sc-500, lanes 5,7,8,10 and 11 relates to H4, H5, H6, H7 and H8, respectively. Lanes 4, 6, 9: candidate strains which did not results as hybrid.

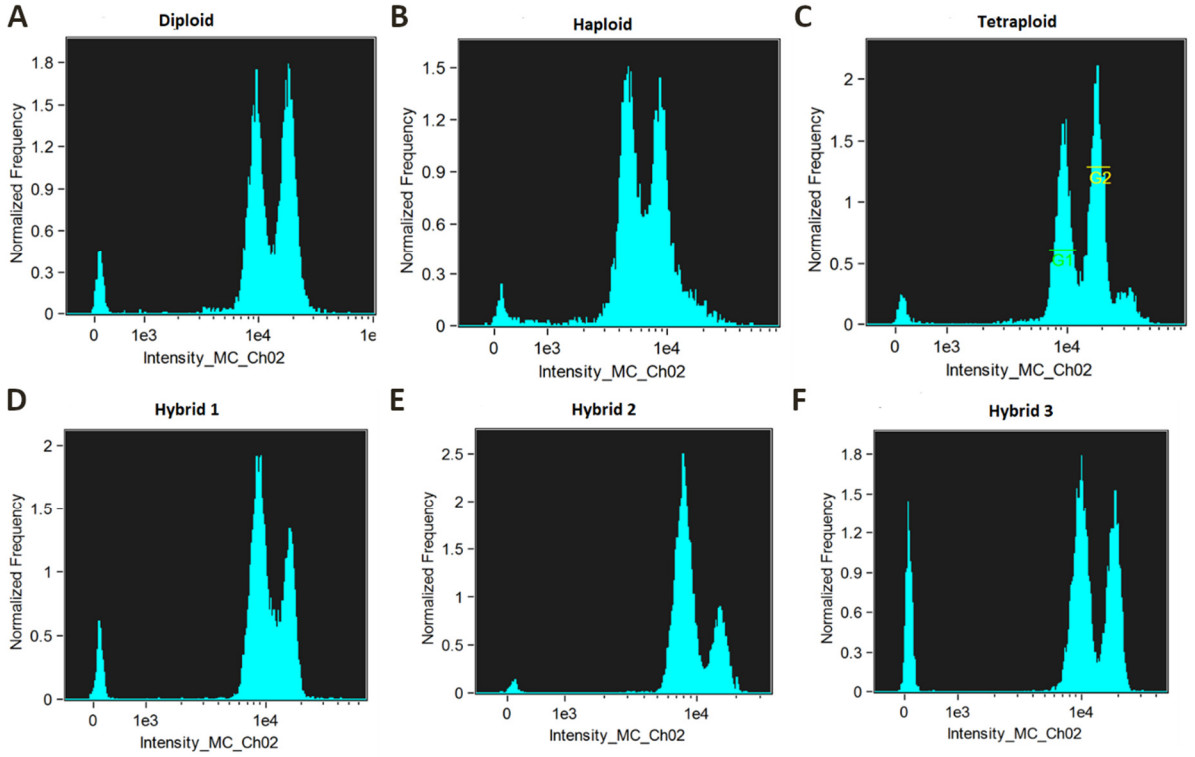

Figure B-3 | Fluorescence flow cytometry analysis. Data for DNA content of Sj-95 (diploid, panel A), BY4742 (haploid, panel B), PB7 (tetraploid, panel C), hybrid strains H1 (panel D), H2 (Panel E) and H3 (Panel F).

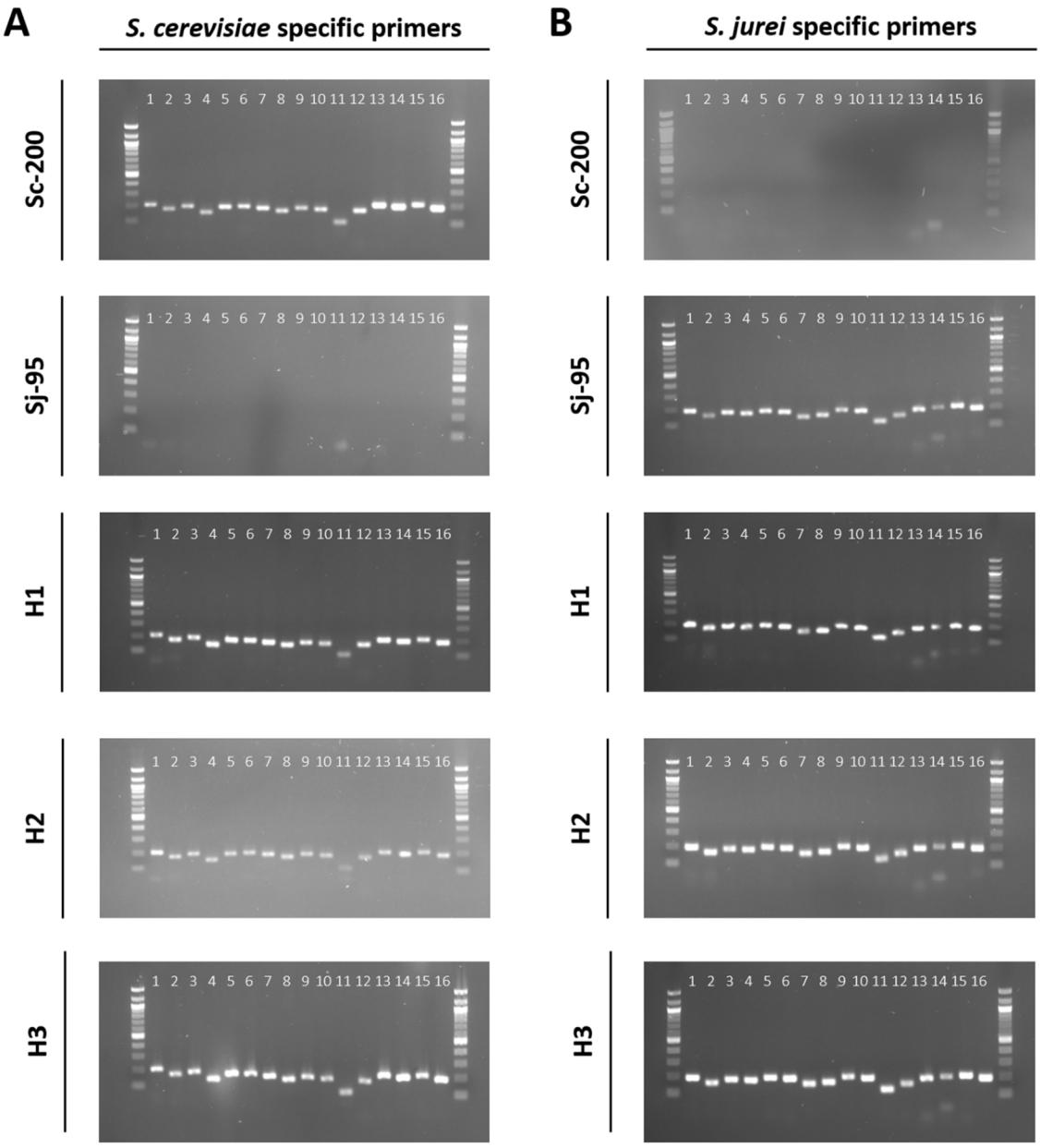

Figure B-4 | Species-specific chromosome-specific PCR. Chromosome specific, species-specific PCR products primers for Sc-200, Sj-95, H1, H2 and H3. Panel A: *S. cerevisiae* specific primers set for chromosomes 1-16. Panel B: *S. jurei* specific primers sets for chromosomes 1-16. The molecular weight size marker utilized in all the gel was the 100bp DNA Ladder (New England Biolabs)

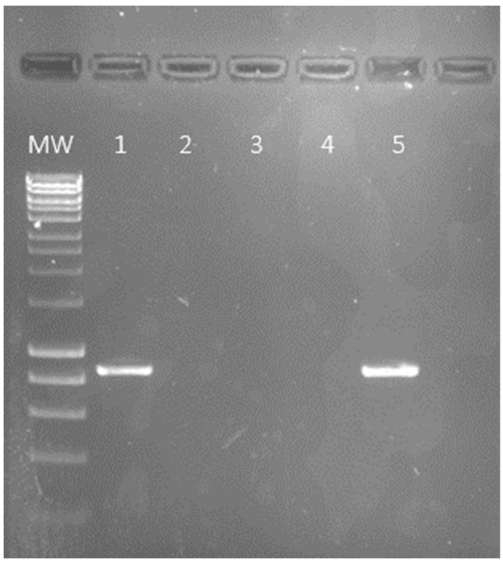

Figure B-5 | Detection of *STA1* gene via PCR. Lanes 1-5: PCR product from genomic DNA of Sc-200, Sj-95, H1, H2, and H3, respectively. Molecular weight marker (MW): Hyperladder 1kb, Bioline.

Table B-1 | Sj-88 and Sj-95 similarities in nucleotide and protein level in selected genes related with maltose and maltotriose utilisation.

Gene	Function	Nucleotide similarity %	Protein similarity %
MTT1	Maltrotriose transporter	100	100
MAL13	Maltose activator protein	100	100
AGT1	Maltotriose transporter	100	100
MAL61	Maltose permease	93	92
MAL32	Maltase	99	98
MAL33	Maltose fermentation regulatory protein	74	73

Table B-2 | Sporulation and spore viability of selected *S. cerevisiae* commercial strains.

Strain name	Sporulation	Presence of viable spores
WLP001	Not present	NA
WPL400	Yes (Low sporulation)	none
WLP008	Not present	NA
A38	Not present	NA
WLP715	Yes (good sporulation)	few
OYL200	Yes (good sporulation)	all
OYL500	Yes (good sporulation)	all
WLP007	Not present	NA
WLP066	Not present	NA
WY1318	Not present	NA
WLP095	Not present	NA
WLP028	Not present	NA
OYL052	Not present	NA
OYL057	Not present	NA
OYL033	Yes (good sporulation)	few
WLP4000	Not present	NA

Table B-3 | Growth parameters of strains Sj-95, Sj-88, Sc-200, Sc-500 and H1-8 in YP-maltose, YP-maltotriose, YPD and unhopped wort after 72h.

		Sj-95	Sc-200	H1	H2	H3	Sj-88	Sc-500	H4	H5	H6	H7	H8
YPD	Specific growth (μ_{max})	0.06 ± 0	0.07 ± 0.01	0.06 ± 0	0.07 ± 0	0.07 ± 0	0.061 ± 0.013	0.056 ± 0.004	0.047 ± 0.018	0.078 ± 0.005	0.041 ± 0.007	0.075 ± 0.016	0.066 ± 0.016
	Lag phase (h)	7.49 ± 0.85	9.57 ± 1.31	8.81 ± 1.21	9.89 ± 0.94	10.4 ± 0.4	9.52 ± 1.01	8.8 ± 2.39	10.45 ± 2.81	23.88 ± 2.8	16.48 ± 3.71	19.22 ± 3.2	14.58 ± 5.99
	Maximum biomass (OD_{600})	1.32 ± 0.01	1.43 ± 0.01	1.37 ± 0.01	1.36 ± 0	1.44 ± 0.01	1.16 ± 0.02	1.18 ± 0.04	0.93 ± 0.04	1.04 ± 0.05	0.79 ± 0.07	1.09 ± 0.08	1.12 ± 0.08
	Integral area	74.1 ± 0.76	78.47 ± 0.22	74.39 ± 0.16	74.71 ± 0.92	79.58 ± 0.81	56.68 ± 2.93	58.87 ± 1.51	42.06 ± 4.52	44.13 ± 4.18	37.17 ± 3.05	49.42 ± 5.88	54.17 ± 5.48
YP + 2% maltose	Specific growth (μ_{max})	0.032 ± 0.002	0.061 ± 0.002	0.065 ± 0.003	0.043 ± 0.003	0.047 ± 0.012	0.017 ± 0.003	0.025 ± 0.004	0.034 ± 0.001	0.023 ± 0.001	0.018 ± 0.001	0.016 ± 0.003	0.031 ± 0.001
	Lag phase (h)	32.73 ± 1.59	15.09 ± 0.73	16.51 ± 0.74	20.87 ± 1.51	16.23 ± 1.11	2.12 ± 1.22	9.54 ± 1.65	12.88 ± 0.76	11.62 ± 1.93	19.94 ± 3.86	8.11 ± 4.47	12.84 ± 1.67
	Maximum biomass (OD_{600})	1.2 ± 0.018	1.15 ± 0.004	1.17 ± 0.03	1.19 ± 0.041	1.24 ± 0.029	0.6 ± 0.02	1.05 ± 0.01	1.01 ± 0.01	1.08 ± 0.02	0.87 ± 0.05	0.88 ± 0.1	1.01 ± 0.02
	Integral area	31 ± 0.69	55.07 ± 0.85	54.68 ± 0.83	44.59 ± 0.18	49.72 ± 0.31	24.31 ± 1.92	38.96 ± 3.53	43.19 ± 0.81	37.33 ± 0.96	26.8 ± 1.99	29.08 ± 2.31	42.07 ± 1.19
YP + 2% maltotriose	Specific growth (μ_{max})	0.02 ± 0.001	0.05 ± 0	0.03 ± 0.003	0.05 ± 0.003	0.03 ± 0.001	0.03 ± 0.003	0.035 ± 0.008	0.029 ± 0.004	0.02 ± 0.004	0.022 ± 0.008	0.018 ± 0.001	0.024 ± 0.005
	Lag phase (h)	5.83 ± 1.38	13.66 ± 0.56	14.84 ± 1.17	14.19 ± 0.1	12.79 ± 1.85	3.06 ± 0.64	6.87 ± 1.39	8.13 ± 2.23	2.83 ± 1.51	7.83 ± 3.77	0.43 ± 0.29	2.32 ± 1.61
	Maximum biomass	0.68 ± 0.005	1.21 ± 0.015	1.2 ± 0.009	1.16 ± 0.006	1.29 ± 0.018	0.55 ± 0.04	1.16 ± 0.02	1.08 ± 0.05	0.6 ± 0.07	0.94 ± 0.17	0.66 ± 0.02	0.63 ± 0.08

	(OD_{600})												
	Integral area	24.74 ± 1.42	55.27 ± 0.69	45.96 ± 0.51	54.05 ± 0.22	51.19 ± 0.46	26.56 ± 1.99	49.97 ± 1.21	46.49 ± 2.6	22.15 ± 4.32	37.62 ± 10.69	22.32 ± 1.71	26.09 ± 3.49
DME	Specific growth	0.1309 ± 0.013	0.1475 ± 0.005	0.1265 ± 0.003	0.1385 ± 0.012	0.1139 ± 0.009	0.096 ± 0.01	0.099 ± 0.01	0.105 ± 0.02	0.109 ± 0.01	0.144 ± 0.04	0.107 ± 0.01	0.09 ± 0.01
	Lag phase (h)	15.92 ± 15.97	6.79 ± 0.58	13.09 ± 8.13	8.48 ± 1.81	6.69 ± 0.31	5.23 ± 1.56	15.96 ± 7.47	19.59 ± 14.93	32.41 ± 15.19	9.1 ± 3.07	8.51 ± 2.82	4.79 ± 0.9
	Maximum biomass (OD_{600})	85.21 ± 3.21	74.07 ± 3.27	65.76 ± 7.02	79.63 ± 4.27	80.27 ± 11.28	81.45 ± 10.33	134.61 ± 15.97	98.52 ± 9.12	103.91 ± 19.69	137.27 ± 44.21	120,41 ± 23.85	79.02 ± 6.97
	Integral area	3668 ± 91	3264 ± 127	2856 ± 152	3533 ± 147	3146 ± 355	3736 ± 456	5173 ± 599	4504 ± 629	3953 ± 643	5310 ± 1397	4746 ± 568	3412 ± 454

Table B-4 | Overview of the results and comments from sensory evaluation on 10L beer fermentation by professional tasting panel. Score legend: absent (0); very very low presence (1); very low presence (2); low presence (3); mild presence (4); presence (5); clear presence (6); strong presence (7)

Beers made with strain:		Hybrid 1	Hybrid 2	Hybrid 3	Sj-95	Sc-200
Aroma/Flavour	Malt	4	4.5	3.5	3.5	3
	Hoppy	3	3.5	3.5	1.5	1.5
	Esters	4.5	4	5	3	5
	Phenolic	5	5	4	5	2.5
Comments		Fruity, pear, grape, lemon, estery, sweet, pineapple, banana, slightly sour, vanilla, phenolic, clove, low sulphur	Ethyl acetate, acetaldehyde, isoamyl acetate, estery, pear, light hoppy, sweet, soft, nice body, phenolic, funky, clove, not very carbonated	Lemon, spicy, green apple, dry, low phenolic, light hoppy, light bitter, peach, red berry, yeasty, light sour	Phenolic, low sulphur, higher alcohols, smoky, funky, low estery, pear, pineapple	Floral,estery, dry aftertaste, quite sweet, balanced aroma & flavor, isoamyl acetate, peach
Taste/mouthfeel	Bitterness	2	4	3	2.5	3
	Sweet	4.5	4	4	3.5	2.5
	Body	3	3	2	2	2
	Astringency	3.5	3	4	3	4
	Sour	3	2	2.5	2	1.5
Overall impression	Appreciation	6	6	5	5	4
	Complexity	4	5	5	4	4
	Balance	5	4.5	4	3	4

Table B-5 | Primers used in this study

Primer set name	Forward primer (5'-3')	Reverse primer (5'-3')	Application
Scer	GGTTTTATCTGGCACTCAGGT	GTTGCTGTTGCTGCAAAGGT	Species-specific amplification of *S. cerevisiae* SEC24 allele
Sjur	CTCAAATGGGAATGCCACCG	TCCTGATAGTGGTTGTTGCT	Species-specific amplification of *S. jurei* SEC24 allele
ACT1	GGTTATTGATAACGGTTCTGGTATG	ATGATACCTTGGTGTCTTGGTCTAC	Amplification of *ACT1* in *S. cerevisiae* and *S. jurei* for qPCR
FDC1_sc	GAAGACAACGCCTGAAGAAT	TGACATCATCAAAAGCCATC	Amplification of *S. cerevisiae* FDC1 allele for qPCR
FDC1_sj	ACGTACGGAATGTGGATTCT	ATTTCCTTTGCCAATAGCTG	Amplification of *S. jurei* FDC1 allele for qPCR
PAD1_sc	AACCCCTTTATCTTCCATCC	TTTTATTCCTTCCCAACGAG	Amplification of *S. cerevisiae* FDC1 allele for qPCR
PAD1_sj	TGCAATCAAAGAAAACCGTA	ATTCTACCGACGCTTTGTTC	Amplification of *S. jurei* FDC1 allele for qPCR
STA1	CAACTACGACTTCTGTCATA	GATGGTGACGCAATCACGA	Amplification of *STA1*
Chr.1_Sc	CTTCACAGCTGGAGACATTG	TCACCAGCTCTTTTCAACAA	Chromosome-specific, species-specific amplification of S. *cerevisiae* ACS1 allele in chromosome I
Chr.1_Sj	GGCTGGAGTACCTTCAAAGA	AAGGTGTCCAACATTCCACT	Chromosome-specific, species-specific amplification of *S. jurei ACS1* allele in chromosome I
Chr.2_Sc	TCAAGTCATGGAGAAAAGCA	ATCTGTGGCATTTCCAATTT	Chromosome-specific, species-specific amplification of S. *cerevisiae POA1* allele in chromosome II
Chr.2_Sj	TTGGACCCGTCTCTATCATT	CCACTTAACGTGTCCACAAA	Chromosome-specific, species-specific amplification of *S. jurei* TFC1 allele in chromosome II
Chr.3_Sc	CAAGGTTTGGAAAGGTATGG	TGTTGTATTTGCGAGCGTAT	Chromosome-specific, species-specific amplification of S. *cerevisiae CHA1* allele in chromosome III
Chr.3_Sj	CTACTGTGCATGGCAAAGAC	TGAATGCCTACAACCAAGTG	Chromosome-specific, species-specific amplification of *S. jurei* CHA1 allele in chromosome III
Chr.4_Sc	GTTCCCTTTCGTGATCATTC	GACCACTGGAGCAACTCTCT	Chromosome-specific, species-specific amplification of S. *cerevisiae* DIA3 allele in chromosome IV
Chr.4_Sj	AAATGCAGGCGTTTAATTTC	CCCTCTAAAAAGGCAGTCAA	Chromosome-specific, species-specific amplification of *S. jurei LRG1* allele in chromosome IV

Chr.5_Sc	ATCCAGTTCCAATCCTGAAA	CACATCTCCCACAACAAAGA	Chromosome-specific, species-specific amplification of S. *cerevisiae PUG1* allele in chromosome V
Chr.5_Sj	CGACACCTGTGATGTTCAGT	TACGTTGGTTCCCGTATTTT	Chromosome-specific, species-specific amplification of *S. jurei* CAN1 allele in chromosome V
Chr.6_Sc	GGGTGGTCATTCAGATCTTC	AATCCAGGGCTTTTCTTTCT	Chromosome-specific, species-specific amplification of S. *cerevisiae IRC7* allele in chromosome VI
Chr.6_Sj	ACTGCTTCAGCTCCAAATTC	AGATTCGACAGCCTTTATGG	Chromosome-specific, species-specific amplification of *S. jurei* DAK2 allele in chromosome VI
Chr.7_Sc	CTTTCTTTGGTGAAGGTGCT	GGGTTTGGTTGAGTTTTGTC	Chromosome-specific, species-specific amplification of S. *cerevisiae ADH4* allele in chromosome VII
Chr.7_Sj	TTCTTTGCCATTGTTTGCTA	CATGGTAGATGGATCGTTGA	Chromosome-specific, species-specific amplification of *S. jurei* ADH4 allele in chromosome VII
Chr.8_Sc	AATGGGCTCAAAATAATGGA	ATAAAGCTTGCTGGGAAGTG	Chromosome-specific, species-specific amplification of S. *cerevisiae EFM1* allele in chromosome VIII
Chr.8_Sj	CTCTGTTTCATGTCGCAATC	AGGTAAGGCGGAAGGTAGTT	Chromosome-specific, species-specific amplification of *S. jurei* EMF1 allele in chromosome VIII
Chr.9_Sc	TACACCTGCCTTCAATCAAA	TTTGATAGGCATCCCAGAAT	Chromosome-specific, species-specific amplification of S. *cerevisiae* SGA1 allele in chromosome IX
Chr.9_Sj	TCTCCAAATTACCGATCCAT	ACTCTGAGCCTGAAACCATC	Chromosome-specific, species-specific amplification of *S. jurei* SEC6 allele in chromosome IX
Chr.10_Sc	TGTTCAATTTCATCCGTCAG	ATTTCCATGGTGATTGCTCT	Chromosome-specific, species-specific amplification of S. *cerevisiae SDH9* allele in chromosome X
Chr.10_Sj	ATGCCTCGTCTGAAGAAGTC	CTCCCAAAAGTTTGCTGTTT	Chromosome-specific, species-specific amplification of *S. jurei* CHS6 allele in chromosome X
Chr.11_Sc	TGCCTGGGAAACCACAAGTT	AGGAGGCAACTTGACACCAA	Chromosome-specific, species-specific amplification of S. *cerevisiae URA1* allele in chromosome XI
Chr.11_Sj	TGACGGCCAGTTTAACTACCA	TGCACCCGCTTTAGAGTCAG	Chromosome-specific, species-specific amplification of *S. jurei* URA1 allele in chromosome XI
Chr.12_Sc	TTGTCGGTGGATGACAATAG	TAGATGCTCGTGCAACATTT	Chromosome-specific, species-specific amplification of S. MHT1 ACS1 allele in chromosome XII

Chr.12_Sj	GGCATGTCTGGTAAAACCTC	TTCGTGATGGTACCACTTTG	Chromosome-specific, species-specific amplification of *S. jurei* MHT1 allele in chromosome XII
Chr.13_Sc	AATGCCCAAAGCAGAAATAG	GTAATCAGCAACACCGATGA	Chromosome-specific, species-specific amplification of S. *cerevisiae ERO1* allele in chromosome XIII
Chr.13_Sj	GAACTCCAGCCATTGGATAC	TCTCCTGAAGGGCTTTACAC	Chromosome-specific, species-specific amplification of *S. jurei* UBX2 allele in chromosome XIII
Chr.14_Sc	CGGTGTCAACAATCAACACT	GTGAAAGCCAAACTCGAACT	Chromosome-specific, species-specific amplification of S. *cerevisiae EDT2* allele in chromosome XIV
Chr.14_Sj	TCACTGTGTTACCCAAATCG	GTGTTCACCACTACCAACGA	Chromosome-specific, species-specific amplification of *S. jurei* KRE1 allele in chromosome XIV
Chr.15_Sc	TCTCTTCCGGCAAATCTATC	TCAGCGGTATCCTTAAAAGC	Chromosome-specific, species-specific amplification of S. *cerevisiae ZPS1* allele in chromosome XV
Chr.15_Sj	TAGGTGAAGGCTCTCGTACC	GCGAGTGGTAAAAAGCAAAT	Chromosome-specific, species-specific amplification of *S. jurei* FAA1 allele in chromosome XV
Chr.16_Sc	GCAAGGGCTCTAATCAAAAA	GGCCAAGGACAATAACATTC	Chromosome-specific, species-specific amplification of S. *cerevisiae MDL2* allele in chromosome XVI
Chr.16_Sj	AAATGGGTGATAATGGTGCT	CGATCCTGAACTTGCTTTTT	Chromosome-specific, species-specific amplification of *S. jurei* MRI1 allele in chromosome XVI

Table B-6 | Pale wort recipe

Malts	%
Golden Promise	74.80%
Flaked Oats	13.70%
Wheat	9.20%
Caramel pils	2.30%
Mashing profile	Time
50 ºC	15 min
72 ºC	60 min
77 ºC	5 min
100 ºC (boiling step)	60 min

Blank page